



**APPLICATION OF HORIZONTAL FLOW TREATMENT WELLS FOR *IN SITU*
TREATMENT OF MTBE-CONTAMINATED GROUNDWATER**

THESIS

Preston F. Rufe, Captain, USAF

AFIT/GEM/ENV/04M-15

**DEPARTMENT OF THE AIR FORCE
AIR UNIVERSITY**

AIR FORCE INSTITUTE OF TECHNOLOGY

Wright-Patterson Air Force Base, Ohio

APPROVED FOR PUBLIC RELEASE; DISTRIBUTION UNLIMITED.

The views expressed in this thesis are those of the author and do not reflect the official policy or position of the United States Air Force, Department of Defense, or the United States Government.

AFIT/GEM/ENV/04M-15

APPLICATION OF HORIZONTAL FLOW TREATMENT WELLS FOR *IN SITU*
TREATMENT OF MTBE-CONTAMINATED GROUNDWATER

THESIS

Presented to the Faculty
Department of Systems and Engineering Management
Graduate School of Engineering and Management
Air Force Institute of Technology
Air University
Air Education and Training Command
In Partial Fulfillment of the Requirements for the
Degree of Master of Science in Engineering Management

Preston F. Rufe, B.S.
Captain, USAF

March 2004

APPROVED FOR PUBLIC RELEASE; DISTRIBUTION UNLIMITED.

APPLICATION OF HORIZONTAL FLOW TREATMENT WELLS FOR *IN SITU*
TREATMENT OF MTBE-CONTAMINATED GROUNDWATER

Preston F. Rufe, B.S.

Captain, USAF

Approved:

/signed/

11 Mar 04

Dr. Mark N. Goltz (Chairman)

/signed/

11 Mar 04

Dr. Charles A. Bleckmann (Member)

/signed/

12 Mar 04

Dr. Junqi Huang (Member)

ABSTRACT

Petroleum hydrocarbon releases into the environment have resulted in widespread groundwater contamination by the gasoline oxygenate MTBE. The distribution, mobility, recalcitrance, and potential health hazards of MTBE have resulted in a significant environmental problem across the United States. This study utilized a three-dimensional numerical model to evaluate the potential application of a novel *in situ* bioremediation technology using so-called Horizontal Flow Treatment Wells (HFTWs) to manage MTBE-contaminated groundwater. HFTWs consist of two dual-screened treatment wells. One well operates in an upflow mode, with MTBE-contaminated water extracted from an aquifer through the lower well screen and injected into the aquifer through the upper screen, while the adjacent well operates in a downflow mode, extracting water through the upper screen and injecting it through the lower. As the MTBE-contaminated water flows through the wells, an electron acceptor and/or an electron donor is introduced in order to promote oxidation of MTBE by indigenous microorganisms that grow in bioactive zones adjacent to the injection screens of the treatment wells. In addition to effecting mixing of electron donor/acceptor into the water, the HFTWs recirculate water between the well pairs, resulting in multiple passes of contaminated water through the bioactive treatment zones. In an earlier field study, McCarty *et al.* (1998) used HFTWs to add oxygen and toluene into trichloroethylene (TCE)-contaminated groundwater in order to promote *in situ* aerobic cometabolic biodegradation of TCE.

The model used in this study couples a model that simulates the complex three-dimensional flow field that results from HFTW operation with a transport model to simulate MTBE fate due to advective/dispersive transport and biodegradation. The biodegradation model allows simulation of either direct or cometabolic oxidation of MTBE by indigenous microorganisms. The model was applied to a hypothetical MTBE-contaminated site to demonstrate how this technology might effect *in situ* MTBE treatment.

A sensitivity analysis was conducted using the model to determine the engineering and environmental parameters that impact technology performance. It was observed that technology performance simulated by the model is particularly sensitive to treatment well pumping rate, aquifer hydraulic conductivity, and conductivity anisotropy. It was also observed that simulated technology performance was sensitive to kinetic parameters in both the direct and cometabolic biodegradation sub-models, motivating the need for future research to accurately quantify these parameters for given geochemical and microbiological conditions. This study demonstrates that the HFTW technology has potential for application in managing MTBE-contaminated groundwater.

ACKNOWLEDGMENTS

This work was supported in part by the Air Force Center for Environmental Excellence. I would like to thank all those who assisted me in any way to make this work possible. Furthermore, there are a few people who in particular I owe special thanks and will address them now. Dr. Mark Goltz spent countless hours guiding me in my research efforts and was an invaluable asset to my completion of this thesis. Dr. Junqi Huang wrote all the computer code to support this work and his expertise was instrumental in making this work possible. Dr. Bleckmann provided excellent help through his classroom instruction in microbiology. Finally, the diligence of the research librarians in the AFIT library for providing the resources I needed for this work.

Preston F. Rufe

TABLE OF CONTENTS

	Page
Abstract.....	iv
Acknowledgments	vi
Table of Contents.....	vii
List of Figures.....	xi
List of Tables	xv
 1.0 Introduction.....	 1
1.1 Background.....	1
1.2 Research Goals and Objectives	7
1.3 Research Approach.....	7
1.4 Scope and Limitations of Research	8
 2.0 Literature review	 9
2.1 Overview.....	9
2.2 Definitions	9
2.3 Abbreviations.....	12
2.4 History of MTBE Use.....	13
2.5 Health Effects and Regulatory Issues	16
2.6 Properties of MTBE.....	18
2.7 Occurrence and Distribution in the Environment	21
2.8 Degradation Processes	24
2.8.1 Abiotic Processes.....	24
2.8.1.1 Oxidation by Oxygen.....	27
2.8.1.2 Oxidation by Ozone	29
2.8.1.3 Oxidation by Fenton’s Reagent	30
2.8.1.4 Oxidation by Persulfate	33
2.8.1.5 Oxidation by Permanganate.....	38
2.8.1.6 Oxidation by Ozone and Hydrogen Peroxide.....	40
2.8.1.7 Oxidation by UV Irradiation.....	43

	Page
2.8.1.8 Oxidation by Ultrasound Irradiation.....	45
2.8.1.9 Oxidation by Gamma Irradiation.....	51
2.8.1.10 Oxidation by Dense Medium Plasma	52
2.8.1.11 Hydrolysis.....	53
2.8.2 Biotic Processes	55
2.8.2.1 Direct metabolism.....	57
BC-1 (Aerobic)	57
MC-100 (Aerobic)	58
PM-1 (Aerobic).....	59
ENV735 (Aerobic).....	62
Mycobacterium austroafricanum IFP 2012 (Aerobic).....	63
Isolates 24, 33, 41 (Aerobic).....	64
Uncharacterized Cultures (Aerobic)	64
Uncharacterized Cultures (Anaerobic)	65
2.8.2.2 Cometabolism	65
Graphium sp. (Aerobic)	66
ENV421 and ENV425 (Aerobic).....	67
Mycobacterium vaccae JOB5 (Aerobic).....	68
Arthrobacter (Aerobic).....	70
Cyclohexane-Oxidizing Culture (Aerobic).....	70
Iso-Alkane-Oxidizing Cultures (Aerobic)	71
Pseudomonas aeruginosa (Aerobic).....	72
Uncharacterized Cultures (Aerobic)	72
2.9 Kinetic Models.....	73
2.9.1 First-Order Kinetic Models for Abiotic and Biotic Processes	74
2.9.2 Second-Order Kinetic Models For Abiotic Processes	75
2.9.3 Monod Kinetic Models for Direct Metabolism	76
2.9.4 Monod Kinetic Models for Cometabolism	80
2.9.5 Dual-Monod Kinetic Models for Cometabolism	84
2.10 Horizontal Flow Treatment Wells (HFTWs).....	91
2.10.1 Operation of HFTWs	91
2.10.2 Modeling HFTW Operation.....	93
2.10.2.1 Analytical Models.....	93

	Page
2.10.2.2 Numerical Models	95
3.0 Methodology	98
3.1 Overview.....	98
3.2 Process Selection	98
3.2.1 Process Evaluation Criteria.....	99
3.2.2 Process Evaluation	101
3.2.2.1 Oxidation by Oxygen.....	103
3.2.2.2 Oxidation by Ozone	103
3.2.2.3 Oxidation by Fenton's Reagent	104
3.2.2.4 Oxidation by Persulfate	104
3.2.2.5 Oxidation by Permanganate.....	104
3.2.2.6 Oxidation by Ozone and Hydrogen Peroxide	105
3.2.2.7 Oxidation by UV Irradiation.....	105
3.2.2.8 Oxidation by Ultrasound Irradiation.....	105
3.2.2.9 Oxidation by Gamma Irradiation.....	105
3.2.2.10 Oxidation by Dense Medium Plasma	105
3.2.2.11 Hydrolysis.....	106
3.2.2.12 Aerobic Direct Metabolism	106
3.2.2.13 Aerobic Cometabolism	107
3.2.2.14 Anaerobic Metabolism.....	108
3.2.3 Process Selection	108
3.3 Submodel	110
3.3.1 Submodel Evaluation	110
3.3.2 Submodel Selection	111
3.3.3 Submodel Assumptions	112
3.3.4 Submodel Limitations	113
3.4 Flow and Transport Model	114
3.5 Technology Model.....	116
3.5.1 Kinetic Parameters	117
3.5.2 Model Space Site Conditions	121
3.5.3 Actual MTBE Site Conditions	124
3.5.4 Environmental Parameters	125
3.5.5 Engineering Parameters	126

	Page
3.6 Technology Model Verification	128
3.7 Model Simulations.....	130
4.0 Results and Analysis	132
4.1 Overview.....	132
4.2 Submodel Verification.....	132
4.2.1 Direct Metabolism Verification	132
4.2.2 Cometabolism Verification.....	138
4.3 Technology Model Simulation Results	142
4.3.1 Direct Metabolism Baseline.....	143
4.3.2 Direct Metabolism Sensitivity Analysis Results.....	149
4.3.2.1 Horizontal Hydraulic Conductivity	149
4.3.2.2 Anisotropy Ratio.....	154
4.3.2.3 MTBE Source Concentration	160
4.3.2.4 Time Average Concentration of Hydrogen Peroxide	162
4.3.2.5 Pumping Rate.....	165
4.3.2.6 MTBE Utilization Rate.....	168
4.3.2.7 MTBE Half-Saturation Constant	170
4.3.3 Cometabolism Baseline	172
4.3.4 Cometabolism Sensitivity Analysis Results	181
4.3.4.1 Primary Substrate Utilization Rate	182
4.3.4.2 Primary Substrate Half-Saturation Constant	185
4.3.4.3 MTBE Utilization Rate.....	185
4.3.4.4 MTBE Half-Saturation Constant	187
5.0 Conclusions	189
5.1 Summary.....	189
5.2 Conclusions.....	189
5.3 Recommendations.....	194
Bibliography	196
Vita	208

LIST OF FIGURES

Figure	Page
Figure 1 Elevation View of HFTW Pair	5
Figure 2 Plan View of HFTW Pair	6
Figure 3 Graphical Representation of Chemical Properties of Several Gasoline Constituents and Oxygenates (from Jansen <i>et al.</i> (2002))	20
Figure 4 Molecular Structure of MTBE.....	21
Figure 5 Typical Oxidation Pathway of MTBE by an AOP (After Mitani <i>et al.</i> (2002)).....	27
Figure 6 Generalized Pathway of MTBE Biodegradation Under Aerobic Conditions (From Deeb <i>et al.</i> (2000))	56
Figure 7 HFTW Operation with Biotic Treatment Processes	92
Figure 8 Plan View of Upper Aquifer Region of a 2-Well HFTW System (After Stoppel, 2001)	95
Figure 9 Sample of Finite-Difference Three-Dimensional Grid (From Garrett (1999)).....	97
Figure 10 Plan View of Baseline Model Space	123
Figure 11 Elevation View of Baseline Model Space	124
Figure 12 MTBE Concentration Contours (a) Without Hydrogen Peroxide Injection and (b) With Hydrogen Peroxide Injection at 100 days, Respectively (Layer 2, TAC=57.4 mg/L Hydrogen Peroxide, Baseline Kinetic Data).....	134
Figure 13 (a) Hydrogen Peroxide and (b) Microbial Concentration Contours at 100 days, Respectively (Layer 2, TAC=57.4 mg/L Hydrogen Peroxide, Baseline Kinetic Data).....	135
Figure 14 MTBE Breakthrough Curve at Observation Well 33 m Down Gradient From Source (Layer 2, No Pumping, No Hydrogen Peroxide Injection).....	137
Figure 15 MTBE Concentration Contours (a) Without Electron Donor/Acceptor Injection and (b) With Electron Donor/Acceptor Injection at 100 days, Respectively (Layer 2, TAC=15 mg/L Propane, TAC=171.7 mg/L Hydrogen Peroxide, Baseline Kinetic Data)	139

Figure	Page
Figure 16 (a) Hydrogen Peroxide and (b) Microbial Concentration Contours at 100 days, Respectively (Layer 2, TAC =15 mg/L Propane, 171.7 mg/L Hydrogen Peroxide, Baseline Kinetic Data)	140
Figure 17 Shaded Relief Map Depicting Microbial Concentrations (Layer 2, TAC=15 mg/L Propane, 171.7 mg/L Hydrogen Peroxide, Baseline Kinetic Data)	141
Figure 18 Contour Plots of (a) MTBE, (b) Oxygen, (c) Hydrogen Peroxide, and (d) Microbial Concentrations at 300 days, Respectively (Layer 2, Baseline Data)	144
Figure 19 West-East Axis Profile of MTBE Concentration Contours at 300 days, With Approximate Well Location Shown (All Layers, Baseline Data)	145
Figure 20 North-South Profile of MTBE Concentration Contours at 300 days, With Approximate Well Locations Shown (All Layers, Baseline Data)	145
Figure 21 North-South Profile of Microbial Concentration Contours at 300 days, With Approximate Well Locations Shown (All Layers, Baseline Data)	145
Figure 22 Breakthrough Curve of MTBE at Centerline Observation Well (Layer 2, Baseline Data)	147
Figure 23 Breakthrough Curve of Oxygen at Centerline Observation Well (Layer 2, Baseline Data)	148
Figure 24 MTBE Breakthrough Curves at Centerline Observation Well at Varying Horizontal Hydraulic Conductivities (Layer 2, Baseline Kinetic and Engineering Data, 1200 days)	151
Figure 25 Contour Plots of MTBE (1 st row), Oxygen (2 nd row), and Microbial Concentrations (3 rd row), for Horizontal Hydraulic Conductivities of (a) 2.5 m/day, (b) 25 m/day, and (c) 50 m/day (Layer 2, Baseline Kinetic and Engineering Data, 1200 days)	153
Figure 26 North-South Profiles of MTBE Concentration Contours for (a) Horizontal Hydraulic Conductivity=2.5 m/day and (b) Horizontal Hydraulic Conductivity=50 m/day at 1200 days, With Approximate Well Locations Shown (All Layers, Baseline Kinetic and Engineering Data)	154
Figure 27 MTBE Breakthrough Curves at Centerline Observation Well for Different Anisotropy Ratios (Layer 2)	155
Figure 28 MTBE Breakthrough Curves at Centerline Observation Well for Different Anisotropy Ratios (Layer 3)	156

Figure	Page
Figure 29 North-South Profiles of MTBE Concentration Contours for Anisotropy Ratios of (a) 1 to 1, (b) 20 to 1, and (c) 100 to 1 at 300 days (All Layers, Baseline Kinetic and Engineering Data)	157
Figure 30 Flow Lines Induced by HFTW Operation in Isotropic Conditions	158
Figure 31 North-South Profiles of Oxygen Concentration Contours for Anisotropy Ratios of (a) 1 to 1, (b) 100 to 1 at 300 days (All Layers, Baseline Kinetic and Engineering Data)	159
Figure 32 MTBE Breakthrough Curves at Centerline Observation Well for Different Source Concentrations (Layer 2).....	161
Figure 33 MTBE Breakthrough Curves at Centerline Observation Well at Various Hydrogen Peroxide TACs (Layer 2)	163
Figure 34 Microbial Concentration Contours for Hydrogen Peroxide TACs of (a) 5.72 mg/L, (b) 57.2 mg/L, and (c) 572 mg/L at 300 days (All Layers)....	164
Figure 35 MTBE Breakthrough Curves at Centerline Observation Well for Various Pumping Rates (Layer 2).....	166
Figure 36 Contour Plots for MTBE (1 st Row), Oxygen (2 nd Row), and Microbial Concentrations (3 rd Row), for Pumping Rates of (a) 50 m ³ /day, (b) 100 m ³ /day, and (c) 200 m ³ /day (Layer 2, Baseline Kinetic and Environmental Data, 300 days)	167
Figure 37 MTBE Breakthrough Curves at Centerline Observation Well for Various MTBE Utilization Rates (Layer 2).....	169
Figure 38 MTBE Breakthrough Curves at Centerline Observation Well for Various MTBE Half-Saturation Constant Values (Layer 2).....	171
Figure 39 Contour Plots of (a) Propane, (b) Oxygen, (c) Hydrogen Peroxide, (d) MTBE and (e) Microbial Concentrations at 300 days, Respectively (Layer 2, Baseline Data).....	173
Figure 40 MTBE Mass Degraded for Various Propane TACs and Injection Schedules (All Layers)	176
Figure 41 MTBE Breakthrough Curves at Centerline Observation Well for Various Propane Injection Pulse Schedules (Layer 2, Propane TAC=3.0 mg/L, Baseline Kinetic and Environmental Data)	177

Figure	Page
Figure 42 Contour Plots of (a) Propane, (b) Oxygen, (c) Hydrogen Peroxide, (d) MTBE and (e) Microbial Concentrations at 300 days, Respectively (Layer 2, Baseline Data).....	180
Figure 43 MTBE Breakthrough Curves at the Centerline Observation Well for Various Primary Substrate Utilization Rates (Layer 2).....	182
Figure 44 Microbial Concentrations Observed at the Centerline Observation Well Located Between the Pumping Wells (Layer 2)	184
Figure 45 MTBE Breakthrough Curves at the Centerline Observation Well for Various MTBE Utilization Rates (Layer 2)	186
Figure 46 MTBE Breakthrough Curves at the Centerline Observation Well for Various MTBE Half-Saturation Constant Values (Layer 2)	187

LIST OF TABLES

Table	Page
Table 1 Summary of Chemical Properties of Several Gasoline Constituents and Oxygenates at 25 °C (From Moyer, 2003)	19
Table 2 Summary of USAF MTBE-Contaminated Sites Available From AFCEE ERPIMS Database (AFCEE, 2003)	22
Table 3 Pseudo First-Order Rate Constants for Persulfate Oxidation of MTBE at Various Temperatures (Adapted from Huang <i>et al.</i> (2002)).....	35
Table 4 Pseudo First-Order Rate Constants for Persulfate Oxidation of MTBE at Various Persulfate Concentrations (Adapted from Huang <i>et al.</i> (2002))	35
Table 5 Pseudo First-Order Rate Constants for Persulfate Oxidation of MTBE at Various pH (Adapted from Huang <i>et al.</i> (2002)).....	36
Table 6 Pseudo First-Order Rate Constants for Persulfate Oxidation of MTBE at Various Ionic Strengths (Adapted from Huang <i>et al.</i> (2002))	36
Table 7 Pseudo First-Order Rate Constants for Ultrasound Oxidation of MTBE Under Various Conditions (Adapted from Kang and Hoffman (1998) and Kang <i>et al.</i> (1999)).....	47
Table 8 Pseudo First-Order Rate Constants for Ultrasound Oxidation of MTBE Under Various Conditions (pH = 5.8, Temperature = 25°C) (Adapted from Neppolian <i>et al.</i> (2002)).....	50
Table 9 Summary of First-Order Kinetic Parameters and Conditions of Study	75
Table 10 Summary of Second-Order Kinetic Parameters and Conditions of Study.....	76
Table 11 Summary of Substrate Utilization Rates and Half-Saturation Constants for MTBE-Metabolizing Bacteria	79
Table 12 Summary of Biomass Yields for MTBE-Metabolizing Bacteria.....	80
Table 13 Summary of Decay Rates for MTBE-Metabolizing Bacteria.....	80
Table 14 Summary of Substrate Utilization Rates for Various MTBE-Cometabolizing Microorganisms	82
Table 15 Summary of Half-Saturation and Inhibition Constants for MTBE-Cometabolizing Microorganisms.....	83

Table	Page
Table 16 Summary of Biomass Yields for Various Bacterial Strains Grown on Various Substrates	83
Table 17 Summary of Decay Rate for MTBE-Cometabolizing Bacteria	83
Table 18 Summary of Parameters and Values from Gandhi <i>et al.</i> (2002).....	90
Table 19 Evaluation of Treatment Processes.....	102
Table 20 Summary of Process Selection	108
Table 21 Baseline Kinetic Parameters Used in Direct Metabolism Simulations.....	119
Table 22 Baseline Kinetic Parameters Used in Cometabolism Simulations	120
Table 23 MTBE-Contaminated Site Data.....	125
Table 24 Environmental Parameters Used in Simulations	126
Table 25 Engineering Parameters Used in Direct-Metabolism Model Simulations.....	127
Table 26 Engineering Parameters Used in Cometabolic Model Simulations.....	128
Table 27 Summary of Mass Balance Output for Direct Metabolism Verification Simulations (All Layers, 100 days)	136
Table 28 Summary of Mass Balance Output for Cometabolism Verification Simulations (All Layers, 100 days)	142
Table 29 Summary of Mass Balance Output From Baseline Direct Metabolism Simulation (All Layers, 300 days).....	148
Table 30 MTBE Mass Degraded at Varying Horizontal Hydraulic Conductivities (All Layers, Baseline Kinetic and Engineering Data, 1200 days)	152
Table 31 MTBE Mass Degraded and Microbial Mass at Various Anisotropy Ratios (All Layers, 300 days).....	160
Table 32 MTBE Mass Degraded for Different MTBE Source Concentrations (All Layers, 300 days).....	162
Table 33 MTBE Mass Degraded and Microbial Growth at Various Hydrogen Peroxide TACs (All Layers, 300 days).....	164
Table 34 MTBE Mass Degraded at Various Pumping Rates (All Layers, 300 days)	168

Table	Page
Table 35 MTBE Mass Degraded and Oxygen Remaining at Various Utilization Rates (All Layers, 300 days).....	170
Table 36 MTBE Mass Degraded at Various MTBE Half-Saturation Constant Values (All Layers, 300 days)	171
Table 37 Revised Engineering Parameters Used in Cometabolic Model Simulations...	179
Table 38 Summary of Mass Balance Output for Cometabolism Baseline Simulation (All Layers, 300 days).....	181
Table 39 MTBE Mass Degraded at Various Primary Substrate Utilization Rates (All Layers, 300 days)	185
Table 40 Mass Degraded at Various MTBE Utilization Rates (All Layers, 300 days)..	186
Table 41 Mass Degraded at Various MTBE Half-Saturation Constant Values (All Layers, 300 days)	188

APPLICATION OF HORIZONTAL FLOW TREATMENT WELLS FOR *IN SITU* TREATMENT OF MTBE-CONTAMINATED GROUNDWATER

1.0 INTRODUCTION

1.1 BACKGROUND

Methyl tert-Butyl Ether (MTBE) is a gasoline oxygenate used to improve combustion efficiency and reduce air pollution. Having been added to gasoline for over 20 years as an octane boosting agent, MTBE more recently has been added to reformulated gasoline in National Ambient Air Quality Standards (NAAQS) non-attainment areas (Moyer, 2003). The Clean Air Act Amendments of 1990 require the use of gasoline oxygenates to effect the reduction of ozone and carbon monoxide emissions. According to the Oxygenated Fuels Association (OFA), MTBE is added to some degree in approximately 30 to 50 percent of all gasoline sold in the United States (OFA, 2003).

Releases of MTBE into drinking water generally occur due to gasoline released from leaking underground storage tanks, spills, use in watercraft, and volatilization (Moyer, 2003; Reuter, *et al.*, 1998). Results of the U.S. Geological Survey's National Water-Quality Assessment program from 1993-1994 show MTBE is the second most common volatile organic compound (VOC) found in drinking water sources, where chloroform is the first (Squillace *et al.*, 1996). Along with concerns about the ubiquity of

MTBE contamination are the persistence and mobility of MTBE in groundwater. Due to its low octanol-water partition coefficient (0.94-1.16) and high aqueous solubility (23.2-54.4 g/L at 25 °C) MTBE does not adsorb well to aquifer solids and thus migrates in the dissolved phase along with the flowing groundwater (MacKay *et al.*, 1993).

In 1997 the United States Environmental Protection Agency (EPA) initiated a drinking water advisory for MTBE establishing safe limits at 20 to 40 µg/L (EPA, 1997). Seeking to ensure that drinking water is safe and acceptable for consumer use, the EPA advisory limits are established at or below the most common thresholds for detection of unpleasant odor and taste in water (EPA, 1997). The potential negative health effects of MTBE have been the subject of numerous laboratory studies using rodents, as well as a few human studies (Williams and Sheehan, 2003). Other studies have investigated the potential health effects due to tert-butyl alcohol (TBA), a common metabolite of MTBE (Williams and Sheehan, 2003). Due to inadequate toxicity data for ingestion of MTBE at concentrations commonly found in MTBE-contaminated drinking water, inadequacy of carcinogenicity data, and poor exposure monitoring, the acute and chronic health effects of MTBE and TBA are still in question (Williams and Sheehan, 2003). To this date, the EPA has not established an MCL, MCLG, or a reference dosage for chronic oral exposure to MTBE, apparently due to lack of carcinogenicity and toxicity characterization data.

The MTBE contamination problem is widespread throughout DoD. Since many petroleum products are transported in the same pipelines and processed in the same refineries, cross contamination of MTBE between gasoline and other petroleum products has resulted (Moyer, 2003). Studies indicate that MTBE may be present in fuel oil,

diesel, kerosene, other middle petroleum distillates, and used motor oil (Robbins *et al.*, 1999; Robbins *et al.*, 2000; Cummins *et al.*, 2001; Hinchey *et al.*, 2001; Baker *et al.*, 2002). Potentially the groundwater supply for any installation with a gasoline, diesel, and/or jet fuel distribution system may be contaminated with MTBE due to leaks and spills.

Field and laboratory studies have demonstrated that MTBE can be degraded *in situ* through both abiotic and biotic processes. Studies presented by Kelley *et al.* (2003) show that MTBE can be abiotically oxidized *in situ* using oxygen ($O_{2(g)}$), hydrogen peroxide (H_2O_2), ozone ($O_{3(g)}$), permanganate (MnO_4^-), persulfate ($S_2O_8^{2-}$), Fenton's Reagent, ultraviolet (UV) irradiation, ultrasound irradiation, and dense medium plasma.. Although very effective at degrading MTBE, oxidation processes are dependent on natural environmental parameters such as pH, alkalinity, natural organic matter, and the concentrations of competing electron donors (Acero *et al.*, 2001). Because of these dependencies, chemical oxidation may only be suitable under specific subsurface environmental conditions. In addition, some oxidants are unable to completely mineralize MTBE, resulting in production of potentially hazardous intermediates such as TBA and tert-butyl formate (TBF) (Kelley *et al.* 2003).

Although several early studies have shown MTBE to be recalcitrant to both aerobic and anaerobic biodegradation, more recent studies have demonstrated both direct and cometabolic degradation of MTBE (Stocking *et al.*, 2000). Fuel spills in groundwater commonly result in highly reductive environments. *In situ* anaerobic degradation of MTBE in highly reductive and methanogenic environments appears feasible (Finneran and Lovely, 2003). Anaerobic degradation studies presented by

Finneran and Lovely (2003) show MTBE can be oxidized when nitrate, Mn(IV), Fe(III), sulfate, and carbon dioxide are used as electron acceptors.

Other studies presented by Wilson (2003) show the potential for *in situ* aerobic degradation of MTBE. In order to stimulate aerobic MTBE degradation, dissolved oxygen and in some cases non-native microorganisms must be amended to the groundwater (Wilson, 2003). The production of undesirable intermediates is also an issue for both anaerobic and aerobic MTBE degradation processes. Monitoring for intermediates, such as TBA and TBF, must be accomplished in order to verify complete mineralization of MTBE. The potential for *in situ* aerobic bioremediation of MTBE in groundwater is currently being studied at the Department of Defense (DoD) National Environmental Technology Test Site at Port Hueneme, California (ESTCP, 2003a, b; Salanitro *et al.*, 2000) as well as, Vandenberg Air Force Base, California (Wilson *et al.*, 2002).

An emerging technology that has recently been applied to promote *in situ* biodegradation through biostimulation is the horizontal flow treatment well (HFTW) system. HFTW systems consist of treatment well pairs, with one treatment well operated in an upflow mode, and the other in a downflow mode (Figure 1). As shown in Figure 1, each treatment well is dual-screened, with the upflow well extracting water from the lower screen and injecting it through the upper, and the downflow well operating in reverse. As water flows through the wells, it may be amended with oxidizing agents or nutrients, so that the water that's injected into the aquifer supports microbial growth in bioactive zones adjacent to the treatment well injection screens. In these bioactive zones, the contaminant is biodegraded. Similarly, for situations where biostimulation may not

be appropriate, reactors may be installed in-well as a component of the HFTWs to effect abiotic degradation (Stoppel and Goltz, 2003). Whether biotic or abiotic, HFTWs allow for mixing of contaminated water with chemical reactants in order to destroy the contaminant *in situ*. In addition, the recirculation of contaminated groundwater induced by the HFTW system (as shown by the interflow between the two treatment wells in Figure 2) allows for multiple passes of contaminant through the bioactive zones or reactor, thereby reducing the downgradient concentrations of contaminant.

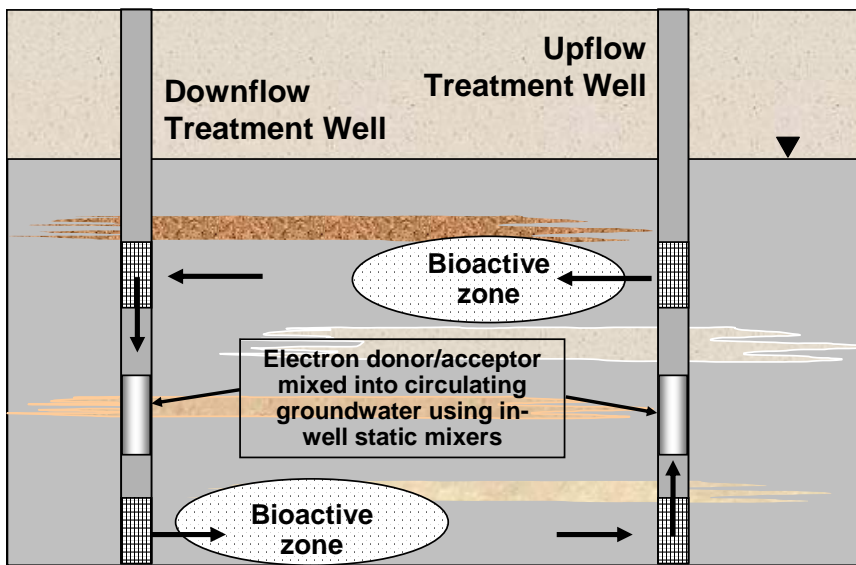


Figure 1 Elevation View of HFTW Pair

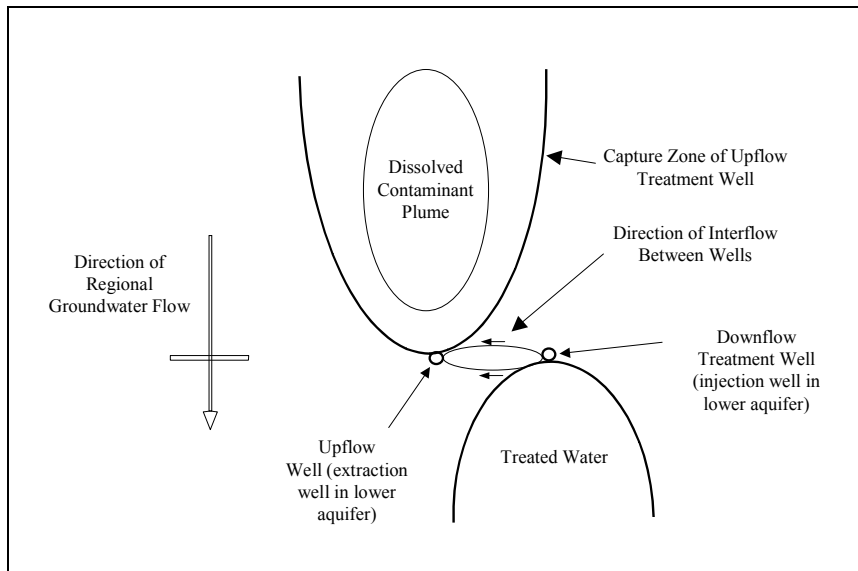


Figure 2 Plan View of HFTW Pair

Using a pair of HFTWs, McCarty *et al.* 1998 demonstrated biodegradation of trichloroethene (TCE) in contaminated groundwater at Site 19, Edwards Air Force Base. At this site, HFTWs were used to mix an electron donor (toluene) and oxidizing agents (hydrogen peroxide and oxygen) into TCE-contaminated groundwater. The demonstration of the HFTW technology at Site 19 achieved high removal of TCE (over 83%) for a single pass of contaminated water through the bioactive zone. Higher removal rates (over 97%) were achieved when comparing TCE concentrations upgradient and downgradient of the HFTWs, due to the recirculation of water between the well pair that resulted in multiple passes of TCE-contaminated water through the bioactive zones (McCarty *et al.* 1998). The potential of HFTW systems to remediate various groundwater contaminants has been the subject of a number of recent studies (McCarty *et al.*, 1998; Stoppel and Goltz, 2003; Parr *et al.*, 2003).

1.2 RESEARCH GOALS AND OBJECTIVES

The objective of this study is to investigate the feasibility of using HFTWs as a technology for the remediation of MTBE-contaminated groundwater. Pursuing this objective will require answering the following questions:

- What chemical and biological processes are capable of converting MTBE to innocuous end products?
- Which of these processes may be incorporated as a component of an HFTW system?
- How will the technology, consisting of the HFTW system coupled with the MTBE destruction process, perform at an MTBE-contaminated site?

1.3 RESEARCH APPROACH

- Review the literature for biological and chemical processes that have the potential to degrade MTBE.
- Select an appropriate process that can be adapted for in-well application as part of an HFTW system.
- Develop an HFTW technology model by combining a model of the selected MTBE degradation process with a model that describes flow and transport resulting from operation of an HFTW system.
- Examine the potential for using HFTWs to manage MTBE-contaminated groundwater by conducting a sensitivity analysis using the technology model and by applying the model to simulate remediation of an actual site.

1.4 SCOPE AND LIMITATIONS OF RESEARCH

- Candidate biological and chemical processes capable of degrading MTBE to innocuous end products will be elicited in the literature review. A suitable process that is capable of being implemented in an HFTW system will be selected for modeling using qualitative criteria (*e.g.* meets regulatory requirements, applicability at many sites, and feasibility for use with HFTW technology).
- The degradation model developed for this research will be based on results of published laboratory studies. This research study does not include a laboratory component.
- Conclusions and recommendations will be made on the results of model analysis only.

2.0 LITERATURE REVIEW

2.1 OVERVIEW

This chapter reviews the history of MTBE use, the chemical properties of MTBE, occurrences and distribution of MTBE in the environment, MTBE health effects and relevant regulatory issues, and both abiotic (physico-chemical) and biotic (biological) MTBE degradation processes. With regard to degradation processes, the review will focus on modeling the rate and extent of the degradation process, identification of degradation byproducts, and the potential of the process for application in the HFTW system. Examples of previous implementations of both *in situ* and *ex situ* processes used to remediate MTBE-contaminated groundwater are examined. Finally, this chapter concludes with a review of models that have been used to simulate performance of HFTW systems.

2.2 DEFINITIONS

Advanced oxidation process (AOP) or advanced oxidation technology (AOT) – A chemical process that makes use of a strong oxidant (typically, the hydroxyl radical, •OH) to oxidize an organic chemical like MTBE.

Bioaugmentation – Inoculation of an aquifer with non-native microorganisms capable of degrading a target compound.

Biostimulation – Amending groundwater with lacking species needed to initiate biodegradation of a target compound.

Cometabolism – The fortuitous oxidation of a secondary substrate due to microbial, enzymatic activity directed at a primary substrate. Further, the energy derived from the oxidation of the secondary substrate is not used to support microbial growth and cell maintenance (Maier *et al.*, 2000).

Direct metabolism – The oxidation of a substrate used as a sole source of carbon and energy supporting microbial growth and cell maintenance (Maier *et al.*, 2000).

First-order reaction kinetics – A process whose rate can be modeled by a mathematical equation that describes the rate of change in concentration of a reactant A as proportional to the concentration of A . Mathematically, $d[A]/dt = -k[A]$, where the constant of proportionality, k , is defined as the first-order rate constant (Clark, 1996).

Half-life – The time it takes reactant concentration to be reduced by 50% in a first-order reaction. Note that the half-life is the reciprocal of the first-order rate constant, k , multiplied by the natural logarithm of 2 (Clark, 1996).

Maximum contaminant level (MCL) – The highest concentration of a contaminant allowed in drinking water as established by the EPA.

Methanogenic – Condition of anaerobic degradation when suitable electron acceptors such as nitrate and sulfate are exhausted, thus resulting in the utilization of carbon dioxide for an electron acceptor and the production of methane (Maier *et al.*, 2000).

Michaelis-Menten/Monod kinetics – Michaelis-Menten kinetics are used to describe the quantitative relationship between substrate concentration and reaction rate of microbial enzyme catalyzed reactions relative to a maximum reaction rate achievable (Rittman and McCarty, 2001). Monod kinetics are used to describe the quantitative relationship between microbial growth and substrate utilization rate relative to a maximum substrate

utilization rate (Rittman and McCarty, 2001). Both Michaelis-Menten and Monod kinetic expressions are of mixed order, which is to say that at low substrate concentrations the reaction is first-order, while at high substrate concentrations the reaction is zero-order (Rittman and McCarty, 2001). Although technically different, the terms Michaelis-Menten and Monod kinetics are used interchangeably throughout this document. The reader is directed to Section 2.9.3 for detailed explanations of Michaelis-Menten/Monod kinetic equations and parameters.

Octanol-water partition coefficient (K_{ow}) – An equilibrium ratio of the concentration of a compound's distribution between the two phases, octanol and water. Mathematically, the octanol-water partitioning coefficient for a concentration of compound 'A' (C^A) is defined as $K_{ow} = C^A_{oct} / C^A_{water}$. The reader should note that compounds with a $\log(K_{ow})$ value less than or equal to 1 are considered hydrophilic, while compounds with a $\log(K_{ow})$ value greater than 1 are considered hydrophobic (Clark, 1996).

Pseudo first-order reaction kinetics – A reaction process with complex kinetics that can be simplified and described by simple first-order kinetics. Often, pseudo first-order kinetics are used to describe reactions where two compounds react with second-order reaction kinetics and since one of the compounds is in great excess when compared to the other reactant, it remains at a relatively constant concentration (Clark, 1996).

Second-order reaction kinetics – A process whose rate can be modeled by a mathematical equation that states that the rate of change in concentration of substance A or B is proportional to the concentration of both A and B , with the constant of proportionality defined as a second-order rate constant, k . Mathematically, $d[A]/dt = d[B]/dt = -k[A][B]$ (Clark, 1996).

Zeolite – A porous aluminum-silicate particle that can potentially function as a catalyst for a host of different reactions.

2.3 ABBREVIATIONS

g – Gram

hr – Hour

kg – Kilogram

L – Liter

M – Molarity

mg – Milligram

min – Minute

µg – Microgram

s – Second

T – Time

AFCEE – Air Force Center for Environmental Excellence

AOP – Advanced Oxidation Process

BTEX – Benzene, Toluene, Ethyl-Benzene, *m*-,*o*-,*p*-Xylene

Cⁿ – (italicized) Concentration of Compound ‘n’

DOD – United States Department of Defense

DOE – United States Department of Energy

DW – Dry Weight

EPA – United States Environmental Protection Agency

ERPIMS – Environmental Resources Program Information Management System

ESTCP – Environmental Security Technology Certification Program

FA – Formic Acid

FR – Fenton’s Reagent

TBF – Tert-Butyl Formate

TBA – Tert-Butyl Alcohol

MCL – Maximum Contaminant Level

MTBE – Methyl Tert-Butyl Ether

MA – Methyl Acetate

NOAEL – No Observed Adverse Effects Limit

RfC – Reference Concentration (inhalation)

RfD – Reference Dosage (ingestion)

RFG – Reformulated Gasoline

TAC – Time Averaged Concentration

TCE – Trichloroethylene

TOC – Total Organic Carbon

US – Ultrasound

UV - Ultraviolet

2.4 HISTORY OF MTBE USE

MTBE is a synthetic compound produced by reacting methanol with isobutylene (Trotta and Miracca, 1997). Initially MTBE was added to gasoline as an octane boosting agent designed to improve engine efficiency and performance by enhancing combustion. As early as the 1920’s, oil companies were researching the potential of ethers as additives

to increase octane in gasoline (Moyer, 2003). It wasn't until the 1970's, however, that MTBE was added to gasoline for commercial use. During the Arab oil embargo and gasoline shortage of the mid-1970's, MTBE was added to gasoline to boost octane as well as to increase supplies by diluting the gasoline (Moyer, 2003). In 1979 MTBE use increased substantially due to the phase out of lead in gasoline. Initially, MTBE was added in quantities of <1% by volume in regular and 2-8% by volume in premium gasoline (Moyer, 2003).

The addition of MTBE to gasoline not only enhanced octane, it also increased the amount of oxygen available for gasoline oxidation during the combustion process. Compounds added to gasoline for the purpose of increasing oxygen content are commonly referred to as oxygenates. The more complete combustion of gasoline results in reduction of ozone and carbon monoxide emissions. Realizing the benefits of improved combustion efficiency and the subsequent effect on air quality, several states in the United States initiated winter oxygenated fuel programs in the late 1980's (Moyer, 2003).

The Clean Air Act Amendments of 1990 established the reformulated gasoline (RFG) program to help achieve carbon monoxide and ozone National Ambient Air Quality Standards in non-attainment areas (Moyer, 2003). The RFG program mandated that oxygenates be added to gasoline in these non-attainment areas; though selection of the specific oxygenate to be added was left to the petroleum refiners (Moyer, 2003). The two most popular oxygenates added to gasoline were ethanol and MTBE (EPA, 1999b). According to the United States Department of Energy (DOE), by the year 2002 over 50 million barrels of ethanol and over 74 million barrels of MTBE were produced in the

U.S., with most of the MTBE being used as a gasoline oxygenate (DOE, 2002; Moyer, 2003).

In 1992 the winter oxygenated fuel program, mandatory in 40 U.S. metropolitan areas, required 2.7% oxygen by weight (15% MTBE or 7.3% ethanol by volume) to be added to gasoline (Moyer, 2003). Shortly thereafter, in 1995, Phase-one of the RFG program mandated year-round use of 2.0% oxygen by weight (11% MTBE or 5.4% ethanol by volume) in gasoline used in 28 metropolitan areas (Moyer, 2003). Phase-two of the RFG program was initiated in 2000, maintaining the requirements established in Phase-one (Moyer, 2003). The use of MTBE in RFG has continued despite an EPA Blue Ribbon Panel on Oxygenates in Gasoline finding that the RFG program be altered in order to reduce MTBE usage (EPA, 1999a).

MTBE is also added to gasoline in areas that currently do not require the use of RFG (Moyer, 2003). Although added in lower quantities than in RFG, MTBE is added to premium gasoline, as well as regular gasoline in lower proportions, for its octane boosting properties (Moyer, 2003). It is estimated that MTBE is present in 30 to 50 percent of all gasoline sold in the United States (OFA, 2003).

Although MTBE is not purposely added to such petroleum products as fuel oil, diesel, kerosene, other middle petroleum distillates, and used motor oil, its presence has been detected in other petroleum products. Baker *et al.* (2002) showed that MTBE is present in used motor oil taken from vehicles fueled with RFG. Studies by Cummins *et al.* (2001) and Robbins *et al.* (1999) indicate that MTBE may be present in diesel fuel and heating oil. Robbins *et al.* (1999) note how a small amount of MTBE-containing gasoline mixed with heating oil may result in significant cross-contamination. As little as

1 cup of MTBE-containing gasoline (15% MTBE by volume) mixed with 5000 gallons of fuel oil would result in an MTBE concentration in the heating oil of 1 mg/L (Robbins *et al.*, 1999). MTBE in significant concentration has also been detected in kerosene and other middle petroleum distillates in a study by Hinchey *et al.* (2001).

MTBE has applications beyond its use as a petroleum additive. MTBE has been used to dissolve gallstones in humans; although its medicinal and laboratory applications are not widespread (Moyer, 2003). Moyer (2003) reports that MTBE has been used to synthesize tert-butyl alcohol (TBA), a compound also used as an oxygenate and in laboratories. MTBE is also used in a refining process to isolate isobutylene (used in the production of synthetic rubbers) from other 4-carbon chain olefins (Trotta and Miracca, 1997). However, the vast majority of MTBE that is produced is used as a gasoline additive (Moyer, 2003).

2.5 HEALTH EFFECTS AND REGULATORY ISSUES

This section includes a discussion of the current health related issues involved with MTBE and its primary intermediate TBA, as well as a discussion of the current regulatory status of the two compounds. The health impacts of MTBE on humans are not completely understood; however, many studies have been conducted on laboratory animals and even some on human volunteers (Williams and Sheehan, 2003). Consequently, the EPA has yet to establish a maximum contaminant level (MCL) for MTBE.

Results from sub-chronic animal studies indicate that the most vulnerable organs to exposure by MTBE are the kidney and liver (Williams and Sheehan, 2003). Increased

kidney weights, cell proliferation, and kidney lesions have been observed in several studies (Williams and Sheehan, 2003). The sub-chronic effects of MTBE are similar for both ingestion of MTBE-contaminated water and inhalation of MTBE vapors. Other reported effects include reversible nervous system ailments (Williams and Sheehan, 2003). Exposure to MTBE has not resulted in any observed adverse effects to reproductive health of laboratory animals (Williams and Sheehan, 2003). The reported effects of TBA exposure are similar to those of MTBE exposure. Human studies investigating inhalation and ingestion of MTBE indicated limited short-term adverse respiratory and neurological effects; however, there are no specific long-term data available for exposure to MTBE or TBA (Williams and Sheehan, 2003).

The EPA has yet to establish a reference dosage (RfD) for MTBE ingestion; however, the EPA has established a reference concentration (RfC) for MTBE inhalation. The EPA designates of the reference dosage or concentration as a level of exposure below which no negative health effects should be observed and is also commonly referred to as the no observed adverse effect limit (NOAEL). The RfC for MTBE exposure has been established at 3 mg/m³ (EPA, 2004). Williams and Sheehan (2003) point out that extrapolation of the RfC is appropriate for determination of the RfD and this extrapolation corresponds to an RfD of approximately 1 mg/kg/day (Williams and Sheehan, 2003). Comparison of threshold values compiled in Williams and Sheehan (2003) indicate that the MTBE concentrations are on the order of 10 times higher than other gasoline constituents such as BTEX, indicating that MTBE may pose less of a health threat than other gasoline constituents (Williams and Sheehan, 2003).

Laboratory studies on the carcinogenicity of MTBE indicate that MTBE does pose a cancer threat to animals (Williams and Sheehan, 2003). The EPA has recognized MTBE as an animal carcinogen but has not officially declared that it is a potential cancer risk to humans (Williams and Sheehan, 2003). The MTBE metabolites, TBA and formaldehyde, also showed marginal evidence of posing a cancer threat to animals (EPA, 1997). Some states have established drinking water standards based on the assumption that MTBE does in fact pose a cancer risk to humans (Williams and Sheehan, 2003).

The EPA has established a drinking water advisory level for MTBE at 20 to 40 $\mu\text{g/L}$ based on taste and odor thresholds (EPA, 1997). Although strictly based on aesthetic considerations, the drinking water advisory levels are considered protective of health since they are 20,000 to 100,000 times lower than reported adverse exposure levels (EPA, 1997). States have established MCLs notwithstanding the lack of guidance from the EPA. California and New Hampshire have established the lowest MCLs for MTBE of any states at 13 $\mu\text{g/L}$ and Texas established an MCL of 240 $\mu\text{g/L}$, the highest of any state (Williams and Sheehan, 2003). The State of California has also established an aesthetically based secondary MCL at 5 $\mu\text{g/L}$. Also reported in Williams and Sheehan (2003), other states have established action levels ranging from 10 to 202,000 $\mu\text{g/L}$.

2.6 PROPERTIES OF MTBE

The chemical properties of MTBE not only influence its fate in the environment but also are important for remediation system design. It is helpful to compare MTBE to other gasoline constituents like BTEX since the compounds are often found together at

hydrocarbon spill sites. Table 1 summarizes several important parameters that characterize MTBE, its daughter-products, and other gasoline constituents.

Table 1 Summary of Chemical Properties of Several Gasoline Constituents and Oxygenates at 25 °C (from Moyer, 2003)

Compound	Molar Weight (g/mole)	Boiling Temp (°C)	Specific Gravity	Solubility (mg/L)	Log K_{ow}	Henry's Constant (atm-m³/gram-mole)
MTBE	88.15	54	0.74	50,000	1.2	1.5 x 10 ⁻³
TBA	74.12	83	0.79	miscible	0.35	1.2 x 10 ⁻⁵
TBF	102.13	82	0.89	~40,000	N/A	2.7 x 10 ⁻⁴
Benzene	78.11	80	0.88	1,780	2.0	5.4 x 10 ⁻³
Toluene	92.13	111	0.87	535	2.6	5.9 x 10 ⁻³
Ethylbenzene	106.16	136	0.87	161	3.2	8.4 x 10 ⁻³
m-Xylene	106.16	139	0.88	146	3.2	7.7 x 10 ⁻³
o-Xylene	106.16	144	0.88	175	3.0	5.1 x 10 ⁻³
p-Xylene	106.17	138	0.86	156	3.2	7.7 x 10 ⁻³

As can be seen from the table, MTBE is extremely soluble in water. Additionally, the low values for log K_{ow} and Henry's constant indicate, respectively, that MTBE does not adsorb well to solids and is not as volatile as the BTEX compounds. The result of the differences in adsorption is that the MTBE plume eventually outpaces and separates from the BTEX compounds that adsorb more readily to aquifer solids. As a result of these properties, some remediation technologies such as vapor extraction and granular activated carbon adsorption are not as effective for MTBE as they may be for BTEX compounds. Figure 3 graphically depicts the relative differences in important chemical properties of several gasoline constituents.

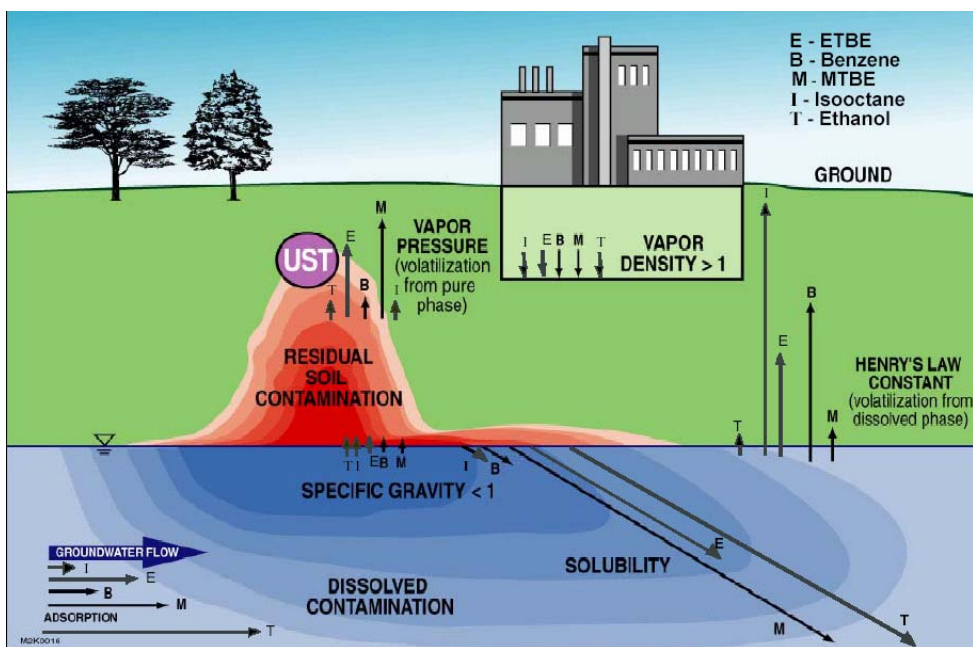


Figure 3 Graphical Representation of Chemical Properties of Several Gasoline Constituents and Oxygenates (from Jansen *et al.* (2002))

Additionally, the transport and fate of MTBE in the environment may not be affected by microbiological activity as early studies of the biodegradation of MTBE have indicated that MTBE may be recalcitrant to biological degradation, hence is very persistent in the environment (Fiorenza and Rifai, 2003). Many studies have attributed MTBE's recalcitrance to biodegradation to the ether bond in its molecular structure, shown below in Figure 4, and the high activation energy required to break it; however, later studies have shown that many species of microorganisms are capable of cleaving the ether bond and degrading MTBE despite the high energy demand (Fiorenza and Rifai, 2003).

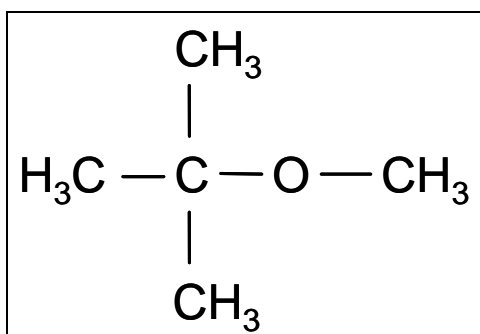


Figure 4 Molecular Structure of MTBE

2.7 OCCURRENCE AND DISTRIBUTION IN THE ENVIRONMENT

The extent of MTBE usage, along with its persistence and mobility in the environment, contribute to making MTBE a common volatile organic chemical that has been detected in many groundwater sources. The sources of MTBE are widespread including fuel leaks and spills, engine emissions, precipitation, and run-off. Additionally, due to the cross-contamination of other petroleum distillates like kerosene by MTBE, as previously discussed, MTBE sources can be difficult to identify. The broad spectrum of sources coupled with the separation of the BTEX-plume from the MTBE-plume may cause significant uncertainty as to the actual source of MTBE contamination in any particular instance (Squillace *et al.*, 1996).

Groundwater samples were taken from 210 wells in urban areas and 549 wells in agricultural areas across the US during a period from 1993 to 1994 as part of the US Geological Survey National Water-Quality Assessment program (Squillace *et al.*, 1996). The results of the analysis of the samples indicated that MTBE is the second most common volatile organic chemical detected (Squillace *et al.*, 1996). Of the urban wells sampled, 27% contained MTBE and of the agricultural area wells sampled, only 1.3%

contained MTBE (Squillace *et al.*, 1996). Squillace *et al.* (1996) suggest that leaking underground storage tanks are most likely the primary source of MTBE releases into the subsurface.

The DoD is also responsible for MTBE releases throughout the country. According to the Air Force Center for Environmental Excellence (AFCEE) Environmental Resources Program Information Management System (ERPIMS) database at least 40 Air Force installations have reported detections of MTBE contamination in groundwater. Table 2 summarizes the installation, source, and magnitude of concentrations of MTBE in groundwater reported.

Table 2 Summary of USAF MTBE-Contaminated Sites Available From AFCEE ERPIMS Database (AFCEE, 2003)

Installation	Sample Site	Maximum Reported MTBE Conc. (µg/L)
Goodfellow AFB, TX	Drum Storage Area	60,400
Andrews AFB, MD	Main Service Station	60,000
Lackland AFB, TX	UST	34,800
Randolph AFB, TX	BX Service Station	21,000
Vandenberg AFB, CA	BX Service Station	11,000
March AFB, CA	N/A	5,500
Travis AFB, CA	North and South Gas Station	5,400
Moody AFB, GA	BX Service Station	3,400
Griffiss AFB, NY	Apron 2	3,180
Nellis AFB, NV	Maint. Fac. (TCE-plume)	1,700
Avon Park AF Range, FL	10,000 gal AST	1,500
Tinker AFB, OK	UST, Site 23	1,200
Seymour-Johnson AFB, NC	BX Service Station	690
Plattsburgh AFB, NY	N/A	529

Installation	Sample Site	Maximum Reported MTBE Conc. (µg/L)
McConnell AFB, KS	N/A	420
Carswell AFB, TX	Base Service Station	330
George AFB, CA	N/A	327
Dover AFB, DE	Tank Farm	260
Chanute AFB, IL	N/A	248
Loring AFB, ME	N/A	190
Williams AFB, AZ	N/A	139
Maxwell AFB, AL	UST	123
Holloman AFB, NM	Military Gasoline Station	120
MA Military Reservation	Residential Wells	73
Patrick AFB, FL	ST-28 Area	59
Keesler AFB, MS	N/A	56
Scott AFB, IL	Military Gasoline Station	56
Charleston AFB, SC	Base Gasoline Station Leak	48.1
Pope AFB, NC	N/A	38
Eglin AFB, FL	Gasoline Dispensing Facility	27.3
Brooks AFB, TX	Fire Protection Training Area	25
Laughlin AFB, TX	Fire Protection Training Area	24
Beale AFB, CA	Test Cell Discharge Area	20.7
Little Rock AFB, AK	Fuel Spill	19
F. E. Warren AFB, WY	Gasoline Spill Site	12.3
Pease AFB, NH	N/A	12
Johnston Island	JP-5 AST	11.4
Offutt AFB, NE	Fire Protection Training Area	11
Tyndall AFB, FL	N/A	9.4
Hickam POL Facility, HI	Fuel Line Leak	2.2
Wurtsmith AFB, MI	Fuel Spill Site	2.1

Installation	Sample Site	Maximum Reported MTBE Conc. (µg/L)
Myrtle Beach AFB, SC	Gasoline Storage Tank	1.4
Hurlburt Field, FL	UST Leak	1.3
McClellan AFB, CA	N/A	1

2.8 DEGRADATION PROCESSES

The purpose of this section is to review processes that have been applied to degrade MTBE. The review will discuss both abiotic and biotic processes and will include descriptions of how process kinetics can be modeled. Applicable kinetic parameters identified in the literature will be summarized in tables later in this section. Additionally, applicable kinetic models relevant to the processes will also be described in detail later in this section.

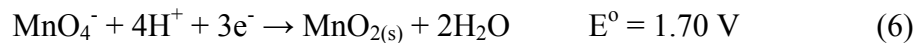
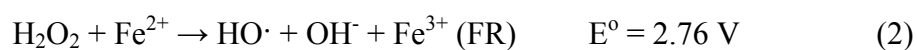
Intended to be comprehensive, this review will include laboratory studies as well as field applications of *in situ* and *ex situ* degradation processes. The material presented in the following sections will be evaluated in Chapter 3.0 for selection of an appropriate degradation process for application in an HFTW system.

2.8.1 ABIOTIC PROCESSES

Abiotic processes that will be discussed in this section include traditional oxidation processes, advanced oxidation processes (AOPs), and hydrolysis. Contaminants such as MTBE have been shown to be directly oxidized using an oxidizing agent or indirectly oxidized via an AOP (Kelley *et al.*, 2003). Several compounds have

been shown capable of directly oxidizing MTBE, to include: ozone (O_3), persulfate ($S_2O_8^{2-}$), hydrogen peroxide (H_2O_2), and permanganate (MnO_4^-). Alternatively, AOPs capable of oxidizing MTBE include: Fenton's Reagent (FR), ozone/hydrogen peroxide, ultraviolet (UV) irradiation, ultrasound (US) irradiation, gamma radiolysis, and dense medium plasma. MTBE has also been demonstrated to degrade via hydrolysis (O'Reilly *et al.*, 2001).

Selection of the proper process to efficiently degrade MTBE as a component of an HFTW *in situ* remediation system depends on several factors. In the case of oxidation processes, the reduction/oxidation potential is a significant factor that may influence oxidant selection. The reduction/oxidation potential is a measure of the tendency of a reaction to proceed in a particular direction. Reduction/oxidation potential is measured in electron volts (E^0). The higher the value for E^0 , the more likely that the reaction will proceed as written. Oxidants that will be discussed are listed below in order of decreasing potential (Kerfoot and LeChaminant, 2003; Kelley *et al.*, 2003):



Although oxidants having a high oxidation potential are more likely to degrade a target compound like MTBE, the oxidant cannot discriminate among other compounds that may also be present, which compete for the oxidant. Therefore, although oxidants

with high oxidation potentials can more easily degrade a target substance, they can also more easily react with and degrade non-target substances, thereby reducing the efficiency of the oxidant. The presence of non-target compounds must thus be compensated for by increasing the oxidant dosage (Safarzadeh-Amiri, 2002). In addition, oxidation of non-target compounds can also result in production of undesirable byproducts (*e.g.* bromide oxidized to bromate) (Kelley *et al.*, 2003). Clearly, the need for higher oxidant dosages (with the associated costs) and the potential for production of hazardous byproducts may rule out the use of certain oxidants or processes for remediation. For these reasons, environmental conditions and the presence of other non-target constituents in the water being treated are important considerations when selecting an oxidizing agent (Kelley *et al.*, 2003). Factors such as alkalinity, pH, natural organic matter and the concentration of interfering compounds may impact the oxidation of MTBE and must be considered when designing an MTBE degradation system (Acero *et al.*, 2001).

Production of intermediates during the degradation of MTBE is another serious concern that will influence selection of any degradation process. The primary intermediates produced during the oxidation and hydrolysis of MTBE have been found to be tert-butyl formate (TBF) and TBA, as indicated in Figure 5 (Kelley *et al.*, 2003). The production of TBA is undesirable due to health concerns, as described in Section 2.5, if it is not subsequently degraded. Additionally, other studies (*e.g.* Barreto *et al.* (1995); Stefan *et al.* (2000); Cooper *et al.* (2003); Kang and Hoffman (1998); Mitani *et al.* (2002)) on oxidants, AOPs, and other abiotic processes have shown that MTBE oxidation results in production of other intermediates, in addition to TBA and TBF, such as acetone, methyl-acetate (MA), formaldehyde, formic acid (FA) and acetic acid.

Ultimately, the production of intermediates may not be problematic as many biological degradation studies (eg. Bradley *et al.* (1999); Bradley *et al.* (2001a); Finneran and Lovely (2001)) have shown that MTBE breakdown products may be easily biodegraded under both anaerobic and aerobic conditions.

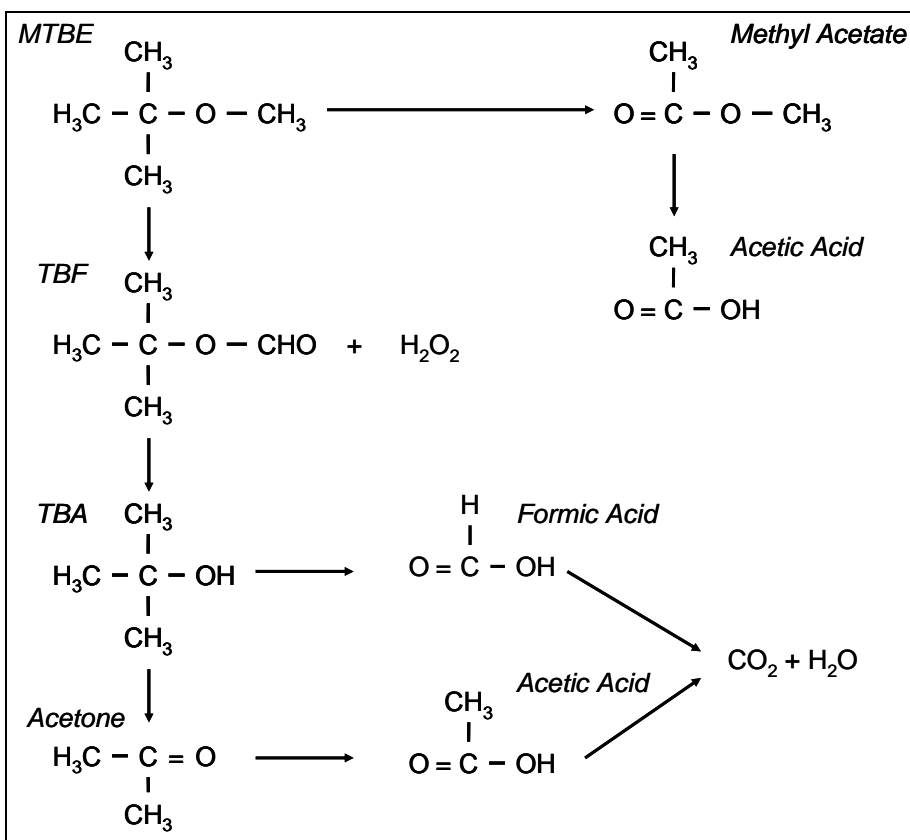


Figure 5 Typical Oxidation Pathway of MTBE by an AOP (After Mitani *et al.* (2002))

2.8.1.1 OXIDATION BY OXYGEN

The oxidation of MTBE by molecular oxygen (O₂) is thermodynamically feasible; however, due to reaction kinetics, molecular oxygen will not spontaneously oxidize

MTBE under normal environmental conditions (Lien and Wilkin, 2002b). Despite the stability of MTBE at normal environmental conditions, Lien and Wilkin (2002a;b) have shown that MTBE can be oxidized by molecular oxygen in the presence of bifunctional aluminum. Bifunctional aluminum is formed by sulfating aluminum with sulfuric acid (Lien and Wilkin, 2002b). The formation of sulfate on the surface of the metal provides sites where electron transfer between aluminum and molecular oxygen can occur (Lien and Wilkin, 2002b). The formation of the reactive reduced form of oxygen ($O\cdot$) is described by Equation 7, below (Lien and Wilkin, 2002a).



$O\cdot$ can oxidize MTBE to TBA, TBF, acetone, and MA (Lien and Wilkin, 2002b); however, the accumulation of TBA may indicate that this process may not be effective at degrading some MTBE intermediates. Alternatively, the reductive sites can also serve to directly reduce other contaminants, thus the bifunctionality of the aluminum (Lien and Wilkin, 2002b).

Lien and Wilkin (2002b) has shown that the degradation of MTBE by bifunctional aluminum follows first-order kinetics. The first-order rate constant (k) for the degradation of MTBE by bifunctional aluminum was found to be $0.31 \times 10^{-4} \text{ s}^{-1}$; this rate constant corresponds to an MTBE half-life of 6.3 hr (Lien and Wilkin, 2002b). Lien and Wilkin (2002b) also demonstrated that the rate constant could be increased by increasing the surface concentration of sulfate on the aluminum. Bifunctional aluminum in the presence of molecular oxygen is capable of degrading MTBE through oxidation and is also capable of degrading other contaminants susceptible to reduction, such as chlorinated solvents (Lien and Wilkin, 2002b). Lien and Wilkin (2002b) suggest that

bifunctional aluminum may potentially be applied to degrade contaminants *in situ* as part of a permeable reactive barrier (PRB) system; although, there is no known documentation that oxidation by oxygen is capable of reducing MTBE concentrations below regulatory requirements and there are no known field implementations of this technology as yet.

2.8.1.2 OXIDATION BY OZONE

Ozonation has gained attention as a treatment process with the potential to oxidize drinking and wastewater contaminants that are difficult or too expensive to remove by conventional technologies (Mitani *et al.*, 2002). Increased availability of ozone at lower costs has spurred more interest in investigating ozone's potential as an oxidant (Mitani *et al.*, 2002). Ozone added to water is capable of degrading MTBE directly or indirectly (Kelley *et al.*, 2003). Ozone, as the oxidant, can directly oxidize MTBE, or the oxidation can occur indirectly, using hydroxyl radicals (OH•) that are produced during ozone decay. Although ozone has a relatively high oxidation potential, studies by Acero *et al.* (2001), Mitani *et al.* (2002), and Liang *et al.* (2001) have shown that whether oxidation by ozone is direct or indirect, reaction kinetics are too slow for drinking water applications; accordingly, ozone alone may not be a good choice for use *in situ* as an oxidant.

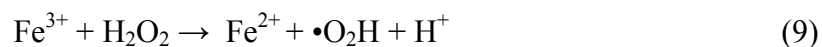
In addition to its slow rate of reaction, ozonation also is problematic because it has been shown to produce bromate as an unwanted by-product if bromide is present in the water being treated (Kelley *et al.*, 2003). The EPA considers bromate a potential carcinogen and has established a maximum contaminant level (MCL) for bromate at 10 µg/L (EPA, 1998). If bromide levels are in the range of <20µg/L in the water, the production of bromate during ozonation should not be significant (Von Gunten, 2003).

However, for concentrations of bromide in the range of 50µg/L to 100µg/L, the production of bromide byproducts may be significant and measures should be taken to minimize bromate production (Von Gunten, 2003). Bromide concentrations in excess of 100µg/L may result in severe bromate production (Von Gunten, 2003). Ultimately, minimization of the production of harmful by-products requires consideration of other compounds in the water being treated and often requires optimization of the process being used (Acero *et al.*, 2001).

A field implementation where ozone has been used to oxidize MTBE is described by Kerfoot and LeCheminant (2003). Ozone microbubble sparging in the saturated and vadose zone was implemented at a fuel storage site in California (Kerfoot and LeCheminant, 2003). MTBE concentrations were reduced 71 to 99%, and in some cases to less than 5 µg/L, over the period of three months. TBA, which was also present, was also degraded at a similar rate (Kerfoot and LeCheminant, 2003).

2.8.1.3 OXIDATION BY FENTON'S REAGENT

Fenton's reagent (FR) is one of the oldest AOPs that have been used to remediate contamination (Li *et al.*, 2003). The simplicity of implementation and the versatility of the FR process make FR an attractive choice as an oxidant (Ray *et al.*, 2002; Li *et al.*, 2003). The Fenton reaction occurs when ferrous iron (Fe^{2+}) oxidizes in the presence of hydrogen peroxide (H_2O_2) to yield ferric iron (Fe^{3+}), hydroxide ion (OH^-) and hydroxyl radical (OH^\bullet) (Li *et al.*, 2003). The ferric iron may subsequently react with the hydrogen peroxide, yielding ferrous iron, hydrogen ion (H^+), and hydroperoxyl radical ($\bullet\text{O}_2\text{H}$) in a cyclic reaction, according to the following equations (Li *et al.*, 2003).



The oxidation of MTBE would subsequently take place due to the presence of the hydroxyl radicals. Regeneration of ferrous iron during the FR process is highly dependent on pH, thus the cyclic nature of the process is also highly dependent on pH (Li *et al.*, 2003). Ferrous iron regeneration is slowed significantly at neutral to alkaline pH due to the precipitation of iron (III) hydroxide ($\text{Fe}^{\text{III}}(\text{OH})_3$ (s)). Yeh and Novak (1995) indicate that the optimal pH for the FR process is between 2 and 3, which may preclude using FR for the *in situ* remediation of contaminated groundwater.

Yeh and Novak (1995) investigated the effects of ferrous iron concentration, hydrogen peroxide concentration, and pH on the degradation of MTBE in solution and in soil/water microcosms. They first demonstrated that hydrogen peroxide by itself is not reactive with MTBE; thus confirming that ferrous iron must also be present to effect the oxidation of MTBE. Additionally, the concentration of the ferrous iron added to the solution did not seem to influence the extent of degradation, rather the extent of degradation was dependent upon the initial hydrogen peroxide concentration (Yeh and Novak, 1995). Increasing the hydrogen peroxide dosage resulted in more MTBE oxidized (Yeh and Novak, 1995). For the same dosage of hydrogen peroxide, however, more MTBE was oxidized in the solution than in the soil/water microcosms (Yeh and Novak, 1995). The reduction in oxidation may be due to competition for the hydrogen peroxide by the organics in the soil or the slower rate of diffusion of hydrogen peroxide at the soil/water interface (Yeh and Novak, 1995). Increased oxidation occurred at lower pH, although there was still significant degradation at pH = 6.5 (Yeh and Novak, 1995).

The primary intermediates identified during the oxidation of MTBE by FR were TBA and acetone (Yeh and Novak, 1995).

A study by Burbano *et al.* (2002) investigated oxidation of MTBE by FR and production of intermediates (TBA, TBF, acetone, and MA) in a batch study. The study was run with a molar ratio of FR to each of the compounds studied (MTBE, TBA, TBF, acetone, MA) of 10:1, a molar ratio of ferrous iron to hydrogen peroxide of 1:1, and pH = 3 (Burbano *et al.*, 2002). In a similar study by Ray *et al.* (2002) the optimal ratio of ferrous iron to hydrogen peroxide was determined to be 1:1 at a pH of 5; curiously, the rate of degradation of MTBE using the 1:1 ratio was faster at a pH of 5 than pH of 3 (Ray *et al.*, 2002). Ray *et al.* (2002) does not offer an explanation for this observation, which is contrary to previous studies (*e.g.* Yeh and Novak, 1995), but only suggest that further study is required.

Burbano *et al.* (2002) suggest a pseudo first-order kinetic rate law for the degradation of MTBE and its degradation products by FR. A pseudo first-order degradation rate constant was found by establishing initial concentrations of compounds according to the molar ratios described previously (10:1 FR to target compound, 1:1 FR to hydrogen peroxide; where, [MTBE] = 2 mg/L, [Fe²⁺] = 12.68 mg/L, and [H₂O₂] = 7.67 mg/L) (Burbano *et al.*, 2002). The pseudo first-order degradation rate constant (k') was found to be $2.9 \times 10^{-2} \text{ s}^{-1}$.

The primary intermediates of MTBE oxidation by FR identified by Burbano *et al.* (2002) included TBF, acetone, TBA, and MA. The only intermediate that showed a continuous build up during the degradation of MTBE was acetone, indicating that the hydroxyl radical oxidized acetone more slowly than it oxidized the other compounds

(Burbano *et al.*, 2002). Formaldehyde and acetic acid were also identified in low concentrations (Burbano *et al.*, 2002).

Additionally, Bergendahl and Thies (2004) have demonstrated the potential for using zero-valent iron (Fe^0) as a source for Fe^{2+} needed for the degradation of MTBE by FR. Experiments performed by Bergendahl and Thies (2004) resulted in approximately 99% degradation of MTBE by FR at molar ratios of Fe^0 to H_2O_2 and H_2O_2 to MTBE of 1.8:1 and 440:1, respectively. Bergendahl and Thies (2004) used a second-order rate law relating the degradation rate of MTBE to the concentration of MTBE and hydroxyl radicals. The second-order degradation rate constants determined for FR in this configuration were $1.9 \times 10^8 \text{ M}^{-1} \text{ s}^{-1}$ at pH of 7 and $4.4 \times 10^8 \text{ M}^{-1} \text{ s}^{-1}$ at pH of 4 (Bergendahl and Thies, 2004). Using regression analysis, Bergendahl and Thies (2004) also found the pseudo first-order degradation rates of MTBE for steady state hydroxyl radical concentrations of approximately $1.19 \times 10^{-2} \text{ s}^{-1}$ and $1.4 \times 10^{-2} \text{ s}^{-1}$ at pH of 7 and 4, respectively. The primary intermediate identified in the study by Bergendahl and Thies (2004) was acetone, which was subsequently degraded.

There are no known field implementations of the FR process for the remediation of MTBE-contaminated groundwater; however, Ray *et al.* (2002) have shown that oxidation by FR can reduce MTBE concentrations to or below the lower limit of the EPA's drinking water advisory of 20 $\mu\text{g/L}$ in laboratory studies.

2.8.1.4 OXIDATION BY PERSULFATE

Oxidation by persulfate ion has demonstrated success in degrading MTBE-contaminated water (Huang *et al.*, 2002). A study conducted by Huang *et al.* (2002) analyzed the kinetics of the degradation of MTBE by persulfate in a buffered

groundwater solution under various temperatures, pH and oxidant concentrations.

Although persulfate has a relatively high oxidation potential (2.01 V), it has had little success being used as an oxidant at ambient temperatures (Huang *et al.*, 2002).

Persulfate is typically used to oxidize substances in the presence of UV or metal catalysts, at elevated temperatures due to increased sulfate radical and hydroxyl radical production under such conditions (Huang *et al.*, 2002). In an earlier study discussed by Huang *et al.* (2002), Dogliotti and Hayon (1967) indicated that oxidation due to the photolysis of persulfate was dominated by the sulfate radical in neutral to acidic solutions (Huang *et al.*, 2002). Alternatively, in the study by Huang *et al.* (2002), oxidation of MTBE was attributed to the hydroxyl radical as indicated by the production of TBA and TBF (Huang *et al.*, 2002).

The kinetics of MTBE oxidation by persulfate have been shown to follow a pseudo first-order model and seem to result from MTBE oxidation dominated by the sulfate radical (Huang *et al.*, 2002). Huang *et al.* (2002) indicate that the pseudo first-order degradation rate constant (k') is proportional to the temperature, concentration of sodium persulfate, and the ionic strength of the water. Values of the rate constant (k') at under various conditions, as measured by Huang *et al.* (2002), are summarized below.

Experiments to determine temperature dependence of the rate constant were conducted in a buffered solution (pH \approx 7) using the same MTBE concentration (5.3-6.2 mg/L) (Huang *et al.*, 2002). The temperature of the buffered solution was varied from 20 to 50 °C in separate experiments (Huang *et al.*, 2002). The results of the experiments indicated a direct relationship between rate constant and temperature; when temperature increased, the rate constant increased (Huang *et al.*, 2002). According to tabulated results

by Huang *et al.* (2002) and shown here in Table 3, the rate constant obtained at 50 °C was approximately 45 times the rate constant obtained at 20 °C.

Table 3 Pseudo First-Order Rate Constants for Persulfate Oxidation of MTBE at Various Temperatures (Adapted from Huang *et al.* (2002))

Temp (°C)	Ionic Strength (M)	C^{MTBE} (mg/L)	$C^{persulfate}$ (mg/L)	pH _{init} /pH _{final}	k' (s ⁻¹)
20	0.11	5.29	5956	6.9/6.8	0.13×10^{-4}
50	0.11	5.29	5956	6.9/6.6	5.8×10^{-4}

Similar experiments were conducted in the buffered solution to determine the dependence on the oxidant concentration (Huang *et al.*, 2002). The concentration of sodium persulfate was varied from 1364 to 10010 mg/L (Huang *et al.*, 2002). Results of the experiment by Huang *et al.* (2002) shown in Table 4 indicates that higher oxidant concentrations resulted in faster MTBE degradation. These results indicate a direct relationship between degradation rate and initial oxidant concentration (Huang *et al.*, 2002).

Table 4 Pseudo First-Order Rate Constants for Persulfate Oxidation of MTBE at Various Persulfate Concentrations (Adapted from Huang *et al.* (2002))

Temp (°C)	Ionic Strength (M)	C^{MTBE} (mg/L)	$C^{persulfate}$ (mg/L)	pH _{init} /pH _{final}	k' (s ⁻¹)
40	0.07-0.15	6.17	1364	7.0/6.9	0.38×10^{-4}
40	0.07-0.15	6.17	10010	6.9/6.9	3.74×10^{-4}

Experiments conducted where pH was varied between 2 and 11 indicated that the degradation rate of MTBE by persulfate oxidation is pH dependent (Huang *et al.*, 2002).

As the pH increased, the rate of reaction decreased, indicating an inverse relationship between pH and rate of reaction. Huang *et al.* (2002) explains that this result was expected and follows the trend indicated by results published by Hayon and McGarvey (1967) where sulfate radicals and hydroxyl radicals quickly decayed in the presence of hydroxyl ions (Huang *et al.*, 2002). The effects of pH on the rate constant are indicated in Table 5.

Table 5 Pseudo First-Order Rate Constants for Persulfate Oxidation of MTBE at Various pH (Adapted from Huang *et al.* (2002))

Temp (°C)	Ionic Strength (M)	C^{MTBE} (mg/L)	$C^{persulfate}$ (mg/L)	pH _{init} /pH _{final}	k' (s ⁻¹)
40	0.11	5.29	6052	2.5/2.4	3.05 x 10 ⁻⁴
40	0.11	5.29	6052	6.8/6.3	2.14 x 10 ⁻⁴

Increased ionic strength of the solution also inhibited the degradation of MTBE as depicted in Table 6 (Huang *et al.*, 2002). Experiments conducted where the ionic strength of the solution was varied from 0.11 to 0.53 M indicated an inverse relationship between reaction rate and ionic strength (Huang *et al.*, 2002). Huang *et al.* (2002) suggests that the reduction in rate is most likely due to the decreased activity of the reacting species with increased ionic strength.

Table 6 Pseudo First-Order Rate Constants for Persulfate Oxidation of MTBE at Various Ionic Strengths (Adapted from Huang *et al.* (2002))

Temp (°C)	Ionic Strength (M)	C^{MTBE} (mg/L)	$C^{persulfate}$ (mg/L)	pH _{init} /pH _{final}	k' (s ⁻¹)
40	0.11	7.05	6052	7 (buffered)	2.94 x 10 ⁻⁴
40	0.53	7.05	6052	7 (buffered)	1.48 x 10 ⁻⁴

In a duplicate experiment, the degradation of MTBE was shown to be significantly inhibited when heated groundwater, rather than a buffered solution, was used (Huang *et al.*, 2002). Properties of the groundwater, as reported by Huang *et al.* (2002), were temperature of 40 °C, pH of 8.2, total alkalinity of 314 mg/L as CaCO₃, and total organic carbon (TOC) of 2.3 mg/L. Huang *et al.* (2002) suggest that the inhibition is a result of the presence of bicarbonate ions. Also, the pH of the solution decreased significantly from the starting pH value. Over the course of 30 hours, the pH of the solution dropped from 8.2 to 3.2 (Huang *et al.*, 2002). As indicated by the degradation pathway suggested by Huang *et al.* (2002), and depicted previously in Figure 5, the decrease in pH may be a result of the first step of MTBE degradation where a hydrogen abstraction takes place on the methoxyl group (Huang *et al.*, 2002).

The oxidation of MTBE by persulfate produced the intermediates TBA, TBF, acetone, and methyl acetate, which were subsequently oxidized as well (Huang *et al.*, 2002). Acetone had the highest concentration and longest persistence of all the intermediates (Huang *et al.*, 2002). The results of the intermediate analysis and mass balance suggest that TBA, TBF, and acetone are the primary intermediates formed by persulfate oxidation of MTBE (Huang *et al.*, 2002).

As demonstrated by the experiments with groundwater, the application of persulfate for the remediation of MTBE-contaminated groundwater may be limited by the water temperature, pH, ionic strength, and alkalinity of natural waters, as well as by production of intermediates (Huang *et al.*, 2002). The advantages of using persulfate are that persulfate is more stable in the subsurface than other oxidants and it is very soluble in water, thereby decreasing the difficulties of transporting it to contaminated zones for

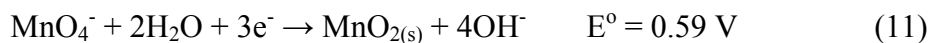
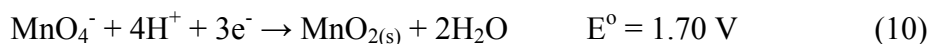
use as part of an *in situ* remediation process (Huang *et al.*, 2002). Despite these potential advantages, however, there is no known evidence to show that oxidation by persulfate can reduce MTBE concentrations to or below regulatory levels and there are no known field implementations of MTBE oxidation by persulfate (Kelley *et al.*, 2003).

2.8.1.5 OXIDATION BY PERMANGANATE

Studies have shown that permanganate (MnO_4^-) is capable of effectively oxidizing several types of contaminants to include chlorinated ethenes and ethanes (Clayton *et al.*, 2000). The potential of permanganate to oxidize MTBE has been the subject of several studies including Clayton *et al.* (2000), Oberle and Schroder (2000), and Damm *et al.* (2002). These studies showed that the effectiveness of permanganate as an MTBE oxidant varies. Reported by Damm *et al.* (2002), studies conducted by Oberle and Schroder (2000) indicate no degradation of MTBE in a 24-hour period. Alternatively, the study conducted by Clayton *et al.* (2000) showed that MTBE can be degraded 99.9% when permanganate was applied *in situ*; however, TBA produced during the oxidation of MTBE was not oxidized in the presence of permanganate (Clayton *et al.*, 2000).

Oxidation by permanganate can occur through several processes. The potential processes of oxidation by permanganate include hydrogen atom abstraction, electron exchange, and/or oxygen donation (Walton *et al.*, 1991). For more information on these processes as they relate to a particular type of target compound the reader is directed to Walton *et al.* (1991). The number of electrons involved (*i.e.* one, three, or five) and hence oxidation potential of the reaction is highly dependent on the pH of the solution. For pH in the range of 3.5 to 11, three electrons will be accepted by permanganate to form manganese dioxide according to Equations 10 and 11, below (Walton *et al.*, 1991).

Equation 10 is applicable to acidic pH conditions and Equation 11 is applicable to alkaline pH conditions (Walton *et al.*, 1991).



The study by Damm *et al.* (2002) investigated the kinetics of the oxidation of MTBE by permanganate through a series of laboratory batch experiments where MTBE concentrations varied from 23.9 to 238.8 mg/L and permanganate concentrations were varied between 1.1, 3.8, and 7.5 g/L. The kinetics of the reaction were found to be described by a second-order rate law. The overall second-order degradation rate constant, k , was determined to be $3.96 \times 10^{-10} \text{ L mg}^{-1} \text{ s}^{-1}$ (Damm *et al.*, 2002). Additional experiments were conducted to determine the effect of pH on the reaction rate. Ultimately it was determined that pH has little effect on the rate of reaction and does not require adjustment (Damm *et al.*, 2002). The oxidation of MTBE by permanganate also yields the common intermediates of TBA and TBF (Damm *et al.*, 2002). The accumulation of TBA and TBF during the study showed that MTBE did not completely oxidize to carbon dioxide (Damm *et al.*, 2002).

The half-lives of the reactants in the experiment by Damm *et al.* (2002) varied from 55 to 495 hours, which is longer than the half-lives when other oxidants are used to oxidize MTBE (Damm *et al.*, 2002). The slow kinetics combined with the apparent inability of permanganate to oxidize TBA severely limits its use as an oxidant for *in situ* MTBE remediation.

Clayton *et al.* (2000) present results from a multi-site evaluation of *in situ* chemical oxidation processes using permanganate to degrade various contaminants.

Degradation of 99% was reported for both low and high concentrations of MTBE (Clayton *et al.*, 2000). Unfortunately, no other information about conditions, kinetics, or results of the study was provided (Clayton *et al.*, 2000).

2.8.1.6 OXIDATION BY OZONE AND HYDROGEN PEROXIDE

The effectiveness of the ozone/hydrogen peroxide couple to oxidize MTBE has been the subject of several studies (*e.g.* Vel Leitner *et al.*, 1994, Acero *et al.*, 2001, Liang *et al.*, 2001, Mitani *et al.*, 2002, and Safarzadeh-Amiri, 2001; 2002). The addition of hydrogen peroxide increases the rate of ozone decay, thus increasing the rate of production of the hydroxyl radical (Acero *et al.*, 2001). Not only does the addition of hydrogen peroxide accelerate the production of hydroxyl radicals, it also helps minimize the production of bromate, which was noted earlier in the discussion of ozone as an oxidant to be a problem (Acero *et al.*, 2001; Mitani *et al.*, 2002, Liang *et al.*, 2001).

The degradation of MTBE by ozone and hydrogen peroxide has been modeled using second-order kinetics (Hoigne, 1998; Acero *et al.*, 200; Liang *et al.*, 2001; Mitani *et al.*, 2002; Safarzadeh-Amiri, 2001). The following rate equation describes the second order reaction,

$$\frac{d[MTBE]}{dt} = -k_{\bullet OH / MTBE} [MTBE][\bullet OH] \quad (12)$$

The rate equation states that the change in concentration of MTBE is proportional to the concentration of MTBE ($[MTBE]$) and the concentration of hydroxyl radical ($[\bullet OH]$).

Second order rate constants for the degradation of MTBE in the presence of the hydroxyl radical are presented by Buxton *et al.* (1988) and Mitani *et al.* (2002): $k_{\bullet OH / MTBE} = 1.6 \times 10^9 \text{ M}^{-1} \text{ s}^{-1}$ and $k_{\bullet OH / MTBE} = 1.2 \times 10^9 \text{ M}^{-1} \text{ s}^{-1}$, respectively.

Safarzadeh-Amiri (2001) proposed that the degradation of MTBE can be modeled in two stages by pseudo first-order kinetics (Safarzadeh-Amiri, 2001). For concentrations of MTBE above 10 mg/L, the rate of MTBE degradation is limited by the mass transfer of ozone; however, at MTBE concentrations below 10 mg/L the degradation is not mass transfer limited (Safarzadeh-Amiri, 2001). Although Safarzadeh-Amiri (2001) presents different pseudo first-order rate constants at different ozone flow rates, hence different ozone concentrations, the author does not describe all relevant experimental parameters, particularly the concentrations of MTBE.

The effect of the presence of carbonates on the MTBE degradation rate by the O_3/H_2O_2 process was investigated by Vel Leitner *et al.* (1994). Bicarbonate ions added to the solution resulted in no impact on the degradation rate of MTBE (Vel Leitner *et al.*, 1994), indicating that carbonate alkalinity of groundwater may not affect the degradation of MTBE using the O_3/H_2O_2 process. Acero *et al.* (2001) demonstrated how the production of bromate during the AOP can be controlled by altering the ozone dose with respect to the hydrogen peroxide dose, and pH. Higher pH ultimately yields less bromate though high pH also slows degradation of MTBE. Optimizing the ozone dose with relation to interfering groundwater constituents is critical to achieving low bromate production (Acero, *et al.*, 2001).

The primary intermediates identified during the degradation of MTBE by ozone/hydrogen peroxide include TBA, TBF, acetone, and MA (Liang *et al.*, 2001; Mitani *et al.*, 2002; Vel Leitner *et al.*, 1994; Safarzadeh-Amiri *et al.*, 2001). Intermediates that are formed only are oxidized after a significant amount of MTBE has been degraded (Acero *et al.*, 2001). Although the intermediates are oxidized by the AOP, the rates of oxidation

are an order-of-magnitude smaller than the rate of MTBE degradation, so there is intermediate build-up (Acero *et al.*, 2001).

Safarzadeh-Amiri (2001) presents a unique cost comparison technique that quantifies the cost of operating the ozone/hydrogen peroxide AOP by using an efficiency index. The efficiency index for this AOP is proportional to the energy (kWh) required, bulk material costs (*i.e.* hydrogen peroxide), and the number of orders of magnitude of concentration reduction desired (Safarzadeh-Amiri, 2001). The treatment cost to reduce MTBE concentration from 10 to 0.01 mg/L (3 orders of magnitude), using 120 mg/L ozone and 10 mg/L hydrogen peroxide, where electricity costs are \$0.06/kWh and 1 kg of 100% hydrogen peroxide costs \$1.50, was shown to be approximately \$0.18 per m³ of water treated.

Lory (2003) describes the ozone/hydrogen peroxide treatment technique that is currently being implemented at Port Hueneme National Environmental Technology Test Site (NETTS). The so-called HiPOx (ozone/hydrogen peroxide AOP) being used is an *ex situ* technology using a pump-and-treat system (Lory, 2003). MTBE-contaminated groundwater is extracted at a rate of 19 L/min (5 gpm) (Lory, 2003). The contaminated water is then passed through 18 reactors in series where ozone and hydrogen peroxide are injected. Results of this study, which are summarized in an EPA report, show that the application of this technology was not successful under the test conditions (EPA, 2002). MTBE concentrations were reduced to or below the regulatory limit of 5 µg/L; however, resultant TBA and bromate concentrations exceeded regulatory limits (EPA, 2002).

2.8.1.7 OXIDATION BY UV IRRADIATION

Degradation of MTBE by UV irradiation has been the subject of many studies (*e.g.* Barreto *et al.*, 1995; Chang and Young, 2000; Cater *et al.*, 2000; O'Shea *et al.*, 2002b; Stefan *et al.*, 2000). In particular, there are two main processes for MTBE destruction by UV; one process uses UV to oxidize the MTBE in the presence of a titanium dioxide catalyst (TiO₂, titania) (Barreto *et al.*, 1995; O'Shea *et al.*, 2002b) and the other process is in the absence of a catalyst (Cater *et al.*, 2000; Chang and Young, 2000; Stefan *et al.*, 2002). The oxidation of pollutants by UV irradiation without titania catalyst is typically accomplished by amending the water with hydrogen peroxide (Cater *et al.*, 2000; Chang and Young, 2000; Stefan *et al.*, 2002). Irradiation by UV light in the optimal wavelength range of 200-280 nm with hydrogen peroxide present results in the excitation of the hydrogen peroxide to form hydroxyl radicals (Cater *et al.*, 2000; Chang and Young, 2000). The oxidation of pollutants by UV irradiation in the presence of a titania catalyst slurry is the result of the activation of the catalyst producing superoxide anion radicals (O₂^{-•}) (in the presence of oxygen) and reductive sites where water or hydrogen peroxide is reduced to form hydroxyl radicals (Barreto *et al.*, 1995; O'Shea *et al.*, 2002b).

Both studies by Cater *et al.* (2000) and Chang and Young (2000) indicate that the degradation of MTBE in the presence of hydrogen peroxide and UV can be modeled as a pseudo first-order reaction (Cater *et al.*, 2000; Chang and Young, 2000). Additionally, the degradation rate of MTBE increased with increased initial concentration of hydrogen peroxide up to 100 mg/L hydrogen peroxide; above 100 mg/L hydrogen peroxide, the rate of MTBE degradation decreased indicating that the excess hydrogen peroxide

competed for the hydroxyl radicals (Cater *et al.*, 2000). The presence of BTEX compounds in concentrations over 2 mg/L also impeded the degradation of MTBE (Cater *et al.*, 2000). Optimal pseudo first-order rate constants (k') obtained in these studies were $2.17 \times 10^{-3} \text{ s}^{-1}$ for a molar ratio of hydrogen peroxide to MTBE of 15:1 (Chang and Young, 2000) and $1.18 \times 10^{-1} \text{ s}^{-1}$ for concentrations of hydrogen peroxide and MTBE of 30 mg/L and 0.08 mg/L, respectively at or near neutral pH (Cater *et al.*, 2000). Both studies identified the primary intermediates of TBA, TBF, acetone, and MA (Stefan *et al.*, 2000; Chang and Young, 2000). Chang and Young (2000) identified TBF as the most persistent and abundant intermediate produced; however, Stefan *et al.* (2000) (in a companion paper to Cater *et al.* (2000)) indicated that acetone is the most abundant and persistent intermediate produced during UV irradiation of MTBE with hydrogen peroxide. Detailed intermediate production information and degradation pathways can be found in Stefan *et al.* (2000).

Barreto *et al.* (1995) showed that the degradation of MTBE in the presence of a titania slurry also occurred according to pseudo first-order kinetics (Barreto *et al.*, 1995). The pseudo first-order degradation rate constant (k') found $1.2 \times 10^{-3} \text{ s}^{-1}$ (Barreto *et al.*, 1995). The experiment was begun at or near neutral pH (pH \approx 6.8) but pH decreased over the duration of the experiment to approximately 4.2 (Barreto *et al.*, 1995). The primary intermediates identified include TBA and TBF; however, both were shown to be degraded photocatalytically (Barreto *et al.*, 1995). O'Shea *et al.* (2002b) also showed that the degradation of MTBE by UV in the presence of titania can be modeled using first-order kinetics. A rate constant of $k = 0.16 \text{ min}^{-1}$ was measured (O'Shea *et al.*, 2002b). Additionally, O'Shea *et al.* (2002b) applied the Langmuir-Hinshelwood (L-H) kinetic

model to describe the relationship between degradation rate and the initial concentration of MTBE. The L-H kinetic model is used extensively to describe photocatalytic reactions and for more detail on the L-H kinetic model, the reader is directed to O'Shea *et al.* (2002b). The relationship can be useful as a tool to assist in predicting degradation rates of MTBE at various concentrations (O'Shea *et al.*, 2002b). The typical intermediates produced (*i.e.* TBA, TBF, acetone, and MA), as well as isobutylene, formaldehyde, and methane were identified during this study (O'Shea *et al.*, 2002b).

Safarzadeh-Amiri (2001) estimated the cost of UV degradation of MTBE using an efficiency factor. The treatment cost to reduce MTBE concentrations from 10 to 0.01 mg/L (3 orders of magnitude) using the UV/hydrogen peroxide system was shown to be approximately \$0.30 per m³ of water treated.

The author is unaware of any field implementations of this technology.

2.8.1.8 OXIDATION BY ULTRASOUND IRRADIATION

Ultrasound (US) irradiation in the medium frequency ultrasound range (300-1000 kHz) is used for thermo-chemical reactions (Ince *et al.*, 2001). The AOP principle of US irradiation is based on the development, growth, and violent collapse of microbubbles (Ince *et al.*, 2001). The continuous ultrasonic compression and rarefaction cycles, or vibrations, applied to water result in the production of microbubbles (Ince *et al.*, 2001). Dependent on the intensity of the applied vibrations, the microbubbles grow in diameter (Ince *et al.*, 2001). Upon reaching a critical or resonant diameter, the microbubbles violently implode (Ince *et al.*, 2001). This implosion results in superheating of the water vapor inside the bubbles to temperatures as high as 5000 °K and pressures up to 500 atm (Ince *et al.*, 2001). The extreme temperature and pressure results in the direct pyrolytic

destruction of contaminants within the microbubbles or indirect destruction through reaction with byproducts produced during the dissociation of water (hydroxyl radicals, hydrogen radicals, and hydrogen peroxide from recombination) (Ince *et al.*, 2001).

Ince *et al.* (2001) go on to explain how sonolysis can be optimized by deliberately controlling the relevant parameters of the system. Frequency and intensity of the sonolysis, as well as physical dimensions of the reactor are important parameters that can be optimized to maximize contaminant destruction (Ince *et al.*, 2001). These are explored in a study by Kang *et al.* (1999). Intensity of the sonolysis is a function of the acoustic amplitude (energy per unit area per time), fluid density, and the velocity of sound in the fluid. Additionally, the intensity of degradation can be optimized by constantly bubbling a gas through the liquid during sonolysis (Ince *et al.*, 2001).

Although ultrasound irradiation alone is capable of degrading MTBE, amending water with ozone during sonolysis has been shown to accelerate the degradation process (Kang and Hoffman, 1998). The presence of ozone during sonolysis increases the production of the hydroxyl radical, which in turn oxidizes MTBE (Kang and Hoffman, 1998). The destruction of MTBE by ultrasound irradiation in the presence of ozone can be described by a pseudo first-order rate law. The effects of varying ozone, oxygen, and/or MTBE concentrations, during ultrasound at a constant intensity, were investigated by Kang and Hoffman (1998). A later study by Kang *et al.* (1999) investigated the optimization of ozone concentration, hydrogen peroxide production, frequency, and power density (Kang *et al.*, 1999). Relevant results of both studies are summarized in Table 7.

Table 7 Pseudo First-Order Rate Constants for Ultrasound Oxidation of MTBE Under Various Conditions (Adapted from Kang and Hoffman (1998) and Kang *et al.* (1999))

Condition (US=ultrasound)	[MTBE] (mg/L)	[O ₃] or [O ₂] (mg/L)	Power Density (W L ⁻¹)	Frequency (kHz)	<i>k'</i> (s ⁻¹)
US	0.88	N/A	200	205	8.5 x 10 ⁻⁴
US	4.41	N/A	200	205	8.7 x 10 ⁻⁴
US	88.15	N/A	200	205	4.1 x 10 ⁻⁴
US + O ₃	0.88	14.4	200	205	33.2 x 10 ⁻⁴
US + O ₃	4.41	14.88	200	205	31.3 x 10 ⁻⁴
US + O ₃	88.15	12.48	200	205	6.3 x 10 ⁻⁴
US + O ₂	4.41	8.0	200	205	8.7 x 10 ⁻⁴
O ₂ w/o US	61.71	8.0	N/A	N/A	Negligible
O ₃ w/o US	27.33	12.0	N/A	N/A	0.6 x 10 ⁻⁴
US	0.88	N/A	200	358	16.5 x 10 ⁻⁴
US	88.15	N/A	200	358	6.8 x 10 ⁻⁴
US + O ₃	0.88	9.6	200	358	88.3 x 10 ⁻⁴
US + O ₃	88.15	11.04	200	358	12.3 x 10 ⁻⁴

Observations from the study by Kang and Hoffmann (1998) suggest that there are several factors that contribute to the rate of MTBE degradation. Clearly, the effects of ozone alone, oxygen alone, and amending the water with oxygen during sonolysis are negligible when compared to the rates of degradation achieved by the addition of ozone in combination with sonolysis. Additionally, the rate of degradation of MTBE decreased with increasing MTBE concentration indicating that the pseudo first-order rate constant is a function of the initial concentration of MTBE (Kang and Hoffmann, 1998).

The optimization study by Kang *et al.* (1999) found that the optimal frequency for sonolysis occurs at 358 kHz at a power density of 100 W L⁻¹ (Kang *et al.*, 1999). At

frequencies above 358 kHz, the vibration cycles are too short to permit growth of the microbubbles to sizes necessary to cause significant implosion effects (Kang *et al.*, 1999). The effects of power density were investigated by measuring the production of hydrogen peroxide, as hydrogen peroxide production is attributed to the production and recombination of hydroxyl radicals (Kang *et al.*, 1999). Optimal power density for the production of hydrogen peroxide was determined at 240 W L^{-1} (Kang *et al.*, 1999). At power densities above 240 W L^{-1} , hydrogen peroxide production is inhibited by the scavenging effect of the hydroxyl radical on the accumulating hydrogen peroxide (Kang *et al.*, 1999). No rate constants for the degradation of MTBE were presented by Kang *et al.* (1999) at power density of 240 W L^{-1} . Additionally, Kang *et al.* (1999) investigated the influence of TOC on the degradation rate of MTBE and concluded that the presence of organic competitors for the hydroxyl radical did not significantly impact the degradation of MTBE (Kang *et al.*, 1999). Kang *et al.* (1999) suggest that the results of their investigation confirm that the degradation of MTBE occurs in the vapor phase interface with the surrounding liquid and not in the bulk fluid (Kang and Hoffman, 1998; Kang *et al.*, 1999).

The primary degradation products detected during the sonolysis and ozonolysis of MTBE were found to be TBA, TBF, MA and acetone (Kang and Hoffmann, 1998). The first intermediate produced was TBF, which was subsequently degraded after 40 minutes of continuous sonolysis (Kang and Hoffmann, 1998). MA and acetone were also produced and completely removed after 60 minutes of continuous sonolysis (Kang and Hoffman, 1998). The production of innocuous end products and readily biodegradable TBA is evidence of the effectiveness of MTBE degradation by sonolysis in the presence

of ozone, although there are no known field implementations of this technology (Kang and Hoffman, 1998).

A later study by Neppolian *et al.* (2002) investigated the effect of sand, power density, temperature, persulfate ion, and Fenton's reagent (FR) on the degradation rate of MTBE in the presence of US irradiation. Although similar to the Kang and Hoffman (1998) and Kang *et al.* (1999) studies, this study used a sonicator operating at 20 kHz, which is categorized as low frequency ultrasound (Ince *et al.*, 2001). Neppolian *et al.* (2002) suggest that treatment of MTBE-contaminated groundwater may occur in the presence of sand, dictating investigation of the impact of sand on the rate of MTBE degradation. Comparison of rate constants with and without sand present indicates that the impact of sand on the degradation rate of MTBE by US irradiation is insignificant (Neppolian *et al.*, 2002). In agreement with Kang and Hoffmann (1998) and Kang *et al.* (1999), results of the study by Neppolian *et al.* (2002) suggest that MTBE degradation rate increases with increasing power density. Similar to power density, temperature also directly impacted the degradation rate of MTBE (Neppolian *et al.*, 2002). As temperature of the water was increased, the rate of MTBE degradation by US alone increased, suggesting that more MTBE was vaporized into the microbubbles where it underwent pyrolytic destruction (Neppolian *et al.*, 2002).

The addition of persulfate ion and FR exhibited similar results. Persulfate salt (potassium persulfate) was added to MTBE-spiked water at 25 °C and then exposed to US irradiation (Neppolian *et al.*, 2002). The optimal persulfate concentration was determined to be 1920 mg/L (Neppolian *et al.*, 2002). Neppolian *et al.* (2002) suggest that persulfate concentrations above 1920 mg/L result in sulfate radical interaction rather

than sulfate radical-MTBE destruction (Neppolian *et al.*, 2002). Similar behavior has also been observed for other AOPs. The rate constants obtained in the study of Neppolian *et al.* (2002) for US destruction of MTBE in the presence of persulfate under various conditions are summarized in Table 8.

Table 8 Pseudo First-Order Rate Constants for Ultrasound Oxidation of MTBE Under Various Conditions (pH = 5.8, Temperature = 25°C) (Adapted from Neppolian *et al.* (2002)).

Condition (US=ultrasound)	[MTBE] (mg/L)	[S ₂ O ₈ ²⁻] (mg/L)	Power Density (W L ⁻¹)	Frequency (kHz)	<i>k'</i> (s ⁻¹)
US	2.47	N/A	N/A	20	1.27 x 10 ⁻⁴
US	5.02	N/A	N/A	20	1.12 x 10 ⁻⁴
US	9.96	N/A	N/A	20	0.88 x 10 ⁻⁴
US	25.03	N/A	N/A	20	0.79 x 10 ⁻⁴
US + S ₂ O ₈ ²⁻	2.47	1921.2	N/A	20	6.30 x 10 ⁻⁴
US + S ₂ O ₈ ²⁻	5.02	1921.2	N/A	20	2.02 x 10 ⁻⁴
US + S ₂ O ₈ ²⁻	9.96	1921.2	N/A	20	1.56 x 10 ⁻⁴
US + S ₂ O ₈ ²⁻	25.03	1921.2	N/A	20	1.25 x 10 ⁻⁴

Neppolian *et al.* (2002) also showed that the FR process in the presence of US irradiation increased the degradation rate of MTBE (Neppolian *et al.*, 2002). The concentration of Fe²⁺ ion was varied from 0.008 to 0.06 mg/L while the concentration of H₂O₂ was held constant at 17.0 mg/L (Neppolian *et al.*, 2002). The rate of degradation of 25 mg/L MTBE by US was increased by the presence of ferrous iron, which indicates that the coupled FR/US process can increase the degradation rate of MTBE relative to rates achieved using US alone (Neppolian *et al.*, 2002).

The primary intermediates identified by Neppolian *et al.* (2002) include TBF and acetone (Neppolian *et al.*, 2002). The degradation of the intermediates was shown to be

dependent on the presence or absence of oxidant in the US process (Neppolian *et al.*, 2002). Less than 50% degradation of TBF and acetone was achieved for US alone, whereas 80 and 95% degradation was achieved for the persulfate/US and FR/US processes respectively, after 5 hours of US irradiation (Neppolian *et al.*, 2002). The ability of the FR/US process to degrade MTBE and its intermediates to innocuous and biodegradable end products indicates the potential viability of this process for use in the remediation of MTBE-contaminated groundwater; however, the residence time required for complete degradation of MTBE and its intermediates may preclude it from use in an HFTW system. Furthermore, the author is unaware of any field implementations of this technology.

2.8.1.9 OXIDATION BY GAMMA IRRADIATION

The viability of gamma irradiation as an MTBE remediation technology has been the subject of several studies (*e.g.* Cooper *et al.* (2003), Mezyk *et al.* (2001), O'Shea *et al.* (2002a), and Wu *et al.* (2002)). In gamma irradiation, electrons are fired into contaminated water using an electron accelerator (Lory, 2003). The electrons excite the water molecules which then form both hydrogen radicals (reductant) and hydroxyl radicals (oxidant) (Lory, 2003). The electron beam is a unique AOP in that both reducing and oxidizing species are created during the process (Lory, 2003). The hydroxyl radicals degrade the MTBE by hydrogen abstraction to form the primary intermediates of TBA and TBF (Wu *et al.*, 2002). A study by O'Shea *et al.* (2002a) demonstrated that the presence of BTEX compounds along with MTBE significantly retards the degradation of MTBE due to competition for the hydroxyl radical by BTEX.

Kinetic rate laws and constants for the gamma radiolysis of MTBE are discussed by O'Shea *et al.* (2002a). MAKSIMA-CHEMIST, a modeling program developed by Carver *et al.* (1979), was used to simulate MTBE destruction kinetics (O'Shea *et al.*, 2002a). Although no kinetic rate law was explicitly stated, the rate constant used in the model that most closely resembled the measured data was dependent on the number 'N' of contaminant species (*i.e.* MTBE and/or BTEX) present in the solution (O'Shea *et al.*, 2002a). The rate constant was determined to be, $k = 5.0 \times 10^9 \text{ N M}^{-1} \text{ s}^{-1}$, where 'N' is the number of groups of species (O'Shea *et al.*, 2002a). The reader is directed to O'Shea *et al.* (2002a) for more details on the kinetic rate law used in this study.

A field demonstration of the electron beam technology at the Port Hueneme National Technology and Test Site (NETTS) is described by Lory (2003). The electron beam process successfully degraded MTBE at concentrations of 1,400 and 1,640 µg/L to concentrations between 1 and 1.6 µg/L (Lory, 2003). The field demonstration of the technology was conducted above ground as part of a pump-and-treat system; the electron beam, pumps, tanks, and control system all co-located within a mobile 48-foot trailer (Lory, 2003).

2.8.1.10 OXIDATION BY DENSE MEDIUM PLASMA

Johnson *et al.* (2003) used a dense medium plasma (DMP) reactor to successfully degrade MTBE in water. In the DMP discharge process, a plasma field is generated where target organic compounds are dissociated to their atomic constituents while simultaneously reactive species such as hydroxyl radical, hydrogen peroxide, and oxide radical are produced that subsequently react with the target species (Johnson *et al.*, 2003). The degradation of MTBE in the DMP reactor was shown to occur through both of these

processes (Johnson *et al.*, 2003). The kinetics of the degradation of MTBE were shown to follow a pseudo first-order rate law. Degradation of MTBE by the DMP reactor produced the primary intermediates common to most, if not all, AOPs including acetone, TBF, and formaldehyde. More information about the DMP reactor and its operation can be found in Johnson *et al.* (2003).

2.8.1.11 HYDROLYSIS

Ethers such as MTBE are susceptible to cleavage by strong acids at very low pH (pH = 1) (O'Reilly *et al.*, 2001). Due to the highly acidic conditions required to achieve degradation of MTBE, hydrolysis has been discounted as a viable process for remediating MTBE (O'Reilly *et al.*, 2001). Through batch studies, O'Reilly *et al.* (2001) determined that hydrolysis of MTBE occurs between the pH ranges of 1 to 3; however, hydrolysis does not occur or is extremely slow at pH above 3. The results of this study indicate that hydrolysis of MTBE at environmental conditions is not possible. At neutral pH, the half-life of MTBE would be on the order of thousands of years (O'Reilly *et al.*, 2001).

Since acid hydrolysis is effective at low pH, the potential use of acidic ion-exchange resins was also investigated by O'Reilly *et al.* (2001). During the batch study, a second-order rate constant was derived; however, the rate of MTBE degradation was still too slow even for above ground application as part of a pump-and-treat system (O'Reilly *et al.*, 2001). Degradation rates would dictate residence times over six days to achieve 99% reduction of MTBE (O'Reilly *et al.*, 2001). O'Reilly *et al.* (2001) propose that the rate of degradation of MTBE via an acidic ion-exchange process is limited by the rate of adsorption of MTBE to the resin material. According to O'Reilly *et al.* (2001),

there are currently no resins capable of adsorbing MTBE sufficiently to make acidic ion-exchange a viable process.

Centi and Perathoner (2003) and Centi *et al.* (2002) investigated the potential use of acid zeolites to catalyze the acid hydrolysis of MTBE at environmental pHs. The investigators looked at several different commercially available zeolites for potential use as part of an *in situ* remediation process such as a PRB. Of the zeolites examined, only those with suitable surface characteristics were effective in hydrolyzing MTBE (Centi and Perathoner, 2003). The effectiveness of MTBE hydrolysis was a function of the ability of MTBE molecules to diffuse into the pore structure of the zeolites (Centi *et al.*, 2002). The zeolites acted as adsorbent for MTBE and the degradation products, TBA and methanol (Centi *et al.*, 2002). Following the hydrolysis of MTBE, TBA and methanol were slowly released from the zeolites (Centi *et al.*, 2002). Since TBA and methanol are easily biodegraded, the slow release of TBA and methanol may be beneficial to their biodegradation (Bradley *et al.*, 1999; Centi *et al.*, 2002). No kinetic models or rate constants were presented by Centi and Perathoner (2003) or Centi *et al.* (2002); however, relatively slow rates of reaction are indicated by the experimental data presented by Centi *et al.* (2002). The degradation of 2000 mg/L of MTBE to approximately 300 mg/L at 22°C occurred over 160 hrs in both un-stirred and stirred batch reactors (Centi *et al.*, 2002).

Although several laboratory studies have been conducted analyzing the hydrolysis of MTBE, to this date there are no known field implementations of this process.

2.8.2 BIOTIC PROCESSES

Early biological degradation studies done on MTBE indicated little or no degradation and very low to negligible cellular yields; consequently many considered MTBE recalcitrant to biological degradation processes. Since the publication of these studies, more recent studies have shown that MTBE is in fact susceptible to biological degradation by pure and mixed cultures as well as at least one species of fungus. Bradley *et al.* (2001c) reported that naturally occurring bacterial colonies found in streambed and lakebed sediments obtained throughout the U.S. readily mineralized MTBE under aerobic conditions. The extent of the mineralization was found to be inversely proportional to the grain size distribution and independent of the history of exposure to MTBE. Results of a study by Landmeyer *et al.* (2001) demonstrated the intrinsic capability of native microorganisms to degrade MTBE simply by providing oxygen to the groundwater. Many studies including Bradley *et al.* (1999), Bradley *et al.* (2001c), Kane *et al.* (2001), Landmeyer *et al.* (2001), Moreels *et al.* (2002) and Hristova *et al.* (2003) reveal the intrinsic capability of naturally occurring bacteria to mineralize MTBE.

The primary breakdown products of MTBE have been identified as TBF and TBA; however, other intermediates such as 2-methyl-2-hydroxy-1-propanol (MHP) and 2-hydroxyisobutyric acid (HIBA) have also been identified (Deeb *et al.*, 2000). For reference, a generalized pathway that describes the aerobic degradation of MTBE including its breakdown products is presented in Figure 6.

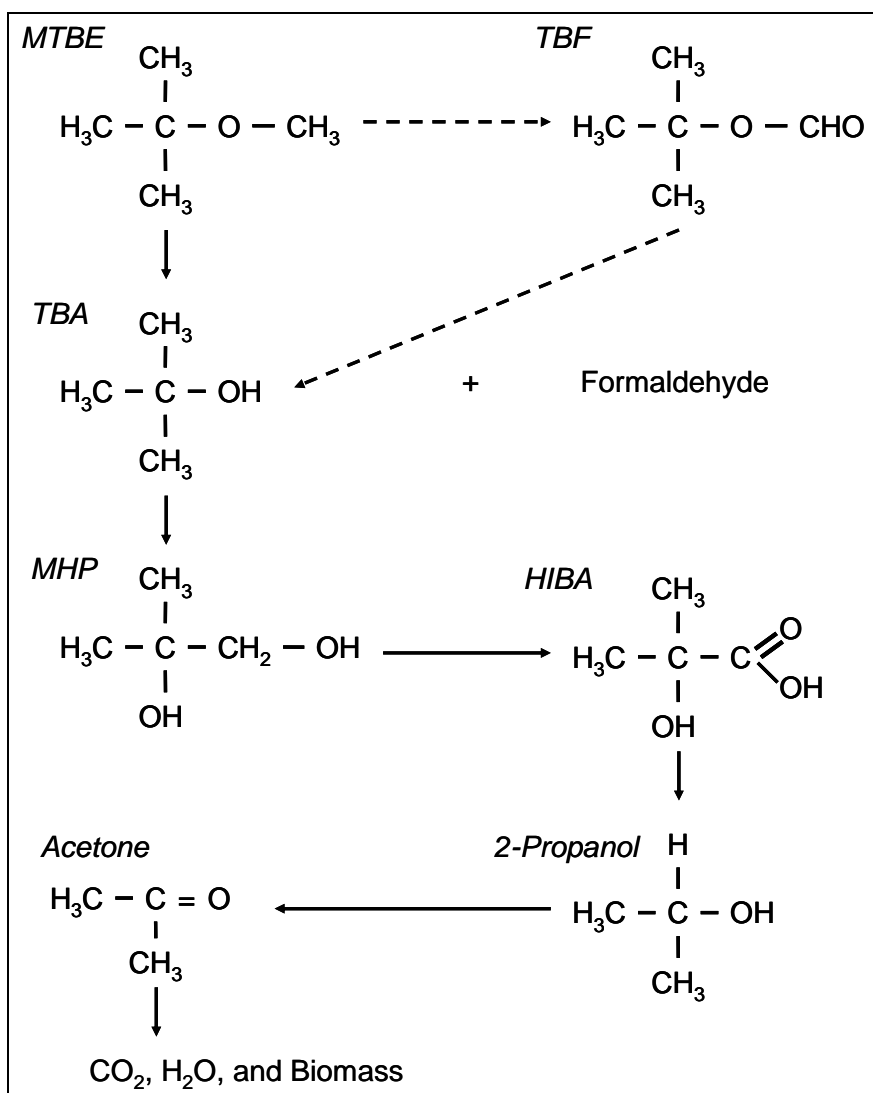


Figure 6 Generalized Pathway of MTBE Biodegradation Under Aerobic Conditions (From Deeb *et al.* (2000))

The purpose of this section is to present and discuss biological processes capable of degrading MTBE and its metabolites to innocuous end-products, the relevant kinetics of the processes, and any field implementations involving the process. In an effort to better facilitate the discussion of the specific mechanisms of biological degradation, the mechanisms will be categorized as either direct or cometabolic.

2.8.2.1 DIRECT METABOLISM

In addition to native microorganisms that have been shown capable of direct metabolism of MTBE through biostimulation under oxic conditions, many non-native microorganisms have also demonstrated the capability to directly degrade MTBE in both laboratory and field studies through bioaugmentation. The purpose of this section is to describe MTBE-degrading microorganisms and present significant findings from the relevant research that has been done. Kinetic models, parameters, and other significant factors will be presented as available from literature. Relevant kinetic parameters from the literature are summarized below in Section 2.9.

BC-1 (Aerobic)

The MTBE oxidizing culture designated BC-1 was isolated from activated sludge used in an industrial biotreatment system (Salanitro *et al.*, 1994). Salanitro *et al.* (1994) conducted both continuous flow and batch studies on BC-1. In aerobic continuous flow conditions, with nutrients added, BC-1 achieved up to 90% conversion of MTBE to carbon dioxide; however, when nutrient flow was decreased, removal of MTBE also decreased. Salanitro *et al.* (1994) concluded that the presence of nitrifying organisms in the microbial consortium have an indirect or direct effect on the degradation rate of MTBE. Additionally, the results of a batch study showed the primary intermediate of MTBE oxidation is TBA (Salanitro *et al.*, 1994). Batch studies investigating the rate of MTBE destruction were conducted at 22 to 25 °C with MTBE concentrations of 120 to 130 mg/L and at an initial dissolved oxygen concentration of 20 mg/L (Salanitro *et al.*,

1994). The degradation rates of MTBE and TBA were 0.57 mg/g cells/min and 0.24 mg/g cells/min, respectively (Salanitro *et al.*, 1994).

There are no known field studies of MTBE biodegradation by BC-1.

MC-100 (Aerobic)

Salanitro *et al.* (2000) conducted a field demonstration of bioaugmentation and biostimulation using a bacterial culture called MC-100 at the U.S. Navy Hydrocarbon National Environmental Test Site at Port Hueneme, CA. The MC-100 culture was derived from the consortium BC-1 (Salanitro *et al.*, 2000). The field demonstration involved three separate test plots consisting of a control plot, a plot where only oxygen was injected, and a plot where both oxygen and MC-100 were injected. The injections were accomplished in both shallow and deep portions of the contaminated aquifer. The initial dissolved oxygen concentration in the aquifer was <1 mg/L and MTBE concentrations ranged from 2 to 9 mg/L (Salanitro *et al.*, 2000).

The results of the field demonstration and batch study indicate that rapid MTBE-degradation can be achieved by maintaining aerobic conditions through oxygen injection and inoculating the aquifer with MTBE-degrading organisms. Salanitro *et al.* (2000) point out that TBA is also rapidly degraded by the MC-100 bacteria, similar to the BC-1 culture. Additionally, results of the study indicate that native MTBE-degrading organisms exist in the Port Hueneme aquifer although a lag time of approximately 230 days was observed before any significant reduction in MTBE concentrations occurred in the oxygen only test plot. Moreover, the degradation of MTBE occurred 3-5 times slower in the oxygen-only test plot as compared to the plot with the MC-100 culture (Salanitro *et al.*, 2000). Salanitro *et al.* (2000) suggest that the lag time is due to the slow

growth rate, small population, and spatial variation of population distribution of native MTBE-degrading bacteria. The native bacteria in the oxygen-only test plot also degraded TBA; however, the rate of TBA degradation was slower than in the bioaugmented plot (Salanitro *et al.*, 2000). Although no kinetic parameters or models were presented by Salanitro *et al.* (2000), Deeb *et al.* (2003) references a first-order decay rate for MTBE of 0.008 day^{-1} for this study.

Another study at the Port Hueneme site by Bruce *et al.* (2002) implemented a biobarrier treatment system where biostimulation through aeration and oxygenation, as well as bioaugmentation with MC-100 and SC-100 (an MTBE-degrading isolate) were used. Dissolved oxygen concentrations achieved by air sparging and oxygen sparging were 4 and 20 mg/L, respectively (Bruce *et al.*, 2002). Similar to the demonstration by Salanitro *et al.* (2000), the study by Bruce *et al.* (2002) demonstrated the capability of the MC-100 and SC-100 cultures and the intrinsic capability of native microorganisms to degrade MTBE *in situ*.

PM-1 (Aerobic)

The pure culture PM-1 was isolated from a compost biofilter at the Los Angeles County Joint Water Pollution Control Plant and then characterized by Hanson *et al.* (1999). Batch studies by Hanson *et al.* (1999) confirmed that PM-1 can degrade MTBE as a sole energy and carbon source. The observed degradation rates were 0.07, 1.17, and 3.56 mg/L/hr for MTBE concentrations of 5, 50, and 500 mg/L, respectively at an inoculation density of 2×10^6 cells/mL and temperature of 25 °C (Hanson *et al.*, 1999); as reported by Wilson (2003), the study by Hanson *et al.* (1999) yielded a half-saturation constant of approximately 50 mg/L MTBE. Further batch studies using MTBE-

contaminated aquifer matrix samples indicated that PM-1 may be an effective culture for bioaugmentation (Hanson *et al.*, 1999).

Deeb *et al.* (2001) investigated the effects of the presence of BTEX compounds on the degradation of MTBE by PM-1. The maximum MTBE degradation rate observed without BTEX present was 5.0 mg/L/hr (Deeb *et al.*, 2001). The presence of ethylbenzene and xylenes severely inhibited the degradation of MTBE; though, benzene and toluene only slightly inhibited MTBE degradation by PM-1. The introduction of benzene and toluene resulted in a lag period before their degradation initiated and a reduction in the rate of MTBE degradation (Deeb *et al.*, 2001). The results of this study indicate that the degradation of MTBE and the degradation of benzene and toluene occur via two different enzymatic processes (Deeb *et al.*, 2001). Additionally, if naturally occurring bacteria found in aquifers behave similarly to the PM-1 bacteria, these results indicate that significant MTBE degradation may not occur until the MTBE plume separates from the BTEX plume (Deeb *et al.*, 2001).

A study by Kane et al. (2001) revealed the presence of PM-1-like microorganisms in anoxic MTBE-contaminated aquifers in two of four sites sampled in California. The presence of the PM-1-like organisms was detected by 16S rDNA sequence analysis. Samples taken from a leaking underground storage tank (LUST) site at Palo Alto demonstrated significant degradation of MTBE and transient production of the metabolite TBA under oxic conditions (Kane et al., 2001). Samples taken from a similar site at Travis AFB also demonstrated significant degradation of MTBE under oxic conditions; however, the production of TBA was not observed in this sample. Similar to the results published by Deeb et al. (2001), presence of BTEX compounds inhibited the degradation

of MTBE and resulted in higher and more persistent transient concentrations of TBA (Kane et al., 2001). The specific component(s) of the BTEX compounds that caused the inhibition was not identified. Although MTBE degradation was observed under oxic conditions for two of the samples, no degradation under oxic conditions was observed for the other two samples. Ultimately, this indicates that simply adding oxygen to anoxic MTBE-contaminated aquifers may not be effective in all cases (Kane et al., 2001).

In a study at Vandenberg AFB, Wilson *et al.* (2002) demonstrated that adding oxygen to MTBE-contaminated groundwater flowing through an *in situ* longitudinal test facility (described in Wilson *et al.* (2002)) resulted in significant reductions in MTBE concentrations (influent concentrations as high as 2.1 mg/L). The pseudo first-order rate constant (k') derived from the study by Wilson *et al.* (2002) was $6.1 \times 10^{-5} \text{ s}^{-1}$ (Wilson *et al.*, 2002). In this case, creating oxic conditions by releasing oxygen into the aquifer resulted in the degradation of MTBE. Wilson *et al.* (2002) concluded that the results of their study indicate that MTBE-degrading microorganisms are native to the aquifer at Vandenberg AFB. A subsequent study by Hristova *et al.* (2003) that used 16S rDNA sequencing with polymerase chain reaction methods confirmed that at a minimum, the known MTBE-degrading culture PM-1 or PM-1-like microorganisms are in fact present at Vandenberg AFB, CA.

The bacterial culture PM-1 has also been used in bioaugmentation efforts. Stavnes *et al.* (2002) describe a field implementation at a site in Montana of a biobarrier consisting of PM-1 along with a solid oxygen source, and/or air installed to remediate an MTBE plume. The success demonstrated by Stavnes *et al.* (2002) provides evidence of the effectiveness of bioaugmented PM-1 culture to degrade MTBE.

ENV735 (Aerobic)

Steffan *et al.* (2000b) isolated a pure bacterial culture capable of mineralizing MTBE and designated it ENV735. Degradation of MTBE to carbon dioxide was confirmed by batch, microcosm, and membrane bioreactor studies conducted by Steffan *et al.* (2000b). The ENV735 culture was derived from MTBE-contaminated groundwater and a fluid bed bioreactor that was used to treat MTBE-contaminated water. The slow growth rate of ENV735 on MTBE and TBA, typical of most MTBE-degrading bacteria, could be accelerated by the addition of a small amount of yeast extract (0.01%) (Steffan *et al.*, 2000b). In addition, Steffan *et al.* (2000b) reported that despite the culture's inability to degrade BTEX compounds, its capacity to degrade MTBE and TBA are unaffected by the presence of the BTEX compounds (Steffan *et al.*, 2000b). The initial degradation rate achieved by ENV735 during the study by Steffan *et al.* (2000b) was ~4.05 mg/g cell protein/min for the degradation of 25 mg/L MTBE to below detectable limits at 25 °C (Steffan *et al.*, 2000b).

Further study of the ENV735 bacterial strain was conducted by Hatzinger *et al.* (2001). Confirming Steffan *et al.*'s (2000b) results, it was shown that ENV735 was able to most rapidly degrade MTBE when the culture was grown in rich media such as yeast extract or sucrose (Hatzinger *et al.*, 2001). Likewise, the growth rate of ENV735 was enhanced by the addition of yeast extract (Hatzinger *et al.*, 2001). Hatzinger *et al.* (2001) suggest that the low growth rates of organisms that use MTBE as the sole carbon source may be attributed to the toxic effects of metabolites produced during the degradation of MTBE (Hatzinger *et al.*, 2001). The maximum initial degradation rate achieved by

ENV735 during the study was 7.58 mg/g cell protein/min for the degradation of 25 mg/L MTBE at 25 °C (Hatzinger *et al.*, 2001).

There are no known field studies of the bacterial culture ENV735.

Mycobacterium austroafricanum IFP 2012 (Aerobic)

Francois *et al.* (2002) identified a pure bacterial strain capable of degrading MTBE and TBA. The bacterial strain IFP 2012 was isolated from activated sludge taken from an urban wastewater treatment plant located near Paris, France (Francois *et al.*, 2002). Isolated by its ability to directly degrade TBA, IFP 2012 demonstrated its ability to also degrade MTBE during the study by Francois *et al.* (2002). Similar to the ENV735 bacteria, the growth rate of the cells and hence the degradation rate of MTBE could be accelerated by the addition of 100 mg/L of yeast extract (Francois *et al.*, 2002). This study also showed that IFP 2012 was able to grow on *p*-xylene and *m*-xylene, as well as toluene (Francois *et al.*, 2002). The degradation rate of MTBE was higher for cells that were grown on TBA versus MTBE (Francois *et al.*, 2002). Although IFP 2012 is able to degrade TBA, when initial concentrations of MTBE exceeded 20 mg/L, IFP 2012 was unable to degrade the TBA produced (Francois *et al.*, 2002). The half-saturation constant derived for IFP 2012 for the degradation of MTBE was not reported; however, the half saturation constant for TBA was found to be 81.5 mg/L (Francois *et al.*, 2002). Additionally, Francois *et al.* (2002) reported an MTBE degradation rate of 1.76 mg/g of cell protein/min.

Isolates 24, 33, 41 (Aerobic)

The bacterial isolates 24, 33, and 41 were all isolated from activated sludges and the soil surrounding fruit of a Ginko tree (Mo *et al.*, 1997). Isolates 24, 33, 41 were identified through lipid analysis as *Methylobacterium mesophilicum*, *Rhodococcus* sp., and *Arthrobacter ilicis* respectively. In batch studies using radio-labeled MTBE, after seven days of incubation the maximum conversion to carbon dioxide observed was 8.2% (Mo *et al.*, 1997). The author is unaware of any further kinetic or field studies that have been done on Isolates 24, 33, and 41.

Uncharacterized Cultures (Aerobic)

An unidentified bacterial consortium was isolated by Fortin and Deshusses (1999) for use in a biotrickling filter treating MTBE vapors. The consortium was obtained from MTBE-contaminated soil and groundwater (Fortin and Deshusses, 1999). Zero-order kinetic behavior was observed when the reactor was operating in steady-state at high MTBE loadings (Fortin and Deshusses, 1999). The degradation rate observed for the unidentified cultures was 0.18 mg/g dry weight cells/min (Fortin and Deshusses, 1999).

Kinetic studies on an MTBE-degrading culture obtained from activated sludge in a petroleum plant wastewater treatment facility were conducted by Cowan and Park (1996) and Park and Cowan (1997). Wilson (2003) reports the maximum degradation rate for the Cowan and Park (1996) study to be 0.25 mg/g cells/day and the half saturation constants for Cowan and Park (1996) and Park and Cowan (1997) to be 4.8 and 0.33 mg/L, respectively. While the earlier study by Cowan and Park (1996) investigated kinetics of the biodegradation of MTBE, the later study by Park and Cowan (1997)

investigated the sensitivity of the MTBE-degrading culture to variations in water temperature and dissolved oxygen concentrations, revealing a high degree of sensitivity to both parameters. Lower water temperatures slowed the already low degradation rate, and dissolved oxygen concentrations below 1 mg/L inhibited MTBE degradation (Park and Cowan, 1997).

Uncharacterized Cultures (Anaerobic)

The anaerobic degradation of MTBE by indigenous bacteria has been the subject of many studies. Microcosm studies (*e.g.* Bradley *et al.*, 2001a; Bradley *et al.*, 2001b; Finneran and Lovley, 2001; and Somsamak *et al.*, 2001) of aquifer and surface water sediments have demonstrated the capability of indigenous bacteria to degrade MTBE to carbon dioxide and/or methane under various terminal electron acceptor conditions. Studies have shown that mineralization of MTBE is directly related to the increasing oxidation potential of the terminal electron acceptor where sulfate < iron (III) < manganese (IV) < nitrate < oxygen (Bradley *et al.*, 2001a). Bradley *et al.* (2001a) also showed that the accumulation and subsequent degradation of TBA occurred under anaerobic conditions; however, under methanogenic conditions nominal amounts of MTBE were converted to TBA which was not subsequently degraded.

2.8.2.2 COMETABOLISM

Both bioaugmentation and biostimulation have been used to achieve MTBE cometabolism. The cometabolism of MTBE can be initiated when bioaugmented or native organisms are supplied with a primary energy and carbon source. The purpose of this section is to describe characterized and uncharacterized MTBE-cometabolizing

microorganisms and present significant findings from the relevant research that has been done. Kinetic models, parameters, and other significant factors will be presented as available from literature. Relevant kinetic parameters from the literature are summarized below in Section 2.9.

Graphium sp. (Aerobic)

Graphium sp. is the only documented case of MTBE degradation by a filamentous fungus. Hardison *et al.* (1997) investigated the cometabolic degradation of MTBE by *graphium sp.* with several different primary substrates. The maximum degradation rate observed in this study was 0.93 mg MTBE/g cells DW/hr for inoculums grown on *n*-butane (Hardison *et al.*, 1997). Hardison *et al.* (1997) attribute the degradation of MTBE to its fortuitous oxidation by the same enzyme responsible for the oxidation of the *n*-alkane and di-ethyl ether (DEE) (Hardison *et al.*, 1997). Additionally, the maximum rate of degradation observed in this study may not be the actual maximum rate of degradation capable by *graphium sp.* since saturation was never achieved (Hardison *et al.*, 1997). Common to most, if not all, MTBE-degradation processes, the intermediates observed during the degradation of MTBE were TBF and TBA (Hardison *et al.*, 1997).

The degradation of MTBE by *graphium sp.* was also studied by Martinez-Prado *et al.* (2002). The objective of this study was to identify Monod-kinetic parameters for *graphium sp.* grown on and utilizing propane as a primary substrate. Martinez-Prado *et al.* (2002) found that the rate of MTBE degradation was faster for filter-attached grown cultures than liquid suspension cultures and propose that this observation may be due to cellular damage caused during handling the liquid suspension culture. Typical

breakdown products including TBA and TBF were identified in this study; neither of which appeared to be toxic to the *graphium* sp. cultures (Martinez-Prado *et al.*, 2002).

ENV421 and ENV425 (Aerobic)

Naturally occurring propane-oxidizing bacteria (POB) strains were isolated for study by Steffan *et al.* (1997). The POB that produce the propane mono-oxygenase enzyme demonstrated the capability to oxidize trichloroethylene (TCE) and hydrochlorofluorocarbons in addition to propane in several studies (Steffan *et al.*, 1997). Steffan *et al.* (1997) investigated the potential for POB strains ENV421 and ENV425 to cometabolize MTBE. Batch study results conducted using ENV421 and ENV425 at temperatures of 28 °C resulted in maximum MTBE degradation rates of 0.81 mg MTBE/g cell protein/min and 0.41 mg/g cell protein/min, respectively (Steffan *et al.*, 1997). Batch studies conducted at 13 °C resulted in lower MTBE degradation rates. The primary intermediate observed during MTBE degradation was TBA, which was subsequently degraded, although at slower rates than those of MTBE (Steffan *et al.*, 1997). Confirming that this is an aerobic process, no degradation was observed in the absence of oxygen (Steffan *et al.*, 1997). The widespread distribution of POB in the environment may prove to be beneficial for MTBE-remediation efforts (Steffan *et al.*, 1997).

Further investigation of POB by Steffan *et al.* (2000a) showed that POB are present in some MTBE-contaminated aquifers, but not in all. For sites where naturally occurring POB were not present, a seed culture of ENV425 was introduced and subsequently degraded the MTBE. For all cases studied, native POB or ENV425 cultures were able to degrade MTBE to levels less than 10 µg/L (Steffan *et al.*, 2000a).

Regarding the difficulties that may be associated with propane sparging at an MTBE-contaminated site (*i.e.* danger of introducing an explosive mixture of propane and oxygen in the aquifer matrix), Steffan *et al.* (2000a) proposed two measures to help mitigate these difficulties. First, propane sparging should be limited to only 10% of the propane LEL. Second, soil vapor extraction techniques should be employed to capture any excess propane. Additionally, Steffan *et al.* (2000a) states that a bubble-less propane delivery technique using plugged silicon tubing is currently being used at a TCE remediation site and may also be utilized effectively at MTBE remediation sites in an effort to reduce the explosive hazard posed by gaseous propane and oxygen in the aquifer matrix.

Mycobacterium vaccae JOB5 (Aerobic)

A study by Martinez-Prado (2002) investigated the kinetics of the degradation of MTBE and its breakdown products by JOB5. Monod-kinetic parameters were determined from liquid suspension batch studies conducted using propane and *iso*-pentane as primary substrates. The Monod-kinetic parameters were determined through both non-linear least squares regression and a direct linear plot method proposed by Kim *et al.* (2002). The results of this study indicate that MTBE and TBA are both fortuitously oxidized by the same propane monooxygenase enzyme responsible for oxidation of the alkane primary substrates. Additionally, it was shown that the oxidation of all compounds was inhibited by the presence of acetylene.

Although the primary substrate utilization rate of propane (k_{Donor}) was higher than that of *iso*-pentane, the half-saturation constant ($K_{s-Donor}$) for propane was much lower (Martinez-Prado, 2002). This indicates that JOB5 has a significantly higher affinity for

propane than *iso*-pentane (Martinez-Prado, 2002). Despite this, the MTBE utilization rate by JOB5 that utilized *iso*-pentane (k_{MTBE}) was faster than that of the JOB5 culture that utilized propane. Thus, the *iso*-pentane culture was selected for further kinetic analysis and testing in a growth batch reactor. Further, competitive inhibition kinetic parameters were determined for the *iso*-pentane oxidizing culture.

Both TBA and TBF were identified as break-down products of MTBE (Martinez-Prado, 2002). The presence of TBA and TBF competitively inhibited the degradation of MTBE (Martinez-Prado, 2002). The hydrolysis of TBF to TBA was not found to be a significant contributor to the disappearance of TBF. Furthermore, the utilization rate of TBF was the highest of any substrate utilization by propane-oxidizing JOB5 and second fastest for *iso*-pentane-oxidizing JOB5 (Martinez-Prado, 2002). Overall, the magnitude of substrate utilization rates by the propane and *iso*-pentane oxidizing bacteria for each of the substrates can be described by the following: TBF > propane > MTBE > TBA and *iso*-pentane > TBF > MTBE > TBA, respectively (Martinez-Prado, 2002).

Another recent study of the POB JOB5 was conducted by Smith *et al.* (2003). The POB characterized as *M. vaccae* JOB5 was obtained from the American Type Culture Collection for analysis in a kinetic study by Smith *et al.* (2003). Cells that were grown on propane as the sole carbon and energy source demonstrated the capability to cometabolize MTBE. The oxidation of MTBE is a result of the production of the monooxygenase enzyme used by JOB5 to oxidize propane (Smith *et al.*, 2003). Smith *et al.* (2003) identified the metabolites produced during the oxidation of MTBE by JOB5 as TBF and TBA. The TBF and TBA were formed in that order and were subsequently degraded by JOB5, although at a slower rate than that of MTBE (Smith *et al.*, 2003). The

maximum degradation rate of MTBE (k_{MTBE}) observed in this study for an initial MTBE concentration of 79.3 mg/L was 2.2 mg MTBE/g cell protein/min (Smith *et al.*, 2003). The half-saturation constant for MTBE (K_{s-MTBE}) observed for JOB 5 was 120 mg/L. Additionally, inhibitory effects of propane concentration were analyzed and an average inhibition constant (K_i) for propane of 285 mg/L was derived (Smith *et al.*, 2003).

Arthrobacter (Aerobic)

Liu *et al.* (2001) conducted a kinetic study on an *n*-alkane oxidizing bacteria characterized as *Arthrobacter*. *Arthrobacter* bacteria were isolated from the soil of a natural- and domestic-gas-contaminated site (Liu *et al.*, 2001). Kinetic parameters for the degradation of low concentrations of MTBE (100 to 800 µg/L) by *Arthrobacter* utilizing butane as the sole carbon and energy source were quantified in batch studies. The observed maximum degradation rate for MTBE (k_{MTBE}) was 0.6 mg MTBE /g cell protein/min and half-saturation constant (K_{s-MTBE}) was 2.14 mg/L (Liu *et al.*, 2001). The primary metabolite identified was TBA which was subsequently oxidized at a slower rate. The presence of TBA appeared to inhibit the degradation of MTBE (Liu *et al.*, 2001).

Cyclohexane-Oxidizing Culture (Aerobic)

A cyclohexane-oxidizing culture was obtained from a bio-scrubber being used to treat cyclohexane-contaminated air (Corcho *et al.*, 2000). Batch studies conducted with the culture utilizing cyclohexane as the sole carbon and energy source yielded a maximum MTBE degradation rate (k_{MTBE}) of 6.4 mg MTBE/g cells/hr (Corcho *et al.*, 2000). The sole metabolite identified by Corcho *et al.* (2000) was TBA. Corcho *et al.*

(2000) also conducted batch studies to investigate the inhibitory effects of toluene and benzene on the degradation of MTBE. Low concentrations of toluene (2.5 mg/L) and high concentrations of benzene (120 mg/L) inhibited the degradation of MTBE (Corcho *et al.*, 2000).

Iso-Alkane-Oxidizing Cultures (Aerobic)

A group of nine distinct bacterial strains were isolated from a surface soil sample obtained at a gasoline-contaminated site (Hyman *et al.*, 2000). Genetic sequencing by 16S rRNA analysis indicated that hydrocarbon-oxidizing bacteria including *Rhodococcus*, *Nocardia*, *Pseudomonas*, *Alcaligenes*, and *Rhizobium* bacteria are present *in situ* (Hyman *et al.*, 2000). Batch studies conducted by Hyman *et al.* (2000) showed that all the strains were capable of cometabolically degrading MTBE while utilizing propane, *n*-butane, *n*-pentane, *n*-hexane, *n*-octane, *iso*-butane, and *iso*-pentane individually; although, the strains achieved the highest rates of degradation when *n*-alkanes were utilized as a sole source of carbon and energy (Hyman *et al.*, 2000). The maximum observed MTBE degradation rate (k_{MTBE}) achieved by the strains grown on *iso*-butane was 14.1 nmoles/mg cell protein/min and the half-saturation constant (K_{s-MTBE}) was 482 μ M (Hyman *et al.*, 2000). The maximum observed MTBE degradation rate (k_{MTBE}) achieved by the strains growing on *n*-pentane was 18.3 nmoles/mg cell protein/min (Hyman *et al.*, 2000). The intermediates produced during MTBE cometabolism included TBA and TBF (Hyman *et al.*, 2000).

Pseudomonas aeruginosa (Aerobic)

Dupasquier *et al.* (2002) investigated the cometabolism of MTBE by pentane-oxidizing microorganisms obtained from gasoline-contaminated soil samples. The study investigated the degradation of MTBE vapors in a fixed-film bioreactor. Although this study investigated the degradation of MTBE in the vapor phase, some important and applicable characteristics of cometabolism were observed. Dupasquier *et al.* (2002) used dual-Monod kinetics to model the cometabolic degradation of MTBE by pentane-oxidizing *P. aeruginosa*. Dual-Monod kinetics were used to capture the effects of competitive inhibition due to the presence of a secondary substrate. In order to model the effects of competitive inhibition in a dual-Monod model, Dupasquier *et al.* (2002) state that the inhibition constant of the competitive substrate can be reasonably approximated by the single-substrate half-saturation constant. The substrate utilization rates (k_{Donor} and k_{MTBE}) and substrate half-saturation constants ($K_{s-primary}$ and K_{s-MTBE}) used in modeling were obtained through batch study and are summarized below in Table 14 and Table 15. Dupasquier *et al.* (2002) observed that pentane utilization was inhibited even by low concentrations of MTBE. Finally, results of sensitivity analysis conducted on the model indicate that substrate utilization rates, rather than substrate half-saturation constants, have the greatest effect on the respective compounds (Dupasquier *et al.*, 2002).

Uncharacterized Cultures (Aerobic)

Loll *et al.* (2003) obtained an enrichment of POB from uncontaminated peat-rich topsoil (Loll *et al.*, 2003). Batch studies were conducted at approximately 23°C using the POB enrichment to determine Monod kinetic parameters. The maximum MTBE

degradation rate (k_{MTBE}) and half-saturation constant (K_{s-MTBE}) were estimated to be 267 mg/g cell protein/hr and 40 mg/L, respectively (Loll *et al.*, 2003). Further investigations considered the effects of oxygen and benzene concentrations on the degradation of MTBE. The estimated half-saturation constant for oxygen ($K_{s-Oxygen}$) was 0.28 mg/L, which indicates that significant microbial activity may take place at relatively low oxygen concentrations (Loll *et al.*, 2003). Furthermore, the enrichment was able to degrade benzene; although MTBE degradation was inhibited by the presence of benzene (Loll *et al.*, 2003). An inhibition constant (K_i) of 1 mg/L benzene was estimated from the kinetic studies (Loll *et al.*, 2003).

The inhibitory effects of propane on the degradation of MTBE were also investigated. Propane concentrations above 0.63 mg/L resulted in significantly lower MTBE degradation rates. This observation verifies that the cometabolism of MTBE is sensitive to primary substrate concentration. Loll *et al.* (2003) also calculated preliminary up-scaling parameters needed for field evaluation of their technology. Loll *et al.* (2003) suggest a ratio of 1.5 g propane per 1 g of MTBE for up-scaling the batch reactor.

2.9 KINETIC MODELS

In this section, the kinetic models that have been used to represent the degradation of MTBE will be discussed and relevant model parameters that have been measured will be presented. The models that will be discussed include first-order, second-order, and Monod kinetics. The purpose of presenting these models is to provide information that can be used to select an MTBE degradation submodel that can be used as a component of

an HFTW system model. Selection of an appropriate sub-model will be accomplished in the next chapter.

2.9.1 FIRST-ORDER KINETIC MODELS FOR ABIOTIC AND BIOTIC PROCESSES

First-order or pseudo first-order kinetic models have been used to describe both biotic and abiotic processes. Particularly useful for complex processes that are not explicitly understood, first-order models are the simplest models that have been used to describe the degradation of MTBE. In particular, first-order models have been used to describe MTBE-degradation by oxygen, FR, persulfate, UV irradiation, US irradiation, and biological degradation as discussed in Section 2.8.1.

The degradation of MTBE can be described by Equation 13.

$$\frac{dC^{MTBE}}{dt} = -k \cdot C^{MTBE} \quad (13)$$

Equation 13 indicates that the rate of change of the concentration of MTBE (C^{MTBE}) is proportional to the concentration of MTBE and a first-order degradation rate constant (k). Additionally, reactions that are classified as second-order reactions can also be modeled as pseudo first-order reactions when the concentration of one component is in excess and is effectively constant throughout the duration of the reaction. Pseudo first-order reactions can be described by Equation 14.

$$\frac{dC^{MTBE}}{dt} = -k' \cdot C^{MTBE} \quad (14)$$

Equation 14 states the rate of change of the concentration of MTBE is proportional to the concentration of MTBE and the pseudo first-order rate constant (k').

Table 9 summarizes first-order model parameters and the conditions of the study from which they were measured.

Table 9 Summary of First-Order Kinetic Parameters and Conditions of Study

Process	Rate Constant (s^{-1})	Conditions	Source
Oxygen Oxidation	0.31×10^{-4}	Experimental Batch Study	Lien et al. (2002)
FR Oxidation	2.9×10^{-2}	Experimental Batch Study	Burbano et al. (2002)
FR Oxidation	1.1×10^{-2} , 1.4×10^{-2}	Experimental Batch Study, pH = 7 and 4 respectively	Bergendahl and Thies (2004)
Ozone/Hydrogen Peroxide Oxidation	5.4×10^{-3}	Experimental Batch Study	Safarzadeh-Amiri (2001)
UV Irradiation	1.2×10^{-1} to 2.2×10^{-3}	Experimental Batch Study w/ and w/o TiO ₂ Slurry	Chang and Young (2000) and Baretto et al. (1995)
US Irradiation	88.3×10^{-4}	Experimental Batch Study with Ozone Present	Kang et al. (1999)
Uncharacterized Biotic Degradation	6.1×10^{-5}	Field Study, Oxygen Addition Only	Wilson et al. (2002)
Uncharacterized Biotic Degradation	1.4×10^{-8}	Monitored Natural Attenuation	Schirmer et al. (1999)
MC-100 Biotic Degradation	9.3×10^{-8}	Field Study, Bioaugmentation Plot w/ Oxygen Addition	Deeb et al. (2003)

2.9.2 SECOND-ORDER KINETIC MODELS FOR ABIOTIC PROCESSES

Second-order kinetics have also been used to describe the degradation of MTBE. Second-order models are used particularly when the degradation rate of a compound is dependent on its concentration as well as the concentration of another compound such as an oxidizing agent. Second-order models have been used to describe the oxidation rate of

MTBE by ozone and hydrogen peroxide combination and permanganate as discussed in Section 2.8.1.

The degradation of MTBE according to second-order kinetics can be described by Equation 15.

$$\frac{dC^{MTBE}}{dt} = -k \cdot C^{MTBE} \cdot C^B \quad (15)$$

Equation 15 describes the rate of change of concentration of MTBE as proportional to the concentration of MTBE (C^{MTBE}) and the concentration of compound B (C^B) according to a second-order degradation rate constant. Some reactions that are typically second-order can also be modeled as pseudo first-order reactions, as previously discussed in Section 2.9.1.

Table 10 summarizes second-order model parameters and the conditions of the study from which they were measured.

Table 10 Summary of Second-Order Kinetic Parameters and Conditions of Study

Process	k	Conditions	Source
FR Oxidation	$1.9 \times 10^8, 4.4 \times 10^8 \text{ M}^{-1} \text{ s}^{-1}$	Experimental Batch Study, pH of 7 and 4, respectively	Bergendahl and Thies (2004)
Permanganate Oxidation	$3.96 \times 10^{-10} \text{ L mg}^{-1} \text{ s}^{-1}$	Experimental Batch Study	Damm et al. (2002)
Ozone/Hydrogen Peroxide Oxidation	$1.6 \times 10^9 \text{ M}^{-1} \text{ s}^{-1}$	Experimental Batch Study, Oxidation by Hydroxyl Radical	Buxton <i>et al.</i> (1988)
Ozone/Hydrogen Peroxide Oxidation	$1.2 \times 10^9 \text{ M}^{-1} \text{ s}^{-1}$	Experimental Batch Study, Oxidation by Hydroxyl Radical	Mitani <i>et al.</i> (2002)

2.9.3 MONOD KINETIC MODELS FOR DIRECT METABOLISM

Monod kinetic models are most commonly used to describe the relationship between microbial growth and rate-limiting utilization of a growth substrate (Rittman and

McCarty, 2001). The reader should note that the following Monod model explicitly assumes that the rate limiting substrate (S) is the electron donor and the availability of electron acceptor is not rate limiting. The rate of biomass growth is related to the maximum specific growth rate and concentration of substrate according to Equation 16.

$$\mu_{syn} = \frac{1}{X} \frac{dX}{dt} = \mu_{max} \left(\frac{S}{S + K_s} \right) \quad (16)$$

Where μ_{max} is the maximum specific growth rate, S is the substrate concentration, X is the concentration of active microorganisms, and K_s is the substrate half-saturation constant. It can be observed that at low concentrations of substrate ($S \ll K_s$) the specific growth rate is directly proportional to the substrate concentration, with a constant of proportionality equal to μ_{max}/K_s while at high substrate concentrations ($S \gg K_s$) the specific growth rate is constant and equal to μ_{max} . Additionally, it can be observed that the specific growth rate is equal to one half of the maximum specific growth rate when substrate concentration (S) is equal to the Monod constant (K_s), hence the Monod constant is also commonly referred to as the half-saturation constant (Rittman and McCarty, 2001).

Net cell growth rate is the cell growth rate minus the cell decay rate. Cell decay is represented as a first-order process where cell decay is proportional to the number of cells, with a first-order rate constant (b) (Rittman and McCarty, 2001).

$$\left(\frac{dX}{dt} \right)_{decay} = -bX \quad (17)$$

The indigenous decay rate of a microbial population can then be described by the following equation,

$$\mu_{dec} = \left(\frac{1}{X} \frac{dX}{dt} \right)_{decay} = -b \quad (18)$$

where (μ_{dec}) is the specific growth rate due to cellular decay (Rittman and McCarty, 2001). Combining the cellular growth and cellular decay equations results in the net specific growth rate (μ) as seen in the following equation (Rittman and McCarty, 2001).

$$\mu = \mu_{\max} \left(\frac{S}{S + K_s} \right) - b \quad (19)$$

Since the ultimate concern is the rate of utilization of substrate, the overall rate of substrate utilization (r_{ut}) by a cellular population X can be described by the following equation,

$$r_{ut} = \frac{dC_{MTBE}}{dt} = -k_{MTBE} \cdot \left(\frac{S}{K_s + S} \right) \cdot X \quad (20)$$

where k_{MTBE} is the maximum specific rate of substrate use in units of mass substrate per biomass per time. The net rate of biomass growth then becomes,

$$r_{net} = \frac{dX}{dt} = Y \cdot k_{MTBE} \cdot \left(\frac{S}{K_s + S} \right) \cdot X - b \cdot X \quad (21)$$

where r_{net} is the net specific growth rate (μ) multiplied by the cellular population (X) and Y is the biomass yield defined as biomass per mass of substrate utilized (Rittman and McCarty, 2001). Finally, we see from the previous equations, that the maximum specific rate of substrate use multiplied by the cellular yield gives the maximum growth rate indicated in the following equation.

$$\mu_{\max} = k_{MTBE} \cdot Y \quad (22)$$

The linear relationship between substrate use and biomass growth justifies the use of Monod kinetics, which were traditionally used to describe the kinetics of cellular

growth, to also describe substrate utilization kinetics. Several studies have been conducted on various bacterial cultures, both mixed and pure, to determine Monod kinetic parameters for MTBE degradation. The following tables summarize the parameters available from literature.

Table 11 Summary of Substrate Utilization Rates and Half-Saturation Constants for MTBE-Metabolizing Bacteria

Strain	k_{MTBE} (Max. Substrate Utilization Rate)	K_s (mg/L)	$K_{s-Oxygen}$ (mg/L)	Temp (°C)	Notes	Source
BC-1	34 mg/g cells/hr			22-25	Batch Study	Salanitro <i>et al.</i> (1994)
PM-1	0.07, 1.17, 3.56 g/mL/hr @ [MTBE] = 5, 50, 500 mg/L *	≈ 50 ¹		25	Batch Study, 2 x 10 ⁶ cells/mL	Hanson <i>et al.</i> (1999)
PM-1	50 mg/g cells/hr			N/A		Deeb <i>et al.</i> (2000)
ENV735	134 mg/g cells/hr ² @ [MTBE] = 25 mg/L			25	Batch Study	Steffan <i>et al.</i> (2000b)
ENV735	250 mg/g cells/hr ² @ [MTBE] = 25 mg/L			30	Batch Study	Hatzinger <i>et al.</i> (2001)
IFP2012	58 mg/g cells/hr			30	Batch Study, Culture Grown on TBA	Francois <i>et al.</i> (2002)
Unidentified	3.3 mg/g cells/hr ³			N/A	Batch Study, Gas-phase Biotrickling Filter	Fortin and Deshusses (1999)
Unidentified			≈ 3	N/A		Koeningsberg <i>et al.</i> (1999)
Unidentified	3.1 to 27.3 mg/g cells/hr ⁴	2.2 - 4.8		30	Batch Study	Cowan and Park (1996)
Unidentified	36.4 mg/g cells/hr ⁴	0.33	0.9	20	Batch Study	Park and Cowan (1997)

¹ From Wilson (2003)

² Calculated by assuming 0.55 g cell protein / g cells

³ Calculated by assuming 0.3 g cells DW/g cells

⁴ Calculated by using given values for max. specific growth rate and yield in Equation 22

* Unclear how these values are calculated and will not be considered for further analysis

Table 12 Summary of Biomass Yields for MTBE-Metabolizing Bacteria

Strain	<i>Y</i> (Biomass Yield) (g cells DW/g MTBE utilized)	Source
<i>BC-1</i>	0.21 to 0.28	Salanitro <i>et al.</i> (1994)
<i>PM-1</i>	0.18	Hanson <i>et al.</i> (1999)
<i>ENV735</i>	0.20 to 0.26 (w/ 0.01% wt/vol YE added)	Steffan <i>et al.</i> (2000b)
<i>ENV735</i>	0.4 (w/ 0.01% wt/vol YE added)	Hantzinger <i>et al.</i> (2001)
<i>IFP2012</i>	0.44	Francois <i>et al.</i> (2002)
<i>Unidentified</i>	0.11	Fortin and Dehusses (1999)
<i>Unidentified</i>	0.33 to 0.43 ¹	Cowan and Park (1996)
<i>Unidentified</i>	0.33 to 0.41 ¹ (Temp. 20 to 30 °C)	Park and Cowan (1997)

¹ Assumed dry weight

Table 13 Summary of Decay Rates for MTBE-Metabolizing Bacteria

Strain	<i>b</i> (Decay Rate) (day⁻¹)	Temp (°C)	Source
Unidentified	0.12	25	Cowan and Park (1996)
Unidentified	0.072	20	Park and Cowan (1997)

2.9.4 MONOD KINETIC MODELS FOR COMETABOLISM

As previously discussed, the cometabolism of MTBE generally occurs due to fortuitous oxidation of MTBE by the same enzyme that oxidizes the primary substrate (primary electron donor) microorganisms utilize as a carbon and energy source. Due to the fact that degradation of both the target compound and primary substrate depend on the same enzyme, the degradation rate of the target compound (MTBE) can be inhibited by the presence of the primary substrate (Rittman and McCarty, 2001). This type of

inhibition is called competitive inhibition (Rittman and McCarty, 2001). Competitive inhibition may be modeled by increasing the target compound half-saturation constant (K_{s-MTBE}) by a term that depends on the concentration of the primary substrate (Rittman and McCarty, 2001):

$$K_{eff} = K_{s-MTBE} \left(1 + \frac{C_{Donor}}{K_{i-Donor}} \right) \quad (23)$$

where $K_{i-Donor}$ is defined as the inhibition constant. The overall target compound (secondary substrate) utilization can then be described by modifying Equation 20, to include K_{eff} ,

$$r_{ut} = \frac{dC_{MTBE}}{dt} = -k_{MTBE} \left(\frac{C_{MTBE}}{K_{eff} + C_{MTBE}} \right) \cdot X \quad (24)$$

where k_{MTBE} is the MTBE utilization rate and the secondary substrate concentration is represented as C_{MTBE} . The net rate of biomass growth can then be represented by,

$$r_{net} = \frac{dX}{dt} = Y \cdot k_{Donor} \cdot \left(\frac{C_{Donor}}{K_{s-Donor} + C_{Donor}} \right) \cdot X - b \cdot X \quad (25)$$

where k_{Donor} is the primary electron donor utilization rate and the half-saturation constant for the primary substrate is represented by $K_{s-Donor}$.

Based on the above expressions, Monod kinetics can be used to represent the degradation of a secondary substrate with inhibition by a primary substrate as well as the biomass growth on a primary substrate. Several studies have investigated the kinetic parameters of MTBE-cometabolism in the presence of various primary substrates. The following tables summarize the values of the parameters as available from the literature.

Table 14 Summary of Substrate Utilization Rates for Various MTBE-Cometabolizing Microorganisms

Strain	Primary Substrate	k_{Donor}	k_{MTBE}	Temp (°C)	Source
<i>Graphium</i> sp.	n-butane		0.28 mg/g cells /hr ¹	25	Hardison <i>et al.</i> (1997)
<i>Graphium</i> sp.	propane	10.3 mg/g cells/hr *	6.39 mg/g cells/hr *	25	Martinez-Prado <i>et al.</i> (2002)
ENV421	propane		6.1 mg/g cells/hr	13	Steffan <i>et al.</i> (1997)
ENV421	propane		26.8 mg/g cells/hr	28	Steffan <i>et al.</i> (1997)
ENV425	propane		2.0 mg/g cells/hr	13	Steffan <i>et al.</i> (1997)
ENV425	propane		13.4 mg/g cells/hr	28	Steffan <i>et al.</i> (1997)
ENV425	propane		8.3 mg/g cells/hr	N/A	Liu <i>et al.</i> (2001)
JOB5	propane		70.9 mg/g cells/hr	30	Smith <i>et al.</i> (2003)
JOB5	propane	7.61 mg/g cells/hr	5.46 mg/g cells/hr	20	Martinez-Prado <i>et al.</i> (2002)
JOB5	iso-pentane	60 mg/g cells/hr	17.6 mg/g cells/hr	20	Martinez-Prado <i>et al.</i> (2002)
<i>P. aeruginosa</i>	pentane	63.1 mg/g cells/hr ¹	3.1 mg/g cells/hr ¹	30	Dupasquier <i>et al.</i> (2002)
<i>Arthrobacter</i>	butane		17.9 mg/g cells/hr ³	N/A	Liu <i>et al.</i> (2001)
mixed culture	cyclohexane		6.4 mg/g cells/hr	23	Corcho <i>et al.</i> (2000)
mixed culture	n-pentane		53.2 mg/g cells/hr ³	30	Hyman <i>et al.</i> (2000)
mixed culture	propane	212 mg/g cells/hr ²	147 mg/g cells/hr ²	23	Loll <i>et al.</i> (2003)

¹ Calculated by assuming 0.3 g cells DW/g cells

² Calculated by assuming 0.55 g cell protein/g cells

³ Calculated by assuming 0.5 g cell protein/g cells (as reported by Liu *et al.* (2001))

* Assuming values reported as g cells not g cells DW

Table 15 Summary of Half-Saturation and Inhibition Constants for MTBE-Cometabolizing Microorganisms

Strain	Primary Substrate	$K_{s-Donor}$ (mg/L)	K_{s-MTBE} (mg/L)	$K_{i-Donor}$ (mg/L)	Source
ENV425	propane		1.17		Liu <i>et al.</i> (2001)
JOB5	propane		120		Smith <i>et al.</i> (2003)
JOB5	propane	0.19-0.31	14		Martinez-Prado <i>et al.</i> (2002)
JOB5	<i>iso</i> -pentane	0.51-1.1	12-13	22	Martinez-Prado <i>et al.</i> (2002)
<i>P. aeruginosa</i>	pentane	0.019	185		Dupasquier <i>et al.</i> (2002)
<i>Arthrobacter</i>	Butane		2.14		Liu <i>et al.</i> (2001)
mixed culture	<i>iso</i> -butane		10.5-42.5		Hyman <i>et al.</i> (2000)
mixed culture	propane	0.4	40		Loll <i>et al.</i> (2003)

Table 16 Summary of Biomass Yields for Various Bacterial Strains Grown on Various Substrates

Strain	Y (Biomass Yield)	Source
<i>Graphium</i> sp.	1.63 g cells /g butane utilized ¹	Salanitro <i>et al.</i> (1994)
<i>Graphium</i> sp.	1.1 g cells /g propane utilized	Martinez-Prado <i>et al.</i> (2002)
JOB5	0.8 g cells/g propane utilized ²	Martinez-Prado <i>et al.</i> (2002)
JOB5	0.61 g cells/g <i>iso</i> -pentane utilized ²	Martinez-Prado <i>et al.</i> (2002)
mixed culture	1.8 g cells/g propane utilized ¹	Loll <i>et al.</i> (2003)

¹ Calculated assuming 0.3 g cells DW/g cells

² Assuming 1 g TSS = 1 g cells

Table 17 Summary of Decay Rate for MTBE-Cometabolizing Bacteria

Strain	b (Decay Rate) (day ⁻¹)	Source
<i>Unidentified</i>	0.075 [†]	Martinez-Prado <i>et al.</i> (2002)

[†] Author assumed typical value

2.9.5 DUAL-MONOD KINETIC MODELS FOR COMETABOLISM

Several researchers have used dual-Monod kinetics to describe the degradation of contaminant by microbiological organisms and at least one study used dual-Monod kinetics to describe the degradation of MTBE (Dupasquier *et al.*, 2002). Dual-Monod kinetics differ from basic Monod kinetics described in Section 2.9.4 in that microbial growth, electron donor utilization, and electron acceptor utilization are a function of both the electron donor and acceptor concentrations. Semprini and McCarty (1991) developed a dual-Monod model to describe the degradation of TCE by cometabolism in the presence of methane as a primary substrate. The model developed by Dupasquier *et al.* (2002) is similar to that developed by Gandhi *et al.* (2002b); however, the Gandhi *et al.* (2002b) model can be used to track more components and thus can be adapted for more situations. A more recent model of TCE cometabolism was developed by Gandhi *et al.* (2002b) and is presented in this section. Gandhi *et al.* (2002b) modeled aerobic TCE cometabolism in an HFTW system using toluene as a primary substrate. Hydrogen peroxide was used as a supplemental oxygen source and also to help prevent excessive biomass accumulation near the HFTW well screens (Gandhi *et al.*, 2002b).

The model presented by Gandhi *et al.* (2002b) accounts for microbial growth, electron donor and electron acceptor utilization, competitive inhibition of primary substrate (toluene) utilization by the presence of the target compound (TCE) as well as competitive inhibition of target compound degradation by the presence of the primary substrate, inhibition of microbial growth due to the presence of TCE cometabolism transformation products (accounted for using a transformation capacity term), and

oxygenation and toxicity resulting from hydrogen peroxide injection. Additionally, Gandhi *et al.* (2002b) made the following assumptions in order to develop this model:

- A macroscopic description adequately describes biomass growth
- Biomass is stationary
- Biomass growth does not significantly impact groundwater flow
- Mass transfer is not limited within the biomass
- Only aqueous phase compounds can be biodegraded

The model presented by Gandhi *et al.* (2002b) can be readily modified to accommodate MTBE as the cometabolic substrate, rather than TCE. The main change to the Gandhi *et al.* (2002b) model is to eliminate the transformation capacity term, as there have been no observed toxicity effects due to the cometabolic degradation of MTBE. It should be noted that competitive inhibition due to the presence of another substrate is incorporated into this model by assuming that the half-saturation constants are equal to the inhibition constants for each respective species. The equation then used to describe microbial growth is written below as Equation 26.

$$\frac{dX}{dt} = k_{Donor} \cdot Y \cdot X \cdot I_{per} \cdot \left(\frac{C_{Donor}}{K_{S-Donor} \left(1 + \frac{C_{MTBE}}{K_{S-MTBE}} \right) + C_{Donor}} \right) \cdot \left(\frac{C_{Ox}}{K_{S-Ox} + C_{Ox}} \right) - b \cdot X \cdot \left(\frac{C_{Ox}}{K_{S-Ox} + C_{Ox}} \right) \quad (26)$$

Where

k_{Donor} = maximum primary substrate utilization rate (mg donor/mg biomass/day)

Y = biomass yield (mg biomass/mg donor)

X = concentration of active microorganisms (mg biomass/L)

C_{Donor} = concentration of electron donor (mg/L)

$K_{S-Donor}$ = half-saturation constant of electron donor (mg/L)

C_{MTBE} = concentration of cometabolic substrate (mg/L)

K_{s-MTBE} = half-saturation concentration of cometabolic substrate (mg/L)

C_{Ox} = concentration of oxygen (mg/L)

K_{s-Ox} = half-saturation constant of oxygen (mg/L)

b = biomass decay rate (day^{-1})

and inhibition of bacterial growth due to hydrogen peroxide toxicity (I_{per}) is described by Equation 27 below.

$$I_{per} = \frac{K_{i-per}}{K_{i-per} + C_{per}} \quad (27)$$

Where,

I_{per} = hydrogen peroxide inhibition term (unitless)

K_{i-per} = hydrogen peroxide inhibition constant (mg/L)

C_{per} = concentration of hydrogen peroxide (mg/L)

As indicated by Equation 26 the cell decay rate (b) is modified by the concentration of oxygen present. The inclusion of this term is to ensure that biomass levels are not reduced to very low levels in areas of the aquifer where no or little dissolved oxygen is present. Additionally, the following equation prevents the concentration of active microorganisms from decaying to levels less than the initial concentration in electron donor/acceptor deprived areas.

$$\frac{dX}{dt} = 0; X \leq X_{\min} \quad (28)$$

Equation 29 below states that the utilization of electron donor is affected by the inhibition effects of hydrogen peroxide (I_{per}) as well as the presence of the secondary

substrate (C_{MTBE}) where the MTBE half-saturation constant (K_{s-MTBE}) acts as the inhibition constant.

$$\frac{dC_{Donor}}{dt} = -k_{Donor} \cdot X \cdot I_{per} \cdot \left(\frac{C_{Donor}}{K_{s-Donor} \left(1 + \frac{C_{MTBE}}{K_{s-MTBE}} \right) + C_{Donor}} \right) \cdot \left(\frac{C_{Ox}}{K_{s-Ox} + C_{Ox}} \right) \quad (29)$$

Equation 30 below states that the utilization of oxygen or electron acceptor is also affected by the presence of MTBE. The rate of oxygen utilization is also dependent on the rate of production of oxygen due to the disproportionation of hydrogen peroxide into oxygen and water. Additionally, a term is included to capture the effects oxygen used in the decaying cell mass and oxygen exsolving from solution once dissolved oxygen saturation is achieved. If the dissolved oxygen concentration is less than the saturation concentration, the exsolution rate constant (α) is zero (Gandhi *et al.*, 2002b).

$$\begin{aligned} \frac{dC_{Ox}}{dt} = & -k_{Donor} \cdot F \cdot X \cdot I_{per} \cdot \left(\frac{C_{Donor}}{K_{s-Donor} \left(1 + \frac{C_{MTBE}}{K_{s-MTBE}} \right) + C_{Donor}} \right) \cdot \left(\frac{C_{Ox}}{K_{s-Ox} + C_{Ox}} \right) \\ & - d_c \cdot f_D \cdot X \cdot \left(\frac{C_{Ox}}{K_{s-Ox} + C_{Ox}} \right) + \frac{1}{2} \cdot f_{per} \cdot \varepsilon_{disp} \cdot k_{per} \cdot C_{per} - \alpha \cdot (C_{Ox} - C_{Ox}^{Sat}) \end{aligned} \quad (30)$$

Where,

F = mass ratio of oxygen to electron donor used for cell growth

d_c = biomass decay oxygen demand (kg oxygen/kg biomass)

f_d = fraction of cell mass that is degradable

f_{per} = molar mass ratio of oxygen to hydrogen peroxide

ε_{disp} = fraction of hydrogen peroxide disappearance due to disproportionation

α = exsolution rate constant (T^{-1})

C_{ox} = dissolved oxygen concentration (mg/L)

C_{ox}^{sat} = saturation concentration of oxygen in water (mg/L)

Equation 31 below states that the rate of change in MTBE concentration (C_{MTBE}) is proportional to the concentration of MTBE and oxygen; however, the MTBE degradation rate is inhibited by the presence of the primary electron donor or primary substrate (C_{Donor}). Additionally, a coefficient that represents the fraction of biomass that is active toward MTBE cometabolism is included.

$$\frac{dC_{MTBE}}{dt} = -k_{MTBE} \cdot F_A \cdot X \cdot \left(\frac{C_{MTBE}}{K_{s-MTBE} \left(1 + \frac{C_{Donor}}{K_{s-Donor}} \right) + C_{MTBE}} \right) \cdot \left(\frac{C_{Ox}}{K_{s-Ox} + C_{Ox}} \right) \quad (31)$$

Where,

k_{MTBE} = maximum MTBE degradation rate (T^{-1})

F_A = fraction of biomass actively degrading MTBE

Equation 32 below states that the rate of change in hydrogen peroxide concentration follows a first-order rate law and is proportional to a first-order rate constant (k_{per}) and the concentration of hydrogen peroxide (C_{per}). Additionally, this model assumes that there is no reactivity between hydrogen peroxide and other dissolved species (Gandhi *et al.*, 2002b). This assumption is also valid for MTBE since hydrogen peroxide and MTBE do not react as demonstrated by Yeh and Novak (1995) and reported in Section 2.8.1.3.

$$\frac{dC_{per}}{dt} = -k_{per} \cdot C_{per} \quad (32)$$

Finally, the change in fraction of biomass that is actively degrading MTBE is controlled by a process called deactivation. Deactivation is the reduction in enzyme activity due to the absence of a primary substrate (Semprini and McCarty, 1992). In other words, when

the primary substrate is not present the fraction of biomass that can actively degrade MTBE decreases. This process is expressed below in Equation 33.

$$\frac{dF_A}{dt} = -b_d \cdot F_A \quad \text{if } \frac{dX}{dt} < 0, \text{ otherwise } F_A = 1 \quad (33)$$

Where,

b_d = deactivation first-order rate constant (T^{-1})

The parameters and their associated values used by Gandhi *et al.* (2002b) for TCE aerobic cometabolism using toluene as a primary substrate are summarized in Table 18.

Table 18 Summary of Parameters and Values from Gandhi *et al.* (2002)

Parameter	Description	Value	Source
X_i (kg/m ³)	Initial biomass concentration	1.9×10^{-3}	fit ^a
T_c (kg/m)	TCE transformation capacity	0.05	fit ^a
k_{per} (days ⁻¹)	Hydrogen peroxide disproportionation rate constant	22	fit ^a
K_{I-per} (kg/m ³)	Hydrogen peroxide inhibition constant	3.4×10^{-4}	fit ^a
k_T (days ⁻¹)	Maximum TCE degradation rate constant	9.4	fit ^a
Y (kg/kg)	Yield coefficient	0.77	Jenal-Wanner and McCarty (1997)
F (kg/kg)	Mass ratio of oxygen to toluene for biomass growth	2.1	Jenal-Wanner and McCarty (1997)
K_s (kg/m ³)	TCE saturation constant	0.01	Jenal-Wanner and McCarty (1997)
$k_{primary}$ (days ⁻¹)	Maximum toluene utilization rate constant	1.5	Jenal-Wanner and McCarty (1997)
K_{s-Ox} (kg/m ³)	Dissolved oxygen saturation constant	0.001	Semprini and McCarty (1991,1992)
b (day ⁻¹)	Biomass decay coefficient	0.15	Semprini and McCarty (1991,1992)
f_d	Fraction of biomass that is biodegradable	0.8	Semprini and McCarty (1991,1992)
d_c (kg/kg)	Biomass decay oxygen demand	1.42	Semprini and McCarty (1991,1992)
b_d (days ⁻¹)	Biomass deactivation rate constant	1.0	Semprini and McCarty (1991,1992)
f_{per}	Molar mass of oxygen to hydrogen peroxide	0.94	stoichiometry
ϵ	Hydrogen peroxide disproportionation efficiency	1.0	assumed
α (days ⁻¹)	Dissolved oxygen resolution rate constant	100	assumed
C_{Ox}^{Sat} (kg/m ³)	Dissolved oxygen saturation concentration	0.042	Sawyer <i>et al.</i> (1994)
R_{Ox}	Dissolved oxygen retardation factor	1.0	assumed

2.10 HORIZONTAL FLOW TREATMENT WELLS (HFTWS)

2.10.1 OPERATION OF HFTWS

The operating concept and successful use of HFTWs to remediate trichloroethylene-contaminated groundwater *in situ* was previously discussed in Chapter 1.0. HFTWs can be configured to exploit a physical, chemical, or biological process to remediate groundwater. As depicted in Figure 7, an HFTW system utilizing a biological treatment process can effectively treat groundwater by introducing and mixing electron donor and/or acceptor into contaminated groundwater and injecting the mixture into the aquifer matrix where microorganisms, whose growth is stimulated in bioactive zones surrounding the treatment well injection screens, degrade the target contaminant (McCarty *et al.*, 1998). The treatment efficiency of the process is amplified by the recirculation of contaminated groundwater through the HFTW system resulting in lower down gradient concentrations than would be achieved by a single pass of contaminated groundwater through the bioactive zones (McCarty *et al.*, 1998).

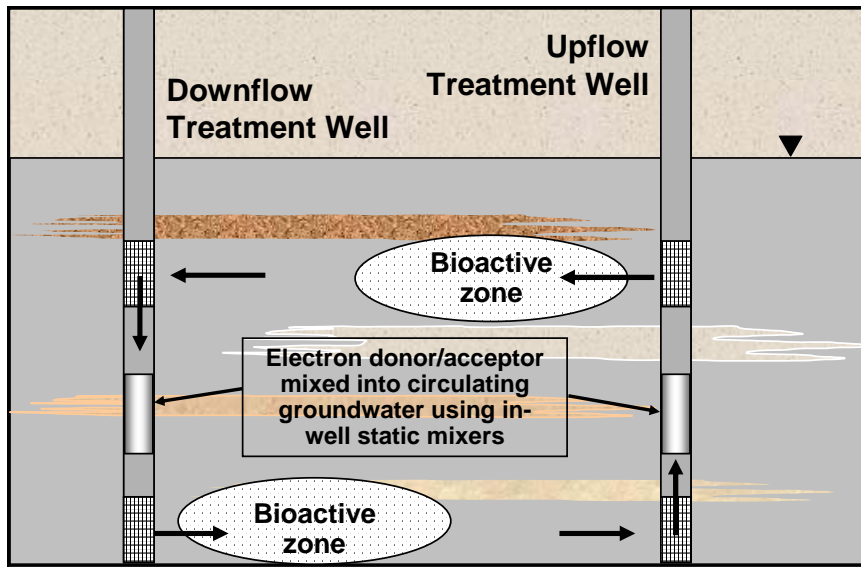


Figure 7 HFTW Operation with Biotic Treatment Processes

The use of HFTWs to remediate contaminated groundwater has been the subject of much research and one pilot study (Stoppel and Goltz, 2003; Parr *et al.*, 2003; McCarty *et al.*, 1998). Using a pair of HFTWs, McCarty *et al.* 1998 demonstrated biodegradation of trichloroethene (TCE) in contaminated groundwater at Site 19, Edwards Air Force Base. At this site, HFTWs were used to mix an electron donor (toluene) and oxidizing agents (hydrogen peroxide and oxygen) into TCE-contaminated groundwater. Goltz *et al.* (2001) demonstrated the effects of the electron donor injection schedule on the growth of microorganisms near the well screens. Goltz *et al.* (2001) suggest that high donor concentration injected with short pulses minimizes microbial growth near the well screens and reduces competitive inhibition (Goltz *et al.*, 2001).

2.10.2 MODELING HFTW OPERATION

Several models (both analytical and numerical) have been used to describe the groundwater flow field induced by operation of HFTWs. Typically, numerical models are used to describe groundwater flow for complex initial and boundary conditions, and under anisotropic and heterogeneous conditions. Analytical models require simplifying assumptions such as isotropy, homogeneity, and steady state flow conditions to solve the differential equations describing groundwater flow. The purpose of this section is to present models that simulate the operation of the HFTW system to include groundwater flow and contaminant fate and transport.

2.10.2.1 ANALYTICAL MODELS

An analytical model that has been used to describe the remediation of TCE-contaminated groundwater using a multiple injection and extraction well system to simulate HFTW operation was developed by Christ *et al.* (1999). In order for this model to simulate the groundwater flow induced by HFTW operation, two-dimensional horizontal flow must be assumed. Vertical flow of water would result in water flowing directly from the discharge screen to the intake screen of a single well. This short-circuiting results in significant loss of treatment efficiency, as contaminated water flowing vertically may be present in the bioactive zones for an insufficient time for adequate degradation to occur. Fortunately, typical aquifer horizontal hydraulic conductivity is often at least an order of magnitude larger than vertical hydraulic conductivity (Domenico and Schwartz, 1998). Thus, short-circuiting during HFTW

operation would be minimal and it is reasonable to assume horizontal flow to model HFTW operation.

Interflow between the treatment wells of the HFTW system dictates the overall treatment efficiency and capture zone width for the HFTW system. Interflow is simply the proportion of water entering an extraction well that originated from an adjacent injection well. Christ *et al.* (1999) present methods for determining well interflow based on properties of the aquifer (hydraulic conductivity, hydraulic gradient, aquifer thickness) and well operation parameters (pumping rate, well spacing). Details on the methods used to determine interflow can be found in Christ *et al.* (1999).

The treatment efficiency and capture zone width are critical variables for design of an HFTW system. The overall treatment efficiency (η_{overall}) of the HFTW system is essentially a comparison of upgradient and downgradient concentrations of contaminant, C_{up} and C_{down} respectively where,

$$\eta_{\text{overall}} = 1 - \frac{C_{\text{down}}}{C_{\text{in}}} \quad (34)$$

The capture zone width of the HFTW system is a measurement of the extent of the contaminant plume that will be captured by the operation of the HFTW.

Figure 8 depicts the upgradient and downgradient contaminant concentrations and the capture zone width in the upper portion of an aquifer for a two-well HFTW system. Thus incorporating the aquifer properties and well operation parameters with knowledge of the degradation properties of the process employed in the HFTW system one can analytically solve for the capture zone width and overall treatment efficiency of the HFTW system.

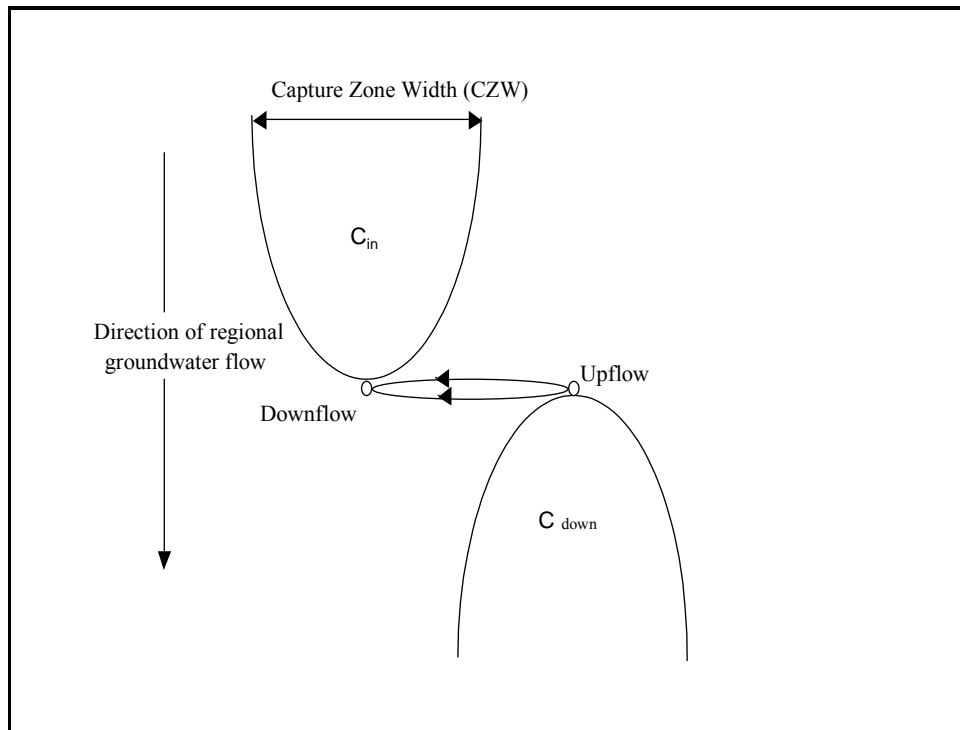


Figure 8 Plan View of Upper Aquifer Region of a 2-Well HFTW System (After Stoppel, 2001)

2.10.2.2 NUMERICAL MODELS

Two numerical models have been developed to describe the flow and transport of groundwater and contaminants in an HFTW system. Huang and Goltz (1998) and Gandhi *et al.* (2002a;b) developed models that were used to describe the aerobic biodegradation of TCE using an HFTW system. Both Huang and Goltz (1998) and Gandhi *et al.* (2002a;b) models are three-dimensional models that incorporate steady-state flow, advective/dispersive transport, rate-limited or equilibrium sorption, and biodegradation.

The Huang and Goltz (1998) model uses MODFLOW (Harbaugh and McDonald, 1996) to calculate the steady-state flow field induced by HFTW operation coupled to a FORTRAN code to describe the fate and transport of dissolved species. The fate and

transport model used by Huang and Goltz (1998) uses a finite difference technique to solve the three-dimensional partial differential equations that describe the advective/dispersive transport of the dissolved species (the target compound (TCE), electron donor (toluene), and acceptor (oxygen)) with a fate term to describe aerobic cometabolic degradation of the TCE. The fate term incorporates a dual-Monod kinetic model that describes the destruction of TCE influenced by the presence of an electron donor and acceptor, where the presence of the donor competitively inhibits TCE degradation. Microorganisms are assumed to be immobile (Huang and Goltz, 1998).

The three-dimensional grid used to represent the conditions of the aquifer can be created manually using Visual MODFLOW. The particular characteristics of the grid such as cell size and cell composition can be modified to accommodate the specifics of the system being investigated. Figure 9 is an example of a three-dimensional finite difference grid. The boundary conditions of the grid along with well location and pumping rates are input into MODFLOW which uses the input to calculate the steady-state velocity and hydraulic head fields. The fate and transport portion of the model then uses the groundwater velocity information with the initial and boundary conditions of the dissolved species to describe the concentration of dissolved components spatially and temporally. System performance can be observed and assessed by determining component concentrations at any location and time within the grid.

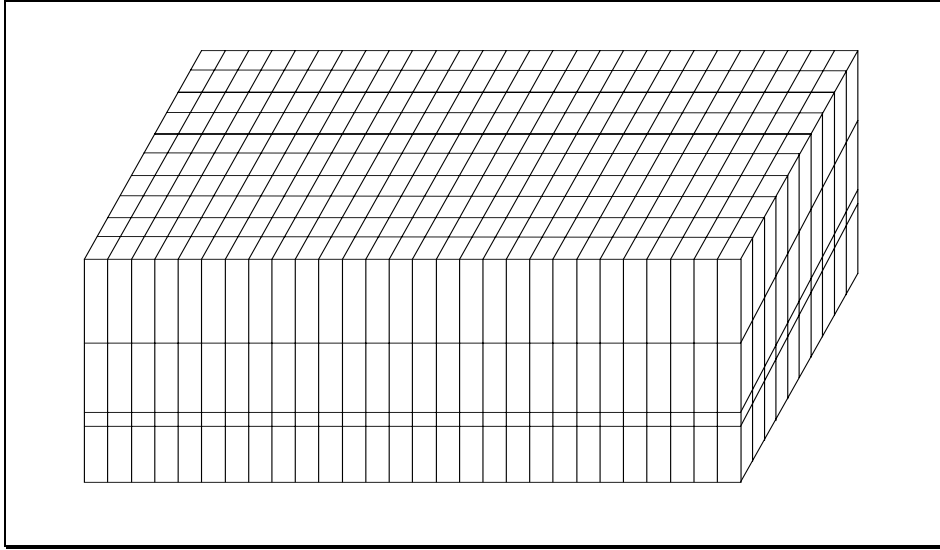


Figure 9 Sample of Finite-Difference Three-Dimensional Grid (From Garrett (1999))

The model developed by Gandhi *et al.* (2002a) is similar to the model just described. The primary differences between the two models are that the Gandhi *et al.* (2002a; b) model uses a finite element technique which accommodates higher cell resolution near the wells. Analysis of the model by Gandhi *et al.* (2002b) indicated that despite the heterogeneity of the aquifer, the model sufficiently described the flow field induced by the operation of the HFTW system. In addition, the results of the study indicate that the impact of heterogeneity on system performance is minimized by the flow field induced by HFTW operation (Gandhi *et al.* (2002b).

3.0 METHODOLOGY

3.1 OVERVIEW

The purpose of this chapter is to select an appropriate process from those discussed in Chapter 2.0 to incorporate into an HFTW system to manage subsurface MTBE contamination. Once a process is selected, a submodel that can be used to represent the process will be developed and then coupled with the hydraulic flow model that simulates the groundwater flow field induced by HFTW operation. The two models coupled together, referred to as the technology model, will be used to represent the *in situ* treatment of MTBE-contaminated groundwater. Verification of the model will be accomplished by individually executing the components of the model to ensure the model is behaving as expected. Finally, in order to answer the research question of how the technology will perform at an MTBE-contaminated site, a sensitivity analysis using the model will be conducted, to ascertain technology performance under various site and contaminant conditions.

3.2 PROCESS SELECTION

The purpose of this section is to evaluate and select an appropriate physicochemical or biological process for further study. Selection of the appropriate physicochemical or biological process for incorporation into an HFTW system will be accomplished through evaluation of each process using a defined set of criteria. The following section will detail the criteria used for evaluating the processes and the

subsequent evaluation of the processes against the criteria. Finally, an appropriate process(es) will be identified for further study.

3.2.1 PROCESS EVALUATION CRITERIA

The criteria for evaluation of degradation processes include: regulatory requirements, in-well applicability, applicability under varying site conditions, and maturity. These criteria are expanded and adapted from criteria established by the Federal Remediation Round Table (FRTR), Remediation Technologies Screening Matrix and Reference Guide, v. 4.0 (FRTR, 2003). Each criterion will be defined in order to provide a baseline for evaluation of the processes. Additionally, the evaluation measures for each respective criterion will be discussed.

The process evaluation criteria include:

- (1) Regulatory requirements - include the ability of the process to degrade MTBE to achieve regulatory cleanup goals. In addition, the process must be likely to obtain regulatory approval for use. For example, a process that requires addition of hazardous materials to an aquifer is unlikely to obtain regulator approval, and therefore would fail this criterion. For purposes of this evaluation, the MTBE cleanup goal will be established at 5 µg/L, which is below the EPA, MTBE drinking water advisory of 20 to 40 µg/L and is at or below all states' maximum contaminant levels (MCLs). Evaluation on this criterion will be pass/fail based on published results from studies of the process' ability to degrade MTBE to or below 5 µg/L and the process' ability to degrade intermediates produced during the degradation of MTBE (primarily, TBA and TBF). Processes that have not demonstrated through lab,

pilot, and/or field study the ability to degrade MTBE and its intermediates fail this criterion.

- (2) In-well applicability - involves the feasibility of implementing a process as an in-well component of an HFTW system. The primary consideration here is that the process must physically be able to be installed for use in an HFTW treatment well. To apply this criterion we will assume that we either must be able to emplace a reactor inside the HFTW treatment well or we must be able to mix a reactant into contaminated groundwater flowing through the treatment well, in order to promote a chemical or biochemical reaction in the aquifer matrix outside the HFTW injection screens. Evaluation on this criterion will be pass/fail based on the ability to readily install and implement a process in-well. A process that would require significant research and development to accommodate an in-well application would fail this criterion.
- (3) Applicability under varying site conditions - requires evaluation of how sensitive process performance is to varying site conditions (*i.e.* contaminant concentrations, groundwater chemistry, site location). Each process will be evaluated against this criterion based on observed effects that have been reported in the literature. The ability of each process to perform well under varying conditions will be rated low or high. A rating of low will be assigned to a process if its efficiency is highly dependant on or requires alteration of the groundwater chemistry or physical properties, or requires the addition of non-native microorganisms. Additionally, a process that produces undesirable byproducts from reaction with other dissolved species that may be present at various sites (*e.g.* bromide to bromate) would also receive a low rating for this criterion. A rating of high will be assigned to a process

that only requires the addition of nutrients, oxidants, electron donor, and/or electron acceptor, that's efficiency is not greatly effected by groundwater chemistry, and does not result in undesirable byproduct production.

- (4) Maturity of the process - requires evaluation to determine how well the process is understood and how confident we are that the process can be successfully implemented and modeled. A mature, well-studied, process will have lots of laboratory and field data available, commercially available solutions, and is presumably well-understood. Each process will be evaluated against this criterion based on the literature. The maturity of each process will be rated low, moderate, or high. Ratings will be assigned based on the extent to which the process has been studied; where, a low rating will be assigned to a process that has been demonstrated in laboratory study only, a moderate rating will be assigned to a process that has been demonstrated in laboratory and pilot study, and a high rating will be assigned to a process that has been demonstrated in laboratory and pilot study as well as full scale implementation.

3.2.2 PROCESS EVALUATION

In this section each process will be evaluated using the criteria discussed previously and a process will be selected for further study. Table 19 summarizes the evaluations of the treatment processes. Following is a discussion of each process explaining the reason for assigning unfavorable ratings.

Table 19 Evaluation of Treatment Processes

	Criteria					Comments
	Meets Regulatory Requirements	In Well Applicability	Applicability Under Varying Site Conditions	Maturity		
Processes	<i>Oxygen</i>	N/A	PASS	N/A	LOW	In laboratory research stage
	<i>Ozone</i>	PASS	PASS	LOW	HIGH	May produce undesirable by-product (bromate)
	<i>Fenton's Reagent</i>	N/A	PASS	LOW	LOW	Rate of reaction is highly dependent on groundwater chemistry
	<i>Persulfate</i>	N/A	PASS	LOW	LOW	Rate of reaction is highly dependent on groundwater physiochemical properties
	<i>Permanganate</i>	FAIL	PASS	HIGH	LOW	Intermediate build-up and persistence
	<i>Ozone/H₂O₂</i>	PASS	PASS	LOW	MOD	May produce undesirable by-product (bromate)
	<i>UV</i>	PASS	FAIL	HIGH	LOW	Not appropriate for in-well application at this time
	<i>Ultrasound</i>	PASS	FAIL	HIGH	LOW	Not appropriate for in-well application at this time
	<i>Gamma</i>	PASS	FAIL	HIGH	MOD	Not appropriate for in-well application at this time
	<i>Plasma</i>	PASS	FAIL	HIGH	LOW	Not appropriate for in-well application at this time
	<i>Hydrolysis</i>	FAIL	FAIL	LOW	LOW	Rate of reaction is highly dependent on groundwater pH; In laboratory research stage
	<i>Aerobic Direct Metabolism</i>	PASS	PASS	LOW	HIGH	MTBE-degrading aerobes are not ubiquitous
	<i>Aerobic Cometabolism</i>	PASS	PASS	HIGH	HIGH	Alkane-degrading aerobes well distributed
	<i>Anaerobic Metabolism</i>	N/A	PASS	LOW	LOW	Minimal degradation under methanogenic conditions

N/A – information required for evaluation not available in literature

3.2.2.1 OXIDATION BY OXYGEN

The oxidation of MTBE by molecular oxygen was shown to be too slow even though the reaction is thermodynamically favorable. To speed the oxidation process, bifunctional aluminum has been used (Lien and Wilkin, 2002b). However, due to the infancy of the research in this particular process, it remains to be seen that this oxidation process is capable of completely mineralizing MTBE or reducing MTBE concentrations to below the target concentration of 5 µg/L. Nor is there any information available that indicates that this process would be suitable under varying geochemical conditions. Also, results of the study by Lien and Wilkin (2002b) indicate that intermediates produced during the oxidation of MTBE may accumulate in solution. Due to these factors, this process does not meet the criteria necessary for use in this study.

3.2.2.2 OXIDATION BY OZONE

The oxidation of MTBE by ozone has shown success at least at one MTBE-contaminated site as described by Kerfoot and LeCheminant (2003). Ozone sparging resulted in reducing MTBE concentrations around most of the sparge points by 71 to 99%; additionally, TBA was also oxidized in the presence of ozone. Unfortunately, ozonation of groundwater can result in the production of dangerous byproducts including bromate (Kelley *et al.*, 2003). As a result, ozonation is not applicable under varying site conditions. Due to these factors, this process does not meet the criteria necessary for use in this study.

3.2.2.3 OXIDATION BY FENTON'S REAGENT

Oxidation of MTBE by FR is capable of reducing MTBE concentrations to at least the lower limit of the EPA's drinking water advisory for MTBE of 20 µg/l (Ray *et al.*, 2002). Despite the evidence from laboratory study by Ray *et al.* (2002), there is no evidence available in the literature to indicate that FR can oxidize MTBE below 5 µg/L. Additionally, several studies have indicated that the FR oxidation process is most effective at pH of 2 to 5, which may preclude its use at various sites (Yeh and Novak, 1995; Burbano *et al.*, 2002; Ray *et al.*, 2002). Due to these factors, this process does not meet the criteria necessary for use in this study.

3.2.2.4 OXIDATION BY PERSULFATE

The oxidation of MTBE by persulfate appears to be limited at ambient temperatures and is greatly affected by groundwater chemistry as indicated in the study by Huang *et al.* (2002). Despite its relatively high oxidation potential, there is no evidence available indicating that persulfate is able to oxidize MTBE below 5 µg/L. Due to these factors, this process does not meet the criteria necessary for use in this study.

3.2.2.5 OXIDATION BY PERMANGANATE

Oxidation of MTBE by permanganate results in the production of TBA which is not further oxidized (Damm *et al.*, 2002). As a result of the TBA production and inability to further oxidize the intermediates of MTBE degradation, oxidation by permanganate fails the criterion to meet regulatory requirements. Due to this factor, this process will not be considered for further investigation in this study.

3.2.2.6 OXIDATION BY OZONE AND HYDROGEN PEROXIDE

Oxidation of MTBE by ozone/hydrogen peroxide appears to be a promising technology that may be applied to remediate MTBE-contaminated groundwater below regulatory limits; however, the ozone used in this process may still react with background species producing undesirable byproducts such as bromate (Acero *et al.*, 2001; Mitani *et al.*, 2001; Liang *et al.*, 2001). Thus, oxidation by ozone/hydrogen peroxide only achieves a low score for applicability under varying site conditions. Due to this factor, this process does not meet the criteria necessary for use in this study.

3.2.2.7 OXIDATION BY UV IRRADIATION

Current state of the technology is not appropriate for in-well application. Due to this factor, this process does not meet the criteria necessary for use in this study.

3.2.2.8 OXIDATION BY ULTRASOUND IRRADIATION

Current state of the technology is not appropriate for in-well application. Due to this factor, this process does not meet the criteria necessary for use in this study.

3.2.2.9 OXIDATION BY GAMMA IRRADIATION

Current state of the technology is not appropriate for in-well application. Due to this factor, this process does not meet the criteria necessary for use in this study.

3.2.2.10 OXIDATION BY DENSE MEDIUM PLASMA

Current state of the technology is not appropriate for in-well application. Due to this factor, this process does not meet the criteria necessary for use in this study.

3.2.2.11 HYDROLYSIS

Ordinary acid hydrolysis of MTBE does not occur at environmental pH (O'Reilly *et al.*, 2001); however, studies by Centi *et al.* (2001) and Centi and Parathoner (2003) indicate that the acid hydrolysis of MTBE can be accomplished at environmental conditions by using acid zeolites. Unfortunately, though, this process results in the production of TBA which is not subsequently hydrolyzed by the acid zeolites. Thus this process does not pass the requirement to meet regulatory requirements. Also, research on the hydrolysis of MTBE is limited to laboratory study only. Due to these factors, this process does not meet the criteria necessary for use in this study.

3.2.2.12 AEROBIC DIRECT METABOLISM

Aerobic direct metabolism has demonstrated success in being able to remediate MTBE-contaminated groundwater to below regulatory limits (Wilson, 2003). As for in-well applicability, *in situ* bioremediation lends itself well to application in an HFTW system as has been demonstrated by McCarty *et al.* (1998). McCarty *et al.* (1998) showed that both an electron acceptor and donor could be added into contaminated groundwater flowing through HFTWs, to biostimulate bacteria to degrade the contaminant in bioactive zones that were established around the HFTW treatment well injection screens.

Studies have shown that microorganism that directly metabolize MTBE occur naturally in the environment (Hristova *et al.*, 2003); although, microorganisms capable of directly metabolizing MTBE may not be ubiquitous in the environment. This, unfortunately, reduces the viability of this process to be applied at various sites where

conditions (*i.e.* microorganism populations) may not support its application. For this reason, aerobic direct metabolism receives a low rating for applicability under varying site conditions.

Biostimulation to treat MTBE-contaminated groundwater is a relatively mature technology. *In situ* bioremediation by biostimulation is well-documented in literature and has been practiced at many MTBE-contaminated sites, as discussed in Section 2.8.2 of Chapter 2.0. Additionally, the materials needed to implement direct metabolism biostimulation (*i.e.* oxygen, hydrogen peroxide) are readily available on the open market. Due to these factors, this process meets the criteria necessary for use in this study.

3.2.2.13 AEROBIC COMETABOLISM

Aerobic cometabolism has also demonstrated the ability to degrade MTBE below regulatory limits (ESTCP, 2003a). As another form of *in situ* bioremediation, aerobic cometabolism also lends itself well to application in an HFTW system, as discussed in the previous section on aerobic direct metabolism. Studies have shown that aerobes that cometabolize MTBE occur naturally in the environment, thus allowing this process to be used at various sites (Steffan *et al.*, 1997). The cometabolic degradation of MTBE may be stimulated simply by amending the groundwater with oxygen and a primary growth substrate such as propane.

Like direct metabolism, cometabolism is a relatively mature technology that has also been well studied and documented in the literature. Likewise, the materials needed to implement cometabolic biostimulation (*i.e.* oxygen, hydrogen peroxide, and propane) are also readily available on the open market from a variety of vendors. Due to these factors, this process meets the criteria necessary for use in this study.

3.2.2.14 ANAEROBIC METABOLISM

Studies have shown that MTBE-degrading anaerobes (Finneran and Lovely, 2001), occur naturally in the environment but this process is just now gaining more attention as a viable remediation strategy. There are no studies that indicate that the anaerobic metabolism of MTBE is capable of degrading MTBE below regulatory limits. Additionally, anaerobic metabolism may not be appropriate at various sites due to the lack of degradation that has been observed under methanogenic conditions (Bradley *et al.*, 2001a). Due to these factors, this process does not meet the criteria necessary for use in this study.

3.2.3 PROCESS SELECTION

The purpose of this section is to identify the process selected for further study. The primary considerations as to why a process will or will not be considered for further study will be discussed. Table 20 provides a summary of the selection process.

Table 20 Summary of Process Selection

Process	Considerations	Status
<i>Aerobic Direct Metabolism</i>	Demonstrated ability to meet regulatory requirements; successful implementation at many sites; easily integrated in existing HFTW model code	Selected for further study
<i>Aerobic Cometabolism</i>	Demonstrated ability to meet regulatory requirements; successful implementation at many sites; potential for universal application; easily integrated in existing HFTW model code	Selected for further study

Eleven physicochemical treatment processes were evaluated for use in this study in the previous section. Processes such as UV irradiation, gamma irradiation, ultrasound

irradiation, and the dense medium plasma reactor, would require significant modification to be suitable for in-well application. Quite simply, attempting to modify these technologies for in-well application would pose too great a risk of failure. Alternatively, other degradation processes such as hydrolysis, oxidation processes including oxidation by oxygen, ozone, persulfate, permanganate, FR, and ozone and hydrogen peroxide, and anaerobic metabolism also have shortcomings that would result in incomplete degradation, and/or production of dangerous byproducts.

Based on the above discussion, *in situ* MTBE aerobic biodegradation (both direct and cometabolic) has been selected as the process that has the best likelihood of success for managing MTBE-contaminated groundwater using an HFTW system. Therefore, this study will investigate the effectiveness of the technology while using either aerobic direct metabolism or aerobic cometabolism of MTBE.

In the study of direct metabolism of MTBE, we will assume that MTBE-degrading aerobes are present and MTBE-degradation is limited only by the absence of oxygen. For this situation, oxygen will be amended to the contaminated groundwater by injecting hydrogen peroxide which rapidly breaks down into oxygen and water. Hydrogen peroxide is also used to inhibit excessive biomass growth near the well screens which could lead to well screen fouling (McCarty *et al.*, 1998).

Alternatively, to investigate the technology effectiveness at sites where MTBE-degrading aerobes are not present, the cometabolic degradation of MTBE will be investigated. It will be assumed that despite the absence of MTBE-degrading aerobes, propane-oxidizing bacteria capable of fortuitous oxidation, or cometabolic degradation, of MTBE are indeed present. In this situation, the factors limiting aerobic cometabolism

of MTBE are the absence of a suitable growth and energy substrate and oxygen; therefore, both propane and hydrogen peroxide will be injected into the contaminated groundwater. Again, hydrogen peroxide will be used for its bactericidal and oxygen releasing properties. Below, we discuss how we will model this technology, in order to evaluate its potential.

3.3 SUBMODEL

Having selected the direct and cometabolic MTBE-degradation processes for in-well implementation as a component of an HFTW system, we are now ready to model the processes. The purpose of this section is to evaluate the applicable models discussed in Section 2.9 of Chapter 2.0 with regard to model assumptions and limitations, and ultimately select the most appropriate model and model parameters for further study and incorporation into a full HFTW technology model.

3.3.1 SUBMODEL EVALUATION

First-order, Monod, and dual-Monod kinetics can all be used to describe the kinetics of biodegradation. Recent studies by Wilson *et al.* (2002) and Martinez-Prado *et al.* (2003) used first-order and Monod kinetics with inhibition to model direct and cometabolic MTBE-biodegradation, respectively. Dupasquier *et al.* (2002) used a dual-Monod model that incorporates competitive inhibition to model MTBE-biodegradation. Additionally, dual-Monod kinetics have also been used to model cometabolic degradation of other compounds such as TCE (Gandhi *et al.*, 2002b).

As discussed in Chapter 2.0, we have seen that first-order models offer a simple representation of MTBE degradation kinetics, making the assumption that the degradation rate is only proportional to the concentration of MTBE itself, and that the rate is unaffected by the availability of any other reactant or catalyst. Monod models, on the other hand, allow us to simulate MTBE degradation kinetics as a first-order process when MTBE concentrations are low and therefore availability of co-reactants or catalysts is virtually unlimited, that transitions to a zero-order process when MTBE concentrations increase and co-reactant or catalyst availability becomes limiting. A dual-Monod model allows us to explicitly model the availability of electron acceptor (in addition to the availability of MTBE, the electron donor) using Monod kinetics. The Monod models of electron donor (and acceptor) degradation can also be coupled to a Monod model of microbial cell growth. In addition to simulating direct MTBE metabolism, Monod and dual-Monod models can be adapted to simulate cometabolic degradation with or without competitive inhibition. Note that a dual-Monod model is the most general description of reaction kinetics that we've discussed, and depending on choice of parameters, can be used to simulate either Monod or first-order kinetics.

3.3.2 SUBMODEL SELECTION

For the reasons discussed above, a dual-Monod model will be used in conjunction with the selected HFTW flow and transport model. A dual-Monod model that can be used to simulate MTBE biodegradation as part of an HFTW system can readily be developed by slightly modifying the model of Gandhi *et al.* (2002b) that has been already used to simulate aerobic cometabolic bioremediation of TCE in an HFTW system, as

described in Section 2.10 of Chapter 2.0. By appropriate choice of model parameters, the Gandhi *et al.* (2002b) model may be used to simulate both direct and cometabolic oxidation of MTBE. The specific parameters that must be changed and their respective values will be discussed later in Section 3.5.1.

3.3.3 SUBMODEL ASSUMPTIONS

- (1) Biomass yield (Y) and decay rate (b) vary among and between MTBE-oxidizing and propane-oxidizing microorganisms. In order to eliminate unnecessary detail, an assumed representative value of both the biomass yield (Y) and decay rate (b) for the direct metabolism study will be selected; likewise, for the cometabolism study an assumed representative value of both parameters will also be selected.
- (2) The kinetic parameters selected for study including substrate utilization rate (k and k_{MTBE}) and half-saturation constants (k_{s-MTBE} , $k_{s-primary}$, and $k_{s-Oxygen}$) were taken from literature. To the author's knowledge, only one dual-Monod kinetic study has been conducted on the biodegradation of MTBE to this date; therefore, is the only source of dual-Monod kinetic parameters available from literature. It will be assumed that Monod kinetic parameters available from other studies can be utilized in a dual-Monod model. This assumption based on the relationship that as electron donor concentrations decrease, the kinetic rate of biodegradation and cell growth will also decrease, thus justifying the use of dual-Monod kinetics with available Monod kinetic parameters.
- (3) It will be assumed that all dissolved species are non-sorbing.

- (4) Microorganisms, hydrogen peroxide, oxygen, MTBE, and propane are the only groundwater components incorporated into the model.
- (5) It will be assumed that hydrogen peroxide does not react with MTBE or any other dissolved species (Yeh and Novak, 1995).
- (6) The electron acceptor used for MTBE direct and cometabolic oxidation will be oxygen.
- (7) The electron donor used to stimulate cometabolic MTBE degradation will be propane.

In both laboratory and field studies, propane has been the alkane most commonly used to promote cometabolic oxidation of MTBE, as indicated in Section 2.8.2.2. Additionally, propane is readily available and is relatively inexpensive.
- (8) MTBE-degrading or propane-degrading microorganisms will be assumed to be ubiquitous at an initial minimum natural population evenly distributed throughout the aquifer matrix prior to biostimulation (Kane *et al.* (2001); Hristova *et al.* (2003); Perry (1980); Steffan *et al.* (1997)).
- (9) It will be assumed that the hydrogen peroxide inhibition constant identified by Gandhi *et al.* (2002b) to model TCE-degrading microorganisms is equal to the hydrogen peroxide inhibition constant for MTBE-degrading microorganisms.

3.3.4 SUBMODEL LIMITATIONS

This model does not incorporate the production and subsequent degradation of the breakdown products of MTBE. The presence and degradation of the breakdown products could potentially impact the rate of MTBE degradation, but for the purpose of this study, these potential effects will not be considered.

3.4 FLOW AND TRANSPORT MODEL

Both analytical and numerical models can be used to describe contaminant fate and transport in the groundwater flow field induced by the operation of an HFTW system, as discussed in Chapter 2.0. The numerical model developed by Huang and Goltz (1998) and described in Section 2.10.2.2 to simulate HFTW operation to cometabolically degrade TCE in groundwater is selected for use in this research. The numerical model developed by Huang and Goltz (1998) is selected for the following reasons:

- Suitability for integration with the non-linear MTBE biodegradation submodel
- Ability to track several components including MTBE, oxygen, hydrogen peroxide, propane, and microorganisms
- Ability to simulate anisotropic and heterogeneous conditions
- Ease of obtaining computer code and technical support from the model developers

The selected three-dimensional model incorporates advective/dispersive transport of dissolved components under steady-state flow conditions, and biodegradation. The model assumes that the microorganisms are attached to the aquifer material, and thus are stationary. The following Equations 35 through 38 represent the fate and transport of the dissolved species (C_{Donor} , C_{MTBE} , C_{Ox} , and C_{per}) including a source/sink term (r_{Donor} , r_{MTBE} , r_{Ox} , and r_{per}) that represents production/decay of the respective species.

$$\frac{\partial C_{Donor}}{\partial t} = D \cdot \nabla^2 C_{Donor} - v \cdot \nabla C_{Donor} + r_{Donor} \quad (35)$$

$$\frac{\partial C_{MTBE}}{\partial t} = D \cdot \nabla^2 C_{MTBE} - v \cdot \nabla C_{MTBE} + r_{MTBE} \quad (36)$$

$$\frac{\partial C_{Ox}}{\partial t} = D \cdot \nabla^2 C_{Ox} - v \cdot \nabla C_{Ox} + r_{Ox} \quad (37)$$

$$\frac{\partial C_{per}}{\partial t} = D \cdot \nabla^2 C_{per} - v \cdot \nabla C_{per} + r_{per} \quad (38)$$

The steady-state flow field velocity (v) is computed by the program MODFLOW (Harbaugh and McDonald, 1996) and then used in the fate and transport model. Dispersion (D) will be modeled using numerical dispersion. Because the primary focus of this research is to simulate MTBE transport and biodegradation, and dispersion is only a secondary process in that regard, numerical dispersion is assumed to adequately describe the process. Numerical dispersion occurs in the model as a result of truncation errors in the finite difference solution of the transport equations (35 through 38) (Charbeneau, 2000). Dispersion can be estimated in the x, y, and z directions as

$$D_{x,y,z} = \frac{v_{x,y,z} \Delta(d_{x,y,z})}{2} + \frac{(v_{x,y,z})^2 \Delta t}{2} \quad (39)$$

where $v_{x,y,z}$ are the groundwater velocities in the x, y, and z directions, $\Delta d_{x,y,z}$ is the cell size in the x, y, and z directions and Δt is the time step (Charbeneau, 2000). The transport model partial differential equations are solved using a self-adaptive, partial implicit finite difference technique.

3.5 TECHNOLOGY MODEL

The technology model combines the process submodel with the transport model. As discussed previously, the process submodel selected for further study is the dual-Monod model modified from Gandhi *et al.* (2002b). The biological degradation of the dissolved species is incorporated into the flow and transport equations as the sink term on the right side of the Equations 35-38. The terms r_{Donor} , r_{Ox} , r_{per} , and r_{MTBE} are calculated from Equations 40-43 respectively:

$$r_{Donor} = \frac{dC_{Donor}}{dt} = -k_{Donor} \cdot X \cdot I_{per} \cdot \left(\frac{C_{Donor}}{K_{S-Donor} \left(1 + \frac{C_{MTBE}}{K_{S-MTBE}} \right) + C_{Donor}} \right) \cdot \left(\frac{C_{Ox}}{K_{S-Ox} + C_{Ox}} \right) \quad (40)$$

$$r_{Ox} = \frac{dC_{Ox}}{dt} = -k_{Donor} \cdot F \cdot X \cdot I_{per} \cdot \left(\frac{C_{Donor}}{K_{S-Donor} \left(1 + \frac{C_{MTBE}}{K_{S-MTBE}} \right) + C_{Donor}} \right) \cdot \left(\frac{C_{Ox}}{K_{S-Ox} + C_{Ox}} \right) - d_c \cdot f_D \cdot X \cdot \left(\frac{C_{Ox}}{K_{S-Ox} + C_{Ox}} \right) + \frac{1}{2} \cdot f_{per} \cdot \varepsilon_{disp} \cdot k_{per} \cdot C_{per} - \alpha \cdot (C_{Ox} - C_{Ox}^{Sat}) \quad (41)$$

$$r_{per} = \frac{dC_{per}}{dt} = -k_{per} \cdot C_{per} \quad (42)$$

$$r_{MTBE} = \frac{dC_{MTBE}}{dt} = -k_{MTBE} \cdot F_A \cdot X \cdot \left(\frac{C_{MTBE}}{K_{S-MTBE} \left(1 + \frac{C_{Donor}}{K_{S-Donor}} \right) + C_{MTBE}} \right) \cdot \left(\frac{C_{Ox}}{K_{S-Ox} + C_{Ox}} \right) \quad (43)$$

where F_A is the fraction of biomass active towards MTBE degradation and is described by the following equation.

$$\frac{dF_A}{dt} = -b_d \cdot F_A \text{ if } \frac{dX}{dt} < 0, \text{ otherwise } F_A = 1 \quad (44)$$

The microbial growth equation is:

$$\frac{dX}{dt} = k_{Donor} \cdot Y \cdot X \cdot I_{per} \cdot \left(\frac{C_{Donor}}{K_{S-Donor} \left(1 + \frac{C_{MTBE}}{K_{S-MTBE}} \right) + C_{Donor}} \right) \cdot \left(\frac{C_{Ox}}{K_{S-Ox} + C_{Ox}} \right) - b \cdot X \cdot \left(\frac{C_{Ox}}{K_{S-Ox} + C_{Ox}} \right) \quad (45)$$

where the inhibition due to the presence of hydrogen peroxide (I_{per}) is described by the following equation.

$$I_{per} = \frac{K_{i-per}}{K_{i-per} + C_{per}} \quad (46)$$

Additionally, the following equation acts as a switch to prevent the population of active microorganisms from completely decaying to zero in areas where there is no electron donor or acceptor present.

$$\frac{dX}{dt} = 0; X \leq X_{min} \quad (47)$$

Limiting the indefinite loss of microorganisms is in accordance with the assumption that microorganisms able to degrade MTBE directly or cometabolically exist at some minimum natural population regardless of the presence or absence of electron donor and electron acceptor.

The reaction submodel differential equations are solved using a Runge-Kutta integration technique. For more information about the submodel equations, the reader is directed to Chapter 2.0, Section 2.9.5 where the equations are discussed in detail.

3.5.1 KINETIC PARAMETERS

The kinetic parameters identified in the literature for direct and cometabolic degradation of MTBE span a range of values. In particular, substrate utilization rates (k_{Donor} and k_{MTBE}), half-saturation constants (K_{S-MTBE} , $K_{S-Donor}$, and K_{S-Ox}), biomass yield

(Y), and decay rate (b) vary significantly between studies. These parameters are summarized in Section 2.9 of Chapter 2.0. For the purpose of this study, selected baseline parameter values are the median or mean values of those reported in the literature for each parameter. The baseline median value is used when the range of values for the parameter is skewed due to unusually high or low reported values from literature. The baseline mean value is used when the range of values are not skewed and appear to be normally distributed. Kinetic parameters for direct and cometabolic degradation simulations are summarized below in Table 21 and Table 22, respectively.

Table 21 Baseline Kinetic Parameters Used in Direct Metabolism Simulations

Parameter	Description	Range	Baseline Value	Source
k_{Donor}	Maximum donor utilization rate constant	0.074 - 6 g/g cells/day	0.87 g/g cells/day [†]	Table 11, Ch 2
$K_{S-Donor}$	Donor half-saturation constant	0.33 - 50 mg/L	3.5 mg/L [†]	Table 11, Ch 2
K_{S-Ox}	Oxygen half-saturation constant	0.9 - 3 mg/L	2.0 mg/L [‡]	Table 11, Ch 2
K_{I-per}	Hydrogen peroxide inhibition constant	-	0.34 mg/L	Gandhi <i>et al.</i> (2002b)
k_{per}	Hydrogen peroxide decay rate	-	22 day ⁻¹	Gandhi <i>et al.</i> (2002b)
Y	Biomass yield	0.11 to 0.44 g cells/g MTBE utilized	0.3 g cells/g MTBE utilized [‡]	Table 12, Ch 2
b	Biomass decay rate	0.072 - 0.12 day ⁻¹	0.096 day ⁻¹ [‡]	Table 13, Ch 2
X	Initial biomass concentration	-	1.9 mg/L	Gandhi <i>et al.</i> (2002b)
F	Mass ratio of oxygen to MTBE utilized	-	2.7	stoichiometry
d_c	Biomass decay oxygen demand	-	1.42 mg/mg	Semprini and McCarty (1991, 1992)
f_D	Fraction of degradable biomass	-	0.8	Semprini and McCarty (1991, 1992)
f_{per}	Molar ratio of hydrogen peroxide to oxygen	-	0.94	Gandhi <i>et al.</i> (2002b)
ϵ_{disp}	Fraction of hydrogen peroxide disappearance due to disproportionation	-	1.0	Gandhi <i>et al.</i> (2002b)
α	Exolution rate constant	-	100 day ⁻¹	Gandhi <i>et al.</i> (2002b)
F_A	Fraction of biomass actively degrading MTBE	-	1	Gandhi <i>et al.</i> (2002b)

- Range of values unavailable

[†] Median value selected from available range

[‡] Mean value selected from available range

Table 22 Baseline Kinetic Parameters Used in Cometabolism Simulations

Parameter	Description	Range	Baseline Value	Source
k_{Donor}	Maximum donor utilization rate constant	0.18 to 5.1 g/g cells/day	2.6 g/g cells/day ‡	Table 14, Ch 2
k_{MTBE}	Maximum MTBE degradation rate	0.048 to 3.53 g/g cells/day	0.3 g/g cells/day †	Table 14, Ch 2
$K_{s-Donor}$	Donor half-saturation constant	0.19 to 0.4 mg/L	0.3 mg/L ‡	Table 15, Ch 2
K_{s-MTBE}	MTBE half-saturation constant	1.17 to 120 mg/L	27.0 mg/L †	Table 15, Ch 2
K_{s-Ox}	Oxygen half-saturation constant	0.9 to 3 mg/L	2.0 mg/L ‡	Table 11, Ch 2
K_{I-per}	Hydrogen peroxide inhibition constant	-	0.34 mg/L	Gandhi <i>et al.</i> (2002b)
k_{per}	Hydrogen peroxide decay rate	-	22 day ⁻¹	Gandhi <i>et al.</i> (2002b)
Y	Biomass yield	0.8 to 1.8 g cells/g propane utilized	1.2 g cells/g donor utilized ‡	Table 16, Ch 2
b	Biomass decay rate	-	0.075 day ⁻¹	Martinez-Prado <i>et al.</i> (2002)
X	Initial biomass concentration	-	1.9 mg/L	Gandhi <i>et al.</i> (2002b)
F	Mass ratio of oxygen to propane utilized	-	3.6	stoichiometry
d_c	Biomass decay oxygen demand	-	1.42 mg/mg	Semprini and McCarty (1991, 1992)
f_D	Fraction of degradable biomass	-	0.8	Semprini and McCarty (1991, 1992)
f_{per}	Molar ratio of hydrogen peroxide to oxygen	-	0.94	Gandhi <i>et al.</i> (2002b)
ϵ_{disp}	Fraction of hydrogen peroxide disappearance due to disproportionation	-	1.0	Gandhi <i>et al.</i> (2002b)
α	Exolution rate constant	-	100 day ⁻¹	Gandhi <i>et al.</i> (2002b)
F_A	Fraction of biomass actively degrading MTBE	-	1	Gandhi <i>et al.</i> (2002b)

- Range of values unavailable

† Median value selected from available range

‡ Mean value selected from available range

Note how parameters are chosen in Table 21 in order to use the cometabolic degradation equations (Equations 40-47) to describe direct metabolism. First, the electron donor in the direct metabolism study is MTBE rather than propane, which was used as the donor to promote MTBE cometabolism; therefore, the values of the source/sink term for donor (r_{Donor}), the donor utilization rate (k_{Donor}), and the donor concentration (C_{Donor}) in Equations 40, 41, and 45 represent the source/sink term for MTBE (r_{MTBE}), the MTBE utilization rate (k_{MTBE}), and the MTBE concentration (C_{MTBE}), respectively. Also in Equations 40, 41, and 45 the half-saturation constant for electron donor ($K_{s-Donor}$) represents the half-saturation constant for MTBE. The parameter K_{s-MTBE} , which appears in the equations to represent inhibition of the primary substrate (propane) due to the presence of the secondary substrate (MTBE), is no longer needed. As this parameter appears in the denominator of the term C_{MTBE}/K_{s-MTBE} , we can “turn off” competitive inhibition by assigning K_{s-MTBE} a very large value. Finally, the source/sink term for secondary substrate (r_{MTBE}) represented in Equation 43 can be eliminated by setting the value of the variable k_{MTBE} to zero. The reader should note that this equation is irrelevant as there is no secondary substrate to track in modeling direct metabolism.

3.5.2 MODEL SPACE SITE CONDITIONS

In order to apply the technology model for simulation, we will describe a hypothetical site. In defining the site conditions it is necessary to establish the initial and boundary conditions for flow and transport in order to numerically solve the partial differential equations that comprise the flow and transport model described by Equations 35-38. In this study, the hypothetical site model space consists of an area that measures

105 m by 105 m by 35 m deep. The area is subdivided using 1225, 3 m by 3 m grid blocks (see Figure 10). The volume of this area extends down 35 m from a water table boundary to a confining layer, which is a no-flow boundary at 35 m bgs. The north and south borders of the model space are no-flow boundaries. The west and east boundaries are constant head boundaries with a gradient that induces flow from the west to the east. The concentration of dissolved MTBE contaminant is initially zero for all cells in the model space except for a rectangular constant source that is 105 m by 3 m and extends through the full depth of the aquifer. A well pair that comprises the HFTW system is 18 m downgradient from the constant source. Simulated observation wells are placed within the HFTW wells and also on a centerline between the pumping well pair 15 m downgradient (Figure 10).

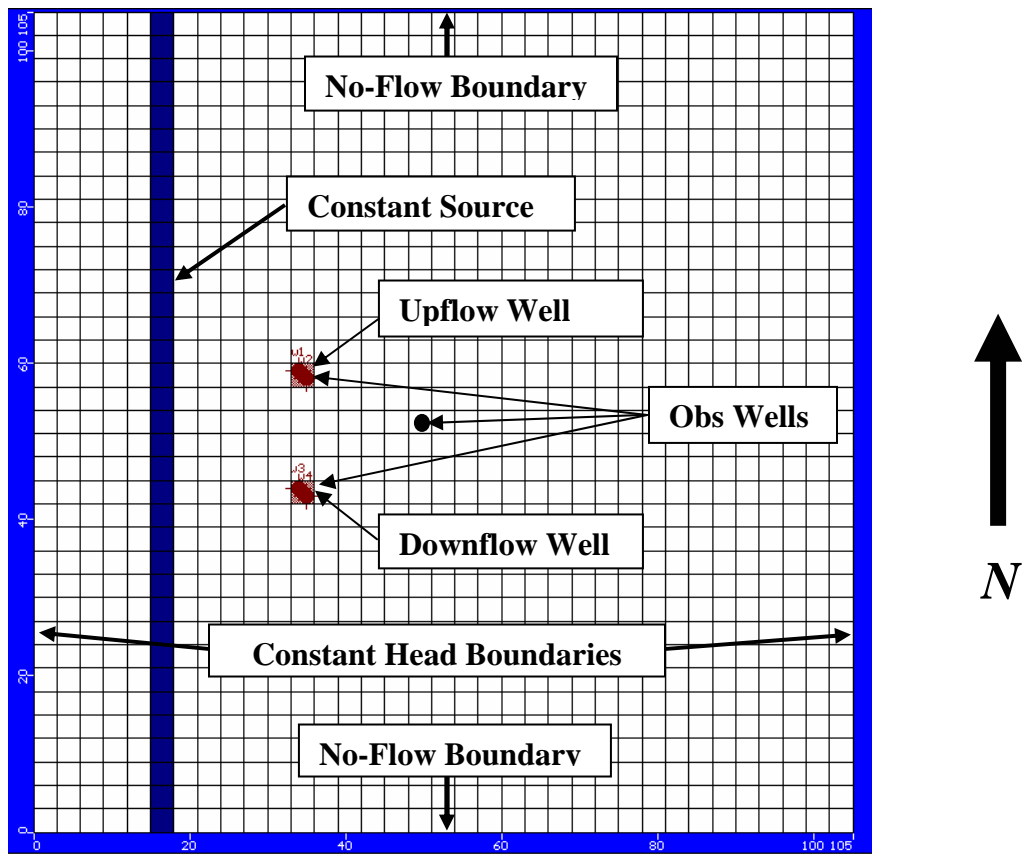


Figure 10 Plan View of Baseline Model Space

The site is divided into four layers that span the full 35 m thickness of the model space (Figure 11). The thickness of layers one, two, three, and four is 10 m, 5 m, 15 m, and 5 m, respectively. The aquifer is unconfined; with the water table at the top of layer one. The HFTW pumping wells are screened the entire depth of layers two and four.

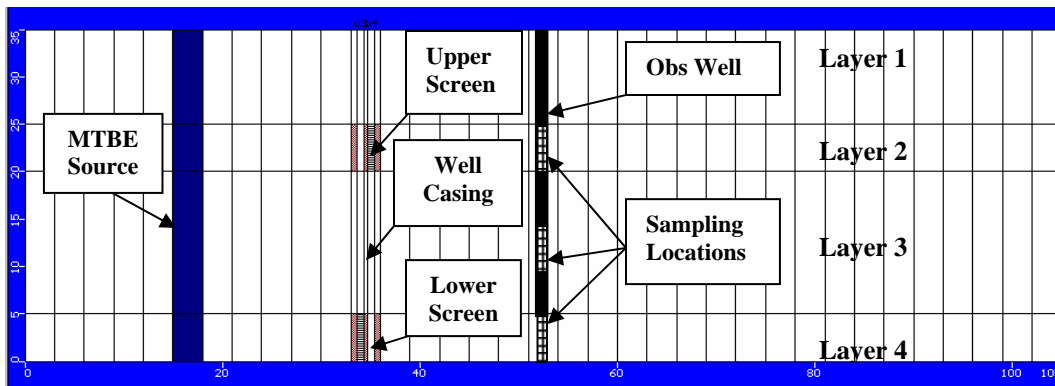


Figure 11 Elevation View of Baseline Model Space

The initial concentrations of all dissolved species except MTBE (*i.e.* propane, oxygen, and hydrogen peroxide) are set to zero. Naturally, before donor and hydrogen peroxide are injected into the aquifer there is none present. Resembling the typical effects of a gasoline release, it will be assumed that all dissolved oxygen in the aquifer has been depleted due to the presence of constituents associated with gasoline; hence, the only source of oxygen will be the dissociation of the hydrogen peroxide. The initial concentration of MTBE will also be set to zero in all areas of the aquifer except for the source area described previously.

3.5.3 ACTUAL MTBE SITE CONDITIONS

To make the simulations of the technology model as realistic as possible, environmental parameter values will be selected from a range of values measured at actual MTBE-contaminated sites. Table 23 shows site conditions from four MTBE-contaminated sites, providing a range of parameter values to choose from to specify hypothetical model parameters.

Table 23 MTBE-Contaminated Site Data

Aquifer Characteristics	Port Hueneme, CA	Vandenberg AFB, CA	Camden County, NJ	CT Site	Range
Horizontal Hydraulic Conductivity (m/day)	0.54 - 55.3	1.47 – 4.58	0.16	0.76 - 45.8	0.16 – 55.3
Hydraulic Gradient	0.001 - 0.003	0.02 – 0.023	0.01	0.01	0.001 – 0.023
Darcy Velocity (m/day)	N/A	0.03 - 0.11	0.06	N/A	0.06 – 0.3
Average Aquifer Thickness (m)	4.6 - 6.1	22	N/A	55	4.6 – 55
Plume Characteristics					
Width of MTBE Plume (m)	152	70 - 90	N/A	N/A	70 – 152
Length of MTBE Plume (m)	1520	520	N/A	N/A	520 – 1520
MTBE Concentration (mg/L)	15	5 - 0.1	N/A	24	0.1 – 24
Dissolved Oxygen Concentration (mg/L)	< 1	< 0.5	< 1	< 1	0 – <1
Source Characteristics					
Continuous Source (yes/no)	yes	N/A	N/A	N/A	N/A
Highest MTBE Concentration (mg/L)	35	N/A	270	40	35 – 270

N/A -- Data not available

3.5.4 ENVIRONMENTAL PARAMETERS

The values of the environmental parameters used in this study are summarized in Table 24. We will simulate technology operation over a range of hydraulic conductivities, hydraulic conductivity anisotropies, and source concentrations in order to

see how technology performance is affected by these environmental factors. The values were selected as typical of actual MTBE contaminated sites (Table 23).

Investigation of the effects of varying Darcy velocity for different sites will be accomplished by varying the horizontal conductivity while holding the hydraulic gradient constant. Additionally, the effects of anisotropy will be investigated by varying the anisotropy ratio (*i.e.* ratio of horizontal to vertical conductivity). The baseline anisotropy ratio will be 20: 1 which Fetter (1994) indicates is a typical ratio. Note that Christ *et al.* (1999) indicate that the ratio of horizontal to vertical conductivity must be approximately 20 to 1 in order for the HFTW system to operate effectively. Finally, the effects of varying source concentrations will be investigated over a range of MTBE concentrations.

Table 24 Environmental Parameters Used in Simulations

Parameter	Baseline Value	Range Tested
Horizontal hydraulic conductivity	25 m/day	2.5, 25, 50 m/day
Anisotropy ratio (horiz. : vert. cond)	20 : 1	1, 20, 100 : 1
Hydraulic gradient	0.01	N/A
Porosity	0.3	N/A
MTBE source concentration	10 mg/L	1, 10, 100 mg/L

3.5.5 ENGINEERING PARAMETERS

The engineering parameters that will be used in model simulations are summarized below in Table 25 and Table 26. Pumping rate and time averaged concentration (TAC) of hydrogen peroxide and propane are the only range of engineering parameter that will be varied to evaluate its effect on the performance of the system. The

effects of varying pumping rate will directly affect the interflow between wells and consequently will affect the treatment efficiency of the system (Christ *et al.*, 1999).

The TAC of hydrogen peroxide for the direct metabolism study was selected by stoichiometry. Hydrogen peroxide will be injected into the aquifer continuously to ensure that oxygen is not limiting the rate or extent of the process.

Table 25 Engineering Parameters Used in Direct-Metabolism Model Simulations

Parameter	Baseline Value	Range Tested
Time-averaged hydrogen peroxide conc.	57.2 mg/L	5.72, 57.2, 572 mg/L
Peroxide injection pulse schedule	continuous	N/A
Well spacing	15 m	N/A
Well screen length	5 m	N/A
Pumping rate	100 m ³ day ⁻¹	50, 100, 200 m ³ day ⁻¹
Well depth	35 m	N/A

The baseline and range of TAC of electron donor used for the cometabolism study were derived from results suggested by Loll *et al.* (2003). For more information regarding these results, the reader is directed to Section 2.8.2.2, of Chapter 2.0. The TAC of electron donor will also be varied to observe the effects on the performance of the system. The reader should note that the solubility of propane at 10 °C is 109 mg/L (Yalkowsky and He, 2003), thus limiting TAC of electron donor used. Electron donor will be injected continuously, versus pulsed, to achieve higher contaminant mass removal (Parr, 2002). The TAC for hydrogen peroxide was determined through stoichiometry and will also be varied.

Table 26 Engineering Parameters Used in Cometabolic Model Simulations

Parameter	Baseline Value	Range Tested
Time-averaged electron donor conc.	15 mg/L	1.5, 15, 109 mg/L
Donor injection pulse schedule	continuous	N/A
Time-averaged hydrogen peroxide conc.	171.7 mg/L	N/A
Peroxide injection pulse schedule	continuous	N/A
Well spacing	15 m	N/A
Well screen length	5 m	N/A
Pumping rate	100 m ³ day ⁻¹	N/A
Well depth	35 m	N/A

3.6 TECHNOLOGY MODEL VERIFICATION

The verification of the flow and transport portion of the technology model has already been completed prior to this study. The reader is directed to Parr (2002) for more information regarding model verification. Despite previous transport verification, verification simulations will be conducted to show that the transport portion of the technology is functioning properly. The submodel, though, has not been verified in previous research.

Verification that the transport portion of the technology model is functioning properly will be verified by accomplishing the following,

- Set the initial concentration of MTBE to 0 mg/L throughout the extent of the model aquifer except for the source area which will be set to 10 mg/L;
- Establish a regional gradient resulting in west to east groundwater flow;
- Set pumping rate in wells to zero;
- Observe MTBE breakthrough at downgradient centerline observation well;

The above conditions will establish proper conditions for the transport of MTBE to the observation well. Breakthrough observations at the observation well will verify that the transport portion of the technology model is functioning as expected.

Verification that the submodel is functioning properly will be accomplished by the following.

- Set the initial concentration of MTBE to 10 mg/L throughout the extent of the model aquifer;
- Set regional groundwater flow to zero by inputting a zero hydraulic gradient;
- Direct metabolism study -- Run the HFTWs for 100 days without hydrogen peroxide injection, check to verify no MTBE degradation and no microorganism growth, then inject hydrogen peroxide and verify MTBE degradation and microorganism growth;
- Cometabolism study -- Run the HFTWs for 100 days without propane and hydrogen peroxide injection, verify no MTBE degradation and no microorganism growth, then inject propane and hydrogen peroxide and verify MTBE degradation and microorganism growth;
- Observe the reduction of MTBE concentration in the aquifer through contour plots and output of total MTBE mass removed;

The above steps will effectively create the conditions necessary to simulate a batch system. The reduction in MTBE concentrations in the aquifer, as evidenced by the concentration contour plots, should verify that the submodel is functioning properly.

3.7 MODEL SIMULATIONS

Upon completion of the verification runs, sensitivity analyses using the technology model will be conducted. Analyses will be conducted separately for direct MTBE metabolism and aerobic cometabolism. A baseline or reference simulation for both degradation processes will be obtained using baseline parameters identified previously. The purpose of the baseline simulation is to provide a reference for measuring the effects of varying the technology model parameters. After establishing baseline values for each parameter, the technology model will be run as the parameters are systematically varied over a range, and the effect of the variation of individual parameters on simulated technology performance noted.

Technology performance will be evaluated by observing propane (cometabolism only), MTBE, oxygen, and peroxide concentration versus time (breakthrough) curves in each layer of the aquifer, at the downgradient monitoring well and in a monitoring well located in the injection screen of the upflow well. Concentration contour plots will show the spatial distribution of propane (cometabolism only), MTBE, oxygen, peroxide, and microorganisms at specific times. Additionally, total mass of MTBE degraded will be tracked. The evaluation of these results will permit evaluation of system performance.

Technology success is measured by the reduction of downgradient MTBE concentrations and the rate at which those reductions are achieved. Simply put, a configuration that achieves lower downgradient MTBE concentrations quickly is desirable. Although this study does not include optimization, performance trends will be observed that may be useful for a future optimization study.

The following series of simulations using the direct metabolism technology model will be accomplished sequentially.

- (1) Establish baseline simulation using baseline parameter values;
- (2) Investigate engineering parameters by varying well pumping rates;
- (3) Investigate environmental parameters by varying horizontal hydraulic conductivity, hydraulic conductivity anisotropy, source concentration, and TAC of electron acceptor;
- (4) Investigate kinetic parameters with the largest ranges reported in the literature, including k_{Donor} and $K_{s-Donor}$ by varying the parameter values appropriately over the ranges reported in literature.

Additionally, the following series of simulations using the cometabolism technology model will be accomplished sequentially.

- (1) Establish baseline simulation using baseline parameters values;
- (2) Investigate kinetic parameters with the largest ranges reported in the literature, including k_{Donor} , $K_{s-Donor}$, k_{MTBE} , and K_{s-MTBE} , by varying the parameter values appropriately over the ranges reported in literature.

4.0 RESULTS AND ANALYSIS

4.1 OVERVIEW

The purpose of this chapter is to present the results obtained by applying the technology model developed in Chapter 3.0. The first section of this chapter discusses the results of the verification of both the direct and cometabolism models. Then results from the baseline simulations of the two models will be presented and discussed. Finally, the results of the sensitivity analysis, where the environmental, engineering, and kinetic parameters are varied, will be presented. Observations and significant findings resulting from the simulations will be discussed.

4.2 SUBMODEL VERIFICATION

The results of the model verification using both the direct and cometabolism submodels will be discussed in this section. The conditions of the verification simulations are described in Section 3.6 of Chapter 3.0. The purpose of the verification simulations is to verify that each submodel (direct and cometabolism) is functioning as expected.

4.2.1 DIRECT METABOLISM VERIFICATION

Two simulations were conducted with the HFTW system operating in “batch” mode (that is, with no regional flow) to verify the direct metabolism submodel. The first simulation was conducted to verify that no MTBE mass would be removed and that

MTBE and microbial concentrations would remain constant if no electron acceptor were injected. The second simulation was conducted to verify that injected electron acceptor would result in MTBE mass removal, reduction in concentration, and an increase in the concentration of microorganisms.

Figure 12(a) and Figure 12(b) show the MTBE concentration contours without electron acceptor injection and with electron acceptor injection, respectively. It can be seen from Figure 12(a) that the simulation run without hydrogen peroxide injection results in no reduction in MTBE concentration. The slight variations in MTBE concentration depicted on the plot most likely are a result of numerical truncation errors generated during the finite difference algorithm used to solve the mass transport partial differential equations. Alternatively, for the simulation run with hydrogen peroxide injection, a “hole” of decreased MTBE concentration develops (Figure 12(b)).

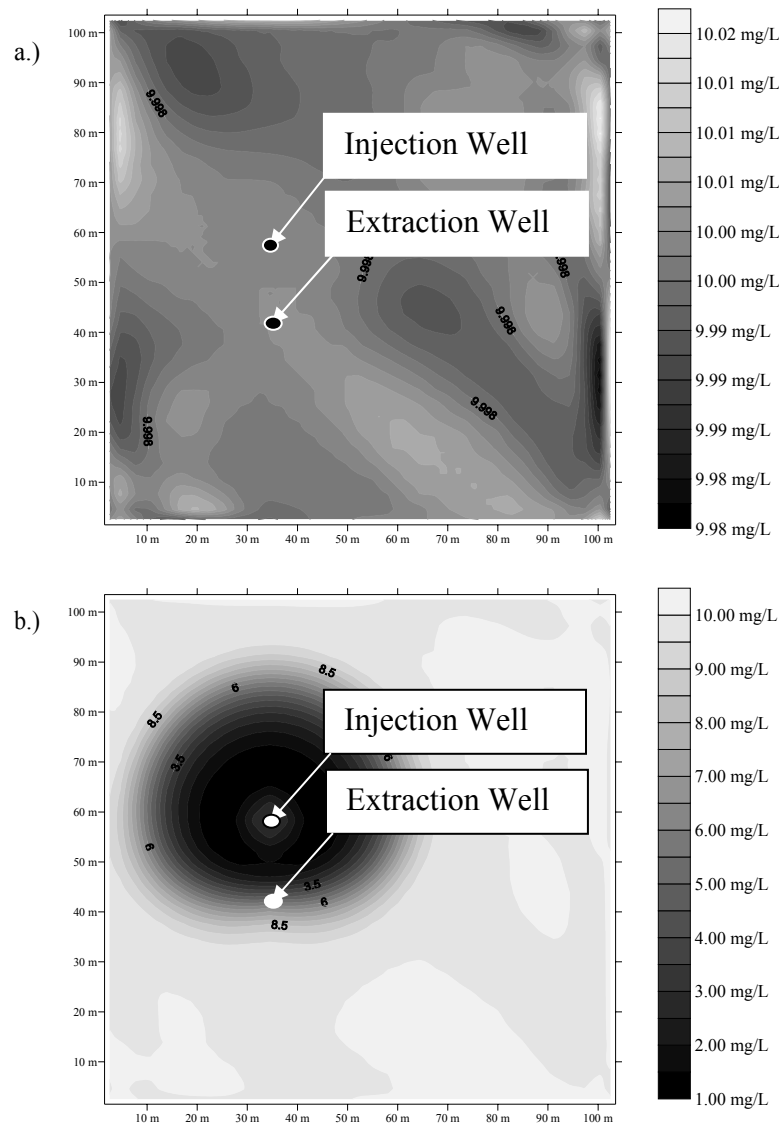


Figure 12 MTBE Concentration Contours (a) Without Hydrogen Peroxide Injection and (b) With Hydrogen Peroxide Injection at 100 days, Respectively (Layer 2, TAC=57.4 mg/L Hydrogen Peroxide, Baseline Kinetic Data)

Figure 13(a) and Figure 13(b) show contour plots of the hydrogen peroxide and microbial concentrations, respectively. Within an approximate 5 m radius of the injection well there appears to be a hydrogen peroxide residual concentration resulting in decreased microbial concentrations surrounding the well. The decreased microbial

concentration near the well seems to signify the toxic effects of hydrogen peroxide on the growth of microorganisms.

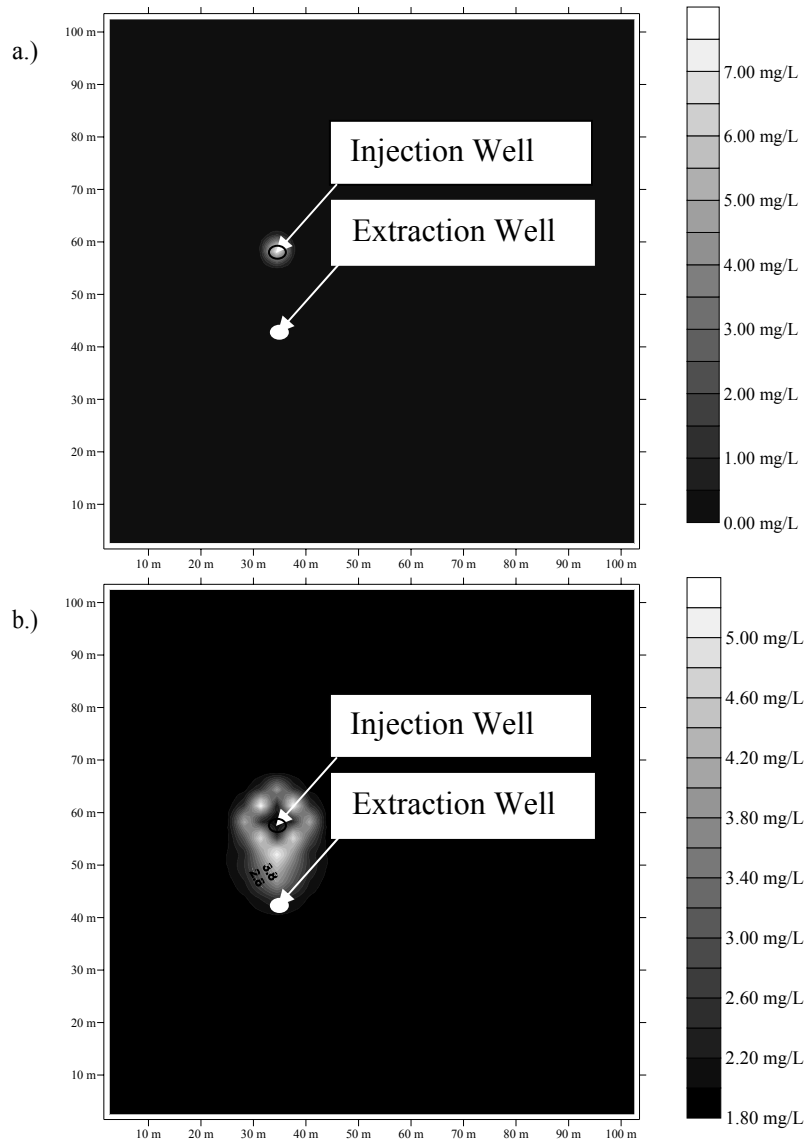


Figure 13 (a) Hydrogen Peroxide and (b) Microbial Concentration Contours at 100 days, Respectively (Layer 2, TAC=57.4 mg/L Hydrogen Peroxide, Baseline Kinetic Data)

Mass balance output from each direct metabolism simulation, summarized in Table 27, indicates that the submodel is functioning as expected. The mass quantities depicted in Table 27 represent net changes in mass of the respective species within the

model space, which is to say that mass leaving the model space due to groundwater flow is not considered a decrease in mass. A positive value indicates a net increase or growth of that species. A negative value indicates a net decrease or decay of that species. For example, the net mass of oxygen in the model space at the end of the simulation period with hydrogen peroxide injection is 0.34 kg, which may seem lower than expected. The mass of oxygen introduced into the model space is stoichiometrically proportional to the mass of hydrogen peroxide injected resulting in approximately 540 kg oxygen added; however, the oxygen is consumed during microbial activity. Therefore the net oxygen remaining is the difference between the mass of oxygen introduced and the mass of oxygen utilized in the microbial processes including MTBE degradation.

Table 27 Summary of Mass Balance Output for Direct Metabolism Verification Simulations (All Layers, 100 days)

	MTBE (kg)	Oxygen (kg)	Hydrogen Peroxide (kg)	Microorganisms (kg)
Without hydrogen peroxide injection				
Injected	0.0	0.0	0.0	0.0
(+) Growth (-) Decay	0.0	0.0	0.0	0.0
With hydrogen peroxide injection				
Injected	0.0	0.0	1144.8	0.0
(+) Growth (-) Decay	- 88.024	0.34	- 1144.6	2.51

According to the results presented in Table 27, the simulation run without hydrogen peroxide injection shows no reduction in MTBE mass, nor does it show an increase in microbial mass. The simulation run with hydrogen peroxide injection, on the other hand, shows that a significant quantity of MTBE mass has been removed. Additionally, the mass balance output depicts an increase in microbial mass.

Finally, in order to verify the transport portion of the model was behaving as expected, the well pumping rate was set to zero and regional flow was “turned on” by creating a 0.01 m/m gradient from west to east. The initial MTBE concentrations were set to zero throughout the model space grid, except at the MTBE source which was set to 10 mg/L. Breakthrough was observed at the centerline observation well located 33 m downgradient of the MTBE source and is depicted below in Figure 14.

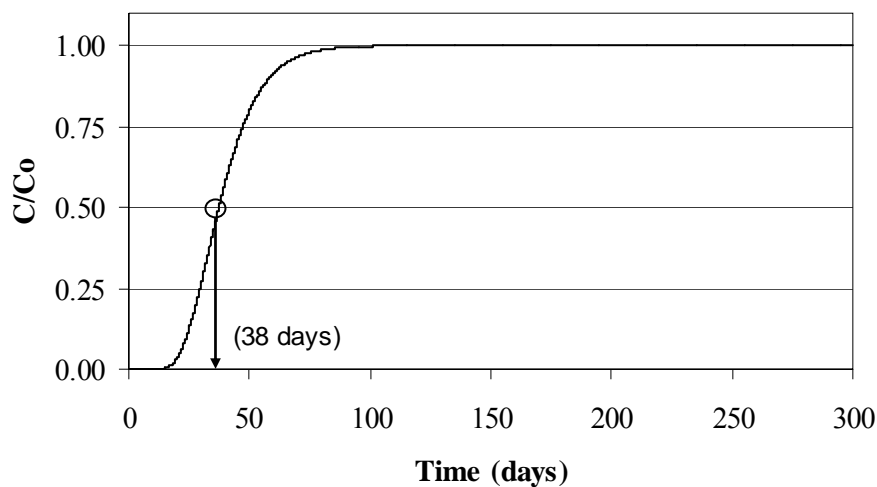


Figure 14 MTBE Breakthrough Curve at Observation Well 33 m Down Gradient from Source (Layer 2, No Pumping, No Hydrogen Peroxide Injection)

Using the pore water velocity of 0.83 m/day (gradient=0.01 m/m, horizontal conductivity=25 m/day, and porosity=0.3), the expected breakthrough for MTBE at the observation well located 33 m downgradient would be approximately 40 days, assuming advective transport only. Using the model, the breakthrough of 50% of the source concentration at the downgradient observation well occurred in approximately 38 days, as depicted in Figure 14. The approximate 5% difference between the two times may be attributed to the fact that the species transport in the numerical model includes both advection and dispersion. The transport time estimated by assuming advective transport

alone would be greater than the time estimated assuming advective/dispersive transport (Domenico and Schwartz, 1998).

4.2.2 COMETABOLISM VERIFICATION

Two simulations were run to verify the cometabolism biological submodel was functioning as expected. Like the direct metabolism submodel verification, one simulation was run without electron donor to verify that no mass was removed, MTBE concentrations remained constant, and no microbial growth was observed. The second simulation was run with electron donor and electron acceptor injection to verify that mass was removed, MTBE concentrations decreased, and microbial growth was observed.

Figure 15(a) and Figure 15(b) show the concentration contours of the system operating without and with electron donor and electron acceptor injection, respectively. It can be seen that the simulation run without propane and hydrogen peroxide injection results in no reduction in MTBE concentration. Like the results of the direct metabolism verification runs, the slight variations in MTBE concentration depicted on the plot most likely are a result of numerical truncation errors generated by the finite difference algorithm used to solve the mass transport partial differential equations. Alternatively, for the simulation run with propane and hydrogen peroxide injection, a “hole” of decreased MTBE concentration develops.

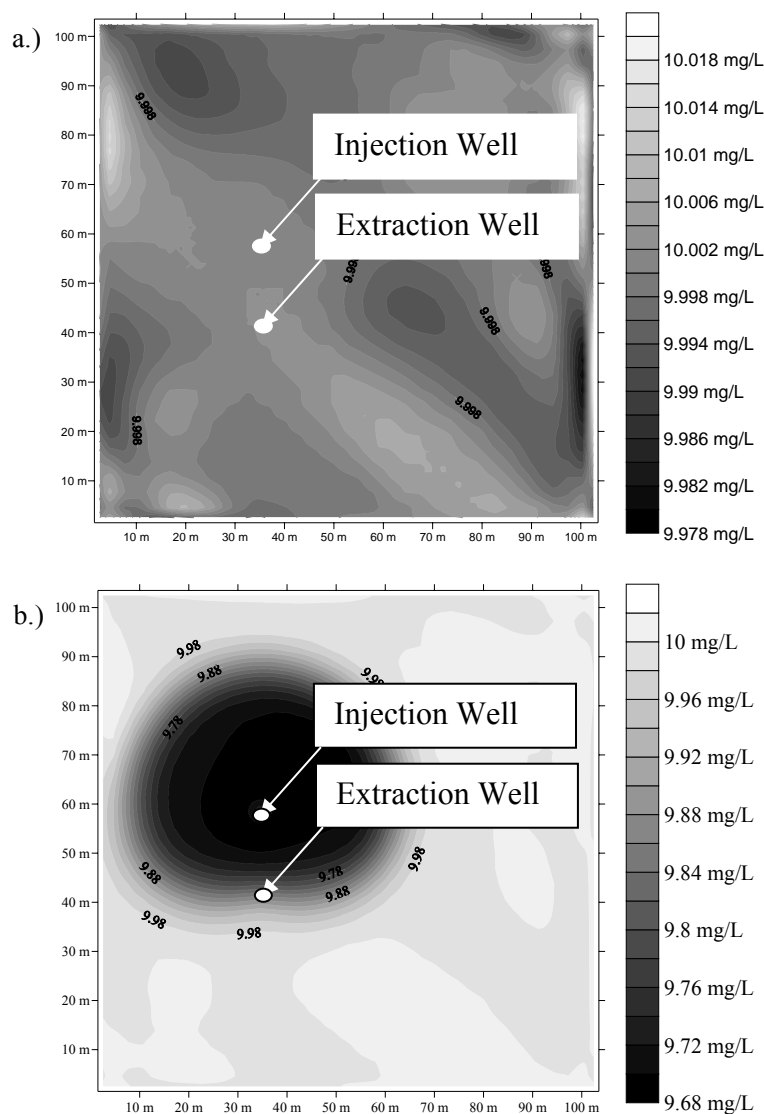


Figure 15 MTBE Concentration Contours (a) Without Electron Donor/Acceptor Injection and (b) With Electron Donor/Acceptor Injection at 100 days, Respectively (Layer 2, TAC=15 mg/L Propane, TAC=171.7 mg/L Hydrogen Peroxide, Baseline Kinetic Data)

Figure 16(a) and Figure 16(b) depict hydrogen peroxide and microbial concentrations, respectively. Similar to the phenomena observed in the output from the direct metabolism verification simulation, microbe concentrations are lower within the immediate vicinity of the injection well. Figure 17 provides additional evidence of this as the relief depicts a depression of microbial concentration near the well. Because

hydrogen peroxide is also used as the oxygen source for both direct and cometabolism it is speculated that the inhibitory effects of hydrogen peroxide also are significant in the cometabolism submodel.

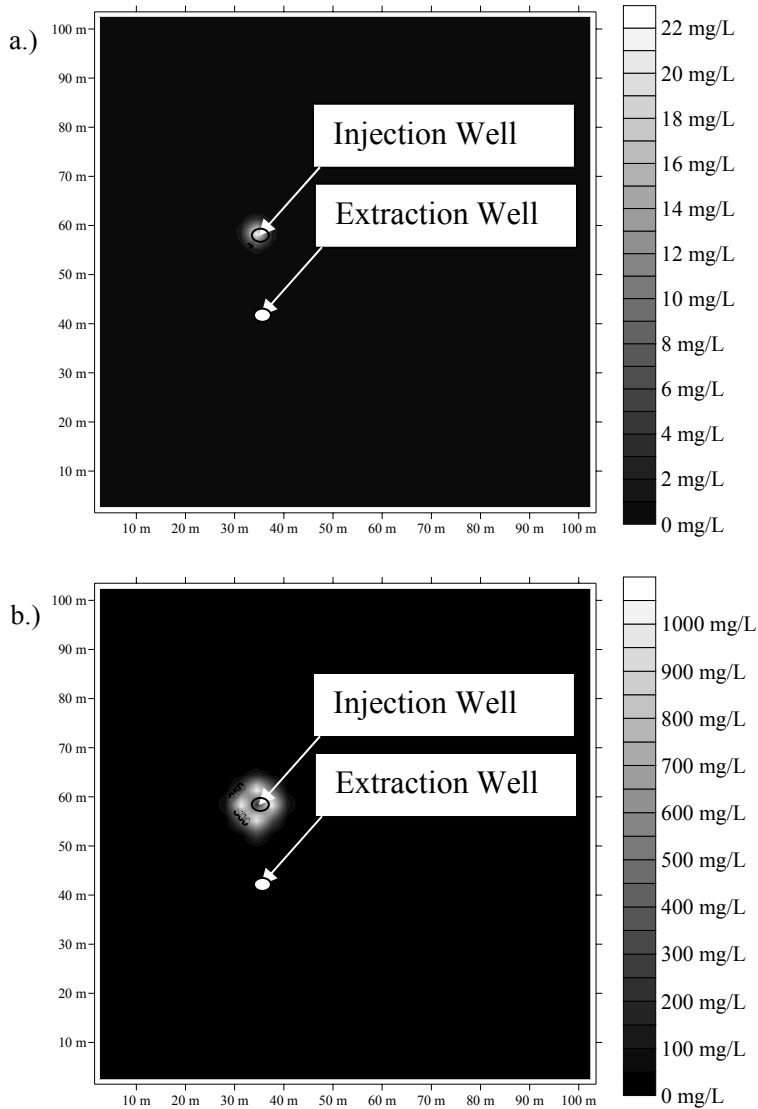


Figure 16 (a) Hydrogen Peroxide and (b) Microbial Concentration Contours at 100 days, Respectively (Layer 2, TAC =15 mg/L Propane, 171.7 mg/L Hydrogen Peroxide, Baseline Kinetic Data)

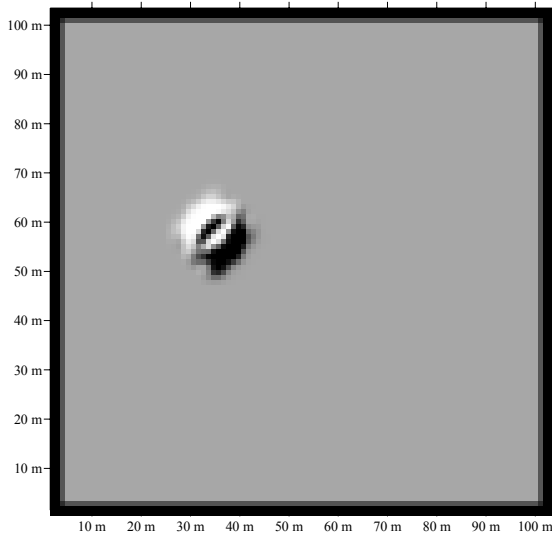


Figure 17 Shaded Relief Map Depicting Microbial Concentrations (Layer 2, TAC=15 mg/L Propane, 171.7 mg/L Hydrogen Peroxide, Baseline Kinetic Data)

Mass balance output from each simulation indicates that the submodel is functioning as expected. The mass balance output is summarized in Table 28. The simulation run without propane and hydrogen peroxide injection shows no net change in MTBE mass, nor does it show an increase in microbial mass. The simulation run with propane and hydrogen peroxide injection, on the other hand, indicates a net reduction in MTBE mass indicating MTBE mass has been degraded. Additionally, the mass balance output depicts a net increase in microbial mass.

Table 28 Summary of Mass Balance Output for Cometabolism Verification Simulations (All Layers, 100 days)

	Propane (kg)	Oxygen (kg)	Hydrogen Peroxide (kg)	MTBE (kg)	Microorganisms (kg)
Without propane and hydrogen peroxide injection					
Injected	0.0	0.0	0.0	0.0	0.0
(+) Growth (-) Decay	0.0	0.0	0.0	0.0	0.0
With propane and hydrogen peroxide injection					
Injected	300.0	0.0	3434.2	0.0	0.0
(+) Growth (-) Decay	- 201.1	- 1.48	- 3433.1	- 3.57	181.6

4.3 TECHNOLOGY MODEL SIMULATION RESULTS

Baseline simulations of the technology model for both direct and cometabolism were run using environmental parameters for a theoretical MTBE-contaminated site described previously in Chapter 3.0. The kinetic, environmental, and engineering parameter values used for these simulations were selected from the literature and previous HFTW research (*i.e.* Parr, 2002). The reader is directed to Section 3.5 of Chapter 3.0 for more details on the parameter values.

The purpose of developing baseline simulations is to establish a benchmark from which results of the sensitivity analysis can be compared. The results of the baseline and sensitivity analyses for both direct and cometabolism will be presented separately. The first part of this section addresses the technology model utilizing direct metabolism and the second part addresses the technology model utilizing cometabolism.

4.3.1 DIRECT METABOLISM BASELINE

Baseline technology model simulations for direct metabolism were conducted using baseline kinetic, engineering, and environmental parameter values identified in Section 3.5, of Chapter 3.0. The parameter values selected for the baseline simulations are “best guess” parameters based on the literature review of MTBE direct metabolism studies, stoichiometry, and previous studies of the HFTW system. The time horizon used for the baseline simulation was 300 days.

Figure 18 depicts the concentration contours of MTBE, oxygen, hydrogen peroxide, and microbes, respectively. Similar to the observations in the direct metabolism verification simulation, Figure 18(a) shows that a MTBE depleted hole develops around the layer-2 injection well, and due to regional groundwater flow, downgradient MTBE concentrations are reduced. Microbial growth is supported by the injection of hydrogen peroxide that disproportionates into oxygen and water. The presence of oxygen and MTBE results in favorable conditions for microbial growth and an increase in microbe concentration depicted in Figure 18(d). Interestingly, microbe concentrations near the injection well appear to decrease within a few meters of the well. Figure 18(c) depicts a residual concentration of hydrogen peroxide within the immediate area of the injection well. The reduced microbial concentration may be the result of toxicity effects of hydrogen peroxide inhibiting the growth of microorganisms near the well. Although excess hydrogen peroxide may be detrimental to microbial growth, hydrogen peroxide may reduce the potential for bioclogging near the well screens and thus benefit the operation of HFTW technology.

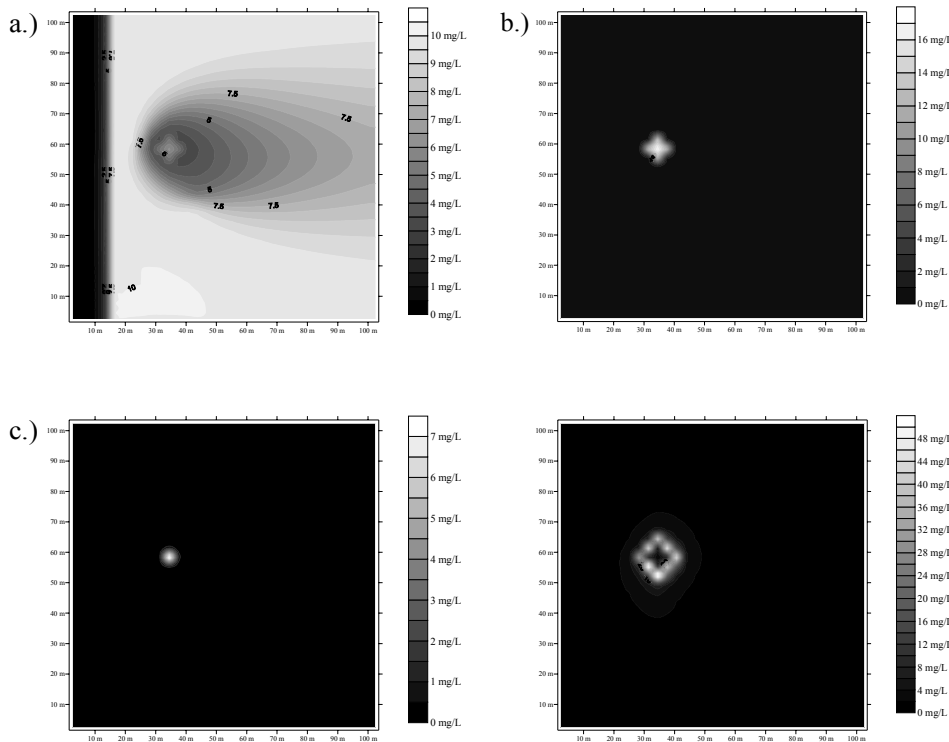


Figure 18 Contour Plots of (a) MTBE, (b) Oxygen, (c) Hydrogen Peroxide, and (d) Microbial Concentrations at 300 days, Respectively (Layer 2, Baseline Data)

The diamond shaped concentration contours depicted in Figure 18 are most likely an artifact of the grid size chosen for this study. Reduced grid size may allow for finer resolution and smoother contours but comes at computational cost in the form of increased simulation run times.

Figure 19 and Figure 20 depict profile views of the MTBE concentrations along the west-east and north-south axes, respectively. Included in Figure 19 and Figure 20 are approximate well and well screen locations for illustration. It can be seen that a zone of decreased MTBE concentrations develops near and between the screens in the pumping wells. Additionally, Figure 21 clearly shows the increased microbial concentrations near the well screens creating a bioactive treatment area where recirculated MTBE-contaminated water can undergo biological treatment.

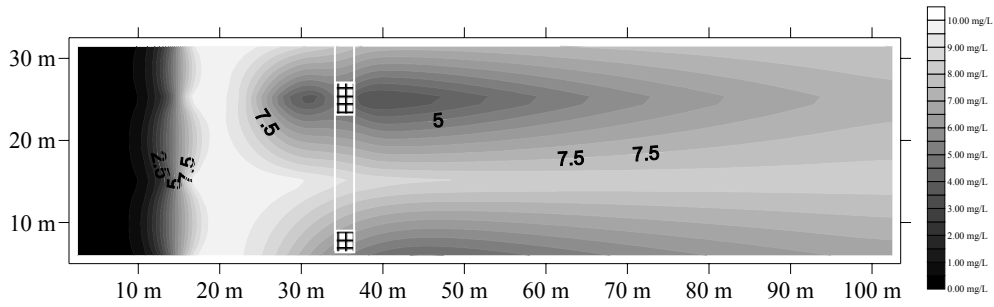


Figure 19 West-East Axis Profile of MTBE Concentration Contours at 300 days, With Approximate Well Location Shown (All Layers, Baseline Data)

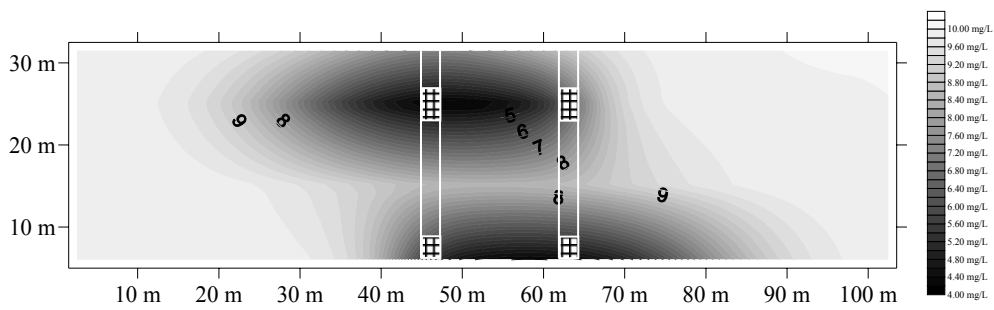


Figure 20 North-South Profile of MTBE Concentration Contours at 300 days, With Approximate Well Locations Shown (All Layers, Baseline Data)

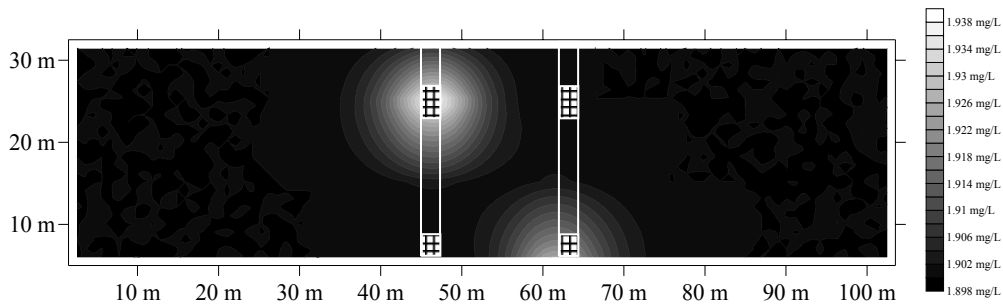


Figure 21 North-South Profile of Microbial Concentration Contours at 300 days, With Approximate Well Locations Shown (All Layers, Baseline Data)

The baseline simulation was conducted with an anisotropy ratio of horizontal to vertical hydraulic conductivity of 20 to 1 which results in somewhat restricted vertical flow between layers. Thus the majority of hydrogen peroxide injected into layers 2 and 4 is transported horizontally as opposed to vertically. One potential disadvantage of the

HFTW technology is that treatment efficiency is much better in layers where the hydrogen peroxide is injected. Evidence of this phenomenon is depicted above in Figure 19 and Figure 20 and is also supported by results from Parr (2002). Despite the anisotropy ratio, though, some degree of vertical mixing does occur and treatment takes place in the layers without injection but to a lesser degree.

Figure 22 shows the breakthrough curve of MTBE at the downgradient, centerline observation well. The maximum observed MTBE concentration at the observation well is approximately 4.1 mg/L, while the upgradient MTBE source concentration is 10 mg/L. Although MTBE concentrations decrease at the centerline observation well, microbe concentrations remain at or near the natural population concentration of 1.9 mg/L (not shown).

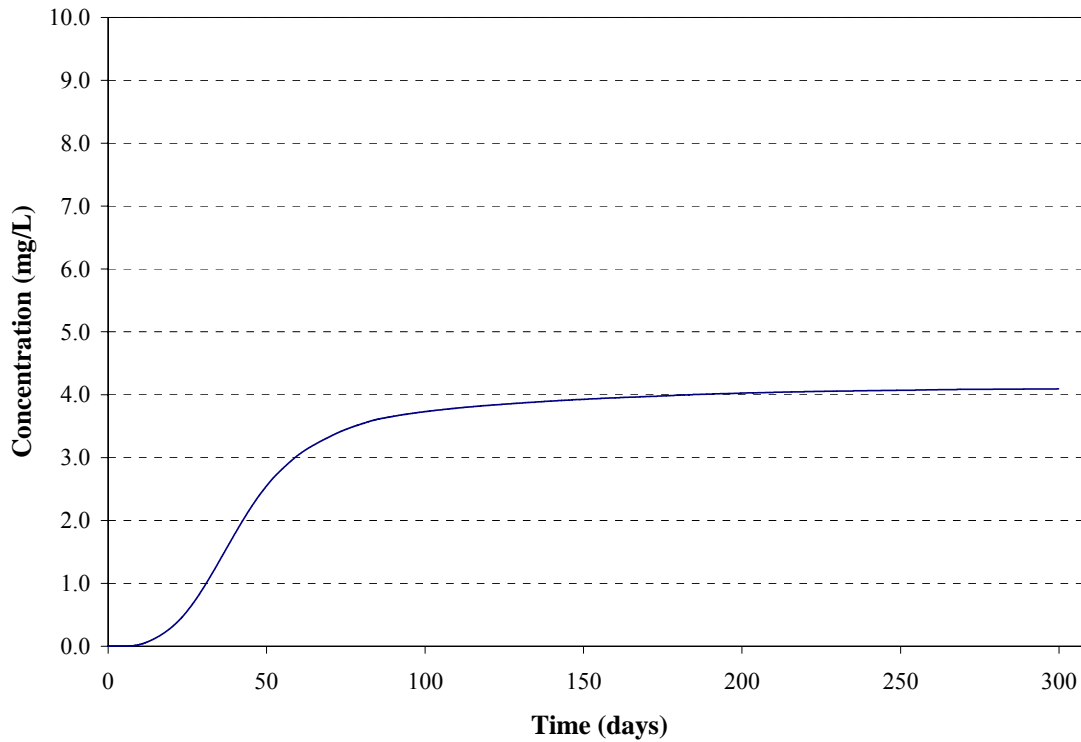


Figure 22 Breakthrough Curve of MTBE at Centerline Observation Well (Layer 2, Baseline Data)

Figure 23 shows that early in the simulation, the concentration of oxygen at the downgradient, centerline observation well increases but then rapidly decreases shortly afterwards. This behavior may be due to the low initial population of microbes. As the population increases, particularly near the pumping wells, oxygen is depleted rather rapidly within a short distance from the injection well. The rapid consumption of oxygen by microorganisms near the injection wells may limit the amount of oxygen transported downgradient and subsequently limit the amount of degradation occurring in the downgradient MTBE plume as no electron acceptor is available for microbial activity.

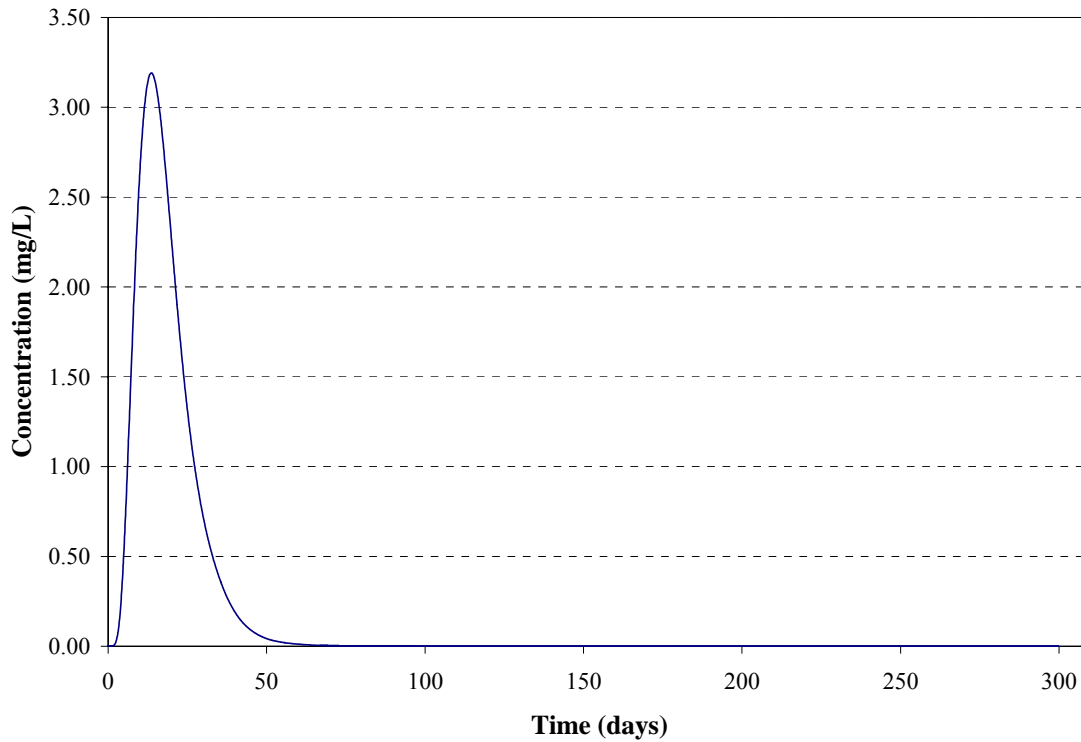


Figure 23 Breakthrough Curve of Oxygen at Centerline Observation Well (Layer 2, Baseline Data)

Mass balance output from the baseline direct metabolism simulation, summarized in Table 29 indicates that approximately 270 kg of MTBE was removed by day 300 and approximately 14.9 kg of microorganisms have grown by day 300.

Table 29 Summary of Mass Balance Output From Baseline Direct Metabolism Simulation (All Layers, 300 days)

	MTBE (kg)	Oxygen (kg)	Hydrogen Peroxide (kg)	Microorganisms (kg)
Injected	0.0	0.0	3434.8	0.0
(+) Growth (-) Decay	-269.89	10.06	-3430.5	14.9

4.3.2 DIRECT METABOLISM SENSITIVITY ANALYSIS RESULTS

Environmental, engineering, and kinetic parameters were varied independently during the sensitivity analysis of the direct metabolism model. The environmental parameters varied during this study include horizontal conductivity, anisotropy ratio, and MTBE source concentration. The engineering parameters varied include TAC of hydrogen peroxide and well pumping rate. Finally, the kinetic parameters varied in the sensitivity analysis include substrate utilization rate (k_{Donor}) and half-saturation constant ($K_{s-Donor}$). The specific values used during the sensitivity analysis can be found in Section 3.5, of Chapter 3.0.

Simulations were conducted over a time horizon of 300 days which was adequate based on the kinetic parameters; however, the time horizon had to be expanded to 1200 days for low hydraulic conductivity simulations. Due to the decreased groundwater Darcy velocity of the low hydraulic conductivity scenario, contaminant would not reach the downgradient centerline observation well within 300 days. The engineering, environmental, and kinetic parameter sensitivity results were analyzed by examining breakthrough curves at the centerline observation well and the observation well located in the layer 2 injection well, concentration contour plots, and total mass degraded, when applicable. Long-term behavior of the technology, although important, is beyond the scope of this research and may be the subject of a future optimization study.

4.3.2.1 HORIZONTAL HYDRAULIC CONDUCTIVITY

The sensitivity of the direct metabolism technology model to changes in horizontal hydraulic conductivity was investigated. The results of that investigation are

discussed in this section. The reader should note that changing the hydraulic conductivity changes the groundwater velocity. Three simulations were conducted using three different values for horizontal hydraulic conductivity, 2.5, 25, and 50 m/day. The anisotropy ratio of horizontal to vertical hydraulic conductivity was fixed at 20 to 1 for all three simulations. As noted above, because the pore water velocity for horizontal hydraulic conductivity of 2.5 m/day is so slow, the simulation run time had to be increased from the baseline 300 days to 1200 days to allow sufficient time for the contaminant to travel from the source to the east boundary.

The breakthrough curves depicted in Figure 24 indicate that horizontal hydraulic conductivity has a significant impact on downgradient MTBE concentrations. The breakthrough curves depicted in Figure 24 clearly show a direct relationship between hydraulic conductivity and downgradient MTBE concentrations. As the horizontal hydraulic conductivity increases, the downgradient MTBE concentration also increases. The reader should note that the breakthrough curve for the 50 m/day hydraulic conductivity simulation (Figure 24) shows perturbations in the concentration which may be an artifact of the numerical method used to approximate the solution of the transport differential equations. The high groundwater velocity relative to the grid size and time step used in this study may have resulted in increased numerical error.

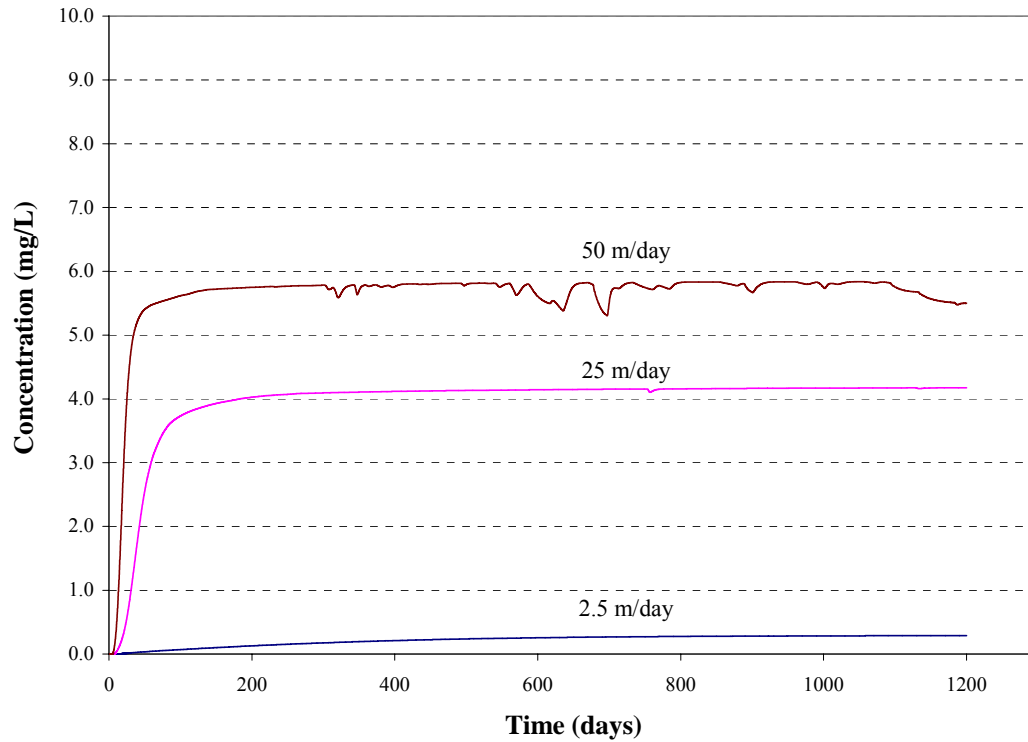


Figure 24 MTBE Breakthrough Curves at Centerline Observation Well at Varying Horizontal Hydraulic Conductivities (Layer 2, Baseline Kinetic and Engineering Data, 1200 days)

Table 30 summarizes the MTBE mass degraded for each value of horizontal hydraulic conductivity. Despite lower downgradient MTBE concentrations, lower horizontal hydraulic conductivity appears to decrease the MTBE mass removed. These results may seem counterintuitive, however, are most likely due to the effects of hydraulic conductivity on capture zone width and well interflow. An analytical method for calculating interflow was developed by Christ *et al.* (1999). This method assumes 2-dimensional flow and is based on properties of the aquifer (hydraulic conductivity, hydraulic gradient, aquifer thickness) and well operation parameters (pumping rate, well spacing). Application of the Christ *et al.* (1999) analytical solution shows that for a given pumping rate and well spacing, interflow decreases as Darcy velocity increases.

Table 30 MTBE Mass Degraded at Varying Horizontal Hydraulic Conductivities (All Layers, Baseline Kinetic and Engineering Data, 1200 days)

Horiz. Hydraulic Conductivity (m/day)	MTBE Degraded (kg)
2.5	703
25	1077
50	1179

Higher hydraulic conductivity results in higher Darcy velocity, which reduces the interflow between the circulating wells and increases the capture zone width. When the interflow between two pumping wells is high, groundwater is circulated through the bioactive treatment zones multiple times, resulting in low downgradient concentrations and high treatment efficiency. Unfortunately, though, a high percentage of interflow decreases capture zone width and consequently results in less mass removed since less contaminant from upgradient is drawn into the HFTW system.

Another factor that may contribute to mass removal is illustrated in Figure 25. The concentration contours depicted in Figure 25 allow for comparison of the concentration of each species (*i.e.* MTBE, oxygen, and microbes) at day 1200 for the different hydraulic conductivity simulations. The low conductivity simulation depicted in Figure 25(a) shows that some of the MTBE source is forced upgradient due to pumping and the small capture zone width of the system results in significant contaminant bypass, as it is not captured by the pumping wells; however, Figure 25(a) also shows significant MTBE degradation and a relatively large area of increased oxygen concentration, yet only a small area of increased microbial concentration which is displaced from the region surrounding the injection well screen, relative to those depicted in Figure 25(b) and (c). As the availability of oxygen does not appear to be limiting, the

low concentration and spatial orientation of the microbes must be the result of low concentrations of MTBE available to the microbes. The increased microbial concentrations depicted in Figure 25(a) show that microbial growth is limited in the regions of very low MTBE concentrations (<1 mg/L) and occurs in a region where increased MTBE and oxygen concentrations coexist.

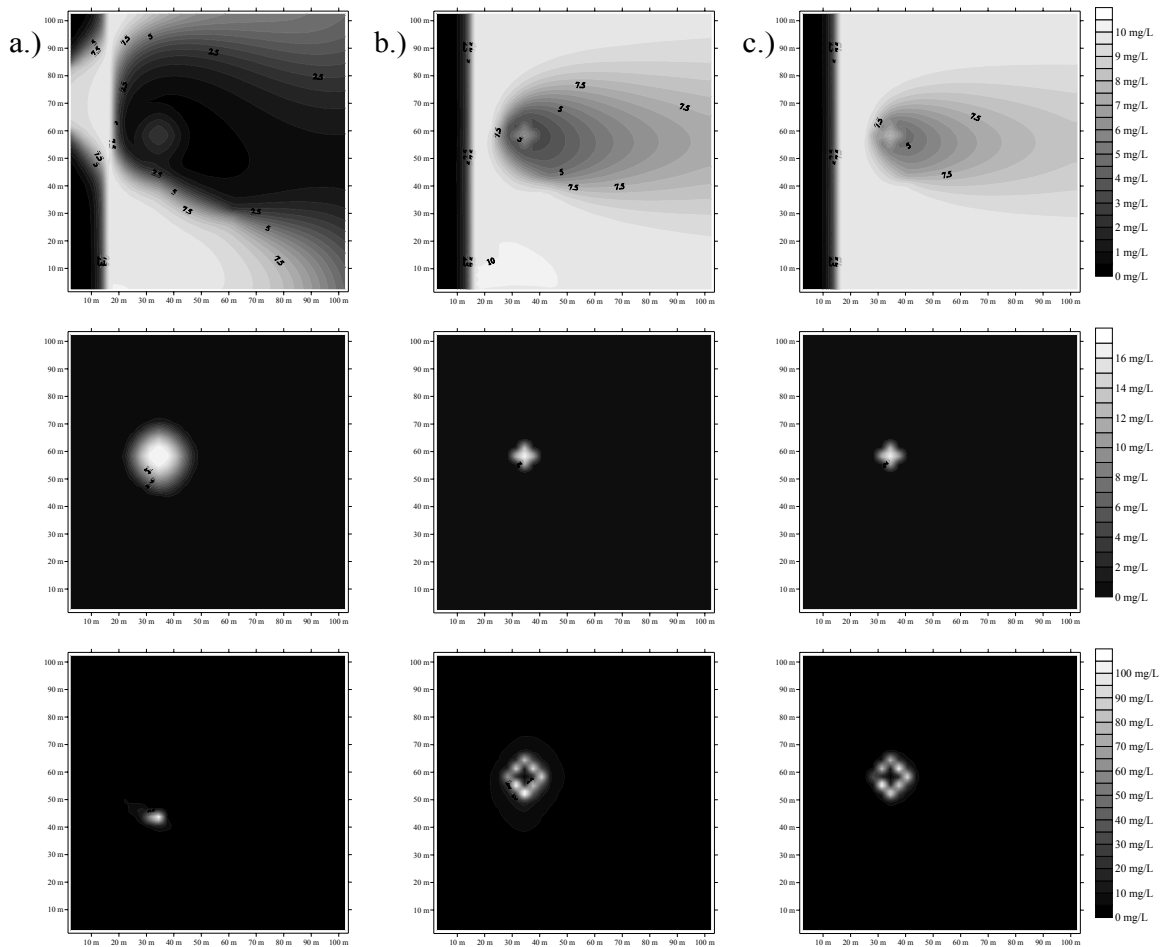


Figure 25 Contour Plots of MTBE (1st row), Oxygen (2nd row), and Microbial Concentrations (3rd row), for Horizontal Hydraulic Conductivities of (a) 2.5 m/day, (b) 25 m/day, and (c) 50 m/day (Layer 2, Baseline Kinetic and Engineering Data, 1200 days)

The low concentration of MTBE in the bioactive zones, due to high interflow resulting from low horizontal hydraulic conductivity, is depicted in Figure 26. The low

concentration and limited distribution of microbes resulting from high interflow may have together contributed to the lower mass removal in the 2.5 m/day hydraulic conductivity simulation.

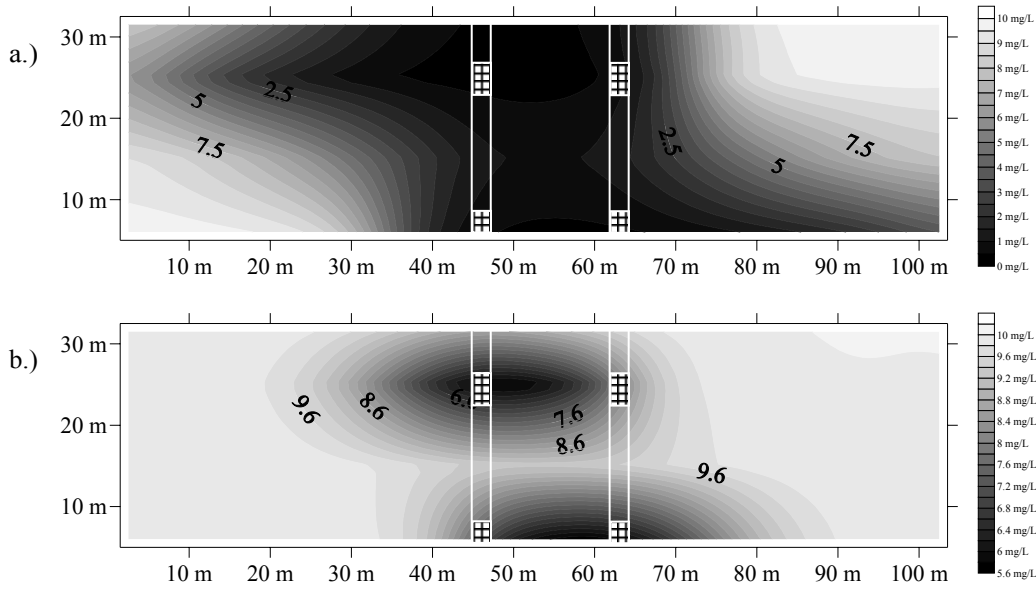


Figure 26 North-South Profiles of MTBE Concentration Contours for (a) Horizontal Hydraulic Conductivity=2.5 m/day and (b) Horizontal Hydraulic Conductivity=50m/day at 1200 days, With Approximate Well Locations Shown (All Layers, Baseline Kinetic and Engineering Data)

4.3.2.2 ANISOTROPY RATIO

This section discusses the results of the sensitivity analysis of the direct metabolism technology model to various anisotropy ratios. Anisotropy ratios (horizontal to vertical hydraulic conductivity) of 100 to 1, 20 to 1, and 1 to 1 were varied while all other parameters remained fixed at their respective baseline values. The primary purpose of varying this parameter was to investigate the potential for well short-circuiting under isotropic conditions. Well short-circuiting occurs when water exits the injection screen of a well and travels vertically to the extraction screen of the same well.

Figure 27 shows the MTBE breakthrough curves at the downgradient, centerline observation well for each anisotropy ratio simulation. According to the breakthrough curves, isotropic conditions result in higher downgradient MTBE concentrations in layer 2 than those simulations conducted under anisotropic conditions. Note that there's very little difference between anisotropy ratios of 20 to 1 and 100 to 1. Flow appears to be essentially horizontal for anisotropies greater than about 20 to 1.

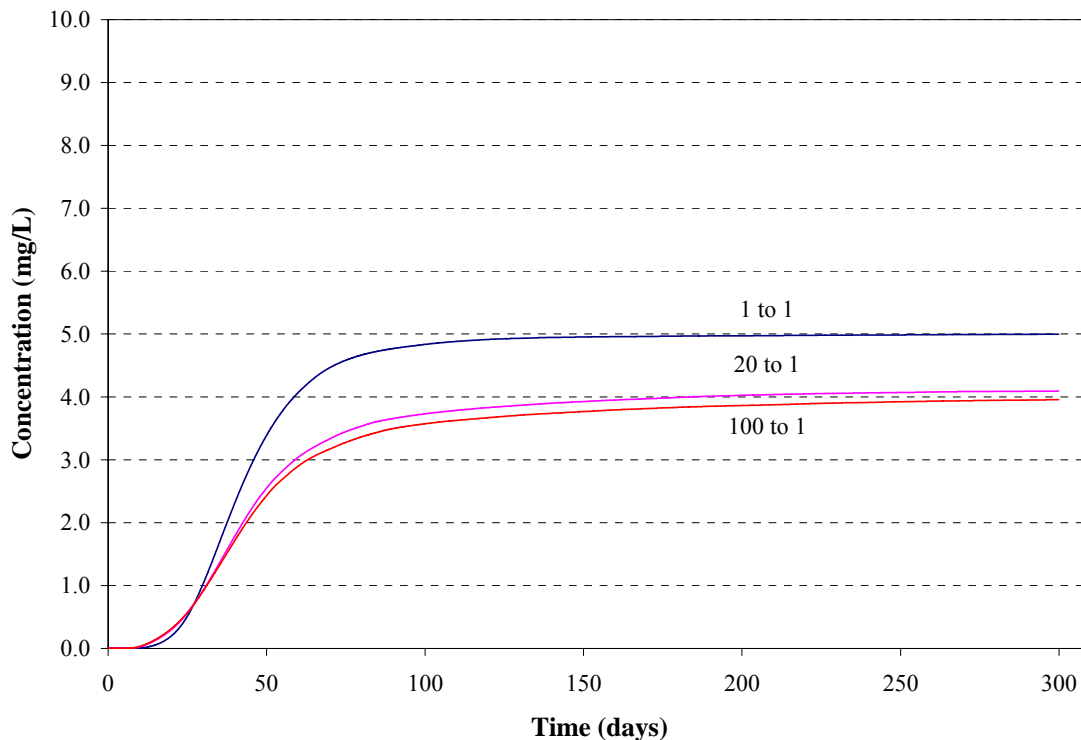


Figure 27 MTBE Breakthrough Curves at Centerline Observation Well for Different Anisotropy Ratios (Layer 2)

Different concentration behavior is seen at a centerline observation well in layer 3 (Figure 28). Here, the lowest concentrations are seen when conductivity is isotropic. The reason for the lower MTBE concentrations observed in layer 3 may be vertical

mixing with treated water from layers 2 and 4, as well as vertical mixing of electron donor into layer 3 thus stimulating microbial activity within the layer.

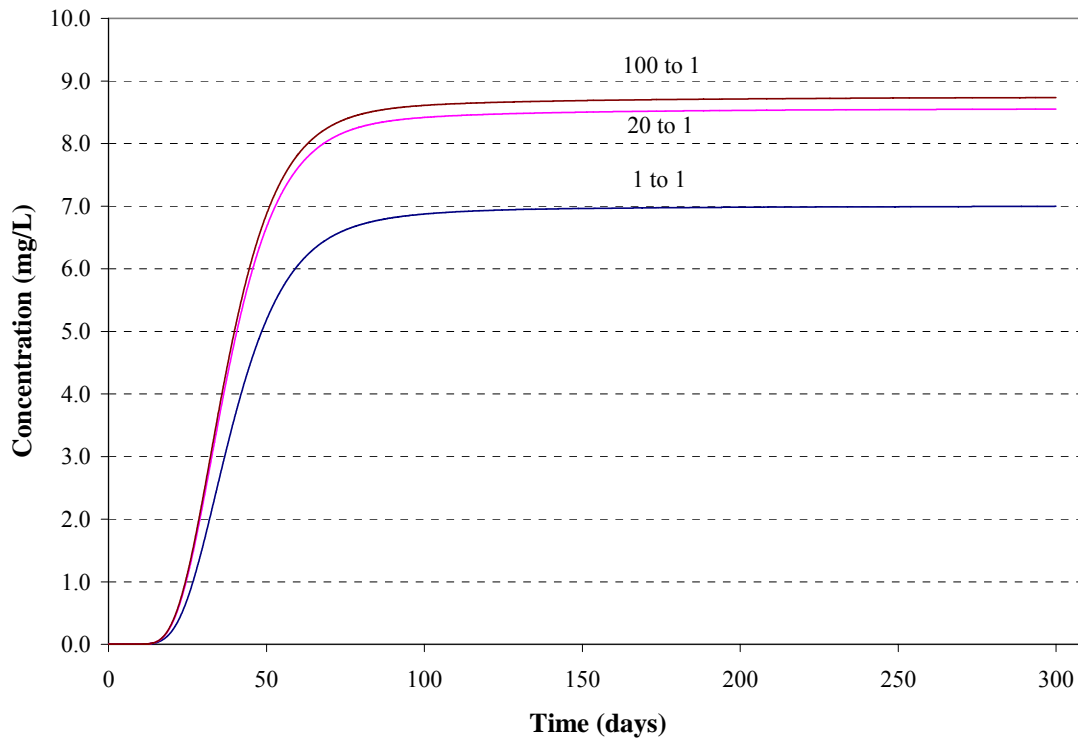


Figure 28 MTBE Breakthrough Curves at Centerline Observation Well for Different Anisotropy Ratios (Layer 3)

Figure 29 depicts the MTBE concentrations at day 300 along the north-south axis for each anisotropy ratio simulation. Isotropic conditions, which are depicted in Figure 29(a), may result in some degree of vertical flow and perhaps well short circuiting. Alternatively, Figure 29(b) and (c) show MTBE concentration reductions spread predominantly in the horizontal direction. The vertical spread of reduced MTBE concentrations in the isotropic simulation, suggests that significant vertical flow is occurring.

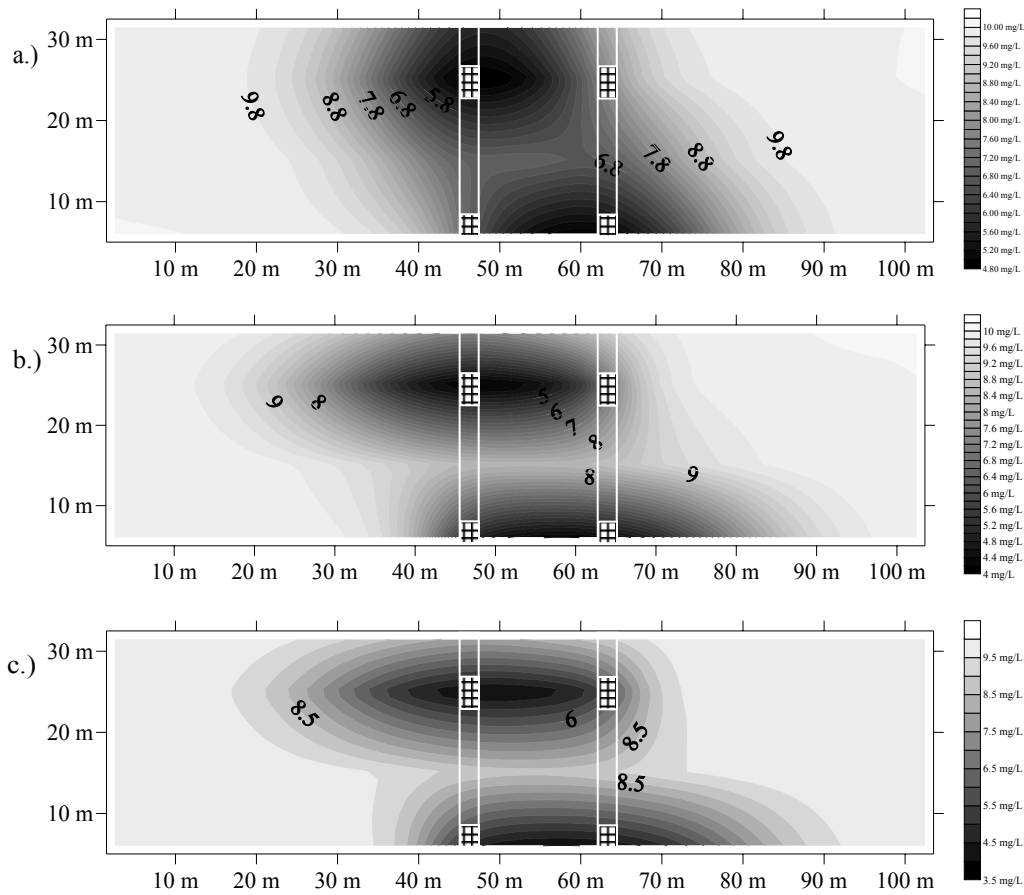


Figure 29 North-South Profiles of MTBE Concentration Contours for Anisotropy Ratios of (a) 1 to 1, (b) 20 to 1, and (c) 100 to 1 at 300 days (All Layers, Baseline Kinetic and Engineering Data)

Figure 30 shows the flow lines induced by the operation of the HFTWs under isotropic conditions. Vertical flow lines clearly indicate that well short circuiting is occurring; however, the figure also indicates that there is also interflow between the upflow and downflow treatment wells.

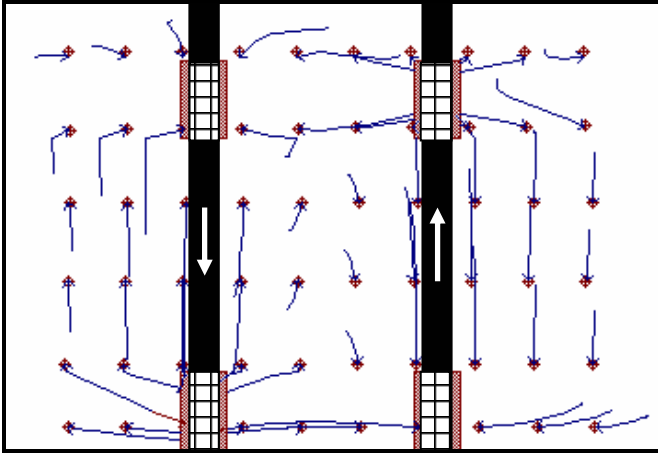


Figure 30 Flow Lines Induced by HFTW Operation in Isotropic Conditions

Evidence of vertical flow is also supported by Figure 31, which depicts oxygen concentrations along the north-south profile. Figure 31(a) clearly shows oxygen concentrations are spread both horizontally and vertically. Figure 31(b) shows that at an anisotropy ratio of 100 to 1, oxygen is also spread vertically, but not to the extent that it is under isotropic conditions. There appears to be more oxygen spreading in the vertical than in the horizontal direction for the isotropic simulation, which is expected if vertical flow and some degree of well short circuiting is occurring. The well screens in a single well in this study were separated by a vertical distance of 15 meters. This spacing may not be sufficient to prevent short circuiting under the simulated isotropic conditions.

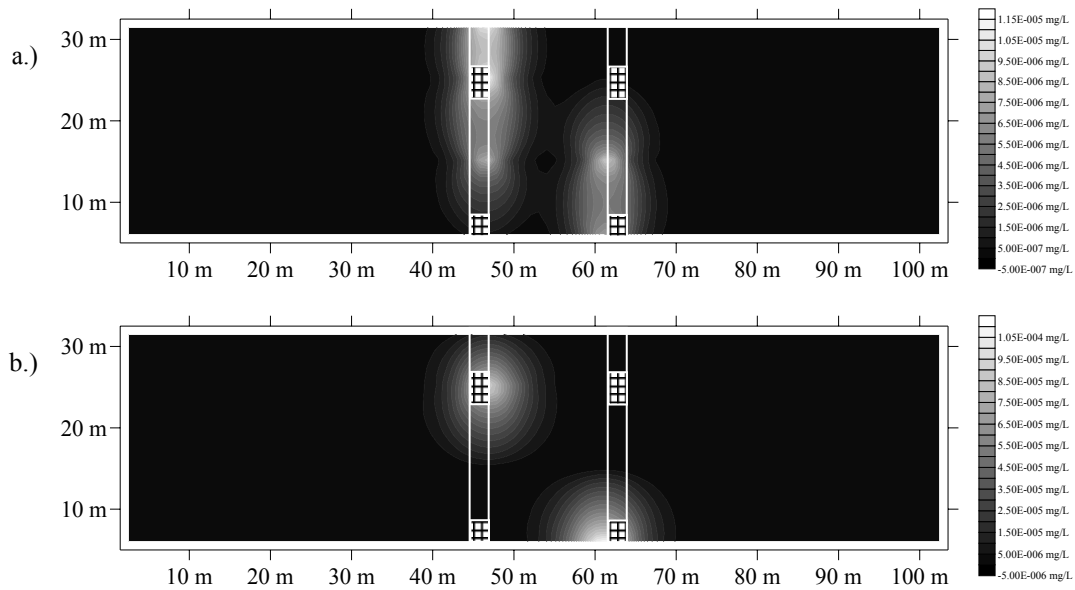


Figure 31 North-South Profiles of Oxygen Concentration Contours for Anisotropy Ratios of (a) 1 to 1, (b) 100 to 1 at 300 days (All Layers, Baseline Kinetic and Engineering Data)

Finally, mass balance output from the anisotropy simulations in Table 31 shows that slightly more MTBE mass is degraded and more microorganisms remain in the system at day 300 at isotropic aquifer conditions. The reason for this may be a result of the vertical flow of oxygen into other layers of the aquifer supporting significant microbial activity. Furthermore, these results indicate that the kinetic parameters assumed for the baseline simulations may be adequate to support significant MTBE degradation despite any vertical flow that may be occurring. Fortunately, according to these results, well short circuiting may not be detrimental to the performance of this technology under the simulated isotropic conditions.

Table 31 MTBE Mass Degraded and Microbial Mass at Various Anisotropy Ratios (All Layers, 300 days)

Anisotropy Ratio (Horiz. Cond : Vert. Cond.)	MTBE Degraded (kg)	Microorganism Mass (kg)
1 : 1	287	24.5
20 : 1	270	14.9
100 : 1	266	12.8

4.3.2.3 MTBE SOURCE CONCENTRATIONS

The sensitivity of the model to changes in source concentration is discussed in this section. A high and low MTBE concentration source, 100 and 1 mg/L respectively, was used for this analysis in addition to the baseline MTBE source concentration of 10 mg/L. The TAC for hydrogen peroxide was also adjusted appropriately to maintain a consistent stoichiometric ratio of MTBE to oxygen for all three simulations. Although this analysis does not specifically involve varying the kinetic parameters used in the model, varying source concentrations may provide some insight into the sensitivity of the model to the value of some biodegradation kinetic parameters including half-saturation constant ($K_{s-Donor}$) and maximum substrate utilization rate (k_{Donor}).

Figure 32 depicts the breakthrough curve concentrations at the downgradient, centerline observation well for each source concentration simulation as a percentage of the source concentration. It is clear from the figure that the downgradient concentration of the 10 mg/L source is reduced by the greatest percentage, approximately 60%. The reduction in downgradient concentrations of the 100 and 1 mg/L sources is less substantial, approximately 20% and 30% respectively.

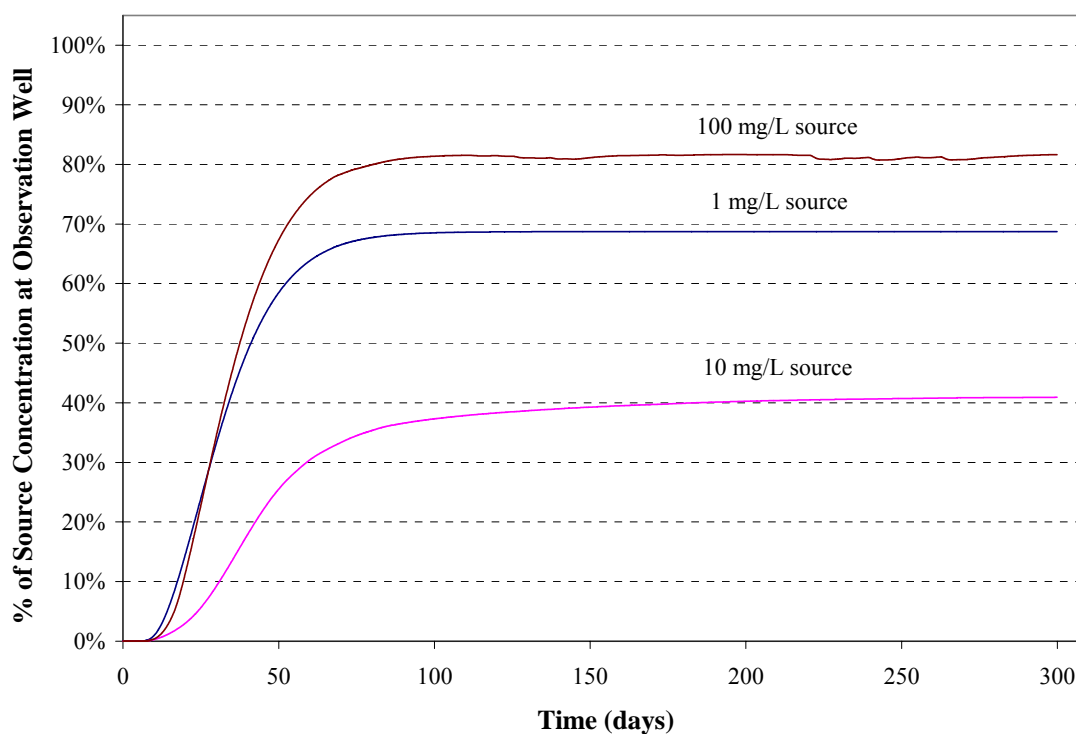


Figure 32 MTBE Breakthrough Curves at Centerline Observation Well for Different Source Concentrations (Layer 2)

This behavior depicted in Figure 32 may be attributed to the effect of varying source concentrations on the rate of MTBE utilization dictated by dual-Monod kinetics. At high MTBE concentrations the MTBE utilization rate is zero-order, thus the rate is essentially fixed at or near the maximum utilization rate. Under these conditions one would expect that significant mass be removed, although due to rate limitations greatly reduced downgradient concentrations may not be achieved because the MTBE mass loading rate is too high relative to the utilization rate. On the other hand, at low MTBE concentrations, the MTBE utilization rate is significantly impaired due to the characteristics of dual-Monod kinetics. Under these conditions, the rate of MTBE degradation is most certainly first-order, thus is highly dependant on MTBE

concentration. Under these circumstances, one would expect that little mass be removed, while lower downgradient concentrations may not be achieved even though the MTBE mass loading rate is relatively low. The breakthrough curve for the 10 mg/ L source indicates that the utilization rate may be zero- or first-order, yet is substantial enough to significantly reduce downgradient concentrations at the MTBE mass loading rate. The MTBE breakthrough curves depicted in Figure 32 for the various source concentrations seem to support this phenomenon.

Table 32 shows the MTBE mass degraded for each source concentration simulation. It can be seen that the most mass removed occurred during the 100 mg/L source simulation; although, that simulation resulted in only 20% reduction in downgradient MTBE concentration. The behavior seems reasonable due to the effect of source concentration on kinetics which was discussed previously.

Table 32 MTBE Mass Degraded for Different MTBE Source Concentrations (All Layers, 300 days)

Source Concentration (mg/L)	MTBE Degraded (kg)
1	13.4
10	270
100	829

4.3.2.4 TIME AVERAGE CONCENTRATION OF HYDROGEN PEROXIDE

The sensitivity of the model to changes in TAC of hydrogen peroxide injected was also investigated. Because the hydrogen peroxide is the source of oxygen added to the MTBE-contaminated groundwater, as well as a biocide, the purpose of this sensitivity analysis is two-fold. First, this investigation may provide insight into the effect on

system performance of hydrogen peroxide inhibition of microbial growth. Second, this investigation may indicate the sensitivity of the model to oxygen concentrations.

The MTBE breakthrough curves at the downgradient, centerline observation well in layer 2 depicted in Figure 34 show that the lowest downgradient concentrations are achieved at the hydrogen peroxide TAC = 572 mg/L. This observation is intuitive. One would guess that more MTBE would be degraded if more oxygen is available to support microbial activity.

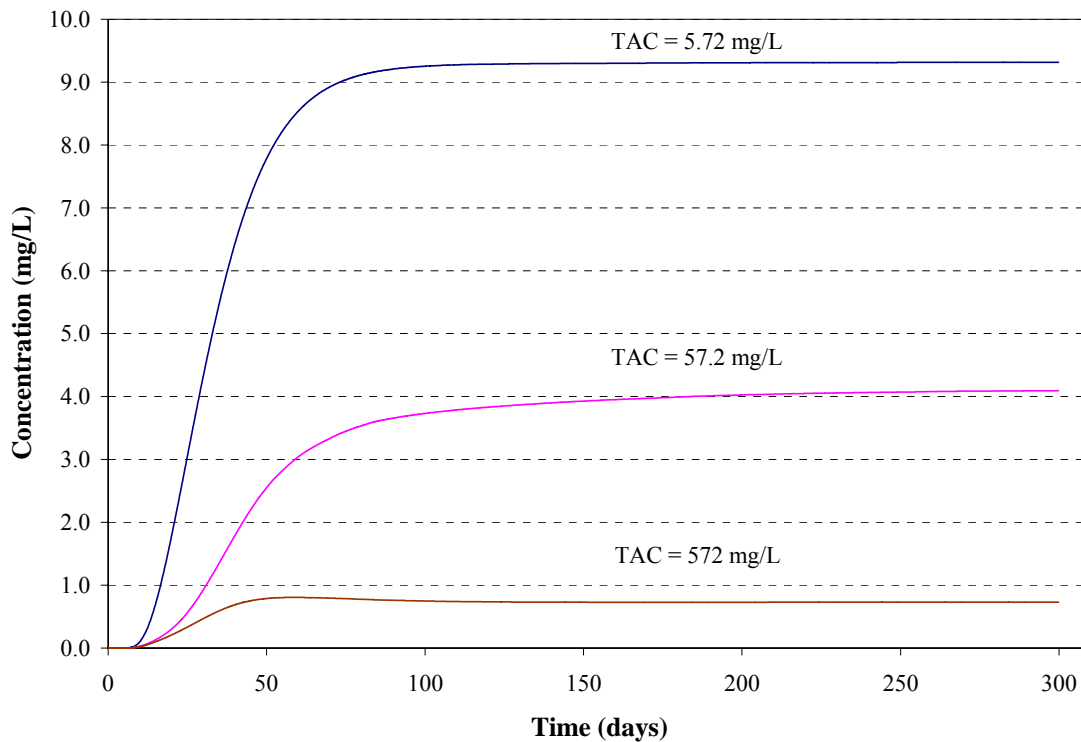


Figure 33 MTBE Breakthrough Curves at Centerline Observation Well at Various Hydrogen Peroxide TACs (Layer 2)

Increased TACs of hydrogen peroxide also have an effect on microbial growth. Higher TACs of hydrogen peroxide appear to inhibit microbial growth near the injection

well, as illustrated in Figure 34. In particular, comparison of Figure 34(a) to Figure 34(c) shows that microbial growth is strongly impacted by the TAC of hydrogen peroxide injected.

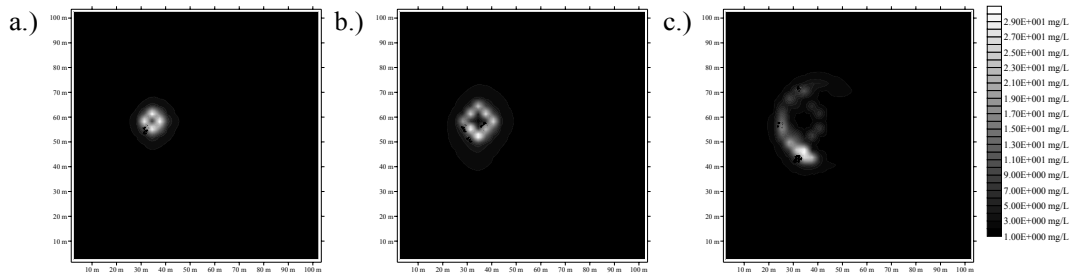


Figure 34 Microbial Concentration Contours for Hydrogen Peroxide TACs of (a) 5.72 mg/L, (b) 57.2 mg/L, and (c) 572 mg/L at 300 days (All Layers)

Intuitively, higher oxygen concentrations ultimately lead to more MTBE mass removal, as shown below in Table 33. As more oxygen is available for microbial growth and activity, more MTBE is degraded at the higher hydrogen peroxide TAC. Despite the inhibition on microbial growth, high TACs of hydrogen peroxide do not seem to negatively impact the performance of the technology model. It appears, at least for the parameters used in these simulations, that higher hydrogen peroxide TACs may benefit the performance of the technology more than hinder it.

Table 33 MTBE Mass Degraded and Microbial Growth at Various Hydrogen Peroxide TACs (All Layers, 300 days)

TAC Hydrogen Peroxide (mg/L)	MTBE Degraded (kg)	Microbial Growth (kg)
5.72	30.9	3.3
57.2	270	14.9
572	457	16.5

4.3.2.5 PUMPING RATE

The sensitivity of the technology model to various pumping rates was investigated and is discussed in this section. Three simulations were conducted at pumping rates of 50, 100 and 200 m³/day, respectively. In order to maintain the baseline TAC of hydrogen peroxide, the mass loading rate of hydrogen peroxide was adjusted for each simulation. The consequence of adjusting the mass loading rate of hydrogen peroxide is that more hydrogen peroxide was injected during the simulation period at the 200 m³/day pumping rate than during the simulations of lower pumping rates.

The lower downgradient MTBE concentrations depicted in Figure 35 achieved at the higher pumping rate may be the result of two complementary functions, increased interflow and higher MTBE and oxygen mass loading at higher pumping rates. The reader should note that interflow is directly proportional to pumping rate, as described by Christ *et al.* (1999). By increasing interflow between wells, MTBE-contaminated groundwater is recirculated through the bioactive treatment zones multiple times, resulting in lower downgradient MTBE concentrations.

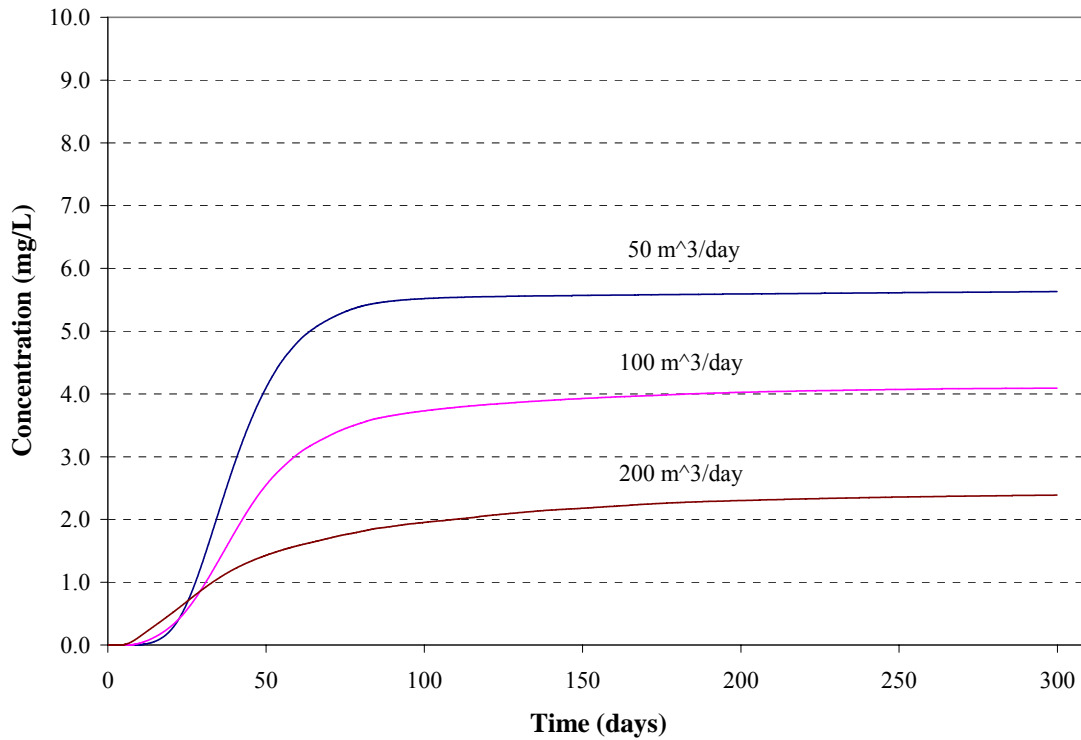


Figure 35 MTBE Breakthrough Curves at Centerline Observation Well for Various Pumping Rates (Layer 2)

Contour plots of MTBE, oxygen, and microbial concentrations for each of the various pumping rates are depicted in Figure 36. The hole of decreased MTBE concentrations is larger and more pronounced in the higher pumping rate simulations, supporting the previous observation of reduced downgradient concentrations at the monitoring well. Additionally, the apparent effects of increased MTBE and hydrogen peroxide/oxygen mass loading are shown in the contour plots of oxygen and microbial concentration, which increase with increasing pumping rate. The earlier observation regarding the effects of hydrogen peroxide inhibition on microbial growth is also seen in Figure 36, with decreased microbial growth near the injection well at the higher pumping rates and consequent higher hydrogen peroxide loadings.

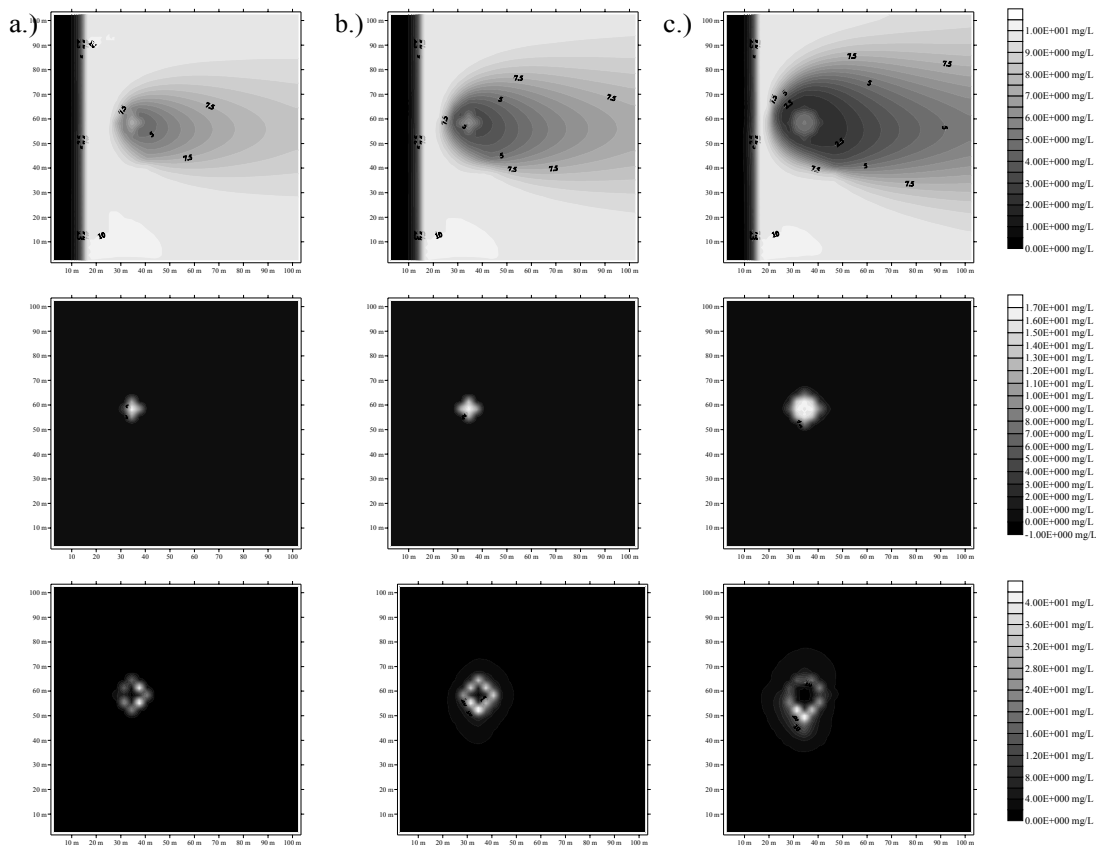


Figure 36 Contour Plots for MTBE (1st Row), Oxygen (2nd Row), and Microbial Concentrations (3rd Row), for Pumping Rates of (a) 50 m³/day, (b) 100 m³/day, and (c) 200 m³/day (layer 2, Baseline Kinetic and Environmental Data, 300 days)

Although it may be difficult to distinguish the effects of increased interflow from the effects of higher MTBE and oxygen mass loading, it is conceivable that higher interflow is responsible for lower downgradient concentrations, while higher pumping rates are responsible for the greater MTBE mass degradation shown in Table 34. Although the benefits of interflow and oxygen mass loading are combined in these simulations, they really have separate impacts on the system. High interflow between pumping wells results in multiple passes of contaminated water through the bioactive zones which leads to lower downgradient concentrations and high treatment efficiency.

Evidence supporting this relationship is also present in the sensitivity analysis of horizontal conductivity in Section 4.3.2.1. Alternatively, increased pumping rates result in a relative increase in capture zone width and increased MTBE mass loading in the bioactive zones. This requires a proportional increase in oxygen mass loading. The combination of increased MTBE and oxygen mass loading in the bioactive zones results in more MTBE mass degraded at higher flow rates.

Table 34 MTBE Mass Degraded at Various Pumping Rates (All Layers, 300 days)

Pumping Rate (m³/day)	MTBE Degraded (kg)	Hydrogen Peroxide Injected (kg)
50	146	1717
100	270	3435
200	515	6870

4.3.2.6 MTBE UTILIZATION RATE

The MTBE utilization rates (k_{Donor}) reported in the literature for MTBE metabolizing aerobes span a significant range of over three orders of magnitude. To analyze the sensitivity of the model to changes in k_{Donor} , simulations were conducted using the lowest and highest reported values and results were compared to the baseline simulation. The downgradient MTBE concentrations observed at the downgradient, centerline observation well in layer 2 varied from almost 9 mg/L to slightly more than 3 mg/L for the low and high values of k_{Donor} , respectively. Figure 37, below, shows the MTBE breakthrough curves at the downgradient, centerline observation well in layer 2 for various values of k_{Donor} . Clearly, as the value of k_{Donor} increases, downgradient concentrations of MTBE are reduced. Although the hydrogen peroxide TAC injected

was held constant, thus fixing the oxygen mass loading for this sensitivity analysis, the reader should note that increased MTBE utilization will also result in increased oxygen utilization.

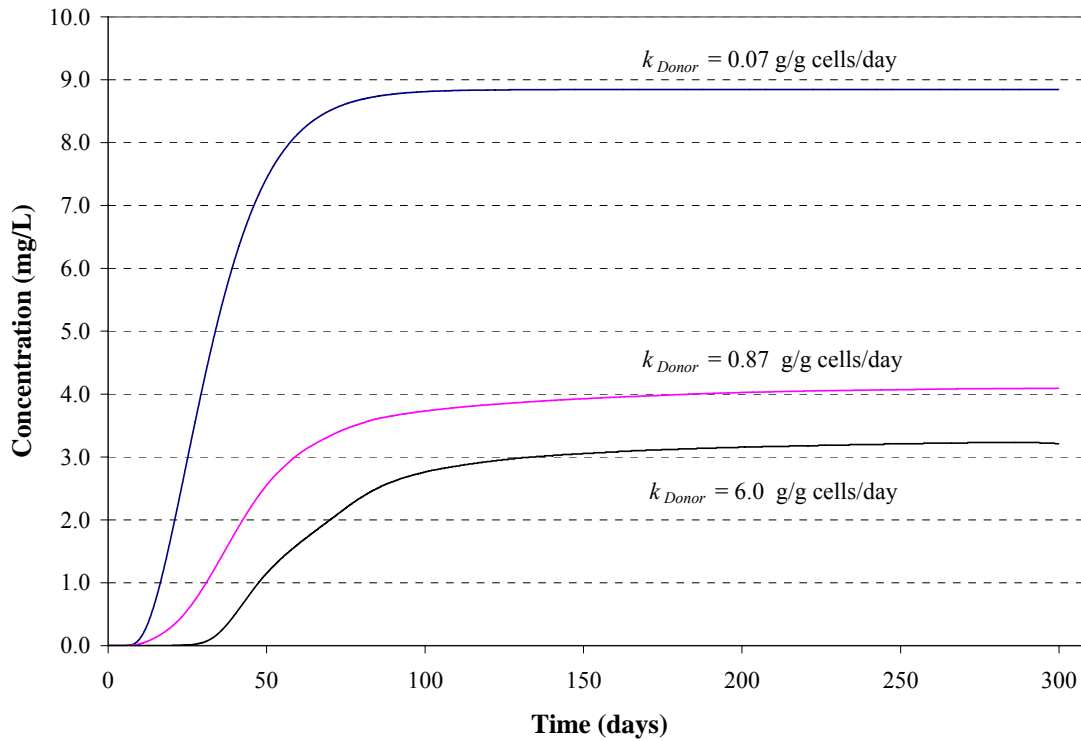


Figure 37 MTBE Breakthrough Curves at Centerline Observation Well for Various MTBE Utilization Rates (Layer 2)

Despite the variations in MTBE utilization rates over three orders of magnitude, the MTBE mass degraded only varied over two orders of magnitude. Table 35, below, shows the mass of MTBE removed for each utilization rate and the mass of oxygen remaining in the system at the end of the simulation period. In accordance with the downgradient MTBE concentrations, more mass was removed in simulations run with higher values of k_{Donor} ; however, as shown in Table 35, the mass of oxygen remaining in

the system at day 300 appears to indicate that MTBE mass removal may become limited by oxygen available.

Table 35 MTBE Mass Degraded and Oxygen Remaining at Various Utilization Rates (All Layers, 300 days)

MTBE Utilization Rate (g/g cells/day)	MTBE Degraded (kg)	Oxygen Remaining (kg)
0.07	56.3	55.4
0.87	270	10.1
6.0	316	2.91

Although the exact values of the kinetic parameter k_{Donor} are not known, care must be taken to ensure abundant oxygen is available for the oxidation reactions to proceed at the maximum rate achievable. The results of the sensitivity analysis on the TAC of hydrogen peroxide discussed previously appear to confirm this observation.

4.3.2.7 MTBE HALF-SATURATION CONSTANT

The values of MTBE half-saturation constant ($K_{s-Donor}$) also vary significantly in the literature. Values of $K_{s-Donor}$ reported in the literature span three orders of magnitude. The sensitivity of the model to variations in $K_{s-Donor}$ was analyzed by comparing the results of the simulations conducted at low, baseline, and high values for $K_{s-Donor}$, of 0.33, 3.5, and 50 mg/L respectively. Figure 38, below, shows the MTBE breakthrough at the downgradient, centerline observation well for various values of $K_{s-Donor}$. As would be expected, the downgradient concentrations of MTBE are lower for lower values of $K_{s-Donor}$. This observation can be explained by the relationship that lower values for $K_{s-Donor}$ indicate a higher microbial affinity towards a particular substrate.

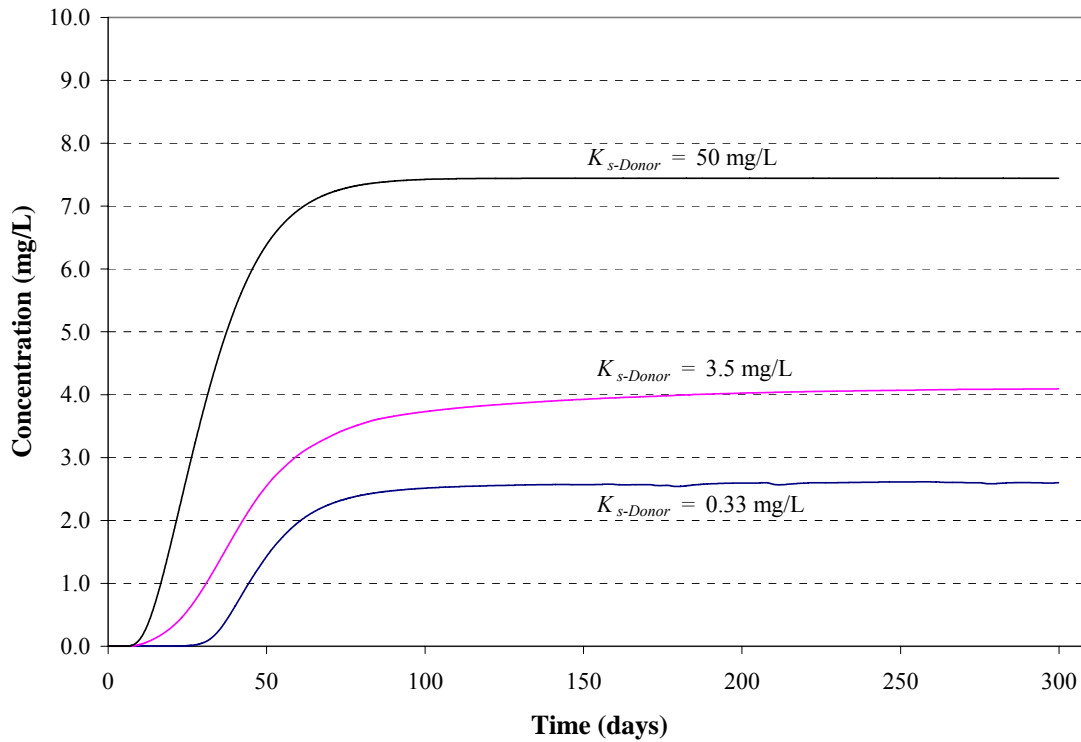


Figure 38 MTBE Breakthrough Curves at Centerline Observation Well for Various MTBE Half-Saturation Constant Values (Layer 2)

The mass of MTBE degraded at each respective value of $K_{s-Donor}$ also is as expected. Table 36, below, shows that more MTBE mass is degraded for lower values of $K_{s-Donor}$. Also, similar to results from the sensitivity analysis conducted on the MTBE utilization rate, lower values of $K_{s-Donor}$ may result in MTBE degradation rates that are limited by oxygen availability.

Table 36 MTBE Mass Degraded at Various MTBE Half-Saturation Constant Values (All Layers, 300 days)

MTBE Half-Saturation Constant (mg/L)	MTBE Degraded (kg)	Oxygen Remaining (kg)
0.33	331	7.85
3.5	270	10.1
50	117	48.9

The sensitivity of the model to variations in the values of the kinetic parameters k_{Donor} and $K_{s-Donor}$ clearly shows the need to obtain accurate or at least reasonable kinetic parameter values in order to accurately model this technology.

4.3.3 COMETABOLISM BASELINE

Baseline technology model simulations for cometabolism were conducted using baseline kinetic, engineering, and environmental parameter values identified in Section 3.5, of Chapter 3.0. The parameter values selected for the baseline simulations are “best guess” parameters based on the literature review of MTBE cometabolism studies, stoichiometry, and previous studies of the HFTW system. The time horizon used for the baseline simulation was 300 days.

Unfortunately, the simulation conducted using baseline kinetic, environmental, and engineering parameter values did not effectively reduce downgradient MTBE concentrations and removed only approximately 8.2 kg of MTBE. Figure 39(a) indicates that there is an excess of propane injected into the aquifer that is not subsequently degraded. Despite injection of stoichiometric proportions of hydrogen peroxide needed to oxidize the propane and MTBE, Figure 39(b and c) indicate that there is minimal oxygen and hydrogen peroxide residual at day 300, respectively. Additionally, Figure 39(d and e) show no appreciable MTBE concentration changes; although there are increased microbial concentrations near the well at day 300.

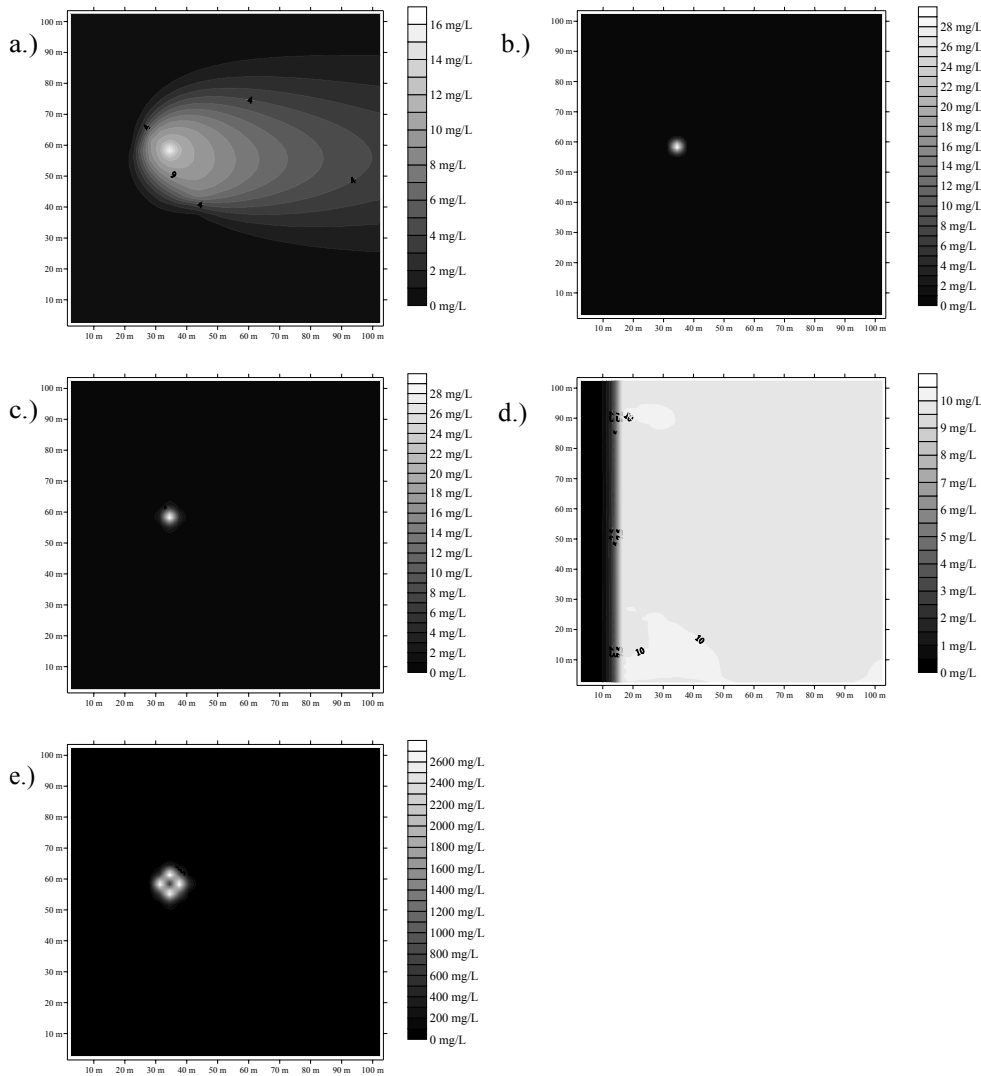


Figure 39 Contour Plots of (a) Propane, (b) Oxygen, (c) Hydrogen Peroxide, (d) MTBE and (e) Microbial Concentrations at 300 days, Respectively (Layer 2, Baseline Data)

The baseline simulation conducted using the best guess parameter values is not adequate to evaluate the performance of the technology model, nor is it adequate for comparison purposes in the sensitivity analysis. It was concluded that one or more of the engineering parameters may need to be changed to achieve more desirable results. As depicted in Figure 39, there is an excess of electron donor and depletion of electron acceptor, therefore a logical parameter to change is the TAC of hydrogen peroxide.

Although there is a danger that an increased TAC of hydrogen peroxide could significantly inhibit microbial activity, the TAC of hydrogen peroxide was doubled from 171.7 mg/L to 343.4 mg/L in the hopes that increased oxygen concentrations would result in promoting additional microbial growth, propane utilization, and substantial MTBE degradation.

The results of the simulation run with TAC of hydrogen peroxide of 343.4 mg/L indicate that 32.6 kg of MTBE was degraded; however, downgradient concentrations of MTBE were only slightly reduced to approximately 9.5 mg/L. Additionally, excess propane continued to accumulate in the system and was transported downgradient while very little oxygen remained in the system at day 300. These results seem to indicate that despite the increased TAC of hydrogen peroxide injected, the propane mass loading may be too high.

Considering the results of the previous simulation, the TAC of propane was reduced to 1.5 mg/L while the hydrogen peroxide TAC was fixed at the baseline value of 171.7 mg/L for the following simulation. Results of this simulation indicate a modest increase of MTBE degraded from the previous simulation to 33.3 kg. Interestingly, downgradient MTBE concentrations initially stabilized at approximately 9 mg/L for about 100 days, but later began to rise, eventually approaching the upgradient source concentration of 10 mg/L. Observations of solute and microbial concentrations taken in layer 2, between the pumping wells, show the microbe concentration increases rapidly initially, but then declines to what appears to be a sustainable steady state level. The decline and subsequent stabilization of the microbe population may have caused the observed trend of increasing downgradient MTBE concentrations after concentrations

appeared to stabilize at 9 mg/L. Propane was not transported downgradient nor were significant concentrations observed more than 10 meters from the injection well. Also, concentration contour plots (not shown) of oxygen concentrations in layer 2 show an excess of oxygen in the region surrounding the injection well.

Considering the results of these previous simulations, the baseline parameter values were re-evaluated. Reducing the TAC of propane to 1.5 mg/L resulted in only modest differences between MTBE mass degraded and downgradient MTBE concentrations compared to the simulation run with the baseline propane TAC and increased hydrogen peroxide TAC; however, injecting less propane and less hydrogen peroxide is economically favorable, therefore subsequent parameter value selection was made under this premise. Despite findings from Parr (2002), who concluded that perchlorate metabolism using an HFTW system was best facilitated by continuous injection of an electron donor, it is possible that continuous injection of electron donor may not be optimal for the MTBE cometabolism technology model. This conclusion is supported by McCarty *et al.* (1998) and Goltz *et al.* (2001), who found that continuous injection is not optimal for stimulating cometabolic biodegradation.

For the following simulations the propane pulse schedule was changed from continuous (8 hours on, 0 hours off) to 1 hour on and 7 hours off for the first series of simulations, and to 4 hours on and 4 hours off for the second series of simulations for various propane TACs. The TAC of hydrogen peroxide was fixed at 171.7 mg/L and injected continuously for all simulations, thus oxygen availability for microbial activity should not be limiting. Simulations were conducted for propane TACs of 1.5, 3.0, 6.0, and 12.0 mg/L.

Figure 40 shows the MTBE mass degraded for different propane TACs for the two pulsed propane injection schedules. The two simulations with the propane TAC of 3.0 mg/L resulted in the most MTBE mass degraded, with slightly more mass removed for the 1 hour on and seven hour off schedule. Mass balance outputs show that approximately 112 kg of MTBE were degraded in the 300 day simulation with the revised pulse schedule and propane TAC compared to only 8.2 kg of MTBE removed with continuous propane injection at the same propane TAC of 3 mg/L.

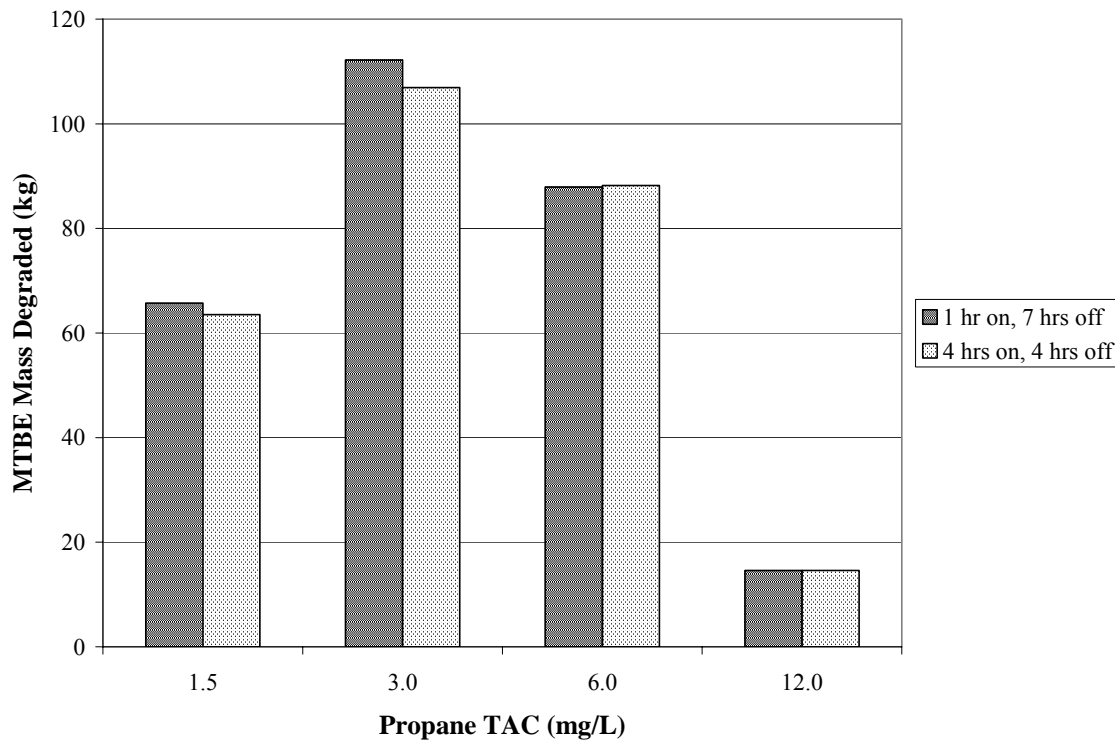


Figure 40 MTBE Mass Degraded for Various Propane TACs and Injection Schedules (All Layers)

Figure 41 shows the MTBE breakthrough curves at the downgradient, centerline observation well in layer 2 for various propane injection pulse schedules. The TAC of

propane and hydrogen peroxide injected was held constant for each simulation at 3.0 mg/L and 171.7 mg/L, respectively. Although the long-term downgradient concentrations achieved by the 1 hour on, 7 hours off and 4 hours on, 4 hours off pulse schedules are approximately the same, shorter pulses result in lower downgradient concentrations earlier, and hence are preferable. Clearly the downgradient concentration achieved with continuous propane injection is the least favorable as the downgradient concentration initially stabilizes but later (approximately day 210) rapidly approaches the source concentration (10 mg/L).

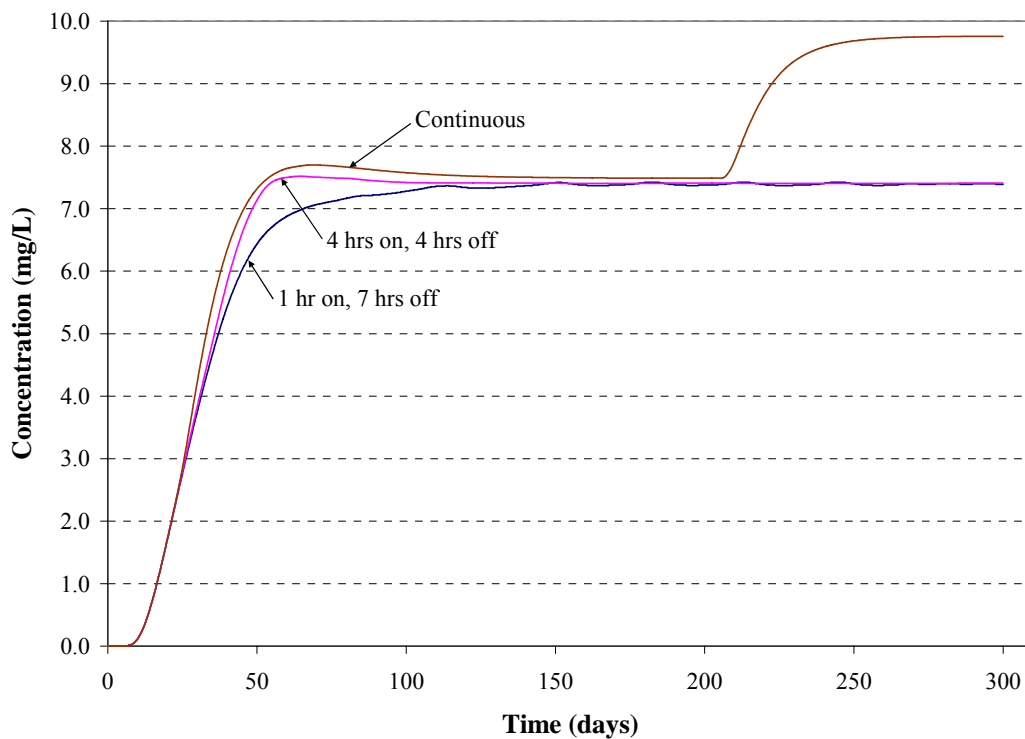


Figure 41 MTBE Breakthrough Curves at Centerline Observation Well for Various Propane Injection Pulse Schedules (Layer 2, Propane TAC=3.0 mg/L, Baseline Kinetic and Environmental Data)

The rapid rise in MTBE concentrations seen on day 210 in Figure 41 is also observed for other breakthrough simulations when propane is continuously injected at low TACs (*i.e.* 1.5 to 3.0 mg/L). In these simulations, propane injection appears to stimulate rapid microbial growth near the injection wells. This growth is followed by rapid consumption of propane, resulting in near depletion of propane in the bioactive zones close to the injection wells. Following this depletion of propane, the microbial population declines to a low concentration of approximately 1.9 mg/L. At this low microbial population, propane concentrations rise slightly. At what appears to be steady-state in the bioactive zones, we observe a low propane concentration that virtually shuts down MTBE degradation by competitive inhibition. Thus, MTBE concentrations rise to the upgradient value.

The impact on both mass removal and downgradient concentration for the different pulse schedules are a result of competitive inhibition. Competitive inhibition occurs when both primary and secondary substrates are simultaneously present, consequently reducing secondary substrate utilization (McCarty *et al.*, 1998). Based on results from the simulations, the negative effects of competitive inhibition can be minimized by pulsing the primary substrate (*i.e.* propane).

Slight oscillations in the MTBE concentration at the downgradient observation well can be seen approximately after day 100 (especially for the 1 hour on, 7 hour off pulse schedule). These oscillations, which appear to be dampened by day 300, may be the result of fluctuations in the microbial population near the injection wells. As the value for primary substrate half-saturation constant ($K_{s-Donor}$) is relatively low in the model, it is conceivable that the microbial population response to changes in propane

concentration and pulse injection is very sensitive. Consequently the downgradient MTBE concentration may be affected by slight variations in the microbial population.

Based on the above model simulations, it was determined that the baseline engineering parameter values for propane TAC and propane injection pulse schedule should be changed from the original best guess values to the revised values listed in Table 37. The reader should note that henceforth, baseline engineering parameter values for the cometabolism technology model will refer to the revised values in Table 37.

Table 37 Revised Engineering Parameters Used in Cometabolic Model Simulations

Parameter	Baseline Value	Range Tested
Time-averaged electron donor conc.	3.0 mg/L	N/A
Donor injection pulse schedule	1 hr on, 7 hrs off	N/A
Time-averaged hydrogen peroxide conc.	171.7 mg/L	N/A
Peroxide injection pulse schedule	continuous	N/A
Well spacing	15 m	N/A
Well screen length	5 m	N/A
Pumping rate	100 m ³ day ⁻¹	N/A
Well depth	35 m	N/A

Figure 42 shows the concentration contour plots for propane, oxygen, hydrogen peroxide, MTBE, and microbes at day 300. In contrast to Figure 39(a), Figure 42(a) depicts very little residual propane at day 300 and no excess propane transported downgradient. Figure 42(b) clearly shows there is oxygen remaining near the injection well, confirming that oxygen is not limiting. Most importantly, though, is Figure 42(d) which shows that MTBE concentrations are reduced downgradient.

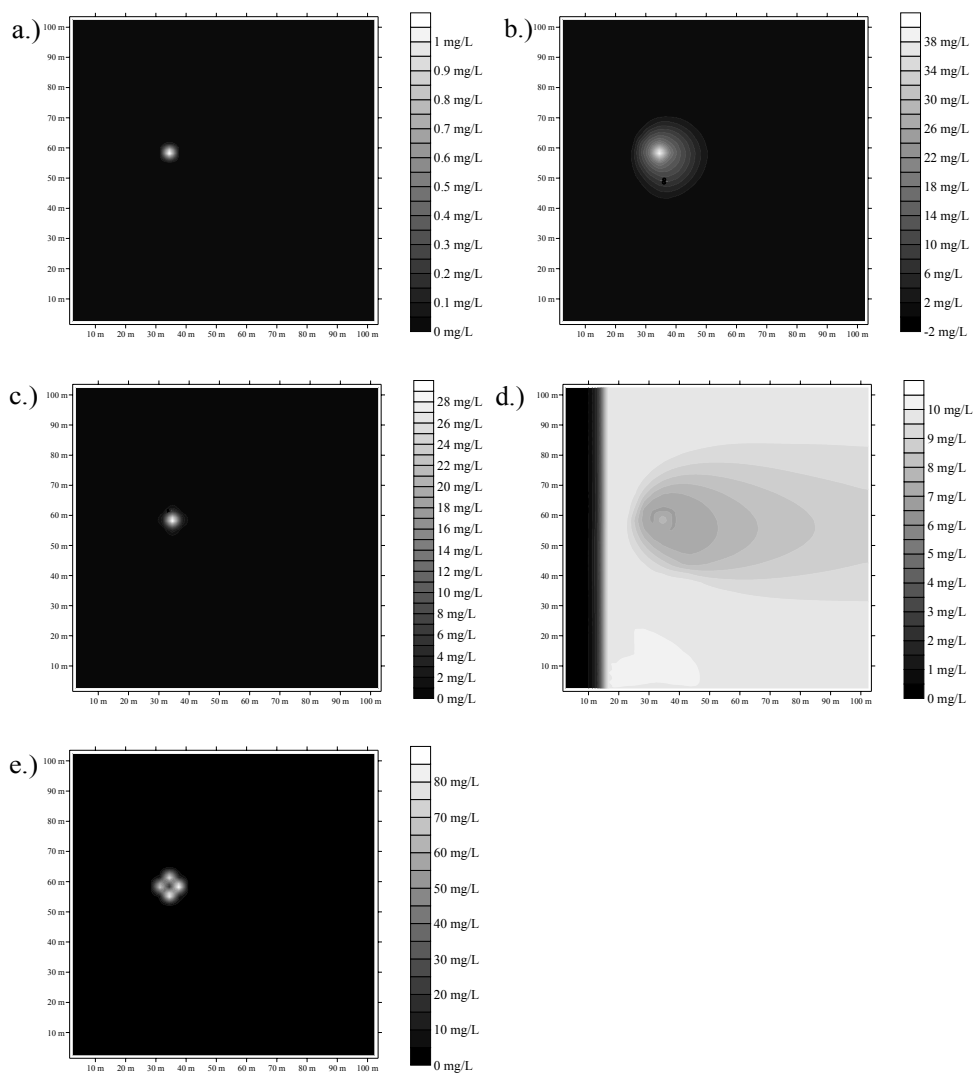


Figure 42 Contour Plots of (a) Propane, (b) Oxygen, (c) Hydrogen Peroxide, (d) MTBE and (e) Microbial Concentrations at 300 days, Respectively (Layer 2, Baseline Data)

Mass balance output from the cometabolism baseline simulation is summarized below in Table 38. Interestingly, only approximately 9.9 kg of microorganisms remain in the system by day 300, yet substantial masses of propane and MTBE have been removed.

Table 38 Summary of Mass Balance Output for Cometabolism Baseline Simulation (All Layers, 300 days)

	Propane (kg)	Oxygen (kg)	Hydrogen Peroxide (kg)	MTBE (kg)	Microorganisms (kg)
Injected	184.1	0.0	10302.0	0.0	0.0
(+) Growth (-) Decay	-183.0	35.2	-10273.0	-112.2	9.9

4.3.4 COMETABOLISM SENSITIVITY ANALYSIS RESULTS

Cometabolism kinetic parameters were varied independently during the sensitivity analysis of the cometabolism model. The kinetic parameters varied in the sensitivity analysis include primary substrate utilization rate (k_{Donor}), primary substrate half-saturation constant ($K_{s-Donor}$), MTBE utilization rate (k_{MTBE}), and the MTBE half-saturation constant (K_{s-MTBE}). Model sensitivity to environmental and engineering parameters was not analyzed for the cometabolism model because these factors were already considered in the sensitivity analysis of the direct metabolism model. The specific kinetic parameter values used during the sensitivity analysis can be found in Section 3.5 of Chapter 3.0.

Simulations were conducted over a time horizon of 300 days, which was a “long” time based on the kinetic parameter values. The kinetic parameter sensitivity results were analyzed by examining breakthrough curves at the centerline observation well and the observation well located in the layer 2 injection well, concentration contour plots, and total mass degraded, when applicable. Again, long-term behavior of the technology, although important, is beyond the scope of this research and may be the subject of a future optimization study.

4.3.4.1 PRIMARY SUBSTRATE UTILIZATION RATE

The primary substrate utilization rate (k_{Donor}) was varied over the range of reported values taken from the literature. In addition to the selected value of k_{Donor} used for the baseline simulation (2.6 g/g cells/day), a low and high value was selected for simulation, 0.2 g/g cells/day and 5.1 g/g cells/day respectively. Although the range of values for k_{Donor} spans two orders of magnitude, Figure 43 shows only modest changes in the downgradient MTBE concentration, with, as expected, downgradient concentrations decreasing with increasing rates.

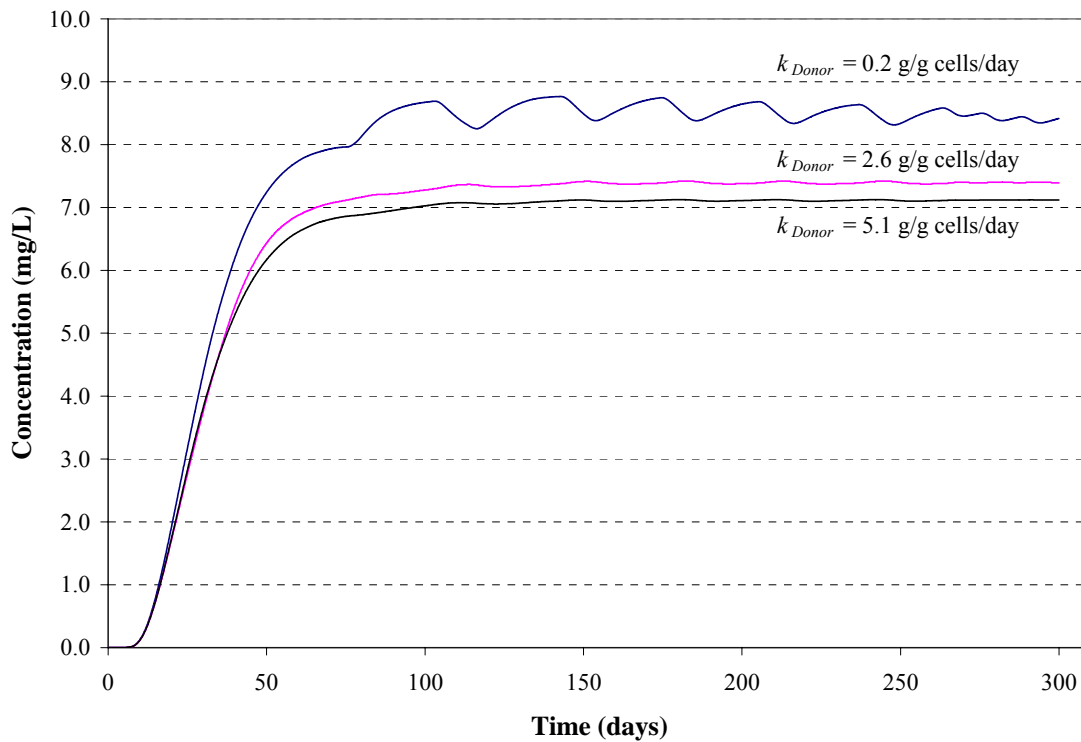


Figure 43 MTBE Breakthrough Curves at the Centerline Observation Well for Various Primary Substrate Utilization Rates (Layer 2)

Interestingly, as the value for k_{Donor} decreased, the amplitude of oscillations observed in the downgradient concentration of MTBE increased, as shown in Figure 43. These oscillations may be attributed to the dual-Monod kinetic equations used to simulate the rate of change of microbial concentrations. The oscillations observed in Figure 43 appear to lead to the oscillations in microbial concentrations observed in Figure 44. Because the value for k_{Donor} is low, propane may accumulate in the system until microbial concentrations slowly respond. As the microbial concentrations increase, the propane is more rapidly consumed by the increased population of microbes until insufficient propane concentrations are available to support the microbial population. It appears that the over-shoot and collapse behavior of the microbes translates into the oscillations of downgradient MTBE concentrations. As this behavior dampens over time, it does not seem to result in long-term impacts to system operation.

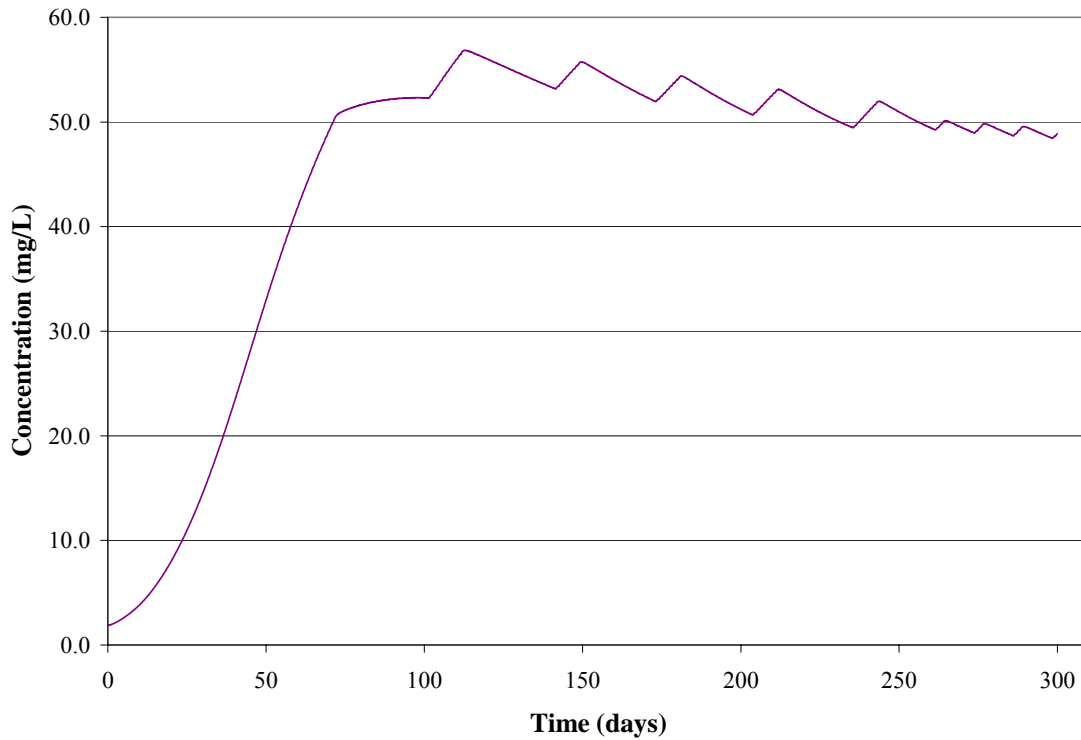


Figure 44 Microbial Concentrations Observed at the Centerline Observation Well Located Between the Pumping Wells (Layer 2)

Table 39 shows, as expected, that increased MTBE mass was removed in simulations run with higher k_{Donor} values. Also, despite the two order of magnitude range of k_{Donor} values used in the sensitivity simulations, the mass of MTBE degraded did not vary as drastically. This may be attributed to the fact that ultimately, propane becomes limiting, and an increase in the value of k_{Donor} does not result in higher MTBE utilization. If k_{Donor} is high, a remediation strategy might be to increase the propane TAC to ensure better system performance.

Table 39 MTBE Mass Degraded at Various Primary Substrate Utilization Rates (All Layers, 300 days)

Primary Substrate Utilization Rate (g/g cells/day)	MTBE Degraded (kg)
0.2	61.4
2.6	112
5.1	124

4.3.4.2 PRIMARY SUBSTRATE HALF-SATURATION CONSTANT

The values for the primary substrate half-saturation constant ($K_{s-Donor}$) are fairly well defined and do not span a significant range of values. The range of values reported in the literature spans from approximately 0.2 to 0.4 mg/L, propane. Simulations were conducted using the low, baseline, and high values of 0.2, 0.3, and 0.5 mg/L, respectively, to observe model sensitivity to variations in the value of $K_{s-Donor}$. Ultimately, only minimal (less than 0.2 mg/L) changes in downgradient MTBE concentrations were observed over the range of $K_{s-Donor}$ values. Additionally, only minimal (less than 3 kg) changes in MTBE mass degraded were observed. Observations of the sensitivity of the model to variations in the value of $K_{s-Donor}$ indicate that the performance of the model is not particularly sensitive to this parameter over the range of values reported in the literature.

4.3.4.3 MTBE UTILIZATION RATE

The values reported in the literature for MTBE utilization rate (k_{MTBE}) varied over three orders of magnitude from 0.048 to 3.5 g/g cells/day. In addition to the selected value of k_{MTBE} used for the baseline simulation (0.3 g/g cells/day), a low and high value

was selected for simulation, 0.048 g/g cells/day and 3.5 g/g cells/day, respectively.

Figure 45 shows the downgradient concentrations of MTBE for the various k_{MTBE} values used in the sensitivity analysis. As expected, the higher the value of k_{MTBE} , the lower the downgradient MTBE concentration observed. Additionally, the mass of MTBE degraded is significantly impacted by variations in k_{MTBE} values, as shown below in Table 40.

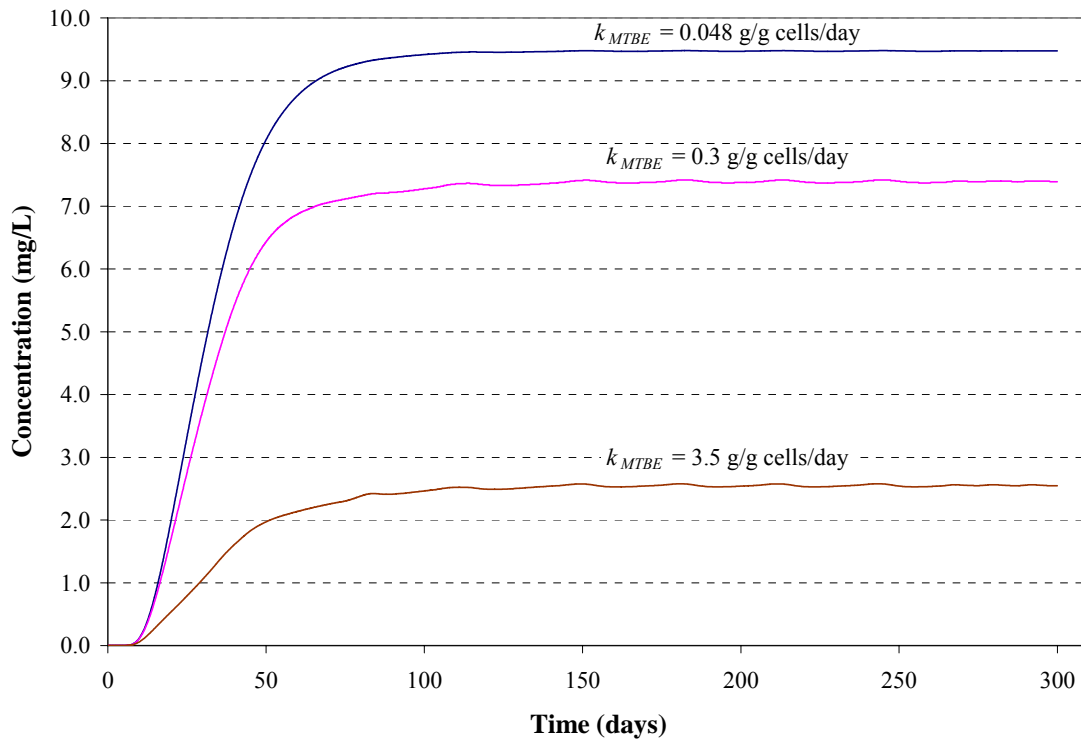


Figure 45 MTBE Breakthrough Curves at the Centerline Observation Well for Various MTBE Utilization Rates (Layer 2)

Table 40 Mass Degraded at Various MTBE Utilization Rates (All Layers, 300 days)

MTBE Utilization Rate (g/g cells/day)	MTBE Degraded (kg)
0.048	22.4
0.3	112
3.5	328

4.3.4.4 MTBE HALF-SATURATION CONSTANT

The values for the MTBE half-saturation constant (K_{s-MTBE}) also vary significantly in the literature as reported values span three orders of magnitude. In addition to the value selected for the baseline simulation (27 mg/L), a low and high value was selected for simulation, 1.2 and 120 mg/L respectively. As one would expect, lower values of K_{s-MTBE} resulted in lower downgradient MTBE concentrations, as shown in Figure 46. The reader should note that a lower value of K_{s-MTBE} indicates a greater enzyme affinity for MTBE. As expected, more MTBE was degraded in simulations run with lower values for K_{s-MTBE} , as shown below in Table 41.

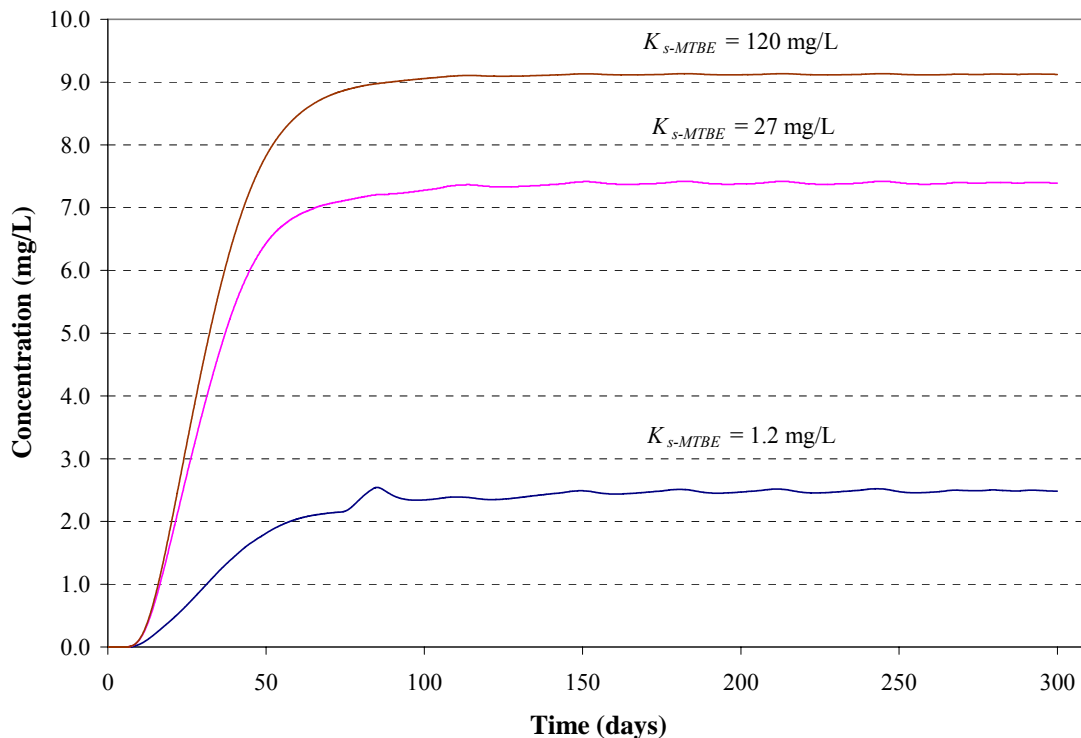


Figure 46 MTBE Breakthrough Curves at the Centerline Observation Well for Various MTBE Half-Saturation Constant Values (Layer 2)

Table 41 Mass Degraded at Various MTBE Half-Saturation Constant Values (All Layers, 300 days)

MTBE Half-Saturation Constant (mg/L)	MTBE Degraded (kg)
1.2	327
27	112
120	37.3

The sensitivity of the model to variations in the kinetic parameters k_{Donor} , $K_{s-Donor}$, k_{MTBE} , and K_{s-MTBE} clearly indicates the necessity to obtain accurate or at least reasonable values to accurately model the technology.

5.0 CONCLUSIONS

5.1 SUMMARY

In this thesis, a technology model simulating the operation of an HFTW system at an MTBE-contaminated site was developed and implemented. The technology model consists of the Huang and Goltz (1998) three-dimensional flow and transport model coupled with a dual-Monod biological kinetic submodel developed by Gandhi *et al.* (2002b) which was used to simulate direct or cometabolic biodegradation of MTBE. Using kinetic parameter values reported in the literature, simulations of this technology model at a hypothetical site resulted in MTBE mass removal and reduced downgradient MTBE concentrations.

5.2 CONCLUSIONS

As stated in Chapter 1.0, the objective of this study was to investigate the feasibility of using HFTWs as a technology for the remediation of MTBE-contaminated groundwater. Pursuing this objective required answering several research questions which are re-stated below. The purpose of this section is to discuss the results of the research by providing answers to these research questions.

- What chemical and biological processes are capable of converting MTBE to innocuous end products?
- Which of these processes may be incorporated as a component of an HFTW system?

- How will the technology, consisting of the HFTW system coupled with the MTBE destruction process, perform at an MTBE-contaminated site?

Section 3.2, of Chapter 3.0 contains a comprehensive list of the chemical and biological processes capable of degrading MTBE along with some relevant characteristics of each which was used to select a process to model. Literature review of these processes revealed that there are 13 processes capable of degrading MTBE but only 11 of those have demonstrated the ability to convert MTBE to innocuous end products. The two processes that appear incapable of complete degradation of MTBE to innocuous end products are oxidation by permanganate and hydrolysis. Studies of MTBE oxidation by permanganate and MTBE hydrolysis have shown that undesirable intermediates may build up that are not subsequently degraded by either process. Conventional oxidation processes including oxidation by oxygen, ozone, and persulfate may be capable of degrading MTBE to innocuous end products. Advanced oxidation processes such as Fenton's Reagent, ozone/hydrogen peroxide, ultraviolet irradiation, ultrasound irradiation, and oxidation by plasma reaction have also demonstrated the ability to degrade MTBE to innocuous end products. Additionally, both aerobic and anaerobic biodegradation through direct or cometabolic processes have been shown capable of degrading MTBE.

The relative immaturity of many of the processes precludes their use as components of an HFTW system. In particular, processes such as ultraviolet irradiation, ultrasound irradiation, and plasma reaction would require significant engineering to apply in-well. Other processes have yet to be demonstrated in field or pilot study applications.

On the other hand, both direct and cometabolic aerobic biodegradation have proven success in field applications and are relatively simple to incorporate as a component of an HFTW system. Thus, aerobic biodegradation was selected for further investigation in this study.

As demonstrated in Chapter 4.0, results from simulation of this technology show that an MTBE-contaminated groundwater plume may be captured and remediated *in situ* using HFTW technology coupled with an aerobic biodegradation process. Model simulations show that both direct and cometabolic degradation processes successfully reduced downgradient MTBE concentrations and removed MTBE mass; however, MTBE concentrations were not reduced below regulatory limits using the baseline kinetic, engineering, and environmental data. The relative uncertainty about actual kinetic parameter values along with best-guess values used for other parameters may have contributed to the lack of success in achieving treatment goals. These limitations will be discussed later in this section. Based on the technology model simulations, though, it appears that the HFTW system appears to be a viable technology that can be applied to stimulate either direct or cometabolic MTBE biodegradation. A cometabolic process may be required when microorganisms capable of direct aerobic MTBE metabolism are not present at a particular site.

Sensitivity analysis on performance of the technology over a range of kinetic parameter values showed that variations in the values of the primary substrate utilization rate (k_{Donor}), primary substrate half-saturation constant ($K_{s-Donor}$), MTBE utilization rate (k_{MTBE}), and MTBE half-saturation constant (K_{s-MTBE}) have a marked effect on the performance of this technology. The values of these parameters vary widely throughout

the literature, motivating future research to determine specific values for given geochemical and microbiological conditions. It is important to note that higher values of K_{s-MTBE} may result in difficulty remediating MTBE-contaminated water below regulatory levels. Furthermore, the assumption that the value of the half-saturation constant for each substrate is equal to its inhibition constant may not be a good one. The half-saturation constant values reported in the literature may not be suitable for use in the inhibition terms of the biodegradation models.

The engineering parameters, including TAC of electron donor and hydrogen peroxide and electron donor pulse schedule, also have a significant impact on the performance of the system. The direct metabolism technology model showed substantial sensitivity to the TAC of hydrogen peroxide. Simulation results using the direct metabolism model indicate that the mass of MTBE degraded is directly related to the TAC of hydrogen peroxide injected, despite peroxide toxicity effects on microbial activity. Accordingly, injecting increased hydrogen peroxide TAC yielded lower downgradient MTBE concentrations. In all, these results indicate that the rate and extent of MTBE degradation by MTBE-degrading aerobes is limited only by the availability of oxygen; however, the TAC of hydrogen peroxide is also directly related to operating expense. The TAC of hydrogen peroxide should be optimized to meet treatment objectives and minimize operation expense.

The cometabolism technology model demonstrated substantial sensitivity to the TAC of electron donor and the electron donor injection pulse schedule. The electron donor TAC and injection pulse schedule is critical for optimizing system performance. The technology model is so sensitive to these parameters that for certain variations in

their values, the downgradient concentration of MTBE was not reduced and only negligible MTBE mass was removed. This sensitivity most likely is a result of competitive inhibition and the selectivity of the enzymes responsible for oxidation for the different substrates.

The efficiency of the system in treating MTBE-contaminated groundwater increases as recirculation and mixing of contaminant occurs due to the operation of the HFTW system. When recirculation between the HFTW well pair increased, either due to increased pumping rates or reductions in groundwater Darcy velocity, lower downgradient MTBE concentrations were achieved. The recirculation of MTBE-contaminated water between the HFTW treatment wells results in multiple passes of contaminated water through the bioactive treatment zones, thus achieving high MTBE removal efficiency; however, the high removal efficiency achieved due to increased recirculation also results in less capture zone width of the upgradient MTBE plume causing less MTBE mass to be removed, if all other parameters remain the same. The counteracting effects of recirculation and capture zone width must be managed properly for a given hydrogeological condition to achieve the desired capture and treatment efficiency objectives.

Results of the simulations conducted under isotropic conditions indicate that some degree of well short circuiting or vertical flow from the injection screen to the extraction screen of the same well is occurring. Despite the occurrence of vertical flow, results from simulations run using the baseline parameter values in the direct metabolism model indicate that well short circuiting may not be a problem for this specific configuration.

Ultimately, the kinetic rate of MTBE degradation for some processes may be fast enough to maintain system performance despite well short circuiting.

The use of hydrogen peroxide as the source of oxygen to support aerobic biodegradation may prevent excessive biomass growth in and around the well screens which could in turn help prevent well screen fouling. High TACs of hydrogen peroxide successfully inhibited microbial growth near the injection screens but did not inhibit the net growth or activity of the microbes.

Overall, the development and implementation of this technology model represents an important step towards the design of a pilot-scale system. The model presented in this study may be used to help researchers design and implement this technology to remediate an MTBE-contaminated site.

5.3 RECOMMENDATIONS

- Further study and investigation is required to determine more accurate values for the kinetic parameters k_{Donor} , $K_{S-Donor}$, k_{MTBE} , K_{S-MTBE} , Y , and b . The literature reveals a wide range of values for these kinetic parameters. Additionally, the specific toxic effects of hydrogen peroxide on a particular microbial culture or species should be considered and/or investigated before use to ensure that excessive microbial inhibition does not occur.
- Optimize the performance of the technology model. A complete sensitivity analysis of the capabilities and limitations of the technology model was not accomplished in this study. An optimization study to help determine the best

operating parameters under various conditions would help us to better understand how this technology may potentially be applied.

- Investigate the utilization of other oxygen sources and electron donors. In this study only hydrogen peroxide and propane were considered as an oxygen source and electron donor, respectively. An investigation into the feasibility of using alternative oxygen sources and electron donors may assist in designing and implementing this technology under various conditions.
- Develop a pilot-scale implementation of this technology at an MTBE-contaminated site. A pilot-scale implementation of the technology would provide invaluable operation and performance data. Furthermore, more accurate kinetic parameters could be determined from the system performance data.
- Validate the technology model using the data collected in the pilot-scale study. By using the pilot-scale data to validate the technology model, the technology model can be improved to better simulate the technology.

BIBLIOGRAPHY

- Acero, J. L., S. B. Haderlein, T. C. Schmidt, M. J. F. Suter and U. Von Gunten, MTBE Oxidation by Conventional Ozonation and the Combination Ozone/Hydrogen Peroxide: Efficiency of the Process and Bromate Formation, *Environmental Science and Technology*, 35(21): 4252-4259, 2001.
- Air Force Center for Environmental Excellence, Environmental Resources Program Information Management System, database queried on 8 August 2003.
- Bagga, A. and H. Rifai, In Situ Bioremediation of MTBE Through Biostimulation and Bioaugmentation, In A.R. Gavaskar and A.S.C. Chen (Eds.), *Bioremediation and Phytoremediation of Chlorinated and Recalcitrant Compounds*, Battelle Press, Columbus, OH, 2002.
- Baker, R. J., E. W. Best, and A. L. Baehr, Used Motor Oil as a Source of MTBE, TAME, and BTEX to Ground Water, *Ground Water Monitoring and Remediation*, 22(4): 46-51, 2002.
- Bergendahl, J. A. and T. P. Thies, Fenton's Oxidation of MTBE with Zero-Valent Iron, *Water Research*, 38: 327-334, 2004.
- Bradley, P. M., J. E. Landmeyer, and F. H. Chapelle, Aerobic Mineralization of MTBE and tert-Butyl Alcohol by Stream-Bed Sediment Microorganisms, *Environmental Science and Technology*, 33(11): 1877-1879, 1999.
- Bradley, P. M., F. H. Chapelle, and J. E. Landmeyer, Effect of Redox Conditions on MTBE Biodegradation in Surface Water Sediments, *Environmental Science and Technology*, 35(23): 4643-4647, 2001a.
- Bradley, P. M., F. H. Chapelle, and J. E. Landmeyer, Methyl t-Butyl Ether Mineralization in Surface-Water Sediment Microcosms Under Denitrifying Conditions, *Applied and Environmental Microbiology*, 67(4): 1975-1978, 2001b.
- Bradley, P. M., J. E. Landmeyer, and F. H. Chapelle, Widespread Potential for Microbial MTBE Degradation in Surface-Water Sediments, *Environmental Science and Technology*, 35(4): 658-662, 2001c.
- Bruce, C. L., P. C. Johnson, and K. D. Miller, Large-Scale MTBE-BTEX Plume Containment Using a Combination of Biostimulation and Bioaugmentation, In A.R. Gavaskar and A.S.C. Chen (Eds.), *Bioremediation and Phytoremediation of Chlorinated and Recalcitrant Compounds*, Battelle Press, Columbus, OH, 2002.
- Burbano, A., D. Dioysiou, T. Richardson, and M. Suidan, Degradation of MTBE Intermediates Using Fenton's Reagent, *Journal of Environmental Engineering*, 128(9): 799-805, 2002.

- Buxton, V. B., C. L. Greenstock, W. P. Helman, and A. B. Ross, Critical Review of Rate Constants for Reactions of Hydrated Electrons, Hydrogen Atoms and Hydroxyl Radicals ($\cdot\text{OH}/\cdot\text{O}$), *Journal of Physical Chemistry Reference Data*, 17: 513-886, 1988.
- Carver, M. B., D. V. Hanley, and K. R. Chapin, MAKSIMA-CHEMIST, a Program for Mass Action Kinetic Simulation and Integration Using Stiff Techniques, Chalk River Nuclear Laboratory Report, Atomic Energy of Canada Ltd., 6313, 1979.
- Cater, S. R., M. I. Stefan, J. R. Bolton, and A. Safarzadeh-Amiri, UV/H₂O₂ Treatment of Methyl tert-Butyl Ether in Contaminated Waters, *Environmental Science and Technology*, 34(4): 659-662, 2000.
- Centi, G., A. Grande, and S. Perathoner, Catalytic Conversion of MTBE to Biodegradable Chemicals in Contaminated Water, *Catalysis Today*, 75: 69-76, 2002.
- Centi, G. and S. Perathoner, Remediation of Water Contamination Using Catalytic Technologies, *Applied Catalysis*, 41: 15-29, 2003.
- Chang, P. B. L. and T. M. Young, Kinetics of Methyl tert-Butyl Ether Degradation and By-product Formation During UV/Hydrogen Peroxide Water Treatment, *Water Research*, 34(8): 2233-2240, 2000.
- Charbeneau, R. J., Groundwater Hydraulics and Pollutant Transport, Prentice-Hall Inc., pp. 428-435, 2000.
- Christ, J. A., M. N. Goltz, and J. Huang, Development and Application of an Analytical Model to Aid Design and Implementation of In Situ Remediation Technologies, *Journal of Contaminant Hydrology*, 37(3): 295-317, 1999.
- Clark, Mark M. Transport Modeling for Environmental Engineers and Scientists. New York: John Wiley and Sons, 1996.
- Clayton, W. S., B. K. Marvin, T. Pac, and E. Mott-Smith, A Multisite Field Performance Evaluation of In-Situ Chemical Oxidation Using Permanganate, Proceedings of the Second International Conference on Remediation of Chlorinated and Recalcitrant Compounds, Chemical Oxidation and Reactive Barriers: Remediation of Chlorinated and Recalcitrant Compounds. 101-108. Columbus, OH: Battelle Press, 2000.
- Cooper, W. J., S. P. Mezyk, K. E. O'Shea, D. K. Kim, and D. R. Hardison, Kinetic Modeling of the Destruction of Methyl tert-Butyl Ether (MTBE), *Radiation Physics and Chemistry*, 67: 523-526, 2003.
- Corcho, D., R. J. Watkinson, and D. N. Lerner, Cometabolic Degradation of MTBE by a Cyclohexane-Oxidising Bacteria, In G.B. Wickramanayake, A.R. Gavaskar, B.C. Alleman, and V.S. Magar (Eds.), Bioremediation and Phytoremediation of Chlorinated and Recalcitrant Compounds, Battelle Press, Columbus, OH, pp. 183-189, 2000.

Cowan, R. M., and K. Park, Biodegradation of the Gasoline Oxygenates MTBE, ETBE, TAME, TBA, and TAA by Aerobic Mixed Cultures, In, Proceedings of the 28th Mid-Atlantic Industrial and Hazardous Waste Conference, Buffalo, NY, July 15-17, pp. 523-530, 1996.

Cummins, T. M., G. A. Robbins, B. J. Henebry, C. R. Goad, E. J. Gilbert, M. E. Miller, and J. D. Stuart, A Water Extraction, Static Headspace Sampling, Gas Chromatographic Method to Determine MTBE in Heating Oil and Diesel Fuel, *Environmental Science and Technology*, 35(6): 1202-1208, 2001.

Damm, J. H., C. Hardacre, R. M. Kalin, and K. P. Walsh, Kinetics of the Oxidation of Methyl Tert-Butyl Ether (MTBE) by Potassium Permanganate, *Water Research*, 36: 3638-3646, 2002.

Deeb, R. A., K. M. Scow, L. Alvarez-Cohen, Aerobic MTBE Biodegradation: An Examination of Past Studies, Current Challenges, and Future Research Directions, *Biodegradation*, 11: 171-186, 2000.

Deeb, R. A., K. H. Chu, T. Shih, S. Linder, I Suffet, M. C. Kavanaugh, and L. Alvarez-Cohen, MTBE and Other Oxygenates: Environmental Sources, Analysis, Occurrence, and Treatment, *Environmental Engineering Science*, 20(5): 433-447, 2003.

Department of Energy, Energy Information Administration, Weekly Petroleum Status Report, EIA-819, December 2002.

Domenico, P. A., and F. W. Schwartz, Physical and Chemical Hydrogeology, New York: John Wiley & Sons, Inc., 1998.

Dupasquier, D. S. Revah, and R. Auria, Biofiltration of Methyl tert-Butyl Ether Vapors by Cometabolism with Pentane: Modeling and Experimental Approach, *Environmental Science and Technology*, 36(2): 247-253, 2002.

Environmental Protection Agency, Office of Water Report, Drinking Water Advisory: Consumer Acceptability Advice and Health Effects Analysis on Methyl Tertiary-Butyl Ether (MtBE), EPA 822-F-97-009, December 1997.

Environmental Protection Agency, Office of Groundwater and Drinking Water Report, Stage 1 Disinfectants and Disinfection Byproducts Rule, EPA 815-F-98-010, December 1998.

Environmental Protection Agency, Achieving Clean Air and Clean Water: The Report of the Blue Ribbon Panel on Oxygenates in Gasoline, EPA 420-R-99-021, September 1999a.

Environmental Protection Agency, Air and Radiation, Office of Mobile Sources Report, Reformulated Gasoline, EPA 420-F-99-040, November 1999b.

- Environmental Protection Agency, Demonstration of the HiPOx Advanced Oxidation Technology for the Treatment of MTBE-Contaminated Groundwater, Final Report, EPA 600-R-02-094, September 2002.
- Environmental Protection Agency, Integrated Risk Information System, Methyl tert-butyl ether (MTBE) (CASRN 1634-04-4), <http://www.epa.gov/iris/subst/0545.htm>, visited 16 January, 2004.
- Environmental Security Technology Certification Program (ESTCP), Cost and Performance Report, In Situ Bioremediation of MTBE in Groundwater, CU-0013, 2003a.
- Environmental Security Technology Certification Program (ESTCP), Cost and Performance Report, In Situ Remediation of MTBE-Contaminated Aquifers Using Propane Biosparging, CU-0015, 2003b.
- Federal Remediation Technology Roundtable, Remediation Technologies Screening Matrix and Reference Guide, Version 4.0, http://www.frtr.gov/matrix2/section3/sec3_int.html, visited November, 2003.
- Fetter, C.W., Applied Hydrogeology, 3rd Ed., Englewood Cliff, NJ: Prentice Hall, 1994.
- Finneran, K. T. and D. R. Lovely, Anaerobic Degradation of Methyl tert-Butyl Ether (MTBE) and tert-Butyl Alcohol (TBA), *Environmental Science and Technology*, 35(9): 1785-1790, 2001.
- Finneran, K. T. and D. R. Lovely, Anaerobic In Situ Bioremediation, in E. E. Moyer and P. T. Kostecki (Eds.), MTBE Remediation Handbook, Amherst Scientific Publishers, Amherst, MA, pp. 265-277, 2003.
- Fiorenza, S. and H. S. Rifai, Review of MTBE Biodegradation and Bioremediation, *Bioremediation Journal*, 7(1): 1-35, 2003.
- Fortin, N. Y. and M. A. Deshusses, Treatment of Methyl *tert*-Butyl Ether Vapors in Biotrickling Filters. 1. Reactor Startup, Steady-State Performance and Culture Characteristics, *Environmental Science and Technology*, 33(17): 2980-2986, 1999.
- Francois, A., H. Mathis, D. Godefro, P. Piveteau, F. Fayolle, and F. Monot, Biodegradation of Methyl tert-Butyl Ether and Other Fuel Oxygenates by a New Strain, *Mycobacterium Austroafricanum* IFP 2012, *Applied and Environmental Microbiology*, 68(6): 2754-2762, 2002.
- Gandhi, R. K., G. D. Hopkins, M. N. Goltz, S. M. Gorelick and P. L. McCarty, Full-Scale Demonstration Of In Situ Cometabolic Biodegradation Of Trichlorethylene In Groundwater, 1: Dynamics Of A Recirculating Well System, *Water Resources Research*, 38(4): 10-1, 10-15, 2002a.

- Gandhi, R. K., G. D. Hopkins, M. N. Goltz, S. M. Gorelick and P. L. McCarty, Full-Scale Demonstration Of In Situ Cometabolic Biodegradation Of Trichlorethylene In Groundwater, 2: Comprehensive Analysis Of Field Data Using Reactive Transport Modeling, *Water Resources Research*, 38(4): 11-1, 11-18, 2002b.
- Garrett, C.A., Optimization Of In Situ Aerobic Cometabolic Bioremediation Of Trichloroethylene-Contaminated Groundwater Using A Parallel Genetic Algorithm. MS Thesis, AFIT/GEE/ENV/99M-02. School of Engineering and Environmental Management, Air Force Institute of Technology, (AU), Wright-Patterson AFB, OH, December 1999.
- Goltz, M. N., E. J. Bouwer, and J. Huang, Transport Issues and Bioremediation Modeling for the In Situ Aerobic Co-metabolism of Chlorinated Solvents, *Biodegradation* 12(2): 127-140, 2001.
- Hanson, J. R., C. E. Ackerman, and K. M. Scow, Biodegradation of Methyl *tert*-Butyl Ether by a Bacterial Pure Culture, *Applied and Environmental Microbiology*, 65(11): 4788-4792, 1999.
- Harbaugh, A. W. and M. G. McDonald, User's documentation for MODFLOW-96, and Update to the US Geological Survey Modular Finite-Difference Groundwater Flow Model, US Geological Survey Open-File Report, 96-485, 56p, 1996.
- Hardison, L. K., S. S. Curry, L. M. Ciuffetti, and M. R. Hyman, Metabolism of Diethyl Ether and Cometabolism of Methyl *tert*-Butyl Ether by a Filamentous Fungus, a *Graphium* sp., *Applied and Environmental Microbiology*, 63(8): 3059-3067, 1997.
- Hatzinger, P. B., K. McClay, S. Vainberg, M. Tugusheva, C. W. Condee, and R. J. Steffan, Biodegradation of Methyl *tert*-Butyl Ether by a Pure Bacterial Culture, *Applied and Environmental Microbiology*, 67(12): 5601-5607, 2001.
- Hinchey, E. J., J. S. Fox, and H. C. Tayeh, Evaluation of MTBE in middle distillate petroleum products in the northeastern United States, Abstract presented at the 17th Annual International Conference on Contaminated Soils, Sediment and Water, University of Massachusetts at Amherst, 22-25 October, 2001.
- Hoigne, J., Chemistry of Aqueous Ozone and Transformation of Pollutants by Ozonation and Advanced Oxidation Processes, In J. Hrubec (Ed.), The Handbook of Environmental Chemistry, Vol. 5, Part C, Quality and Treatment of Drinking Water II, Springer-Verlag, Berlin Heidelberg, 1998.
- Hristova, K., B. Gebreyesus, D. Mackay, and K. M. Scow, Naturally Occurring Bacteria Similar to the Methyl *tert*-Butyl Ether (MTBE)-Degrading Strain PM1 Are Present in MTBE-Contaminated Groundwater, *Applied and Environmental Microbiology*, 69(5): 2616-2623.
- Huang, J. and M. N. Goltz, A Model Of In Situ Bioremediation Which Includes The Effect Of Rate Limited Sorption And Bioavailability, In Proceedings of the 1998

Conference on Hazardous Waste Research, pp 297-295, Snow Bird, UT, 19-21 May 1998.

Huang, K., R. A. Couttenye, and G. E. Hoag, Kinetics of Heat-Assisted Persulfate Oxidation of Methyl tert-Butyl Ether (MTBE), *Chemosphere*, 49: 413-420, 2002.

Hyman, M., C. Taylor, and K. O'Reilly, Cometabolic Degradation of MTBE by Iso-Alkane-Utilizing Bacteria From Gasoline-Impacted Soils, In G.B. Wickramanayake, A.R. Gavaskar, B.C. Alleman, and V.S. Magar (Eds.), *Bioremediation and Phytoremediation of Chlorinated and Recalcitrant Compounds*, Battelle Press, Columbus, OH, pp. 149-155, 2000.

Ince, N. H., G. Tezcanli, R. K. Belen, and I. G. Apikyan, Ultrasound as a Catalyzer of Aqueous Reaction Systems: the State of the Art and Environmental Applications, *Applied Catalysis*, 29: 167-176, 2001.

Jansen, R., E. Moyer, R. Woodward, R. Sloan, MTBE Remediation Seminar, Spring, 2002.

Jenal-Wanner, U., and P. L. McCarty, Development and Evaluation of Semi-Continuous Slurry Microcosms to Simulate In Situ Biodegradation of Trichloroethylene in Contaminated Aquifers, *Environmental Science and Technology*, 31(10): 2915-2922, 1997.

Johnson, D. C., V. A. Shamamian, J. H. Callahan, F. S. Denes, S. O. Manolache, and D. S. Dandy, Treatment of Methyl tert-Butyl Ether Contaminated Water Using a Dense Medium Plasma Reactor: A Mechanistic and Kinetic Investigation, *Environmental Science and Technology*, 37(20): 4804-4810, 2003.

Kane, S. R., H. R. Beller, T. C. Legler, C. J. Koester, H. C. Pinkart, R. U. Halden, and A. M. Happel, Aerobic Biodegradation of Methyl tert-Butyl Ether by Aquifer Bacteria from Leaking Underground Storage Tanks Sites, *Applied and Environmental Microbiology*, 67(12): 5824-5829, 2001.

Kang, J. W. and M. R. Hoffman, Kinetics and Mechanism of the Sonolytic Destruction of Methyl tert-Butyl Ether by Ultrasonic Irradiation in the Presence of Ozone, *Environmental Science and Technology*, 32(20): 3194-3199, 1998.

Kang, J. W., H. Hung, A. Lin, and M.R. Hoffman, Sonolytic Destruction of Methyl tert-Butyl Ether by Ultrasonic Irradiation: The Role of O₃, H₂O₂, Frequency, and Power Density, *Environmental Science and Technology*, 33(18): 3199-3205, 1999.

Kelley, K. L., M. C. Marley, and K. L. Sperry, In Situ Chemical Oxidation, in E. E. Moyer and P. T. Kostecki, (Eds.), *MTBE Remediation Handbook*, Amherst Scientific Publishers, Amherst, MA, pp. 223-241, 2003.

- Kerfoot, W. B. and P. LeCheminant, Ozone Microbubble Sparging at a California Site, in E. E. Moyer and P. T. Kostecki, (Eds.), MTBE Remediation Handbook, Amherst Scientific Publishers, Amherst, MA, pp. 455-472, 2003.
- Kim, Y., D. J. Arp, and L. Semprini, A Combined Method for Determining Inhibition Type, Kinetic Parameters, and Inhibition Coefficients for Aerobic Cometabolism of 1,1,1-Trichloroethane by a Butane-Grown Mixed Culture, *Biotechnology and Bioengineering*, 77(5): 564-576, 2002.
- Koenigsberg, S., C. Sandefur, W. Mahaffey, M. Dehusses, and N. Fortin, In B.C. Alleman, and A. Leeson (Eds.), The Fifth International In Situ and On-Site Bioremediation Symposium, Battelle Press, Columbus, OH, pp. 13-18, 1999.
- Landmeyer, J.E. F.H. Chapelle, H.H. Herlong, and P.M. Bradley, Methyl *tert*-Butyl Ether Biodegradation by Indigenous Aquifer Microorganisms Under Natural and Artificial Oxidic Conditions, *Environmental Science and Technology*, 35(6): 1118-1126, 2001.
- Li, T., R. U. Patel, D. K. Ramsden, and J. Greene, Ground Water Recovery and Treatment in E. E. Moyer and P. T. Kostecki, (Eds.), MTBE Remediation Handbook, Amherst Scientific Publishers, Amherst, MA, pp. 289-348, 2003.
- Liang, S., R. S. Yates, D. V. Davis, S. J. Pastor, L. S. Palencia, and J. M. Bruno, Treatability of MTBE contaminated groundwater by ozone and peroxone, *Journal of the American Water Works Association*, June: 110-120, 2001.
- Lien, H. and R. Wilkin, MTBE Oxidation by Bifunctional Aluminum, In A.R. Gavaskar and A.S.C. Chen (Eds.), Bioremediation of Chlorinated and Recalcitrant Compounds, Battelle Press, Columbus, OH, 2002a.
- Lien, H., and R. Wilkin, Reductive Activation of Dioxygen for Degradation of Methyl *tert*-Butyl Ether by Bifunctional Aluminum, *Environmental Science and Technology*, 36(20): 4436-4440, 2002b.
- Liu, C. Y., G. E. Speitel Jr., and G. Georgiou, Kinetics of Methyl *t*-Butyl Ether Cometabolism by Pure Cultures of Butane-Degrading Bacteria, *Applied and Environmental Microbiology*, 67(5): 2197-2201, 2001.
- Loll, P., C. Larsen, K. Henriksen, and K. Dahlstrom, Treatment of MTBE-Contaminated Groundwater in Sequencing Batch Reactors, In Proceedings of The Seventh Annual In Situ and On-Site Bioremediation Conference, Orlando, FL, 2-5 June 2003.
- Lory, E. E., MTBE Cleanup Technology Evaluations at the Port Hueneme NETTS, in E. E. Moyer and P. T. Kostecki, (Eds.), MTBE Remediation Handbook, Amherst Scientific Publishers, Amherst, MA, pp. 473-502, 2003.
- Mackay, D., Shiu, W. Y., and Ma, K. C., Illustrated handbook of Physical-Chemical Properties and Environmental Fate for Organic Chemicals-Volume III. Volatile Organic Chemicals; Boca Raton: Lewis Publishers, 1993.

- Maier, R. M., I. L. Pepper, and C. P. Gerba, Environmental Microbiology, San Diego, CA: Academic Press, 2000.
- Martinez-Prado, A., Biodegradation of Methyl *tert*-Butyl Ether (MTBE) and its Breakdown Products by Propane and *Iso*-Pentane Grown *Mycobacterium Vaccae* and *Graphium sp.*: Cometabolism, Inhibition, Kinetics, and Modeling, PhD Thesis, Oregon State University, 2002.
- McCarty, P. L., M. N. Goltz, G. D. Hopkins, M. E. Dolan, J. P. Allan, B. T. Kawakami, and T. J. Carrothers, Full-Scale Evaluation of In Situ Cometabolic Degradation of Trichloroethylene in Groundwater through Toluene Injection, *Environmental Science and Technology*, 32(1): 88-100, 1998.
- Mezyk, S. P., W. J. Cooper, D. M. Bartels, K. E. O'Shea, and T. Wu, Radiation Chemistry of Alternative Fuel Oxygenates: Substituted Ethers, *Journal of Physical Chemistry A*, 105: 3521-3526, 2001.
- Mitani, M. M., A. A. Keller, C. A. Bunton, R. G. Rinker, and O. C. Sandall, Kinetics and Products of reactions of MTBE with Ozone and Ozone/Hydrogen Peroxide in Water, *Journal of Hazardous Materials*, B89: 197-212, 2002.
- Mo, K., C. O. Lora, A. E. Wanken, M. Javanmardian, X. Yang, and C. F. Kulpa, Biodegradation of Methyl *t-butyl* Ether by Pure Bacterial Cultures, *Applied Microbiology and Biotechnology*, 47: 69-72, 1997.
- Moreels, D., L. Bastiaens, and L. Diels, Evaluation of the Intrinsic MTBE Biodegradation Potential in MTBE-Contaminated Soils, In A.R. Gavaskar and A.S.C. Chen (Eds.), Bioremediation and Phytoremediation of Chlorinated and Recalcitrant Compounds, Battelle Press, Columbus, OH, 2002.
- Moyer, E. E. Introduction, In E. E. Moyer and P. T. Kostecki (Eds.), MTBE Remediation Handbook, Amherst Scientific Publishers, Amherst, MA, pp. 3-10, 2003.
- Neppolian, B., J. Y. Jung, H. C. Choi, J. H. Lee, and J. W. Kang, Sonolytic Degradation of Methyl *tert*-Butyl Ether: the Role of Coupled Fenton Process and Persulfate Ion, *Water Research*, 36: 4699-4708, 2002.
- Oberle, D. W. and D. L. Schroder, Design Considerations for *In-Situ* Chemical Oxidation, In G.B. Wickramanayake, A.R. Gavaskar, and S.C. Chen (Eds.), Chemical Oxidation and Reactive Barriers: Remediation of Chlorinated and Recalcitrant Compounds, Second International Conference of Chlorinated and Recalcitrant Compounds, Monterey, CA, Battelle Press, Columbus, OH, pp. 91-99, 2000.
- O'Reilly, K. T., M. E. Moir, C. D. Taylor, C. A. Smith, and M. R. Hyman, Hydrolysis of *Tert*-Butyl Methyl Ether (MTBE) in Dilute Aqueous Acid, *Environmental Science and Technology*, 35(19): 3954-3961, 2001.

- O'Shea, K. E., D. K. Kim, T. Wu, W. J. Cooper, and S. P. Mezyk, The Degradation of MTBE-BTEX Mixtures by Gamma Radiolysis. A Kinetic Modeling Study, *Radiation Physics and Chemistry*, 65: 343-347, 2002a.
- O'Shea, K. E., T. Wu, and W. J. Cooper, TiO₂ Photocatalysis of Gasoline Oxygenates, Kinetic Parameters, and Effects of Catalyst Types and Loading on the Degradation of Methyl tert-Butyl Ether, in *Oxygenates in Gasoline: Environmental Aspects*, Washington D.C.: American Chemical Society, 2002b.
- Oxygenated Fuels Association (OFA). MTBE's Role in Reformulated Gasoline, <http://www.cleanfuels.net/article.cfm?id=44>, visited 6 January 2003.
- Park, K. and R. M. Cowan, Effects of Oxygen and Temperature on the Biodegradation of MTBE, In, *Proceedings of the 213th ACS National Meeting, Division of Environmental Chemistry*, San Francisco, CA, pp. 421-424, 1997.
- Parr, J. C. Application of Horizontal Flow Treatment Wells for In Situ Treatment of Perchlorate Contaminated Groundwater. MS thesis, AFIT/GEE/ENV/02M-08. School of Engineering and Environmental Management, Air Force Institute of Technology (AU), Wright-Patterson AFB, OH, March 2002.
- Parr, J. C., M. N. Goltz, J. Huang, P. B. Hatzinger, and Y. H. Farhan, Modeling In Situ Bioremediation of Perchlorate-contaminated Groundwater, *Seventh International In Situ and On-site Bioremediation Symposium*, Orlando, FL, 2-5 June 2003.
- Perry, J. J., Propane Utilization by Microorganisms, *Advances in Applied Microbiology*, 26: 89-115, 1980.
- Pruden, A., M. Sedran, M. Suidan, and A. Venosa, Biodegradation of MTBE and BTEX in an Aerobic Fluidized Bed Reactor, *Water Science and Technology*, 47(9): 123-128, 2003.
- Ray, A. B., A. Selvakumar, and A. N. Tafuri, Treatment of MTBE-Contaminated Waters with Fenton's Reagent, *Remediation: the Journal of Environmental Cleanup Costs, Technologies, and Techniques*, 12(3): 81-93, 2002.
- Reuter, J. E., B. C. Allen, R. C. Richards, J. F. Pankow, C. R. Goldman, R. L. Scholl, and J. S. Seyfried, Concentrations, Sources, and Fate of the Gasoline Oxygenate Methyl tert-Butyl Ether (MTBE) in a Multiple Use Lake, *Environmental Science and Technology*, 32(23): 3666-3672, 1998.
- Rittman, B. E., and P. L. McCarty, *Environmental Biotechnology: Principles and Applications*, 2nd Ed., New York: McGraw-Hill, 2001.
- Robbins, G. A., B. J. Henebry, B. M. Schmitt, F. B. Bartolomeo, A. Green, and P. Zack, Evidence for MTBE in Heating Oil, *Ground Water Monitoring and Remediation*, 19(2): 65-69, 1999.

- Robbins, G. A., B. J. Henebry, T. M. Cummins, C. R. Goad, and E. J. Gilbert, Occurrence of MTBE in Heating Oil and Diesel Fuel in Connecticut, *Ground Water Monitoring and Remediation*, 20(4): 82-86, 2000.
- Safarzadeh-Amiri, A., O₃/H₂O₂ Treatment of Methyl-tert-Butyl Ether (MTBE) in Contaminated Waters, *Water Research*, 35(15): 3706-3714, 2001.
- Safarzadeh-Amiri, A., O₃/H₂O₂ Treatment of Methyl-tert-Butyl Ether (MTBE) in Contaminated Waters: Effect of Background COD on the O₃-Dose, *Ozone Science and Engineering*, 24: 55-62, 2002.
- Salanitro, J. P., L. A. Diaz, M. P. Williams, and H. L. Wisniewski, Isolation of a Bacterial Culture that Degrades Methyl t-Butyl Ether, *Applied and Environmental Microbiology*, 60(7): 2593-2596, 1994.
- Salanitro, J. P., P.C. Johnson, G.E. Spinnler, P. M. Maner, H. L. Wisniewski, and C. Bruce, Field-Scale Demonstration of Enhanced MTBE Bioremediation through Aquifer Bioaugmentation and Oxygenation, *Environmental Science and Technology*, 34(19): 4152-4162, 2000.
- Sawyer, C.N., P.L. McCarty, and G.F. Parkin, Chemistry for Environmental Engineering, 4th Ed, New York: McGraw-Hill, 1994.
- Schirmer, M., B. J. Butler, J. F. Barker, C. D. Church, and K. Schirmer, Evaluation of Biodegradation and Dispersion as Natural Attenuation Processes of MTBE and Benzene at the Borden Field Site, *Physics and Chemistry of the Earth (B)*, 24(6): 557-560, 1999.
- Smith, C.A., K.T. O'Reilly, and M.R. Hyman, Characterization of the Initial Reactants During the Cometabolic Oxidation of Methyl tert-Butyl Ether by Propane-Grown Mycobacterium vaccae JOB5, *Applied and Environmental Microbiology*, 69(2): 796-804, 2003.
- Somsamak, P., R. M. Cowan, and M. M. Haggblom, Anaerobic Biotransformation of Fuel Oxygenates Under Sulfate-Reducing Conditions, *FEMS Microbiology Ecology*, 37: 259-264, 2001.
- Semprini L. and P. L. McCarty, Comparison Between Model Simulations and Field Results for In Situ Bioremediation of Chlorinated Aliphatics: Part 1. Biostimulation of Methanotrophic Bacteria, *Ground Water* 29(3): 365-374, 1991.
- Semprini L. and P. L. McCarty, Comparison Between Model Simulations and Field Results for In-Situ Bioremediation of Chlorinated Aliphatics, Part 2. Cometabolic Transformations, *Ground Water* 30(1): 37-44, 1992.
- Squillace, P. J., J. S. Zogorski, W. G. Wilber, and C. V. Price, Preliminary Assessment of the Occurrence and Possible Sources of MTBE in Groundwater in the United States, 1993-1994, *Environmental Science and Technology*, 30(5): 1721-1730, 1996.

- Stavnes, S. A. *et al.*, MTBE Bioremediation With BioNets™ Containing Isolite®, PM1, Solid Oxygen Source (SOS) or Air, In A.R. Gavaskar and A.S.C. Chen (Eds.), Remediation of Chlorinated and Recalcitrant Compounds, The Third International Conference on Remediation of Chlorinated and Recalcitrant Compounds, Monterey, CA, Battelle Press, Columbus, OH, 2002.
- Stefan, M. I., J. Mack, and J. R. Bolton, Degradation Pathways During the Treatment of Methyl tert-Butyl Ether by the UV/H₂O₂ Process, *Environmental Science and Technology*, 34(4): 650-658, 2000.
- Steffan, R. J., K. McClay, S. Vainberg, C. W. Condee, and D. Zhang, Biodegradation of the Gasoline Oxygenates Methyl tert-Butyl Ether, Ethyl tert-Butyl Ether, and tert-Amyl Methyl Ether by Propane-Oxidizing Bacteria, *Applied and Environmental Microbiology*, 63(11): 4216-4222, 1997.
- Steffan, R. J., C. Condee, J. Quinnan, M. Walsh, S. H. Abrams, and J. Flanders, In Situ Application of Propane Sparging for MTBE Bioremediation, In G.B. Wickramanayake, A.R. Gavaskar, B.C. Alleman, and V.S. Magar (Eds.), Bioremediation and Phytoremediation of Chlorinated and Recalcitrant Compounds, Battelle Press, Columbus, OH, pp. 157-164, 2000a.
- Steffan, R.J., S. Vainberg, C. Condee, K. McClay, and P. Hatzinger, Biotreatment of MTBE With a New Bacterial Isolate, In G.B. Wickramanayake, A.R. Gavaskar, B.C. Alleman, and V.S. Magar (Eds.), Bioremediation and Phytoremediation of Chlorinated and Recalcitrant Compounds, Battelle Press, Columbus, OH, pp. 165-173, 2000b.
- Stocking, A. J., R. A. Deeb, A. E. Flores, W. Stringfellow, J. Talley, R. Brownell, and M. C. Kavanaugh, Bioremediation of MTBE: a review from a practical perspective, *Biodegradation*, 11: 187-201, 2000.
- Stoppel, C. M., A Model for Palladium Catalyzed Destruction of Chlorinated Ethene Contaminated Groundwater. MS Thesis, AFIT/GEE/ENV/01M-21, 2001. School of Engineering and Environmental Management, Air Force Institute of Technology, (AU), Wright-Patterson AFB, OH, 2001.
- Stoppel, C. M. and M. N. Goltz, Modeling Pd-Catalyzed Destruction of Chlorinated Ethenes in Groundwater, *Journal of Environmental Engineering*, 129(2): 147-154, 2003.
- Trotta, R. and I. Miracca, Case History: Synthesis and Decomposition of MTBE, *Catalysis Today*, 34: 447-455, 1997.
- Vel Leitner, N. K., A.-L. Papilhou, J. P. Croue, J. Peyrot, and M. Dore, Oxidation of MTBE and ETBE by Ozone and Combined Ozone/Hydrogen Peroxide, *Ozone Science and Engineering*, 16: 41-54, 1994.

- Von Gunten, U., Ozonation of Drinking Water: Part II. Disinfection and By-Product Formation in Presence of Bromide, Iodide, or Chlorine, *Water Research*, 37: 1469-1487, 2003.
- Walton, J., P Labine, and A. Reidies, The Chemistry of Permanganate in Degradative Oxidations, in W.W. Eckenfelder, A.R. Bowers, and J.A. Roth (Eds.), Chemical Oxidation, Lancaster, Basel: Technomic Publishing Co. Inc., 1991.
- Williams, P. R. D. and P. J. Sheehan, Risk Assessment, In E. E. Moyer and P. T. Kostecki (Eds.), MTBE Remediation Handbook, Amherst Scientific Publishers, Amherst, MA, pp. 121-167, 2003.
- Wilson, J. T., Aerobic In Situ Bioremediation, In E. E. Moyer and P. T. Kostecki (Eds.), MTBE Remediation Handbook, Amherst Scientific Publishers, Amherst, MA, pp. 243-264, 2003.
- Wilson, R. D., D. M. Mackay, and K. M. Scow, In situ MTBE Biodegradation Supported by Diffusive Oxygen Release, *Environmental Science and Technology*, 36(2): 190-199, 2002.
- Wu, T., V. Cruz, S. Mezyk, W.J. Cooper, and K.E. O'Shea, Gamma Radiolysis of Methyl *t*-Butyl Ether: A Study of Hydroxyl Radical Mediated Reaction Pathways, *Radiation Physics and Chemistry*, 65: 335-341, 2002.
- Yalkowsky, S. H. and Y. He, Eds., Handbook of Aqueous Solubility Data, CRC Press, New York, 2003.
- Yeh, C. K. and J. T. Novak, The Effect of Hydrogen Peroxide on the Degradation of Methyl and Ethyl *tert*-Butyl Ether in Soils, *Water Environment Research*, 67(5): 828-834, 1995.

VITA

Captain Preston F. Rufe was born in Doylestown, PA. He grew up in Upper Black Eddy, PA and graduated from Palisades High School in 1995. From there he entered the United States Air Force Academy. In June 1999 he received his officer commission and graduated from the Academy with a B.S. in Civil Engineering. His first assignment in the United States Air Force was to Eielson Air Force Base, AK as a Second Lieutenant. He then entered the Graduate Engineering Management program of the Graduate School of Engineering and Systems Management, Air Force Institute of Technology, in August 2002.

REPORT DOCUMENTATION PAGE				Form Approved OMB No. 074-0188	
The public reporting burden for this collection of information is estimated to average 1 hour per response, including the time for reviewing instructions, searching existing data sources, gathering and maintaining the data needed, and completing and reviewing the collection of information. Send comments regarding this burden estimate or any other aspect of the collection of information, including suggestions for reducing this burden to Department of Defense, Washington Headquarters Services, Directorate for Information Operations and Reports (0704-0188), 1215 Jefferson Davis Highway, Suite 1204, Arlington, VA 22202-4302. Respondents should be aware that notwithstanding any other provision of law, no person shall be subject to a penalty for failing to comply with a collection of information if it does not display a currently valid OMB control number.					
PLEASE DO NOT RETURN YOUR FORM TO THE ABOVE ADDRESS.					
1. REPORT DATE (DD-MM-YYYY) <div style="text-align: center;">23-03-2004</div>		2. REPORT TYPE <div style="text-align: center;">Master's Thesis</div>		3. DATES COVERED (From – To) <div style="text-align: center;">Jun 2003 – Mar 2004</div>	
4. TITLE AND SUBTITLE APPLICATION OF HORIZONTAL FLOW TREATMENT WELLS FOR <i>IN SITU</i> TREATMENT OF MTBE- CONTAMINATED GROUNDWATER				5a. CONTRACT NUMBER 5b. GRANT NUMBER 5c. PROGRAM ELEMENT NUMBER 5d. PROJECT NUMBER 5e. TASK NUMBER 5f. WORK UNIT NUMBER	
6. AUTHOR(S) Rufe, Preston F., Captain, USAF				8. PERFORMING ORGANIZATION REPORT NUMBER AFIT/GEM/ENV/04M-15	
7. PERFORMING ORGANIZATION NAMES(S) AND ADDRESS(S) Air Force Institute of Technology Graduate School of Engineering and Management (AFIT/EN) 2950 Hobson Way, Building 641 WPAFB OH 45433-7765				10. SPONSOR/MONITOR'S ACRONYM(S) 11. SPONSOR/MONITOR'S REPORT NUMBER(S)	
9. SPONSORING/MONITORING AGENCY NAME(S) AND ADDRESS(ES) AFCEE/ERT 210-536-4311 Attn: Ms. Erica Becvar 3207 North Rd., Bldg 532 Brooks AFB TX 78235-5363				12. DISTRIBUTION/AVAILABILITY STATEMENT APPROVED FOR PUBLIC RELEASE; DISTRIBUTION UNLIMITED.	
13. SUPPLEMENTARY NOTES					
14. ABSTRACT <p>This study utilized a three-dimensional numerical model to evaluate the potential application of a novel in situ bioremediation technology using so-called Horizontal Flow Treatment Wells (HFTWs) to manage MTBE-contaminated groundwater. HFTWs consist of two dual-screened treatment wells. One well operates in an upflow mode, with MTBE-contaminated water extracted from an aquifer through the lower well screen and injected into the aquifer through the upper screen, while the adjacent well operates in a downflow mode, extracting water through the upper screen and injecting it through the lower. As the MTBE-contaminated water flows through the wells, an electron acceptor and/or an electron donor is introduced in order to promote oxidation of MTBE by indigenous microorganisms that grow in bioactive zones adjacent to the injection screens of the treatment wells. In addition to effecting mixing of electron donor/acceptor into the water, the HFTWs recirculate water between the well pairs, resulting in multiple passes of contaminated water through the bioactive treatment zones</p> <p>The model used in this study couples a model that simulates the complex three-dimensional flow field that results from HFTW operation with a transport model to simulate MTBE fate due to advective/dispersive transport and biodegradation. The biodegradation model allows simulation of either direct or cometabolic oxidation of MTBE by indigenous microorganisms. The model was applied to a hypothetical MTBE-contaminated site to demonstrate how this technology might effect in situ MTBE treatment. A sensitivity analysis was conducted using the model to determine the engineering and environmental parameters that impact technology performance. It was observed that technology performance simulated by the model is particularly sensitive to treatment well pumping rate, aquifer hydraulic conductivity, and conductivity anisotropy. It was also observed that simulated technology performance was sensitive to kinetic parameters in both the direct and cometabolic biodegradation sub-models, motivating the need for future research to accurately quantify these parameters for given geochemical and microbiological conditions. This study demonstrates that the HFTW technology has potential for application in managing MTBE-contaminated groundwater.</p>					
15. SUBJECT TERMS MTBE, groundwater contamination, bioremediation, modeling					
16. SECURITY CLASSIFICATION OF:			17. LIMITATION OF ABSTRACT <div style="text-align: center;">UU</div>	18. NUMBER OF PAGES <div style="text-align: center;">227</div>	19a. NAME OF RESPONSIBLE PERSON Professor Mark N. Goltz, ENV
a. REPORT U	b. ABSTRACT U	c. THIS PAGE U			19b. TELEPHONE NUMBER (Include area code) (937) 255-3636, ext 4638; e-mail: Mark.Goltz @afit.edu